

Synthesis, catalysis, and electrochemistry of some organic and organometallic compounds

Peng, Hong Mei

2009

Peng, H. M. (2009). Synthesis, catalysis, and electrochemistry of some organic and organometallic compounds. Doctoral thesis, Nanyang Technological University, Singapore.

<https://hdl.handle.net/10356/47503>

<https://doi.org/10.32657/10356/47503>

Nanyang Technological University

Downloaded on 20 Mar 2024 16:39:35 SGT

273
4X
D/B/uc

**Synthesis, Catalysis, and Electrochemistry
Of Some Organic and Organometallic Compounds**

Peng Hong Mei

School of Physical and Mathematical Sciences

A thesis submitted to the Nanyang Technological University
in partial fulfillment of the requirement for the degree of
Doctor of Philosophy in Chemistry

2009

ACKNOWLEDGEMENTS

Words can hardly substitute the enormous depth of gratitude and indebtedness that I owe to my main-supervisor Dr Richard D. Webster and my co-supervisor Dr Li Xingwei for their guidance, continuous encouragement and ongoing motivation in the completion of this PhD work.

I would especially like to thank Dr Li Yongxin for his kind help in the X-ray crystallographic analysis and Prof Peter M. W. Gill for his aid of the theoretical calculations in the vitamin E sections of this work. Miss Ee Ling, Miss Siew Ping, and Ms. Wen-Wei are acknowledged for their assistance in NMR experiments, LCMS and HRMS experiments, and element analyses.

I will always remember with deep sense of gratitude my friends and group members: Jimei, Weiwei, Mengtao, Yanlan, Shanshan, Xianlong, Guoyong, Yongna, Weidong, Xiaofei, Weijuan, Kishan, Xinjiao, Zhang Yao, and Duanghathai, who worked with me during the course of my study for their unstinted cooperation and enthusiastic support during my study at NTU. When I was ill last June, Weiwei and Jimei took so much care of me, and alumni of Suzhou University also expressed their deep concern about my health. I wish to express my heart thanks to them for their moral support in all possible dimensions.

More acknowledgements may not redeem the debt for the blessings and sacrifices from my boyfriend and my family, and no words I can put to express my sincere gratitude to them.

TABLE OF CONTENTS

Acknowledgements	ii
Abbreviations	viii
Abstract	ix

PART I Towards Understanding the Electrochemical Properties of Vitamin E via the Synthesis of Structurally Related Compounds

Chapter 1: Investigation into Phenoxonium Cations of Vitamin E Analogues Produced by Electrochemical Oxidation	2
1.1. Introduction	2
1.1.1. Background	2
1.1.2. Electrochemical Properties of Vitamin E	3
1.1.3. Summary	9
1.2. Results and Discussion	9
1.2.1. Cyclic Voltammetry	9
1.2.2. Electrolysis Experiments	15
1.2.2.1. Class 1 Compounds	16
1.2.2.2. Class 2 Compounds	20
1.3. Conclusions	26
1.4. Experimental Section	27
1.5. References	33

Chapter 2: Long-Lived Radical Cations as Model Compounds for One-Electron

Oxidation Product of Vitamin E	36
2.1. Introduction	36
2.2. Experimental Results	38
2.2.1. Cyclic Voltammetry	38
2.2.2. Controlled Potential Electrolysis (CPE).....	39
2.2.3. UV-vis Spectroscopy.....	41
2.2.4. Chemical Oxidation Experiments	42
2.2.5. Electrochemistry of Films Attached to GC Electrodes	44
2.2.6. Computational Section	47
2.2.7. IR Spectroscopy	49
2.3. Discussion and Conclusions	50
2.4. Experimental Section	52
2.4.1. Chemicals	52
2.4.2. Synthetic Experiments.....	52
2.4.3. Electrochemical Measurements	54
2.4.4. UV-vis-NIR and FTIR Measurements	55
2.4.5. Computational Procedures.....	55
2.5. References	56

PART II Quinoline-Functionalized N-Heterocyclic Carbenes (NHCs)

Metal Complexes: Synthesis, Structures, and Catalysis

Chapter 3: Palladium Complexes of Quinoline-Tethered N-Heterocyclic Carbenes

(NHCs): Synthesis, Structures, Solution Dynamics, and Catalysis	59
3.1. Introduction	59

3.1.1.	General Properties of NHCs	59
3.1.2.	Synthesis and Properties of NHCs Metal Complexes	61
3.1.3.	NHC-Palladium Complexes	64
3.2.	Results and Discussion	68
3.2.1.	Ligand Synthesis and the Corresponding Silver Complexes	68
3.2.2.	Neutral NHC-Palladium Dichlorides	70
3.2.3.	Cationic NHC-Qinoline Palladium Complexes	75
3.2.4.	Neutral NHC-Pd-Allyl Complexes	76
3.2.5.	Cationic NHC-Pd-Allyl Complexes	81
3.2.6.	Catalytic Applications	90
3.3.	Conclusion.....	91
3.4.	Experimental Section.....	91
3.4.1.	General Information	91
3.4.2.	Synthetic Procedures	92
3.5.	References	105

Chapter 4: Quinoline-Tethered N-heterocyclic Carbenes (NHCs) Complexes of

Rhodium and Iridium: Synthesis, Catalysis, and Electrochemistry.....111

4.1.	Introduction	111
4.2.	Results and discussion	115
4.2.1.	Preparation of Rhodium and Iridium Complexes	115
4.2.2.	Rh(I)-Catalyzed [3 + 2] Cycloaddition Reactions	123
4.2.3.	Electrochemistry	126
4.3.	Conclusions	128
4.4.	Experimental Section.....	129
4.4.1.	General Information	129

4.4.2. Synthetic Procedures	130
4.5. References	139

PART III Rhodium-Catalyzed Alkyne Dimerization

and Subsequent Gold-Catalyzed Hydroamination

Chapter 5: Rhodium-Catalyzed Dimerization of N-Functionalized Propargyl

Alkynes.....	144
5.1. Introduction	144
5.1.1. General Considerations of Alkyne Dimerization.....	144
5.1.2. Ruthenium-Catalyzed Alkyne Dimerization	146
5.1.3. Rhodium-Catalyzed Alkyne Dimerization	148
5.1.4. Palladium-Catalyzed Alkyne Dimerization.....	149
5.1.5. Other Transition-Metal-Catalyzed Alkyne Dimerization.....	150
5.1.6. Summary.....	151
5.2. Results and Discussion	151
5.3. Conclusion	156
5.4. Experimental Section	156
5.4.1. General Information	156
5.4.2. Synthetic Procedures and Data	157
5.5. References	167

Chapter 6: Gold-Catalyzed Intramolecular Hydroamination of Functionalized Enynes

Affording Trisubstituted Pyrroles.....	170
6.1. Introduction	170
6.1.1. General Considerations	170

6.1.2.	Hydroamination of Alkynes	170
6.1.3.	Other Nucleophilic Addition Reactions	177
6.1.4.	Summary	179
6.2.	Results and Discussion	180
6.3.	Conclusion	184
6.4.	Experimental Section	185
6.4.1.	General Information	185
6.4.2.	Synthetic Procedures and Data	185
6.5.	References	193

ABBREVIATIONS

Boc *tert*-Butoxycarbonyl

Cbz Carbobenzyloxy

COD 1,5-Cyclooctadiene

COSY Correlation spectroscopy

Cy Cyclohexyl

DCM Dichloromethane

DMSO Dimethyl sulfoxide

dppb 1,3-bis(diphenylphosphino)butane

dppe 1,3-bis(diphenylphosphino)ethane

dppf 1,1'-bis(diphenylphosphino)ferrocene

dppp 1,3-bis(diphenylphosphino)propane

HRMS High resolution mass spectrometry

KHMDS Potassium hexamethyldisilazane

LDA Lithium diisopropylamide

MAO Methylaluminoxane

Mes Mesityl

NHCs N-heterocyclic carbenes

NMR Nuclear magnetic resonance

NOESY Nuclear overhauser effect spectroscopy

ORTEP Oak Ridge Thermal Ellipsoid Plot

ROESY Rotating-frame Overhauser enhancement spectroscopy

TBAC Tetrabutyl ammonium chloride

Ts *p*-Toluenesulfonyl

Xantphos 4,5-Bis(diphenylphosphino)-9,9-dimethylxanthene

ABSTRACT

This thesis contains three parts, and each part consists of two chapters.

Previous research results have demonstrated that vitamin E can undergo a series of reversible electron-transfer and proton-transfer reactions affording unusual long-lived phenoxonium cations under electrochemical oxidation. The purpose of the sequential study is to investigate what structural aspects of α -tocopherol are important in increasing the lifetime of its related phenoxonium cation. In chapter 1, a number of phenolic compounds have been synthesized and their electrochemical behavior tested by CV (cyclic voltammetry) and CPE (controlled potential electrolysis) experiments. In general, these phenols can be classified into two classes. Class 1 compounds can be oxidized to give long-lived phenoxonium cations, which showed similar electrochemical behavior to α -tocopherol. For class 2 compounds, the corresponding phenoxonium cations are voltammetrically undetectable at slow scan rates, and undergo further rapid reactions or convert into *p*-quinones. The methyl group in the aromatic ring and the chromanol structure of vitamin E played crucial roles in stabilizing phenoxonium cations. In addition, in chapter 2, several heterocyclic ethers without free hydroxyl groups have been synthesized and examined as model compounds to study the one-electron oxidation process of vitamin E by a series of electrochemical methods (CV and CPE) and spectroscopic experiments (UV-vis and FTIR).

In part II of this thesis, a series of transition-metal complexes of quinoline-tethered hemilabile N-heterocyclic carbene (NHC^N) have been synthesized, and crystal structures of these metal complexes in each category have been reported. For palladium complexes, different mechanisms of solution dynamics in various settings are discussed, and representative complexes have been proven as efficient catalysts in Suzuki-coupling reactions. Selective η^3 - η^1 - η^3 rearrangement was proposed for Pd(NHC)(allyl)Cl with a

Mes or *n*-Bu wing tip. If the wing tip was replaced by a *tert*-Bu group, the partially hindered Pd-carbene bond rotation was considered as the main reason for its fluxionality. To cationic complexes [Pd(NHC^N)(allyl)]BF₄, a boat-to-boat conversion of the palladacycle was a plausible mechanism *via* a dissociative step. Both deprotonation of imidazolium salts and silver transmetalation methods have been employed to prepare rhodium and iridium NHC complexes, which can undergo one-electron oxidation during cyclic voltammetry experiments. Neutral Rh(COD)(NHC)Cl complexes have proven active in catalyzing cycloaddition of internal alkynes and diphenylcyclopropenone.

Up to now, selective alkyne dimerization to give *gem*-enynes remains a challenge. In the third part of this thesis, a rare head-to-tail mode of dimerization has been achieved for terminal alkynes using rhodium catalysts in combination with phosphine ligands under mild conditions. Dimerization can tolerate propargyl amines which functionalize by sulfonyl, carbamate, or carbonyl groups, but propargyl sulfonamides are relatively more efficient substrates. Importantly, these dimerization enynes can undergo highly efficient gold-catalyzed intramolecular hydroamination to afford tri-substituted pyrroles. One exception is that ^tBu-substituted enyne will cyclize to give oxazoles as a result of the low acidity of the NH group in this substrate.

Most of the work presented in this thesis has been published in refereed journals.

Chapter 1: Peng, H. M.; Webster, R. D. Investigation into Phenoxonium Cations Produced during the Electrochemical Oxidation of Chroman-6-ol and Dihydrobenzofuran-5-ol Substituted Compounds. *J. Org. Chem.* (2008), 73, 2169–2175.

Chapter 2: Peng, H. M.; Choules, B. F.; Yao, W. W.; Zhang, Z.; Webster, R. D.; Gill P. M. W. Long-Lived Radical Cations as Model Compounds for the Reactive One-Electron Oxidation Product of Vitamin E. *J. Phys. Chem. B* (2008), 112, 10367–10374.

Chapter 3: Peng, H. M.; Song, G. Y.; Li, Y.; Li, X. Synthesis, Structures, and Solution Dynamics of Palladium Complexes of Quinoline-Functionalized N-Heterocyclic Carbenes. *Inorg. Chem.* (2008), 47, 8031-8043.

Chapter 4: Peng, H. M.; Webster, R. D.; Li, X. Quinoline-Tethered N-Heterocyclic Carbene Complexes of Rhodium and Iridium: Synthesis, Catalysis, and Electrochemical Properties. *Organometallics* (2008), 27, 4484-4493.

Chapter 5 and Chapter 6: Peng, H. M.; Zhao, J.; Li, X. Synthesis of Trisubstituted Pyrroles from Rhodium-Catalyzed Alkyne Head-to-Tail Dimerization and Subsequent Gold-Catalyzed Cyclization. *Adv. Synth. Cat.* (2009), 351, 1371-1377.

PART I

Towards Understanding the Electrochemical Properties of Vitamin E *via* the Synthesis of Structurally Related Compounds

CHAPTER 1

Investigation into Phenoxonium Cations of Vitamin E Analogues Produced by Electrochemical Oxidation

1.1. Introduction

1.1.1. Background

The term vitamin E is the generic name for a group of eight plant-derived lipid-soluble substances which can be divided into two groups: tocopherols and tocotrienols. Both classes of compounds have four different forms: α , β , γ , and δ , which differ from one another only in the number and position of methyl groups in the aromatic ring (Figure 1.1). Since the discovery of vitamin E by Evans and Bishop in 1922,¹ subsequent studies have demonstrated that it can act as a lipid-soluble antioxidant and radical scavenger, which can inhibit lipid peroxidation and protect biomembranes from being oxidatively damaged.² In order to better understand the relationship between tocopherol's structures and their biological activities, intense research has also been extended to tocopherol analogues, such as chalcogen-substituted species and pyridinol-based compounds.³ The exact antioxidant function of vitamin E is currently not completely clear, although there exists two widely proposed mechanisms (Scheme 1.1).⁴ The first mechanism is termed hydrogen-atom transfer (HAT), and involves the reactive radical removing a hydrogen atom from the phenolic hydrogen on vitamin E directly.⁵ In the second mechanism, the antioxidant gives up an electron to the reactive free radical and itself becomes a radical cation, which is termed partial electron transfer (ET) with subsequent proton tunneling (PT).⁶ For both of these mechanisms, the homolytic OH bond dissociation enthalpy (BDE) and ionization potential (IP) are usually used to evaluate the antioxidant capacity respectively and result in the formation of the neutral radical ArO^\bullet .

In recent years, there is growing evidence that vitamin E has many other biological functions beyond its antioxidant properties, such as activating enzymes, signalling cascades, and

gene regulation.⁷ The biochemistry group of Azzi has even proposed that vitamin E is not an antioxidant *in vivo*, and in fact it must be protected against oxidation.^{7a} In addition, it has never been adequately explained why, although vitamin E has eight forms, α -tocopherol is the only form of vitamin E that is actively maintained in the human body, despite all forms displaying similar antioxidant functions *in vitro* and *in vivo*. Importantly, α -tocopherol shows some unique non-antioxidant properties which are not shared by any other antioxidant molecules.⁸ Therefore, further research is still necessary to define the role of vitamin E in mammalian biological systems and to explain these novel properties of α -tocopherol *in vivo*.

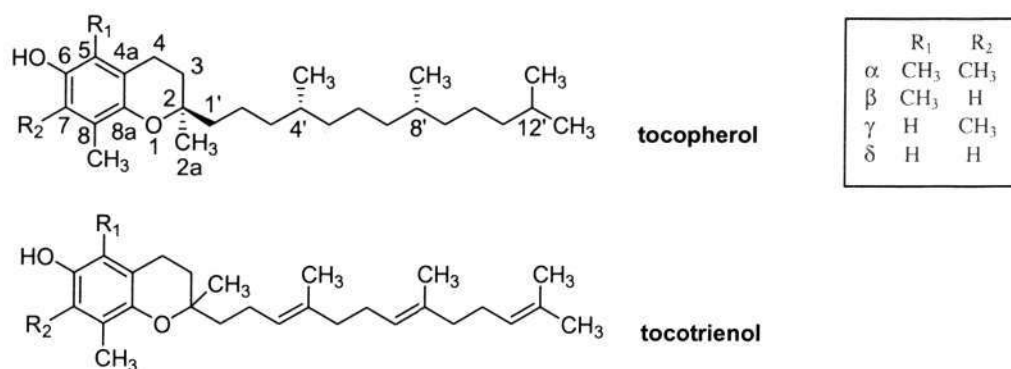
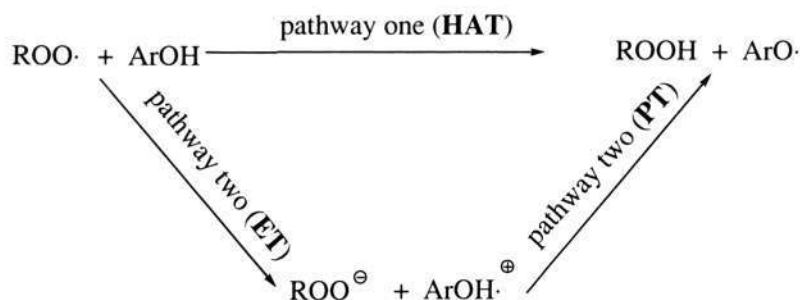


Figure 1.1. Structures of tocopherols and tocotrienols.



Scheme 1.1. The proposed antioxidant mechanisms of vitamin E.

1.1.2. Electrochemical Properties of Vitamin E

Early voltammetric experiments demonstrated the existence of several oxidized forms of α -tocopherol, such as the dication structure and its deprotonated form (figure 1.2).⁹ Later, neutral radicals of vitamin E were measured in benzene at room temperature,¹⁰ in addition, radical cations of tocopherols and tocotrienols were prepared in different solvents and characterized by EPR and ENDOR spectroscopy.¹¹ None of the general methods that were used to study the tocopherols and

tocotrienols showed any significant differences between their antioxidant properties and their structures, other than the neutral radical of α -tocopherol having a slightly longer lifetime under ideal conditions (in organic solvents) compared to the other tocopherols.^{2a,12} However, recent studies by the group of Webster found significant differences in the oxidative behavior of the α -, β -, γ -, and δ -tocopherols when investigated in detail using electrochemical (CV and CPE) and spectroscopic (UV-vis-NIR, FTIR, NMR, and EPR) experiments.¹³

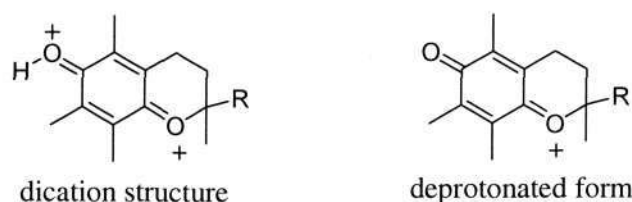


Figure 1.2. Some oxidative forms of α -tocopherols.

Cyclic voltammetry (CV) and electrolysis experiments have shown that α -tocopherol (α -TOH) can be oxidized to form the phenoxonium cation (α -TO⁺) *via* a series of chemically reversible proton and electron transfer processes in a dry aprotic organic solvent such as CH₃CN or CH₂Cl₂.¹⁴ In the presence of the supporting electrolyte Bu₄NPF₆, α -TOH is oxidized by one-electron to the radical cation α -TO^{•+}, at approximately +0.5 V vs Fc/Fc⁺ (Fc = ferrocene), which quickly undergoes a deprotonation reaction to give the neutral free radical α -TO[•]. At the electrode surface, the free radical is immediately oxidized by one-electron affording the phenoxonium cation α -TO⁺, which can be reduced back to the starting material through this reversible route (Scheme 1.2, green line). In general, compounds such as the phenoxonium cations are extremely unstable and positively identified cases are rare.¹⁵ Reports of phenols that form stable phenoxonium ions include two organic compounds with bulky groups in the 2- and 6-positions (**1**) and an aromatic group in the 4-position (**2**),^{16,17} and a metal stabilized phenoxonium complex (**3**), also with bulky groups in the 2- and 6-positions (Figure 1.3).¹⁸ The reverse peak observed during CV experiments indicated that the oxidative intermediate of vitamin E was stable for at least several seconds (Figure 1.4, green line). Controlled potential electrolysis (CPE) experiments further proved the stability of phenoxonium cation α -TO⁺, which has a lifetime of at least several hours in CH₃CN at 243 K.

The oxidation reaction progresses through different pathways when a dry organo-soluble base or acid is added to electrolyte solution of α -tocopherol. For example, in the presence of $\text{CF}_3\text{SO}_3\text{H}$, α -TOH is oxidized in a one-electron step to form the radical cation, $\alpha\text{-TOH}^{\bullet+}$, and then at more positive potentials $\alpha\text{-TOH}^{\bullet+}$ is further oxidized by one-electron to the dication, $\alpha\text{-TOH}^{2+}$ (Scheme 1.2, red line). The addition of an equimolar amount of organo-soluble base (such as Et_4NOH) to CH_3CN solutions of α -TOH immediately forms the phenolate anion ($\alpha\text{-TO}^-$), which can be oxidized in two sequential one-electron steps to also form $\alpha\text{-TO}^+$ (Scheme 1.2, blue line).

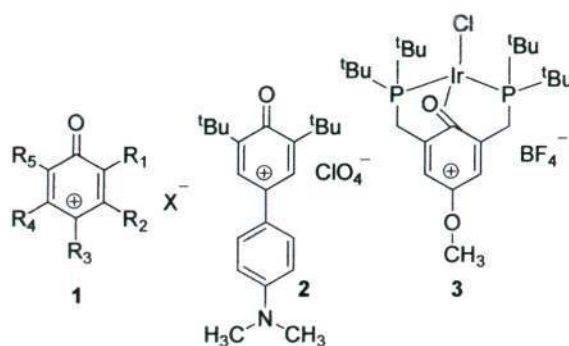
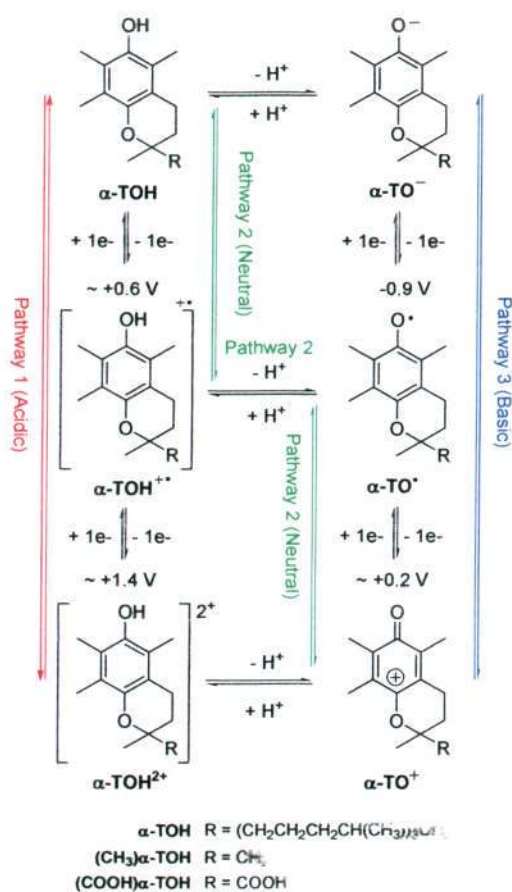


Figure 1.3. Reported examples of stable phenoxonium ions.



Scheme 1.2. Electrochemically induced transformation of α -TOH.^{i4b}

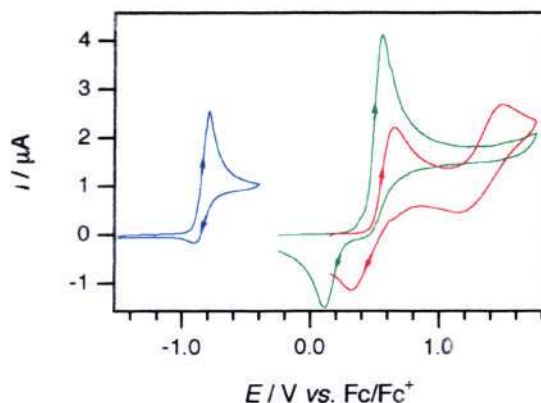
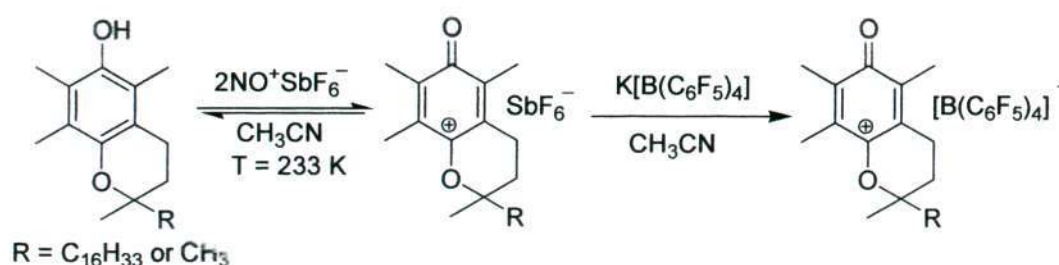


Figure 1.4. Cyclic voltammograms of 2 mM α -TOH at a scan rate of 100 mV s^{-1} at a 1 mm diameter planar Pt electrode in CH_3CN with 0.25 M Bu_4NPF_6 : (green line) α -TOH; (red line) α -TOH with 0.1 M $\text{CF}_3\text{SO}_3\text{H}$; (blue line) R-TO^- prepared by reacting α -TOH with 2 mM Et_4NOH .¹³

The correct assignment of the oxidation pathways described above and the identification of the intermediate compounds were further supported by a series of spectroscopic experiments. Infrared spectra of the electrolyzed solutions provided evidence for the formation of phenoxonium cation, *via* the detection of absorbances at 1649 (C=O) and $1605 \text{ (C=C)} \text{ cm}^{-1}$ is in accordance with a reported iridium-stabilized phenoxonium cation (C=O , 1644 cm^{-1}).^{i8,19} Electrochemical-EPR experiments detected two radical species that were assigned to $\alpha\text{-TOH}^{\bullet}$ and $\alpha\text{-TO}^{\bullet}$, which confirmed the appearance of the radicals during the oxidation process of α -TOH. *In situ* electrochemical-UV-vis experiments led to the detection of unique spectra that could be assigned to both $\alpha\text{-TOH}^{\bullet}$ and $\alpha\text{-TO}^{\bullet}$.^{14b}

In an attempt to synthesize $\alpha\text{-TO}^+$ as a solid compound and to determine its lifetime, a chemical oxidation procedure was employed. The addition of two equivalents of the single electron transfer reagent, $\text{NO}^+\text{SbF}_6^-$, to a solution of α -TOH in CH_3CN , resulted in the phenoxonium cation compound $(\text{CH}_3)\alpha\text{-TO}^+\text{SbF}_6^-$ being obtained (Scheme 1.3).¹⁹ In addition, it was found that when the phytol chain of α -TOH was replaced by a methyl group to form the model compound $(\text{CH}_3)\alpha\text{-TOH}$, the electrochemical behavior was identical, and $(\text{CH}_3)\alpha\text{-TO}^+$ was found to have a very long lifetime in solution.¹⁹ The structure of $(\text{CH}_3)\alpha\text{-TO}^+$ was confirmed by a comparison of experimental ^1H and ^{13}C NMR spectra with theoretical molecular orbital calculations. In the ^{13}C NMR spectrum, the cationic product shows two bands in the carbonyl

region (194.8 and 184.5 ppm), which is consistent with quinoid complex.^{18,19} Attempts to obtain a crystal of $(\text{CH}_3)\alpha\text{-TO}^+\text{SbF}_6^-$ were not successful, but when the SbF_6^- was substituted by the extremely non-nucleophilic anion $[\text{B}(\text{C}_6\text{F}_5)_4]^-$,²⁰ orange crystals could be obtained from a dichloroethane mother liquor. X-ray crystallography confirmed the chromanol structure (Figure 1.5) and further demonstrated the remarkably long lifetime of $\alpha\text{-TO}^+$.²¹ The bond lengths of $\text{C}_4\text{-O}_1$, $\text{C}_2\text{-C}_3$, and $\text{C}_5\text{-C}_6$ are consistent with typical quinone compounds; in addition, the $\text{C}_1\text{-O}_2$ bond length is between a single bond and a double bond, and the $\text{O}_2\text{-C}_9$ bond length (1.520 Å) is much longer than a common single C-O bond (1.44 Å). Thus, it is probable that the chromanol ring structure plays an important role in stabilizing $\alpha\text{-TO}^+$, despite of the weak $\text{O}_2\text{-C}_9$ bond (Figure 1.5).^{13,21}



Scheme 1.3. Chemical oxidation to prepare phenoxonium cation complexes.

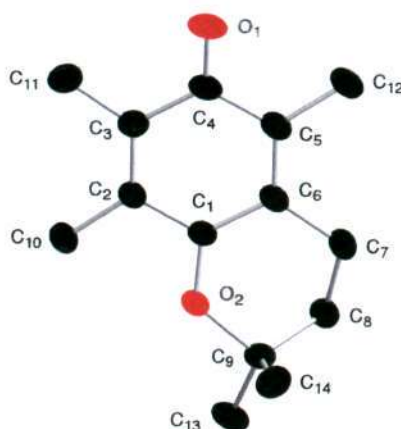


Figure 1.5. ORTEP plot for the molecular structure of $(\text{CH}_3)\alpha\text{-TO}^+$ (crystallized with the $[\text{B}(\text{C}_6\text{F}_5)_4]^-$ counteranion).²¹

The cyclic voltammetric responses obtained for the α -, β -, γ -, and δ -tocopherols show some significant differences (Figure 1.6), which may provide some clues as to why they have very different biological activities, assuming that vitamin E has additional functions to its antioxidant

properties.^{14b} From CV results obtained at a scan rate of 0.1 V s^{-1} , it can be observed that all compounds displayed an oxidation peak at approximately $+0.5$ to $+0.6 \text{ V}$ vs Fc/Fc^+ , but only α -tocopherol and β -tocopherol displayed a clear reduction process when the scan direction was reversed (Figure 1.6). The reverse reduction peaks close to the forward oxidation process for γ - and δ -tocopherols were not observed at a scan rate of 0.1 V s^{-1} , which indicates that their associated phenoxonium cations are relatively short-lived. When the scan rate was increased to 10 V s^{-1} , the reverse reductive peak could be detected for both γ - and δ -tocopherols.

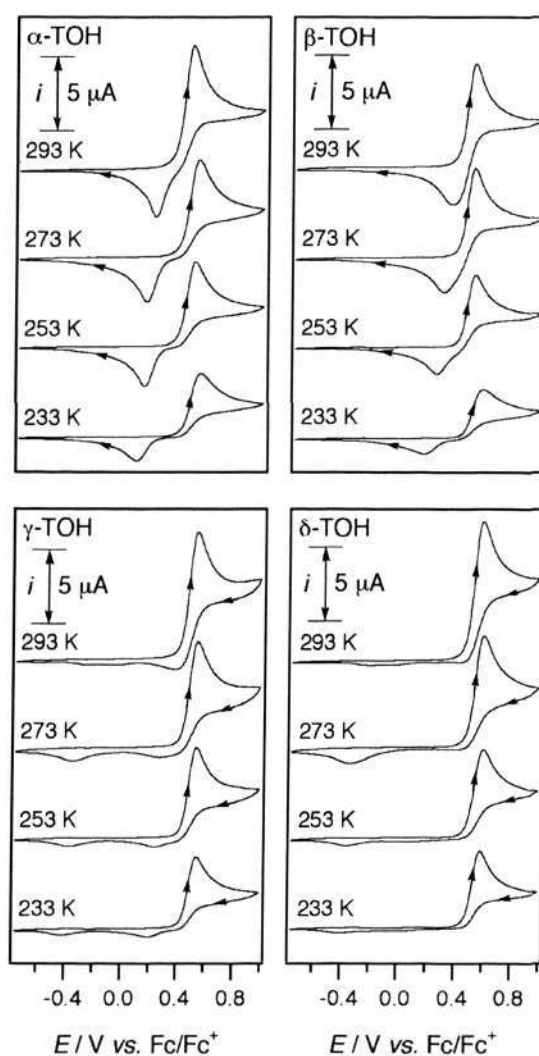


Figure 1.6. Cyclic voltammograms results of α -, β -, γ -, and δ -tocopherols (2 mM) at recorded at a scan rate of 100 mV s^{-1} at a 1 mm diameter planar Pt electrode in CH_3CN with 0.25 M Bu_4NPF_6 .^{14b}

Electrolysis experiments gave a further indication of the stability of the phenoxonium cations of the different tocopherols over longer time intervals (normally greater than minutes), and some conclusions were drawn from the results of the CV and CPE experiments.¹³ Firstly, all forms of the tocopherols undergo the same ECE (E signifies an electron transfer and C represents a chemical step) electrochemical mechanism in CH_3CN in the absence of added acid or base (Scheme 1.2, pathway 2). Secondly, in dry CH_3CN or CH_2Cl_2 , the phenoxonium cation of α -tocopherol is stable for at least several hours, β -tocopherol persists for several minutes, while γ - and δ -tocopherols have lifetimes less than one second. Therefore, only α -tocopherol formed a long-lived phenoxonium cation under electrochemical oxidation, which may be an important property related to its unique non-antioxidant biological functions.

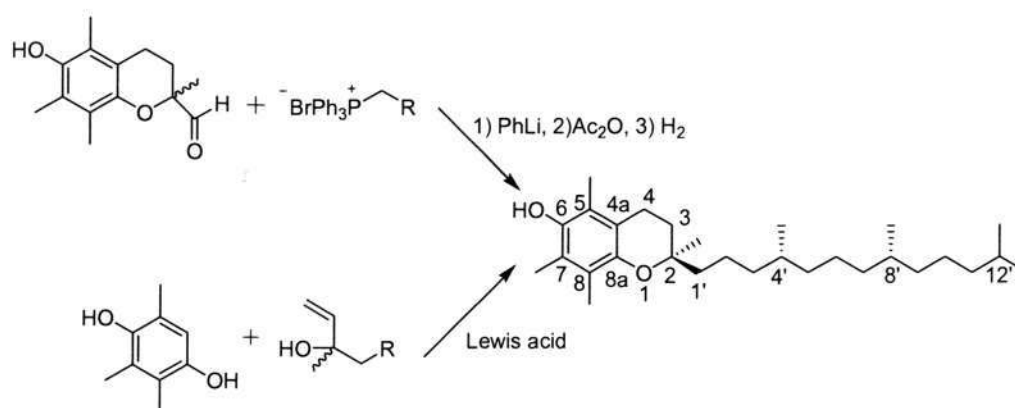
1.1.3. Summary

Previous results showed that the phenoxonium cation of α -tocopherol displayed a long lifetime in dry organic solvents, which is a remarkable observation due to the scarcity of long-lived phenoxonium cations. It is reasoned that the chromanol structure and methyl groups in the aromatic ring impart a special role in the stability of the phenoxonium cation. The subsequent study is devoted to determining what aspects of the structure of α -tocopherol are important in increasing the lifetime of its related phenoxonium cation. A series of similar structurally related compounds of vitamin E were synthesized (chromanol-6-ol and ditrobenzofuran-5-ol based compounds) and their electrochemical behavior was examined by cyclic voltammetry (CV) and controlled potential electrolysis (CPE).

1.2. Results and Discussion

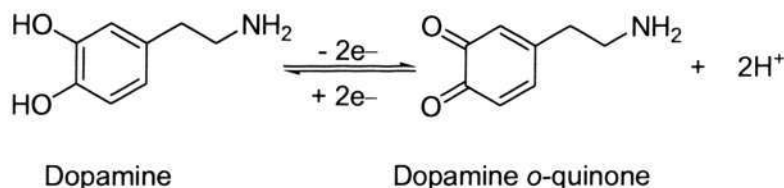
1.2.1. Cyclic Voltammetry (CV)

Mayer, Isler, and co-authors reported the first formal total synthesis of (2R, 4'R, 8'R)- α -tocopherol using Witting reaction (Scheme 1.4).²² Trimethylhydroquinone reacted with allyl-alcohol in the presence of a Lewis acid is another classical synthetic method to synthesize vitamin E (Scheme 1.4).²³



Scheme 1.4. Classical methods to synthesize vitamin E.

In this thesis work, a variety of phenols with structures similar to vitamin E were synthesized (Figure 1.7) by modifying reported methods (see Experimental section) and examined by electrochemical methods. The chemically reversible nature of the two one-electron and one-proton process seen for α -tocopherol is rare compared to what is observed for most phenols, which generally undergo chemically irreversible oxidations to form reaction products that are not readily converted back to the starting material.^{15a} Therefore, CVs performed on phenols do not usually display a reverse cathodic peak when the scan directions are reversed. Some exceptions are: (1) hydroquinones and quinones can interconvert during oxidation/reduction cycling, via a two-electron, two-proton process (Scheme 1.5);^{15a} (2) phenols with nitrogen-included groups adjacent to the hydroxyl group (such as amine, imidazole, and pyridine) that undergo a chemically reversible proton-coupled one-electron transfer;²⁴ (3) in organic solvents containing strong acids some phenol cation radicals can be stabilized against deprotonation resulting in chemically reversible one-electron transfer.²⁵



Scheme 1.5. Electrochemical oxidation mechanism of dopamine in acidic aqueous conditions.

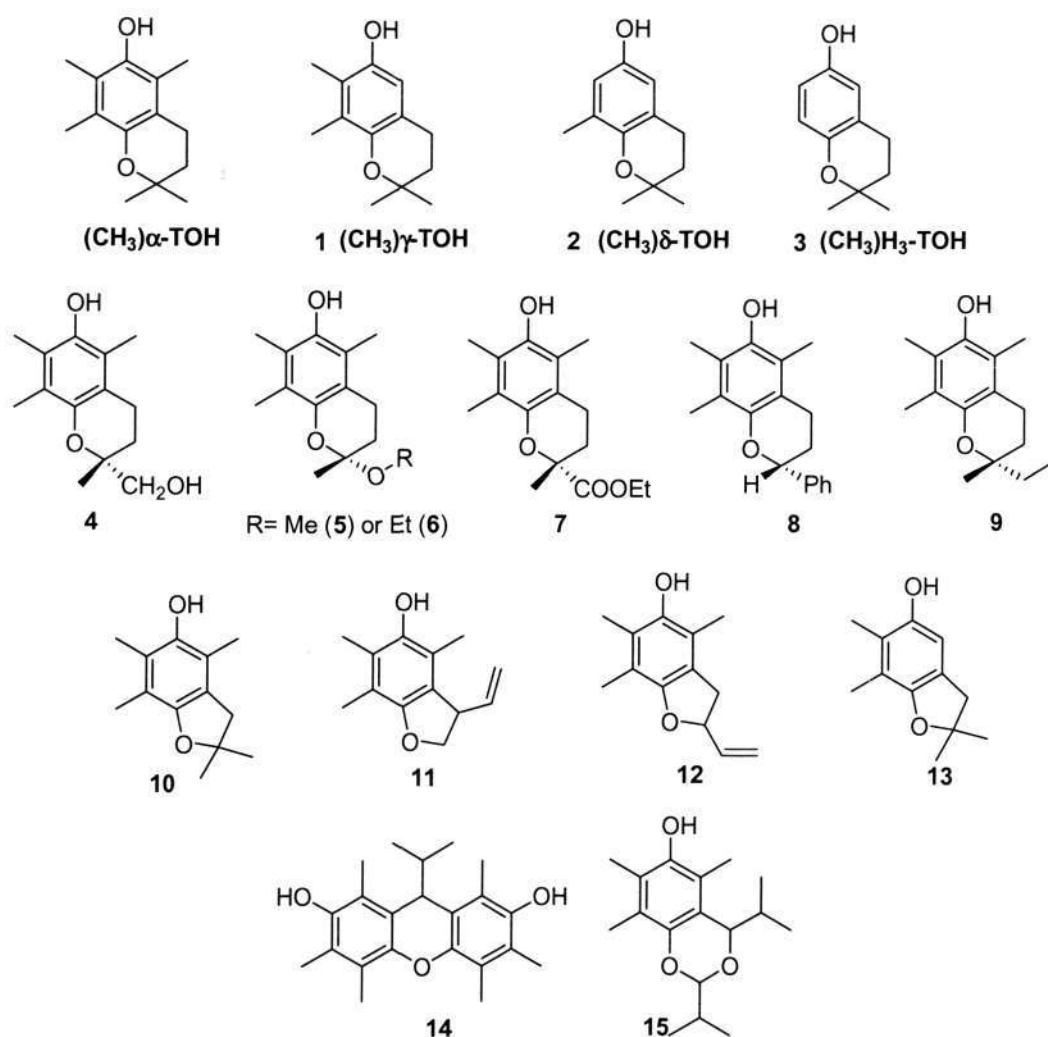


Figure 1.7. Synthesized compounds with structures similar to vitamin E.

CV experiments were firstly conducted on all the compounds in Figure 1.7, in order to make a general assessment about the lifetimes of their oxidized forms. The electrochemical results for the new compounds were interpreted based on the previous experiments performed on the tocopherols and the CVs are shown in Figure 1.8.¹³ The observation of a reverse reductive peak detected during CV experiments, within 0.3 - 0.4 V of the oxidation process, appears to be characteristic of the existence of phenoxonium cations, as observed for α -TOH and β -TOH at $\nu = 0.1 \text{ V s}^{-1}$ and γ -TOH and δ -TOH at $\nu = 10 \text{ V s}^{-1}$ ($\nu = \text{scan rate}$).^{14b} The wide separation between the forward and reverse peaks is similar to that observed during CV experiments on hydroquinones, such as dopamine (a two-electron and two-proton process) (Scheme 1.5).²⁶ However, phenols with one hydroxy group (and an ether group in the *para*-position) cannot form

quinones without breaking an oxygen-carbon bond, which decreases the likelihood of chemical reversibility on the CV timescale. Therefore, the detection of a reverse (reductive) peak during CV experiments on phenols that undergo two-electron oxidation (*and* only contain one hydroxy group), is a good evidence for the presence of persistent phenoxonium cations. The degree of chemical reversibility of the oxidation process can be estimated by the anodic (i_p^{ox}) to cathodic (i_p^{red}) peak current ratio (i_p^{ox}/i_p^{red}). For compounds where the oxidized forms are stable (within the time-scale of the CV), the i_p^{ox}/i_p^{red} -ratio approaches unity (although this relationship is complicated and strictly depends upon the equilibrium constant for the proton transfer reaction).¹³ Compounds **1** - **8** show only very small reverse cathodic peaks when the scan directions are reversed (at a scan rate of 100 mV s⁻¹), therefore, their i_p^{ox}/i_p^{red} -ratios are $\gg 1$, indicating that their associated phenoxonium cations are relatively short-lived and decompose or undergo further reaction before they can be reduced back to the starting material.

Compounds **1-8** all displayed a small cathodic peak at ~ -0.2 to -0.4 V vs. Fc/Fc⁺, which was at a potential that was considered to be too negative to be associated with the reduction of the phenoxonium cation back to the starting material. Multiple cyclic voltammograms indicated that this reductive process does not show a reverse oxidative peak when the scan direction is applied in the positive potential direction (*i.e.* when the CV is conducted over three scans), which means that the species responsible for the peak at -0.2 to -0.4 V vs. Fc/Fc⁺ is short-lived when reduced. Figure 1.9 and Figure 1.10 show cyclic voltammograms recorded at scan rates between 0.1 and 5 V s⁻¹ for compounds **4** and **7**, respectively. Figure 1.10 shows that the cathodic peak at ~ -0.2 to -0.4 V decreases when the scan rate is increased, concomitantly to another peak at +0.2 V becoming bigger. At a scan rate of 5 V s⁻¹, the CV of **7** has a very similar appearance to that observed for (CH₃) α -TOH at $\nu = 0.1$ V s⁻¹. The close similarity in the voltammetry obtained for (CH₃) α -TOH at $\nu = 0.1$ V s⁻¹ and compound **7** at $\nu = 5$ V s⁻¹ supports the presence of the phenoxonium cation of **7**, albeit with a lesser lifetime compared to (CH₃) α -TO⁺.

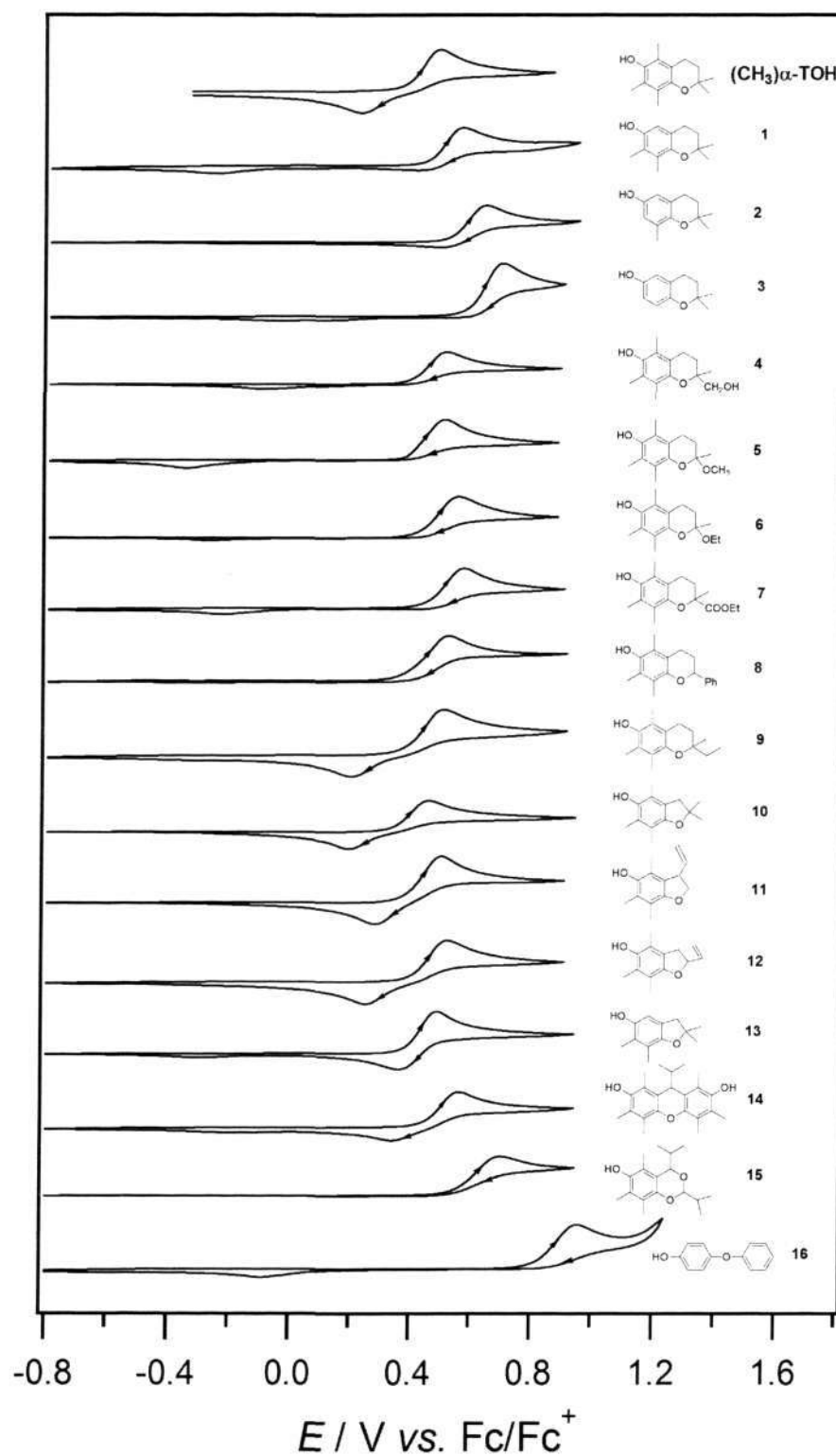


Figure 1.8. Cyclic voltammograms of 2.0 mM substrates in CH_3CN with 0.2 M $n\text{-Bu}_4\text{NPF}_6$ recorded at a 1 mm diameter Pt electrode at a scan rate of 0.1 V s^{-1} at $T = 293 \text{ K}$.

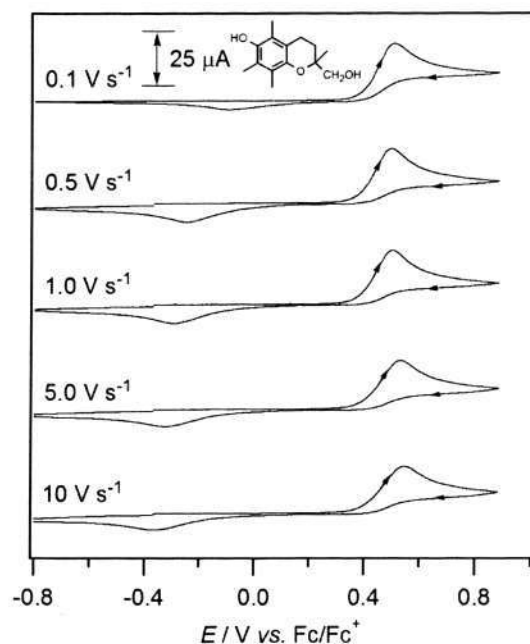


Figure 1.9. Cyclic voltammograms of $2.0 \text{ mM } \mathbf{4}$ in CH_3CN with $0.2 \text{ M } n\text{-Bu}_4\text{NPF}_6$ recorded at a 1 mm diameter Pt electrode at $T = 293 \text{ K}$. The current data were scaled by multiplying by $\nu^{-0.5}$ ($\nu = \text{scan rate} / \text{V s}^{-1}$).

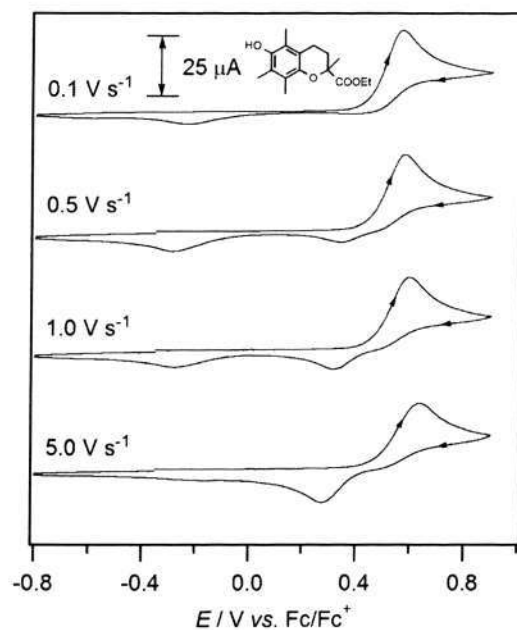


Figure 1.10. Cyclic voltammograms of $2.0 \text{ mM } \mathbf{7}$ in CH_3CN with $0.2 \text{ M } n\text{-Bu}_4\text{NPF}_6$ recorded at a 1 mm diameter Pt electrode at $T = 293 \text{ K}$. The current data were scaled by multiplying by $\nu^{-0.5}$ ($\nu = \text{scan rate} / \text{V s}^{-1}$).

Similar results to compound **7** were obtained for compounds **1** and **2** (the model compounds of γ -TOH and δ -TOH). At a scan rate of 10 V s^{-1} , the voltammograms of **1** and **2** appeared similar to that of $(\text{CH}_3)\alpha$ -TOH at a slow scan rate of 0.1 V s^{-1} . In contrast to compounds **1**, **2**, and **7**, no reductive peak at $+0.2 \text{ V}$ was observed for compounds **4-6** and **8** at a scan rate of 10 V s^{-1} , suggesting that their phenoxonium cations were short-lived (Figure 1.8). In fact, there was no evidence of chemical reversibility of the oxidation processes for compounds **4-6** and **8**, even at scan rates up to 200 V s^{-1} . Therefore, it can be concluded that the phenoxonium cations of **4-6** and **8** were shorter-lived than the phenoxonium cations of **1**, **2**, and **7**.

The voltammetry and peak shapes of the dihydrobenzofuran-5-ol substituted compounds containing a five-membered ring (compounds **10** - **13**) at a scan rate of 0.1 V s^{-1} were also examined and showed similar electrochemical behavior to that observed for $(\text{CH}_3)\alpha$ -TOH at the same scan rate, indicating that their phenoxonium cations were stable for at least several seconds (compound **10** reportedly has antioxidant properties that exceed those of α -TOH^{2a}). Compounds **11** and **12**, with hydrogen atom(s) bonded to the α -carbons adjacent to the ether oxygen also showed chemically reversible voltammetry, indicating that carbon atoms in positions equivalent to C₁₃ or C₁₄ (Figure 1.5) are not essential for the formation of long-lived phenoxonium cations. Compound **13**, with the least methyl groups (among compounds **10-13**) in the aromatic ring, displayed a smaller reverse reductive peak close to the oxidation process suggesting that its phenoxonium cation was less stable than the other dihydrobenzofuran-5-ol based compounds. Compound **14** displayed voltammetric behavior similar to $(\text{CH}_3)\alpha$ -TOH indicating the reversible formation of its phenoxonium ion, while **15** and **16** displayed chemically irreversible voltammetry indicating that their oxidized states were unstable. Compounds **15** and **16** showed no evidence for the formation of the phenoxonium cations at scan rates up to 200 V s^{-1} . (Compound **16** is included to illustrate the typical oxidative behavior of phenols, which generally display chemically irreversible cyclic voltammograms).

1.2.2. Electrolysis Experiments

CV experiments can provide useful information about oxidized or reduced species that have lifetimes on the time scale of less than a few seconds. In order to gain information about the

lifetime of the oxidized compounds over long time scales (minutes), controlled potential electrolysis (CPE) experiments were performed on these compounds and the reaction solutions monitored with CV. On the basis of their behavior under CPE conditions, these compounds can be divided into two classes. Class **1** systems were compounds where their associated phenoxonium cations were detectable during bulk electrolysis experiments indicating that they were stable for at least several minutes. Class **2** compounds were those where their phenoxonium cations were undetectable after electrolysis indicating that they were unstable or reactive. Both of these classes of compounds showed voltammetric evidence of an additional secondary oxidized compound (not the phenoxonium cation) that could be partly reduced back to the starting material under electrolysis conditions. It is difficult to provide accurate kinetic data for the stability of the cations since most were continually decaying during the time scale of the electrolysis. One factor that greatly decreases the lifetime of the cations is the presence of water. Ultra-dry conditions are difficult to achieve under CPE conditions because of the requirement of multi-compartment cells to separate the different electrodes. However, since the electrolysis experiments were all performed under identical conditions, the relative stabilities and subsequent division into Class **1** and Class **2** systems are valid.

1.2.2.1. Class 1 Compounds

All CPE experiments were performed at $-20\text{ }^{\circ}\text{C}$ in order to improve the stability of the phenoxonium cations, which are known to have longer lifetimes at lower temperatures (likely due to slowing down the reaction with trace water that is usually present in mM levels in organic solvents).¹³ Previous results proved that $(\text{CH}_3)\alpha\text{-TOH}$,^{14b,19,21} $\alpha\text{-TOH}$ ¹³ and $\beta\text{-TOH}$ ^{14b} are examples of Class 1 compounds.

Figures 1.11a, 1.12a, 1.13a, 1.14a and 1.15a are cyclic voltammograms recorded at a scan rate of 0.1 V s^{-1} with a 1.0 mm diameter Pt electrode of compounds $(\text{CH}_3)\alpha\text{-TOH}$, **9**, **10**, **12** and **14**, respectively. The black line is the CV of the compounds prior to the CPE, the red line is the CV obtained of the oxidized solution at the completion of the CPE at $+0.6\text{ V vs. Fc/Fc}^+$ (after the transfer of 2 electrons per molecule), and the dashed line is the CV obtained after the oxidized species had been reduced back to the starting material under CPE conditions at 0.0 V vs. Fc/Fc^+ .

Panels b and c in Figures 1.11 to 1.15 are the current (black line) and coulometry data (red line) (plotted as the number of electrons transferred per molecule) for the forward oxidation and reverse reduction processes respectively. The total experiment time was around 2100 s (35 minutes) excluding the time to run the CVs.

Figures 1.12 and 1.13 indicated that compounds **9** and **10** showed the most similar voltammetric results compared to (CH₃) α -TOH (Figure 1.11). There is only a small shift in potential between the first scan (solid black line) and the final scan (dashed line), and the i_p^{ox} -value recorded in the CV of the final product (dashed line) was approximately 80% of the initial i_p^{ox} -value in the CV recorded prior to the electrolysis (black line), indicating that ~20% of the phenoxonium cation was lost during the reaction, which is supported by the coulometry data which indicated the transfer of ~ 1.6 electrons for the reverse reduction reaction. For compound **9**, the residue after electrolysis was purified by silica gel column chromatography giving 70% starting material recovery. All compounds showed a small or big reductive peak at ~ -0.4 V after their exhaustive oxidative electrolysis, which was due to a secondary oxidation product.

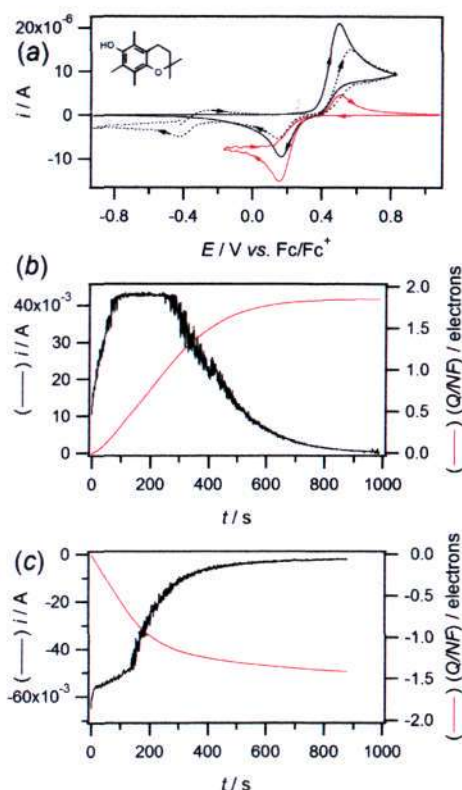


Figure 1.11. Voltammetric and coulometric data obtained at 253 K during the controlled potential electrolysis of 5 mM $(CH_3)\alpha$ -TOH in CH_3CN with 0.2 M Bu_4NPF_6 . (a) Cyclic voltammograms recorded at a scan rate of 0.1 V s^{-1} with a 1.0 mm diameter Pt electrode. (Black line) Prior to the bulk oxidation of $(CH_3)\alpha$ -TOH. (Red line) After the exhaustive oxidation of $(CH_3)\alpha$ -TOH. (Dashed line) After the exhaustive reduction of the oxidized product. (b) Current/coulometry vs. time data obtained during the exhaustive oxidation of $(CH_3)\alpha$ -TOH at $+0.7 \text{ V vs. Fc/Fc}^+$. (c) Current/coulometry vs. time data obtained during the reverse exhaustive reduction of the oxidized product at $0.0 \text{ V vs. Fc/Fc}^+$.

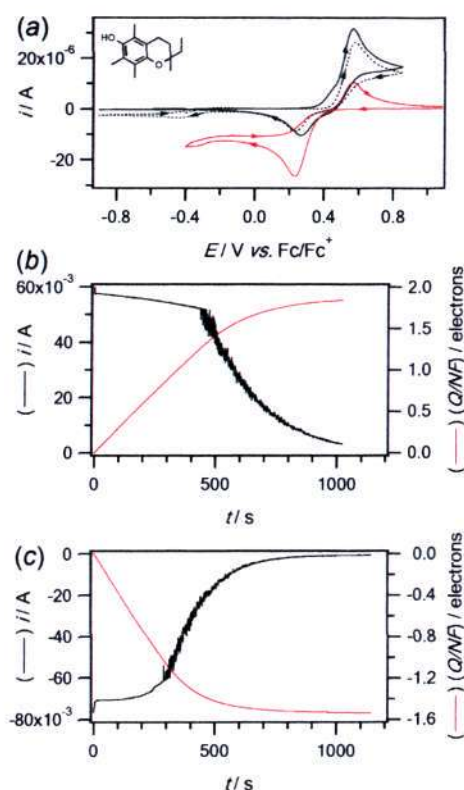


Figure 1.12. Voltammetric and coulometric data obtained at 253 K during the controlled potential electrolysis of 5 mM **9** in CH_3CN with 0.2 M Bu_4NPF_6 . (a) Cyclic voltammograms recorded at a scan rate of 0.1 V s^{-1} with a 1.0 mm diameter Pt electrode. (Black line) Prior to the bulk oxidation of **9**. (Red line) After the exhaustive oxidation of **9**. (Dashed line) After the exhaustive reduction of the oxidized product. (b) Current/coulometry vs. time data obtained during the exhaustive oxidation of **9** at $+0.7 \text{ V vs. Fc/Fc}^+$. (c) Current/coulometry vs. time data obtained during the reverse exhaustive reduction of the oxidized product at $0.0 \text{ V vs. Fc/Fc}^+$.

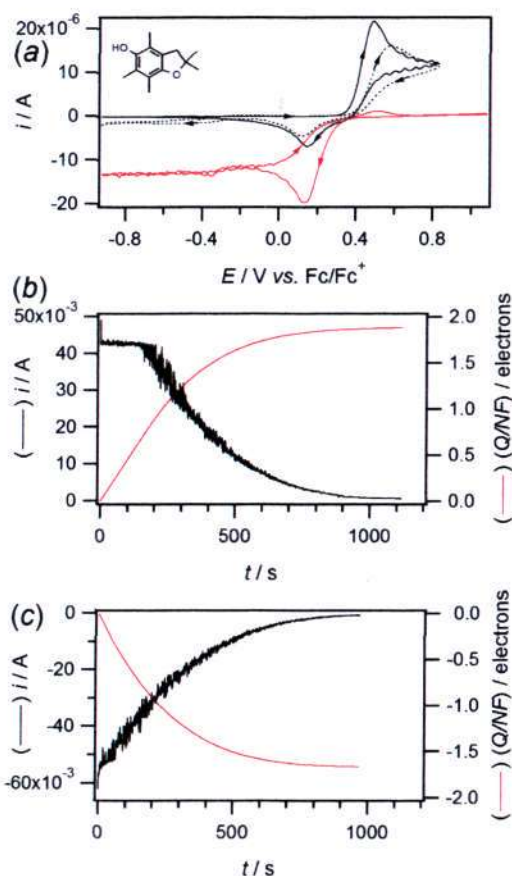


Figure 1.13. Voltammetric and coulometric data obtained at 253 K during the controlled potential electrolysis of 5 mM **10** in CH_3CN with 0.2 M Bu_4NPF_6 . (a) Cyclic voltammograms recorded at a scan rate of 0.1 V s^{-1} with a 1.0 mm diameter Pt electrode. (Black line) Prior to the bulk oxidation of **10**. (Red line) After the exhaustive oxidation of **10**. (Dashed line) After the exhaustive reduction of the oxidized product. (b) Current/coulometry vs. time data obtained during the exhaustive oxidation of **10** at +0.6 V vs. Fc/Fc^+ . (c) Current/coulometry vs. time data obtained during the reverse exhaustive reduction of the oxidized product at 0.0 V vs. Fc/Fc^+ .

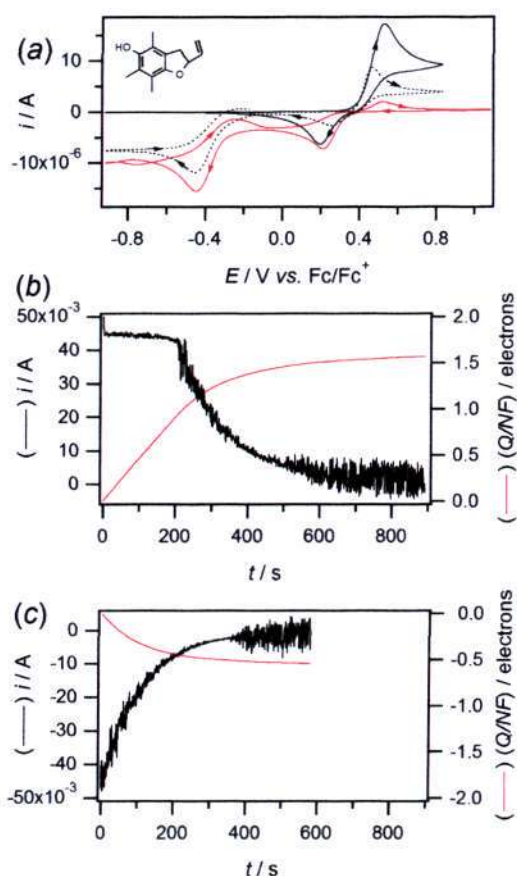


Figure 1.14. Voltammetric and coulometric data obtained at 253 K during the controlled potential electrolysis of 5 mM **12** in CH_3CN with 0.2 M Bu_4NPF_6 . (a) Cyclic voltammograms recorded at a scan rate of 0.1 V s^{-1} with a 1.0 mm diameter Pt electrode. (Black line) Prior to the bulk oxidation of **12**. (Red line) After the exhaustive oxidation of **12**. (Dashed line) After the exhaustive reduction of the oxidized product. (b) Current/coulometry vs. time data obtained during the exhaustive oxidation of **12** at +0.6 V vs. Fc/Fc^+ . (c) Current/coulometry vs. time data obtained during the reverse exhaustive reduction of the oxidized product at 0.0 V vs. Fc/Fc^+ .

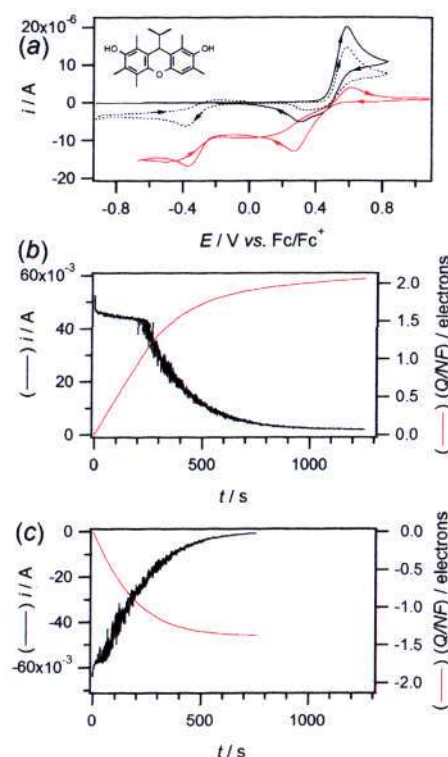


Figure 1.15. Voltammetric and coulometric data obtained at 253 K during the controlled potential electrolysis of 5 mM **14** in CH₃CN with 0.2 M Bu₄NPF₆. (a) Cyclic voltammograms recorded at a scan rate of 0.1 V s⁻¹ with a 1.0 mm diameter Pt electrode. (Black line) Prior to the bulk oxidation of **14**. (Red line) After the exhaustive oxidation of **14**. (Dashed line) After the exhaustive reduction of the oxidized product. (b) Current/coulometry vs. time data obtained during the exhaustive oxidation of **14** at +0.7 V vs. Fc/Fc⁺. (c) Current/coulometry vs. time data obtained during the reverse exhaustive reduction of the oxidized product at 0.0 V vs. Fc/Fc⁺.

1.2.2.2. Class 2 Compounds

Class 2 systems, only showed the peak at ~ -0.4 V at the completion of the electrolysis, and no phenoxonium cation peak could be observed at potentials close to +0.2 V vs. Fc/Fc⁺ (Figure 1.16 and 1.17). Compounds **6** (Figure 1.16) and **7** (Figure 1.17) are used as examples to clarify the electrochemical properties of class 2 compounds. When the oxidized solution was reduced under CPE conditions, CV experiments indicated that the starting material could be partly regenerated in $\sim 50\%$ yield (Figure 1.16a and 1.17a, dashed lines). Considering that the phenol is regenerated, the reaction product at -0.4 V vs. Fc/Fc⁺ cannot be too dissimilar from the starting material, thus a ring opened form is unlikely. Therefore, the species at -0.4 V

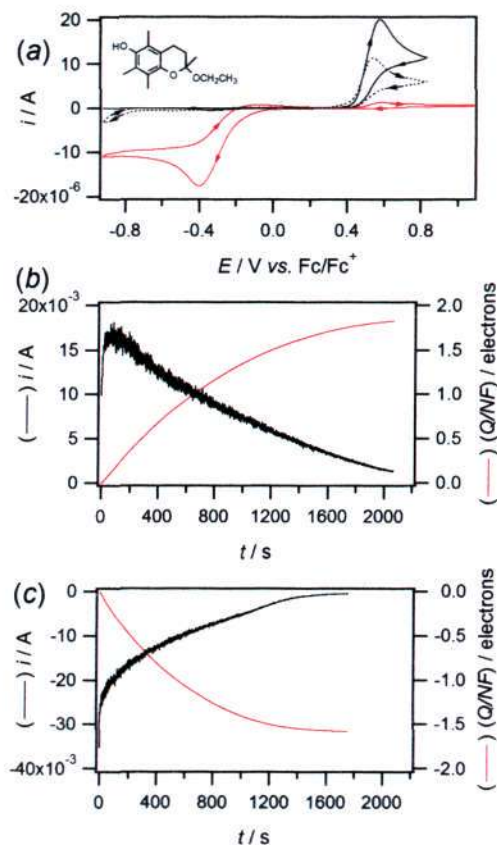


Figure 1.16. Voltammetric and coulometric data obtained at 253 K during the controlled potential electrolysis of 5 mM **6** in CH_3CN with 0.2 M Bu_4NPF_6 . (a) Cyclic voltammograms recorded at a scan rate of $0.1 V s^{-1}$ with a 1.0 mm diameter Pt electrode. (Black line) Prior to the bulk oxidation of **6**. (Red line) After the exhaustive oxidation of **6**. (Dashed line) After the exhaustive reduction of the oxidized product. (b) Current/coulometry vs. time data obtained during the exhaustive oxidation of **6** at +0.8 V vs. Fc/Fc^+ . (c) Current/coulometry vs. time data obtained during the reverse exhaustive reduction of the oxidized product at -0.5 V vs. Fc/Fc^+ .

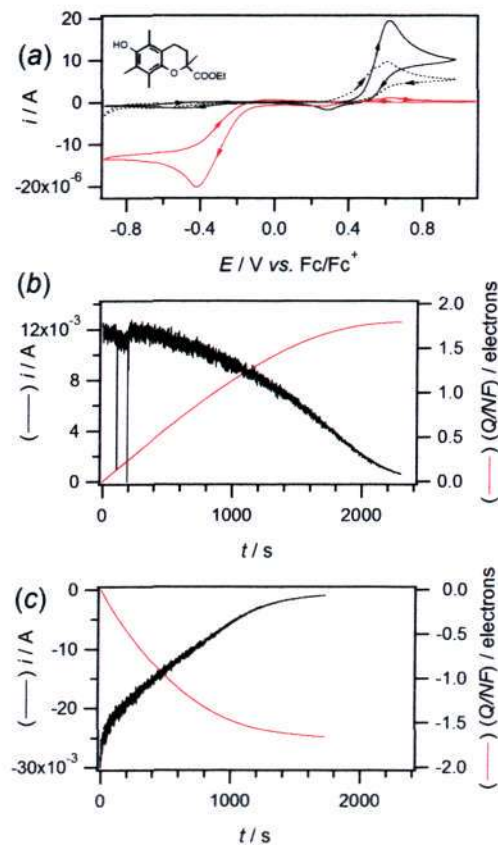
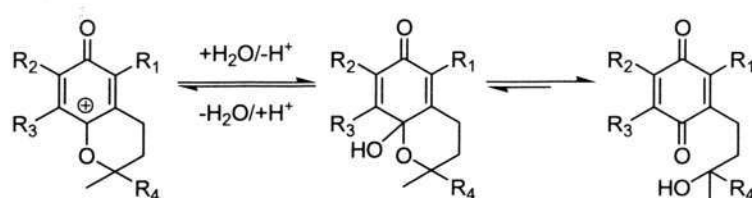


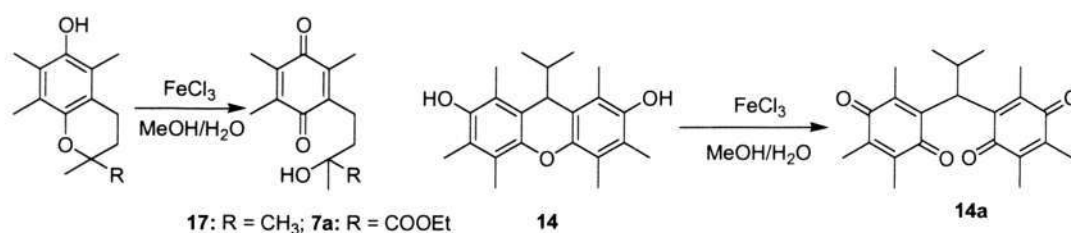
Figure 1.17. Voltammetric and coulometric data obtained at 253 K during the controlled potential electrolysis of 5 mM **7** in CH_3CN with 0.2 M Bu_4NPF_6 . (a) Cyclic voltammograms recorded at a scan rate of $0.1 V s^{-1}$ with a 1.0 mm diameter Pt electrode. (Black line) Prior to the bulk oxidation of **7**. (Red line) After the exhaustive oxidation of **7**. (Dashed line) After the exhaustive reduction of the oxidized product. (b) Current/coulometry vs. time data obtained during the exhaustive oxidation of **7** at +0.8 V vs. Fc/Fc^+ . (c) Current/coulometry vs. time data obtained during the reverse exhaustive reduction of the oxidized product at -0.5 V vs. Fc/Fc^+ .

vs. Fc/Fc^+ have been assigned as the hemiketal chromenol, which are known oxidation products of tocopherols that subsequently convert into the ring opened *para*-quinones (Scheme 1.6).^{27a-c}



Scheme 1.6. Conversion of phenoxonium cation into hemiketals (chromenols) and further conversion into *para*-quinones.

In order to study the long term oxidation products of the class 2 compounds, chemical oxidation experiments using FeCl_3 as the oxidant were conducted on compounds $(\text{CH}_3)_\alpha\text{-TOH}$, **7**, and **14**, which resulted in the formation of the quinone compounds (Scheme 1.7). Figure 1.18 shows the CVs of the different quinones which display a chemically reversible one-electron reduction process at approximately -1.2 V vs. Fc/Fc^+ .



Scheme 1.7. FeCl_3 -catalyzed oxidative reactions of some vitamin E analogues.

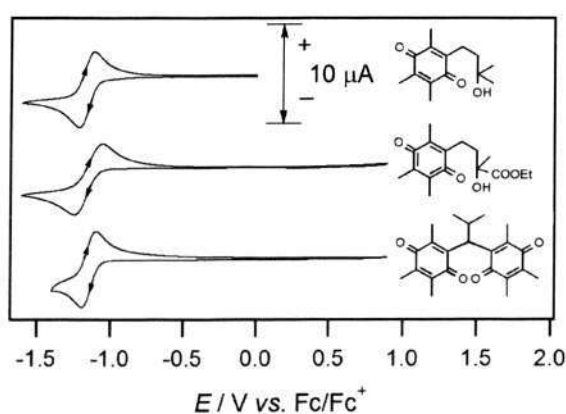


Figure 1.18. Cyclic voltammograms of 2.0 mM substrates CH_3CN with 0.2 M $n\text{-Bu}_4\text{NPF}_6$ recorded at a 1 mm diameter Pt electrode, at $T = 293\text{ K}$ and at a scan rate of 0.1 V s^{-1} .

CPE results for compounds **1-16** (except **8**) were summarized in Table 1.1.

Table 1.1. Calculated number of electrons transferred per molecule (*n*-values) obtained during the controlled potential oxidation of phenols, and in some cases the reverse reduction of their associated phenoxonium cations.

Compound	<i>n</i> -value ^a (oxidation) ^b	<i>n</i> -value ^a (reduction) ^c	Class ^d
(CH ₃) α -TOH	1.9	-1.5	1
1	1.9	<i>e</i>	2
2	1.9	<i>e</i>	2
3	2.1	<i>e</i>	2
4	1.9	<i>e</i>	2
5	1.8	<i>e</i>	2
6	1.8	<i>e</i>	2
7	1.8	<i>e</i>	2
9	1.8	-1.6	1
10	1.9	-1.7	1
11	1.9	-1.2	1
12	1.6	-0.5	1
13	2.5	-0.3	1
14	2.1	-1.4	1
15	1.9	<i>e</i>	2
16	2.2	<i>e</i>	2

^aCalculated from coulometry data using the equation $n = Q/NF$ where Q is the charge passed (coulombs), N is the number of mols and F is the Faraday constant (96485 C mol⁻¹). ^bApplied potential is +0.1 V past oxidation peak potential (E_p^{ox}) of the phenol (see Figure 3.8). ^cApplied potential is -0.1 V past reduction potential of the phenoxonium cation (see Figure 3.8). ^dClass 1 systems are where the phenoxonium cations are voltammetrically detectable for several minutes, and Class 2 systems are where the phenoxonium cations cannot be detected after electrolysis (lifetimes < a few seconds). ^eNot measurable under present conditions.

Based on the knowledge of the identity and voltammetry of the final quinones that form during the oxidation of the phenols (Scheme 1.7), that voltammetry observed during the controlled potential electrolysis of compound **7** was further analyzed (Figure 1.19). At the completion of the CPE of **7**, CV led to the detection of a small reductive peak at -1.0 V vs Fc/Fc⁺

that has been assigned to the *p*-quinone (**7a**) [red line in Figure 1.19(ii)]. Although the hemiketal product in the CVs at -0.4 V vs Fc/Fc⁺ is stable at 253 K for several hours, it quickly reacts further to form a species with a reduction potential peak close to -0.1 V (*p*-quinone structure of **7a**) [Figure 1.19(iii)] when the solution is warmed to 293 K. The voltammetric peak shape of the *p*-quinone is different when it is present in a pure solution of CH₃CN [Figure 1.19(i)], which may be the result of the presence of liberated acid during the oxidation process. When a standard sample of **7a** is added to the solution, the peak at -1.0 V increases in size, supporting the assignment of the *para*-quinone in partial yield [Figure 1.19(iv)]. It is likely that other oxidation products also form at room temperature because the long-term oxidation products of phenols are usually complicated with one product seldom formed in 100% yield.^{27,28}

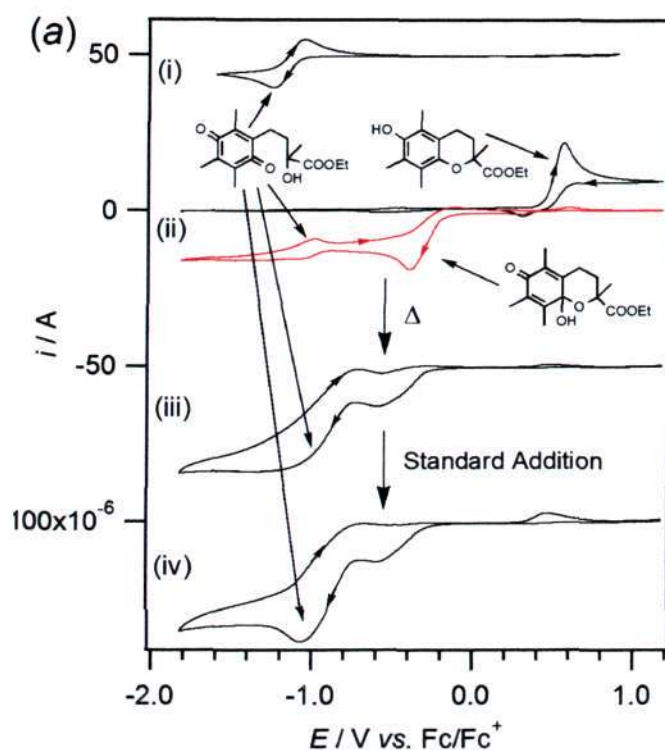


Figure 1.19. Voltammetric and coulometric data obtained in CH₃CN with 0.2 M Bu₄NPF₆. (a) Cyclic voltammograms recorded at a scan rate of 0.1 V s⁻¹ with a 1.0 mm diameter Pt electrode. (i) 2 mM of **7a** at 293 K. (ii) (Black line) Prior to the bulk oxidation of 5 mM **7** at 253 K (Red line) After the exhaustive oxidation of 5 mM **7** at 253 K. (iii) After the electrolyzed solution of **7** had warmed to 293 K. (iv) After **7a** was added to the oxidized solution of **7** at 293 K. (b) Current/coulometry vs. time data obtained during the exhaustive oxidation of **7** at 0.8 V vs. Fc/Fc⁺.

In previous studies, spiro-dimers have been identified as a common product formed *via* chemical oxidation of α -tocopherol.^{27d,27e,29} α -Tocopherol is thought to be initially oxidized to the phenoxyl radical, which further reacts to form the *ortho*-quinone methide, which subsequently undergoes a bimolecular reaction to form the spiro-dimer.^{27d} However, it is unlikely that the species detected at -0.4 V vs. Fc/Fc^+ could be a complicated product such as a dimer, because the CPE experiments indicate that the reaction is at least partially chemically reversible, while the formation of a spiro-dimer is a chemically irreversible process under the mild conditions used in this study.

On the basis of the above discussion, we note that the oxidation reaction of class 2 compounds occurs in two steps under electrolysis conditions: initial one-electron oxidation (and one-proton loss) to form the phenoxyl radical, followed by further one-electron oxidation to form the phenoxonium cation. In comparison with class 1 compounds, the phenoxonium cations of class 2 compounds are more reactive, and are easily attacked by nucleophiles present in the solvent, therefore, the formation of hemiketals *via* the reaction with low levels of water is consistent with the present data (green line in Figure 1.20). The hemiketals can be stable for several hours at lower temperature (such as 253 K), but it will be further converted to related *p*-quinone *via* ring-opening reactions at room temperature (blue line in Figure 1.20).

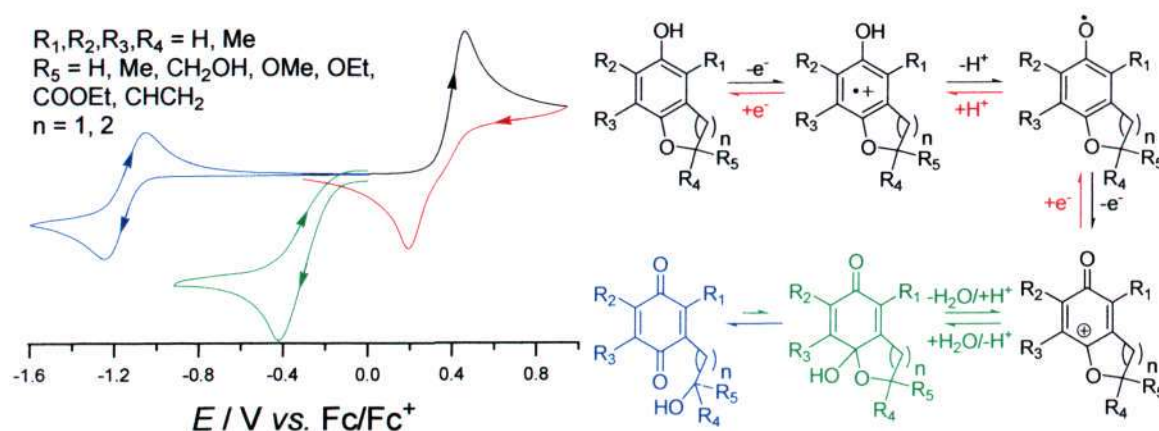


Figure 1.20. The electrochemical mechanism for class 1 and 2 compounds.

1.3. Conclusions

A number of phenols with structures similar to $(\text{CH}_3)\alpha\text{-TOH}$ were synthesized and electrochemical experiments (CV and CPE) were performed in order to determine the relative lifetime of the phenoxonium cations of the oxidized compounds. Both chroman-6-ol and dihydrobenzofuran-5-ol substituted compounds are able to form detectable phenoxonium cations upon oxidation in CH_3CN , several with lifetimes of at least a few seconds. In general, the lifetime of the phenoxonium cations increases with increasing methylation of the aromatic ring, which can be rationalized by improved steric shielding from nucleophilic attack (of trace water), and by the electron donating ability of the methyl groups aiding in stabilizing the increased positive charge.

Previously, results from ^{13}C NMR experiments and data from theoretical calculations indicated that the positive charge in the phenoxonium cation of $\alpha\text{-TOH}$ ($\alpha\text{-TO}^+$) was, surprisingly, mainly located on the quaternary carbon in the chromanol ring, with lesser delocalization into the aromatic ring.¹⁹ Therefore, it would be expected that the properties of the group bonded to quaternary carbon would have a pronounced affect on the lifetimes of the phenoxonium cations. Thus it was found that for the chroman-6-ol compounds with fully methylated aromatic rings and methyl groups in position 2a [$(\text{CH}_3)\alpha\text{-TOH}$, **4-6** and **8**], that the lifetime of their phenoxonium cations followed the order $\text{Me} \gg \text{CH}_2\text{OH} \approx \text{COOEt} \gg \text{OMe} \approx \text{OEt}$ for the groups in position 1' (Figure 1.1). CV and controlled potential electrolysis experiments indicated that the phenoxonium cations of compounds **9-14** were stable at least several minutes in CH_3CN at -20°C . No obvious voltammetric peak for the reduction of the phenoxonium cation peak was observed at potentials 0.3-0.4 V for compounds **1-8**, **15**, and **16**, indicating that the associated phenoxonium cations were relatively short-lived (half lives < 1 s). The presence of a carbon atom or heteroatom in positions 1' or 2a (Figure 1.1) is not a prerequisite for the stability of the phenoxonium cations. It was found that compounds **11** and **12** with hydrogen atom(s) bound to position 2a formed persistent phenoxonium cations upon electrochemical oxidation. Furthermore, compound **10**, containing a 5-membered ring, formed a phenoxonium cation upon oxidation whose lifetime in solution was as high as the 6-membered naturally occurring analogue $\alpha\text{-TO}^+$.

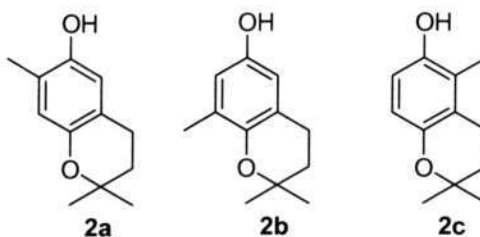
1.4. Experimental Section

Literature methods were used to prepare compounds **1-15**, **7a**, **14a**, and **17**. Other compounds and reagents were obtained from commercial sources.

General procedure for synthesis of 1, 2(a-c) and 3: Substituted hydroquinone (2 mmol) and *p*-toluenesulfonic acid (TsOH) were added to a two-necked flask, and dry toluene was added under argon. After stirring for five minutes, 2-methyl-but-3-en-2-ol (1.1 equiv) was injected dropwise into the flask by syringe. Then, it was stirred for 18 h at 100 °C. After cooling, ethyl acetate was added to dilute the solution, and the organic layer was washed with sodium bicarbonate and water, and dried with Na₂SO₄. After the solvent was removed, the residue was separated by column chromatography (hexane:ethyl acetate = 10:1).

Compound 1: 157 mg; 0.76 mmol; Yield: 38%. ¹H NMR (CDCl₃, 400 MHz): δ 6.38 (s, 1H), 4.37 (s, 1H), 2.69 (t, 2H, *J* = 6.8 Hz), 2.14 (s, 3H), 2.11 (s, 3H), 1.74 (t, 2H, *J* = 6.8 Hz), 1.30 (s, 6H); ¹³C {¹H} NMR (CDCl₃, 100 MHz): δ 162.3 (C_{aromatic}), 146.3 (C_{aromatic}), 125.8, 121.6, 118.1, 112.2, 73.4 (OCCH₃), 32.9 (CH₂), 27.0 (CH₃), 22.6 (Ar-CH₂), 14.1(Ar-CH₃), 11.9 (Ar-CH₃).

Compound 2: the mixtures of three isomers



Compound 3: 117 mg; 0.66 mmol; Yield: 33%. ¹H NMR (CDCl₃, 400 MHz): δ 6.66–6.55 (m, 3H), 4.88 (s, 1H), 2.71(t, 2H, *J* = 6.8 Hz), 1.78 (t, 2H, *J* = 6.8 Hz), δ 1.31 (s, 6H); ¹³C {¹H} NMR (CDCl₃, 100 MHz): δ 148.6 (COH), 147.9, 121.8, 117.8, 115.4, 114.5, 73.9 (OCCH₃), 32.8 (CH₂), 26.7 (CH₃), 22.6 (Ar-CH₂).

Compound 4: A similar method was used as reported in the literature.³⁰ Ethyl 6-hydroxy-2,5,7,8-tetramethyl-3,4-dihydro-2H-chromene-2-carboxylate (439 mg, 1.6 mmol) was dissolved in dried THF, then added dropwise to a THF solution of LiAlH₄ (182 mg, 4.8 mmol) in an ice

bath. After it was warmed to room temperature, the mixture was refluxed for 3 h. TLC showed that there was no starting material remaining. An aqueous solution of sodium hydroxide was added dropwise. After filtration, THF was removed, and ether was used to extract organic layer. Then, it was dried by sodium sulfate. After filtration and concentration, a white solid was obtained (350 mg, 1.48 mmol, 92%). ^1H NMR (CDCl_3 , 400 MHz): δ 4.46 (s, 1H), 3.65-3.61 (m, 2H), 2.68 (br, 2H), 2.17-1.97 (m, 10H), 1.75-1.72 (m, 1H), 1.23 (s, 3H); ^{13}C $\{^1\text{H}\}$ NMR (CDCl_3 , 100 MHz): δ 145.1, 144.9, 122.6, 121.4, 118.8, 117.3, 75.1 (OCCH_3), 69.4 (CH_2OH), 27.9 (CH_2), 20.4, 20.3, 12.2 (Ar-CH_3), 11.9 (Ar-CH_3), 11.3 (Ar-CH_3).

Compound 5:³¹ Trimethyl-hydroquinone (304.4 mg, 2 mmol) was added to a round-bottomed flask, and MeOH (10 mL) was injected under argon. After methyl vinyl ketone (0.32 mL, 2 mmol) was added, conc. sulfuric acid (2 drops) was injected quickly. The solution was stirred for five minutes and trimethyl orthoformate (0.33 mL, 3 mmol) was added. After workup, a white solid product was obtained (302 mg, 1.28 mmol, 64%). ^1H NMR (CDCl_3 , 400 MHz): δ 4.24 (s, 1H), 3.24 (s, 3H), 2.77-2.73 (m, 1H), 2.62-2.57 (m, 1H), 2.19-2.14 (m, 1H), 2.19 (s, 6H), 2.14 (s, 3H), 1.57 (s, 3H); ^{13}C $\{^1\text{H}\}$ NMR (CDCl_3 , 100 MHz): δ 145.4, 143.7, 122.3, 120.9, 118.6, 118.5, 97.2 (OCCH_3), 48.9 (OCH_3), 31.9 (CH_2), 23.1, 20.0, 12.2 (Ar-CH_3), 11.6 (Ar-CH_3), 11.2 (Ar-CH_3).

Compound 6:³² Trimethylhydroquinone (304.4 mg, 2 mmol) was added to a round-bottomed flask, and MeOH (10 mL) was injected under argon. After methyl vinyl ketone (0.32 mL, 2 mmol) was added, conc. sulfuric acid (2 drops) was injected quickly. The reaction was stirred for five minutes and triethyl orthoformate (0.50 mL, 3 mmol) was added. The solution was stirred for 48 h at room temperature. After the solvent was removed, ethyl acetate and water were added. The organic layer was washed with sodium dicarbonate and brine, then dried with Na_2SO_4 . The residue was purified by chromatography (hexane: ether = 5:1) to give the white solid product (276 mg, 1.10 mmol, 55%). ^1H NMR (CDCl_3 , 300 MHz): δ 4.21 (s, 1H), 3.62-3.58 (m, 1H), 3.45-3.41 (m, 1H), 2.78-2.72 (m, 1H), 2.59-2.56 (m, 1H), 2.17-2.11 (m, 10H), 1.79-1.77 (m, 1H), 1.54 (s, 3H), 1.00 (t, 3H, $J = 7.1$ Hz); ^{13}C $\{^1\text{H}\}$ NMR (CDCl_3 , 100 MHz): δ 145.2, 144.0, 122.1, 120.6,

118.6, 118.3, 97.2 (OCCH₃), 56.5 (OCH₂), 32.1 (CH₂), 24.0, 20.0, 15.6, 12.2 (Ar-CH₃), 11.7 (Ar-CH₃), 11.3 (Ar-CH₃).

Compound 7:³⁰ 6-Hydroxy-2,5,7,8-tetramethylchroman-2-carboxylic acid **15** (500 mg, 2 mmol) was dissolved in absolute ethanol (5 mL). Then, conc. sulfuric acid (0.15 mL) was added, and the mixture was refluxed for 5 h. After that, the solvent was removed, and the organic layer was extracted from the mixture of ether and water. The ether layer was washed with sodium bicarbonate and brine, then, dried by sodium sulfate. After filtration, the solution was concentrated to give a white product (542 mg, 1.95 mmol, 97 %). ¹H NMR (CDCl₃, 400 MHz): δ 4.14-4.09 (m, 2H), 2.67-2.40 (m, 3H), 2.19 (s, 3H), 2.16 (s, 3H), 2.06 (s, 3H), 1.91-1.83 (m, 1H), 1.60 (s, 3H), 1.18 (t, 3H, $J = 7.1$ Hz); ¹³C {¹H} NMR (CDCl₃, 100 MHz): δ 173.9 (C_{carbonyl}), 145.7, 145.3, 122.6, 121.2, 118.4, 117.0, 76.9 (OCCH₃), 61.0 (OCH₂), 30.6 (CH₂), 25.3, 21.0, 14.1, 12.2 (Ar-CH₃), 11.8 (Ar-CH₃), 11.2 (Ar-CH₃).

Compound 8: Similar method was used as preparing compound **1** (460 mg, 1.72 mmol, 86%). ¹H NMR (CDCl₃, 400 MHz): δ 7.46-7.29 (m, 5H), 4.96-4.94 (m, 1H), 4.26 (s, 1H), 2.85-2.70 (m, 2H), 2.30-2.25 (m, 1H), 2.20 (s, 3H), 2.19 (s, 3H), 2.13 (s, 3H), 2.06-1.97 (m, 1H); ¹³C {¹H} NMR (CDCl₃, 100 MHz): δ 147.0, 145.2, 142.5, 128.4, 127.5, 125.8, 122.6, 121.1, 118.7, 118.0, 74.6 (OCH), 30.5 (CH₂), 20.3 (Ar-CH₂), 12.2 (Ar-CH₃), 11.9 (Ar-CH₃), 11.3 (Ar-CH₃).

Compound 9: Similar method was used as preparing compound **1** (346 mg, 1.48 mmol, 74%). ¹H NMR (CDCl₃, 400 MHz): δ 4.20 (s, 1H), 2.69 (t, 2H, $J = 6.4$ Hz), 2.17 (s, 3H), 2.12 (s, 6H), 1.82-1.77 (m, 2H), 1.68-1.53 (m, 2H), 1.23 (s, 3H), 0.96 (m, 3H); ¹³C {¹H} NMR (CDCl₃, 100 MHz): δ 145.5, 144.6, 122.7, 121.1, 118.5, 117.4, 74.6 (OCCH₃), 31.9, 31.3, 23.2, 20.8, 12.2 (Ar-CH₃), 11.8 (Ar-CH₃), 11.3 (CH₃), 8.0 (CH₂CH₃).

A literature method was used to synthesize compound **10**.⁵ **Compound 10:** ¹H NMR (CDCl₃, 300 MHz): δ 4.13 (s, 1H), 2.91 (s, 2H), 2.13 (s, 3H), 2.10 (s, 6H), 1.45 (s, 6H).

A literature method was used to synthesize compounds **11** and **12**.³³ Substituted hydroquinone (2 mmol), (Z)-2-butene-1,4-diol (8 mmol) and *p*-toluenesulfonic acid (TsOH, 0.4 mmol) were added to two-necked flask, and dry toluene was added under argon. Then, it was stirred for 16 h at 70 °C. After cooling, ethyl acetate was added to dilute the solution, and the

organic layer was washed with sodium bicarbonate and water, and dried with Na_2SO_4 . After the solvent was removed, the residue was filtered through a short column. Then, the mixture was crystallized from n-hexane to give compound **12**. The residue was concentrated and recrystallized to yield product **11**.

Compound 11: ^1H NMR (CDCl_3 , 400 MHz): δ 5.92-5.83 (m, 1H), 5.12-5.07 (m, 2H), 4.57 (t, 1H, $J = 8.8$ Hz), 4.28-4.25 (m, 1H), 4.20 (s, 1H), 4.04-3.98 (m, 1H), 2.15 (s, 3H), 2.13 (s, 6H); ^{13}C $\{^1\text{H}\}$ NMR (CDCl_3 , 100 MHz): δ 151.9, 145.9, 138.5, 124.3, 122.3, 118.1, 116.1, 115.5, 75.9 (OCH_2), 47.1 (Ar-CH), 12.14 (Ar- CH_3), 12.09 (Ar- CH_3), 12.00 (Ar- CH_3).

Compound 12: ^1H NMR (CDCl_3 , 400 MHz): δ 6.07-5.98 (m, 1H), 5.37 (d, 1H, $J = 17.1$ Hz), 5.20 (d, 1H, $J = 10.3$ Hz), 5.16-5.10 (m, 1H), 4.18 (s, 1H), 3.32-3.26 (m, 1H), 2.93-2.87 (m, 1H), 2.14-2.13 (m, 9H); ^{13}C $\{^1\text{H}\}$ NMR (CDCl_3 , 100 MHz): δ 151.3, 145.7, 138.0, 122.5, 121.5, 117.2, 116.2, 115.8, 82.6 (OCH), 35.9 (Ar- CH_2), 12.9 (Ar- CH_3), 12.2 (Ar- CH_3), 12.0 (Ar- CH_3).

A literature method was used to synthesize compound **13**.³⁴ 2,3-dimethylhydroquinone (1g, 7.2 mmol), 2-methylallyl alcohol (7.2 mmol) were added to a two-necked flask, and anhydride formic acid (40 mL) and two drops of conc. H_2SO_4 were added. Then, it was stirred for 16 h at 100 °C. After cooling, the dark solution was poured onto crushed ice and the solution was extracted with ether. ethyl acetate was added to dilute the solution. The organic layer was washed with sodium bicarbonate and water, and dried with Na_2SO_4 . After the solvent was removed, the residue was dissolved in MeOH (20 mL), and conc. HCl (0.2 mL) was added. The solution was heated to reflux for 15 min. After the solvent was removed, the residue was treated with ether/hexane. After filtration and evaporation, the dark solid was recrystallized from hexane to give a tan colored product. The ^1H NMR spectrum matches that reported. ^1H NMR (CDCl_3 , 300 MHz): δ 6.51 (s, 1H), 4.32 (s, 1H), 2.96 (s, 2H), 2.13 (s, 6H), 1.45 (s, 6H).

A literature method was used to synthesize compounds **14** and **15**.³⁵ Trimethylhydroquinone (2 mmol) and *p*-toluenesulfonic acid (TsOH) were added to a two-necked flask, and dry toluene was added under argon. After stirring for five minutes, 2-methyl-but-3-en-2-ol (1.1 equiv) was injected dropwise into the flask by syringe. Then, it was stirred for 16 h at 80 °C. After cooling, ethyl acetate was added to dilute the solution, and the organic layer was washed with sodium

bicarbonate and water, and dried with Na_2SO_4 . After the solvent was removed, the residue was separated by column chromatography (hexane:ethyl acetate = 10:1).

Compound 14: ^1H NMR (CDCl_3 , 300 MHz): δ 4.36 (s, 2H), 4.05 (d, 2H, $J = 7.1$ Hz), 2.35 (s, 6H), 2.28 (s, 6H), 2.20 (s, 6H), 1.88-1.85 (m, 1H), 0.78 (d, 6H, $J = 6.8$ Hz).

Compound 15: ^1H NMR (CDCl_3 , 300 MHz): δ 4.99 (d, 1H, $J = 1.4$ Hz), 4.44 (d, 1H, $J = 4.8$ Hz), 4.27 (s, 1H), 2.16 (s, 3H), 2.12 (s, 3H), 2.07 (s, 3H), 2.07-1.97 (m, 2H), 1.14 (d, 3H, $J = 6.9$ Hz), 1.05 (t, 6H, $J = 7.5$ Hz), 0.60 (d, 3H, $J = 6.7$ Hz).

Compound 7a:^{27c} $\text{FeCl}_3 \cdot 6\text{H}_2\text{O}$ (762 mg, 2.8 mmol) was added to a solution of ethyl 6-hydroxy-2,5,7,8-tetramethyl-3,4-dihydro-2H-chromene-2-carboxylate (150 mg, 0.68 mmol) in methanol/water/diethyl ether (40 mL, v/v/v = 19: 1: 20) cooled in an ice bath, and the mixture was stirred for 2 h. After that, water (20 mL) was added and the mixture was extracted with ether. The organic layer was washed with water and brine, then dried over sodium sulfate. The residue was separated by column chromatography (hexane:ethyl acetate = 10:1) to give a yellow oil product (125 mg, 76%). ^1H NMR (CDCl_3 , 400 MHz): δ 4.33-4.23 (m, 2H), 3.31 (s, 1H), 2.65-2.58 (m, 1H), 2.43-2.35 (m, 1H), 2.02 (s, 3H), 2.00 (s, 6H), 1.88-1.81 (m, 1H), 1.74-1.67 (m, 1H), 1.42 (s, 3H), 1.34 (t, 3H, $J = 7.1$ Hz); ^{13}C NMR (CDCl_3 , 100 MHz): δ 187.6 (CO *p*-quinone), 186.9 (CO *p*-quinone), 176.9 (CO), 143.4, 140.6, 140.5, 140.4, 74.1 (COH), 62.1 (OCH_2CH_3), 38.3 (CH_2), 26.0, 21.1, 14.2, 12.3 (Ar- CH_3), 12.2 (Ar- CH_3), 11.9 (Ar- CH_3). HRMS calcd. for $\text{C}_{16}\text{H}_{22}\text{O}_5$: 294.15. Found 294.15.

Compound 14a: A literature method was used to synthesize compound **14a**.³⁵ FeCl_3 (1.7 g, 10.5 mmol) was added to a stirred solution of compound **14** (170 mg, 0.50 mmol) in MeOH (15 mL) and water (2 mL), and the resulting mixture was stirred at rt for 2 h. After filtration, the yellow solid was recrystallized from MeOH to afford the pure product in 85% yield (150 mg, 0.42 mmol). ^1H NMR (CDCl_3 , 400 MHz): δ 2.58-2.54 (d, 1H, $J = 11.2$ Hz), 3.05-2.96 (m, 1H), 2.30 (s, 6H), 1.99 (s, 6H), 1.98 (s, 6H), 0.92 (d, 6H, $J = 6.4$ Hz).

Compound 17:^{27c} $\text{FeCl}_3 \cdot 6\text{H}_2\text{O}$ (930 mg, 3.4 mmol) was added to a solution of 6-hydroxy-2,2,5,7,8-pentamethylchroman (150 mg, 0.68 mmol) in methanol/water/diethyl ether (40 mL, v/v/v = 19: 1: 20) cooled in an ice bath, and the mixture was stirred for 2 h. After that, water (20

mL) was added and the mixture was extracted with ether. The organic layer was washed with water and brine, dried over sodium sulfate. The residue was separated by column chromatography (hexane:ether = 3:7) to give yellow oil (150 mg, 93%). ^1H NMR (CDCl_3 , 400 MHz): δ 2.58-2.54 (m, 2H), 2.03 (s, 3H), 2.00 (s, 6H), 1.69 (s, 1H), 1.53-1.50 (m, 2H), 1.28 (s, 6H); ^{13}C NMR (CDCl_3 , 100 MHz): δ 187.7 (CO), 187.3 (CO), 144.3, 140.6, 140.4, 140.3, 70.8 (OCCH_3), 42.1 (CH_2), 29.1 (OCCH_3), 21.6 (CH_2), 12.4, 12.3, 12.0.

1.5. References

1. Evans, H. M.; Bishop, K. S. *Science* **1922**, 56, 650.
2. (a) Burton, G. W.; Ingold, K. U. *Acc. Chem. Res.* **1986**, 19, 194. (b) Finkel, T.; Holbrook, N. J. *Nature* **2000**, 408, 239. (c) Wang, X.; Quinn, P. J. *Mol. Membr. Biol.* **2000**, 17, 143. (d) Niki, E.; Noguchi, N. *Acc. Chem. Res.* **2004**, 37, 45. (e) Traber, M. G.; Atkinson, J. *Free Radic. Biol. Med.* **2007**, 43, 4.
3. (a) Cerecetto, A.; López, G. V. *Mini-reviews in Medicinal Chemistry* **2007**, 7, 315, and references therein. (b) Shanks, D.; Frisell, H.; Ottosson, H.; Engman, L. *Org. Biomol. Chem.* **2006**, 4, 846.
4. Leopoldini, M.; Marino, T.; Russo, N.; Toscano, M. *J. Phys. Chem. A* **2004**, 108, 4916.
5. Burton, G. W.; Doba, T.; Gabe, E. J.; Hughes, L.; Lee, F. L.; Prasad, L.; Ingold, K. U. *J. Am. Chem. Soc.* **1985**, 107, 7053.
6. Nagaoka, S.; Inoue, M.; Nishioka, C.; Nishioku, Y.; Tsunoda, S.; Ohguchi, C.; Ohara, K.; Mukai, K. *J. Phys. Chem. B* **2000**, 104, 856.
7. (a) Ricciarelli, R.; Zingg J-M.; Azzi, A. *Biol. Chem.* **2002**, 383, 457. (b) Zingg, J-M.; Azzi, A. *Curr. Med. Chem.* **2004**, 11, 1113. (c) Monroe, E. B.; Jurchen, J. C.; Lee, J.; Rubakhin, S. S.; Sweedler, J. V. *J. Am. Chem. Soc.* **2005**, 127, 12152. (d) Azzi, A.; Stocker, A. *Progress in Lipid Research* **2000**, 39, 231. (e) Brigelius-Flohé, R. *Free Radic. Biol. Med.* **2009**, 46, 543.
8. (a) Azzi, A. *Eur. J. Nutr.* **2004**, 43, 18. (b) Azzi, A. *Free Radic. Biol. Med.* **2007**, 43, 16.
9. Svanholm, U.; Bechgaard, K.; Parker, V. D. *J. Am. Chem. Soc.* **1974**, 96, 2409.
10. Tsuchiya, J.; Niki, E.; Kamiya, Y. *Bull. Chem. Soc. Jpn.* **1983**, 56, 229.
11. Lehtovuori, P.; Joela, H. *Phys. Chem. Chem. Phys.* **2002**, 4, 1928.
12. Pryor, W. A.; Cornicelli, J. A.; Devall, L. J.; Tait, B.; Trivedi, B. K.; Witiak, D. T.; Wu, M. *J. Org. Chem.* **1993**, 58, 3521.
13. Webster, R. D. *Acc. Chem. Res.* **2007**, 40, 251, and reference therein.
14. (a) Williams, L. L.; Webster, R. D. *J. Am. Chem. Soc.* **2004**, 126, 12441. (b) Wilson, G. J.; Lin, C. Y.; Webster, R. D. *J. Phys. Chem. B* **2006**, 110, 11540.

15. (a) Hammerich, O.; Svensmark, B. In *Organic Electrochemistry*, 3rd ed.; Lund, H., Baizer, M. M., Eds.; Marcel Dekker: New York, **1991**; Chapter 16. (b) Rieker, A.; Beisswenger, R.; Regier, K. *Tetrahedron* **1991**, *47*, 645. (c) Eickhoff, H.; Jung, G.; Rieker, A. *Tetrahedron* **2001**, *57*, 353.
16. Dimroth, K.; Umbach, W.; Thomas, H. *Chem. Ber.* **1967**, *100*, 132.
17. (a) Speiser, B.; Rieker, A. *J. Chem. Res. (S)*, **1977**, 314. (b) Speiser, B.; Rieker, A. *J. Electroanal. Chem.* **1979**, *102*, 373. (c) Speiser, B.; Rieker, A. *J. Electroanal. Chem.* **1980**, *110*, 231.
18. Vigalok, A.; Rybtchinski, B.; Gozin, Y.; Koblenz, T. S.; Ben-David, Y.; Rozenberg, H.; Milstein, D. *J. Am. Chem. Soc.* **2003**, *125*, 15692.
19. Lee, S. B.; Lin, C. Y.; Gill, P. M. W.; Webster, R. D. *J. Org. Chem.* **2005**, *70*, 10466.
20. (a) Reed, C. A.; Kim, K.-C.; Bolskar, R. D.; Mueller, L. J. *Science* **2000**, *289*, 101. (b) Camire, N.; Nafady, A.; Geiger, W. E. *J. Am. Chem. Soc.* **2002**, *124*, 7620. (c) Krossing, I.; Raabe, I. *Angew. Chem. Int. Ed.* **2004**, *43*, 2066.
21. Lee, S. B.; Willis, A. C.; Webster, R. D. *J. Am. Chem. Soc.* **2006**, *128*, 9332.
22. Mayer, H.; Schudel, P.; Rüegg, R.; Isler, O. *Helv. Chim. Acta.* **1963**, *46*, 650.
23. (a) Mizuguchi, E.; Achiwa, K. *Tetrahedron Asymmetry* **1993**, *4*, 2303. (b) Hasegawa, A.; Ishiwa, K.; Yamamoto, H. *Angew. Chem. Int. Ed.* **2003**, *42*, 5731.
24. (a) Rhile, I. J. and Mayer, J. M. *J. Am. Chem. Soc.* **2004**, *126*, 12718. (b) Costentin, C.; Robert, M.; Savéant, J. M. *J. Am. Chem. Soc.* **2006**, *128*, 4552. (c) Rhile, I. J.; Markle, T. F.; Nagao, H.; DiPasquale, A. G.; Lam, O. P.; Lockwood, M. A.; Rotter, K.; Mayer, J. M. *J. Am. Chem. Soc.* **2006**, *128*, 6075.
25. (a) Hammerich, O.; Parker, V. D.; Ronlán, A. *Acta. Chem. Scand. B* **1976**, *30*, 89. (b) Hammerich, O.; Parker, V. D. *Acta. Chem. Scand. B* **1982**, *36*, 63.
26. (a) Hawley, M. D.; Tatawawadi, S. V.; Pierkarski, S. Adams, R. N. *J. Am. Chem. Soc.* **1967**, *89*, 447. (b) Sternson, A. W.; McCreery, R.; Feinberg, B.; Adams, R. N. *J. Electroanal. Chem.* **1973**, *46*, 313.
27. (a) Dürckheimer, W.; Cohen, L. A. *J. Am. Chem. Soc.* **1964**, *86*, 4388. (b) Marcus, M. F.; Hawley, M. D. *J. Org. Chem.* **1970**, *35*, 2185. (c) Patel, A.; Netscher, T.; Gille, L.; Mereiter, K.; Rosenau, T. *Tetrahedron*, **2007**, *63*, 5312. (d) Rosenau, T.; Klosner, E.; Gille,

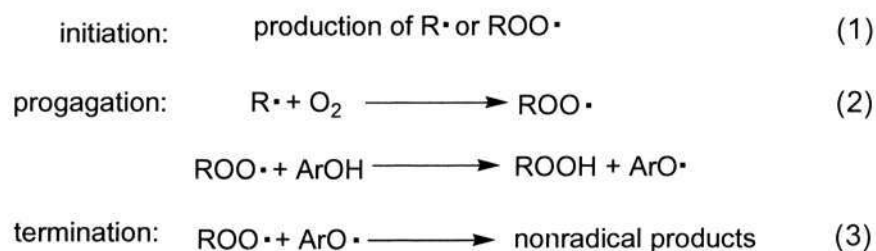
- L.; Mazzini, F.; Netscher, T. *J. Org. Chem.* **2007**, 72, 3268. (e) Bowry, V. W.; Ingold, K. U. *J. Org. Chem.* **1995**, 60, 5456.
28. Parkhurst, R. M.; Skinner, W. A. Chromans and Tocopherols. In *Chemistry of Heterocyclic Compounds*; Ellis, G. P., Lockhart, I. M., Eds.; Wiley: New York, **1981**; Vol. 36, Chapter 3.
29. Rosenau, T.; Potthast, A.; Elder, T.; Kosma, P. *Org. Lett.* **2002**, 4, 4285.
30. Ramachandran, U.; Mital, A.; Bharatam, P. V.; Khanna, S.; Rao, P. R.; Srinivasan, K.; Kumar, R.; Chawla, H. P. S.; Kaul, C. L.; Raichurd S.; Chakrabarti R. *Bioorganic and Medicinal Chemistry* **2004**, 12, 655.
31. Cohen, N.; Schaer, B.; Saucy, G.; Borer, R.; Todaro, R.; Chiu, A. M. *J. Org. Chem.* **1989**, 54, 3282, and references cited therein.
32. Cossy, J.; Rakotoarisoa, H.; Kahn, P.; Desmurs, J.-R. *Tetrahedron Lett.* **2000**, 41, 7203, and references cited therein.
33. Novák, L.; Kovács, P.; Kolonits, P.; Szántay, C. *Heterocycles* **1994**, 38, 177.
34. Lars, J.; Nilsson, G.; Selander, H.; Sievertsson, H.; Skånberg, I. *Tetrahedron* **1970**, 26, 879.
35. Novák, L.; Kovács, P.; Pirok, G.; Kolonits, P.; Szabó, E.; Fekete, J.; Weiszfeiler, V.; Szántay, C. *Synthesis*, **1995**, 693.

CHAPTER 2

Long-Lived Radical Cations as Model Compounds for One-Electron Oxidation Product of Vitamin E

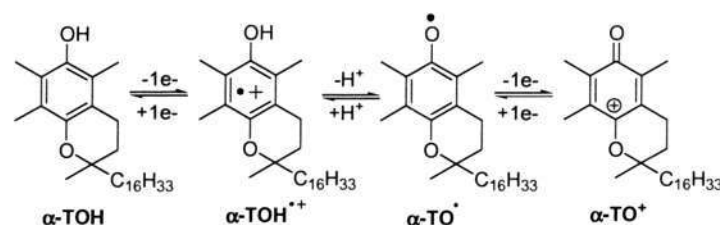
2.1. Introduction

The antioxidant properties of phenolic compounds like vitamin E have been extensively studied. The mechanism can be described by Scheme 2.1, comprising three main steps: radical initiation, propagation, and termination.¹ Highly reactive free radicals such as superoxide ($\text{O}_2^{\bullet-}$), hydroxyl (HO^\bullet), and peroxy (ROO^\bullet) are known to be produced easily in living organisms, and the reactions they undergo are thought to contribute significantly to the aging process.² Vitamin E ($\alpha\text{-TOH}$) and its neutral free radical ($\alpha\text{-TO}^\bullet$) can act as important chain-breaking antioxidants to suppress these free radicals, although other methods have also been developed on how to scavenge free radicals.³ However, the importance of the radical cation ($\alpha\text{-TOH}^{+\bullet}$), which can form through one-electron oxidation of vitamin E by a reactive free radical, in the biological chemistry of vitamin E is presently less known,⁴ although it is potentially an interesting intermediate compound because it is relatively nonacidic (in non-aqueous media) compared to most other phenolic radical cations.⁵ Therefore, $\alpha\text{-TOH}^{+\bullet}$ could potentially be long-lived in a low dielectric constant lipid bilayer environment.



Scheme 2.1. The proposed mechanism for antioxidation of phenolic compounds.

It has been demonstrated that vitamin E and its analogues can be electrochemically oxidized to form surprisingly long-lived phenoxonium cations *via* a series of electron-transfer and proton transfer reactions (see Chapter one).⁶ For vitamin E, initial one-electron oxidation gives rise to the radical cation ($\alpha\text{-TOH}^{+\bullet}$), followed by a proton loss from the hydroxyl group to form the free radical $\alpha\text{-TO}^\bullet$, which is further oxidized to form $\alpha\text{-TO}^+$ (Scheme 2.2). In the present work, a series of model compounds without the hydroxyl groups have been prepared from the reaction between substituted hydroquinones and allyl alcohol (Figure 2.1, **1a**, **2a**, and **3a**). Among them, compound **1a** was obtained as one isomer while compounds **2a** and **3a** contain a mixture of two isomers. The isomers were not separated, so the experimental results were obtained from mixtures of isomers of compounds **2a** and **3a**. It was envisaged that the replacement of the hydrogen atom in vitamin E with a symmetrical ether linkage in compounds **1a-3a** would change the electrochemical response from a two-electron oxidation to a one-electron process, providing that the formed radical cations were long-lived. It was also of interest to determine the difference in potentials between the protic phenolic structure of vitamin E and the aprotic ring closed analogues (**1-3** in Figure 2.1).



Scheme 2.2. The electrochemical oxidation mechanism for α -tocopherol in CH_3CN .

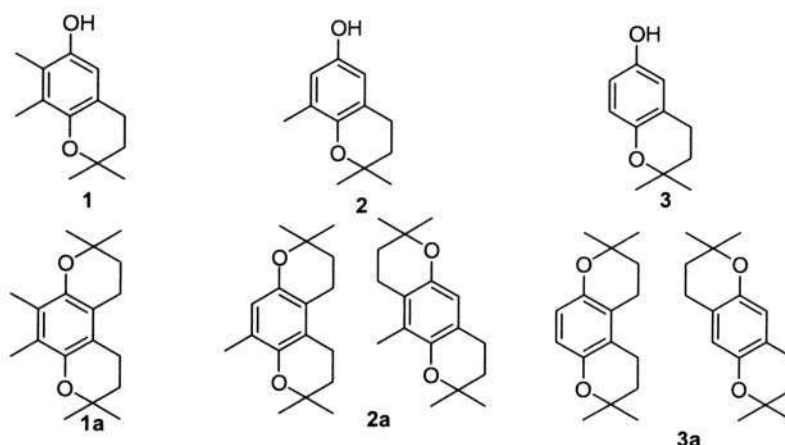


Figure 2.1. Some model compounds of vitamin E.

2.2. Experimental Results

2.2.1. Cyclic Voltammetry

Figure 2.2 shows cyclic voltammograms of compounds **1a** – **3a** recorded at a scan rate of 100 mV s⁻¹ in CH₃CN solutions, along with the α -tocopherol model compound, (CH₃) α -TOH, where the phytol tail is replaced with a methyl group. The voltammograms in Figure 2.2 indicate that the anodic (i_p^{ox}) and cathodic (i_p^{red}) peak currents for (CH₃) α -TOH are larger than those observed for compounds **1a** – **3a**, at equivalent concentrations and scan rates. The larger i_p^{ox} -value observed for (CH₃) α -TOH is due to the transfer of a greater number of electrons, with the oxidation occurring by two electrons (two one-electron steps) and a proton loss to form the phenoxonium cation α -TO⁺ (Scheme 2.2). Compounds **1a** – **3a** with the aprotic cyclic ether in place of the protic phenol are unable to lose a hydroxyl proton; therefore they undergo a one-electron oxidation, with no a follow-up chemical reaction apparent on the time-scale of the CV experiment.

The anodic (E_p^{ox}) to cathodic (E_p^{red}) peak separation (ΔE_{pp}) is much larger for (CH₃) α -TOH ($\Delta E_{\text{pp}} \approx 260$ mV) compared to compounds **1a** – **3a** ($\Delta E_{\text{pp}} \approx 70$ mV) because of the presence of the proton transfer and multiple electron transfer steps (an ECE mechanism) for (CH₃) α -TOH. The $E_{1/2}^{\text{f}}$ values [$E_{1/2}^{\text{f}} = (E_p^{\text{ox}} + E_p^{\text{red}}) / 2$] for compounds **1a** – **3a** were calculated to be +0.440, +0.520, and +0.605 V vs. Fc/Fc⁺ respectively (reported to the nearest 5 mV). The $E_{1/2}^{\text{f}}$ -values for compounds **1a** – **3a** are a good approximation to the formal potentials (E^0) because the oxidation mechanism involves a simple chemically reversible one-electron transfer. For (CH₃) α -TOH, the $E_{1/2}^{\text{f}}$ -value is not a good approximation for the formal one-electron oxidation potential because of the additional electron and proton transfer steps. Instead the formal one-electron oxidation potential for (CH₃) α -TOH in CH₃CN with Bu₄NPF₆ as the supporting electrolyte was previously estimated by digital simulation techniques⁷ to be $+0.50 \pm 0.05$ V vs. Fc/Fc⁺ at 293 K.^{6g} It would be expected that **1a**, rather than **2a** or **3a** should be closest in potential to (CH₃) α -TOH, because it is most closely related in structure (containing a fully methylated aromatic ring). Therefore, the $E_{1/2}^{\text{f}}$

of **1a** obtained by voltammetric simulations may be closer to the lower estimated potential (+0.45 V vs. Fc/Fc⁺).^{6g}

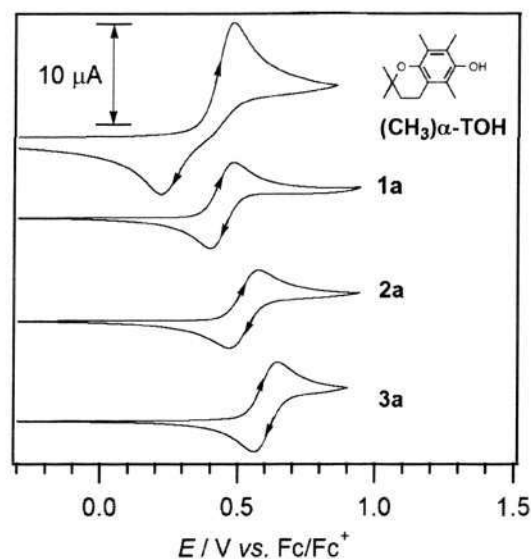


Figure 2.2. Cyclic voltammograms of 2.0 mM compounds in CH₃CN with 0.2 M *n*-Bu₄NPF₆ recorded at a 1 mm diameter Pt electrode at *T* = 293 K.

It can be concluded that the formal one-electron oxidation potential of α-TOH is very close (within 0.1 V) of that observed for compounds **1a** – **3a**, and therefore, that the presence of the phenolic group does not strongly influence the formal one-electron oxidation potential of the chromanol. There is a shift to more negative potentials with decreasing methylation of the aromatic ring for compounds **1a** – **3a**. The shift in potential can be accounted for by the electron donating ability of the methyl groups, which provides evidence that the molecular orbital involved in the one-electron oxidation is located within the aromatic and heterocyclic portions of the molecule. The observation of only one oxidation process for isomers **2a** and **3a** indicates that the *E*_F⁰-values for the isomers are very close to each other. Digital simulation experiments indicate that one-electron processes that are electrochemically and chemically reversible on the CV timescale are indistinguishable if they are within approximately 30 mV of each other.⁷

2.2.2. Controlled Potential Electrolysis (CPE)

In order to gain information about the lifetime of the radical compounds over longer time scales and to confirm the number of electrons transferred in the oxidation process, CPE and

coulometry were conducted on compounds **1a** – **3a**. Figure 2.3(a) shows CV data obtained before (black line) and after (red line) the exhaustive electrolysis of **1a**. Figures 2.3(b) and 2.3(c) show the corresponding current/coulometry vs. time data obtained during the oxidation of **1a** and reduction of **1a⁺**, respectively. The data in Figure 2.3 illustrate that **1a** is oxidized quantitatively in a one electron process to **1a⁺** and that **1a⁺** can be quantitatively reduced back to **1a**. It was found that **1a⁺** is very long-lived in CH₃CN solution, surviving for at least several weeks, and can be isolated as a solid compound *via* chemical oxidation with the one-electron oxidant NO⁺(SbF₆[−]).

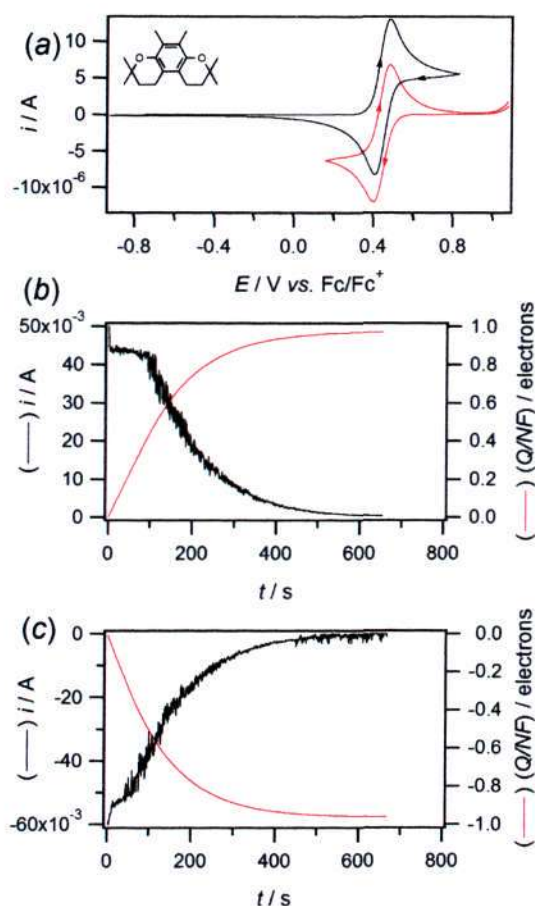


Figure 2.3. Voltammetric and coulometric data obtained at 293 K during the controlled potential electrolysis of 5 mM **1a** in CH₃CN with 0.2 M Bu₄NPF₆. (a) Cyclic voltammograms recorded at a scan rate of 0.1 V s^{−1} with a 1.0 mm diameter Pt electrode. (Black line) Prior to the bulk oxidation of **1a**. (Red line) After the exhaustive oxidation of **1a**. (b) Current/coulometry vs. time data obtained during the exhaustive oxidation of **1a** at 0.6 V vs. Fc/Fc⁺. (c) Current/coulometry vs. time data obtained during the reverse exhaustive reduction of **1a⁺** at 0.2 V vs. Fc/Fc⁺.

In contrast to **1a⁺**, compounds **2a⁺** and **3a⁺** survived for a shorter time under electrolysis conditions and a greater number of electrons were transferred ($n \approx 1.5$ electrons per molecule).

Figure 2.4 shows CV data obtained before (black line) and after (red line) the exhaustive oxidation of **2a**. In this case an additional reduction process is evident at the completion of the electrolysis at -0.4 V vs. Fc/Fc^+ , which is due to the formation of a further reaction product of $\mathbf{2a}^{++}$. The process at -0.4 V remains when $\mathbf{2a}^{++}$ is reduced back to **2a**. The CV data obtained during the electrolysis of **3a** were very similar, with an additional product detected at -0.4 V vs. Fc/Fc^+ at the completion of the electrolysis. Nevertheless, both $\mathbf{2a}^{++}$ and $\mathbf{3a}^{++}$ were able to be detected voltammetrically at the end of the electrolysis, indicating that their half-lives were several minutes in CH_3CN .

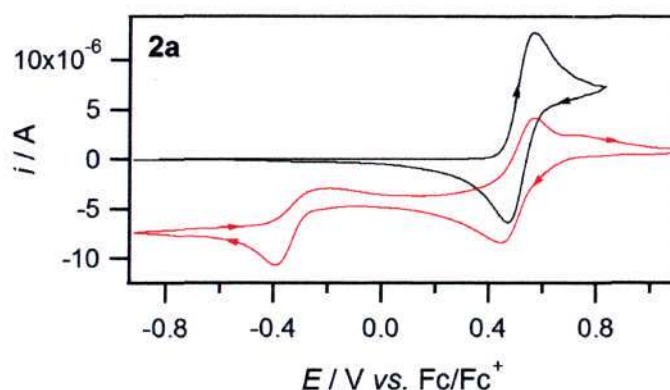


Figure 2.4. Cyclic voltammograms recorded at a scan rate of 0.1 V s^{-1} with a 1.0 mm diameter Pt electrode at 293 K during the controlled potential electrolysis of 5 mM **2a** in CH_3CN with 0.2 M Bu_4NPF_6 . (Black line) Prior to the bulk oxidation of **2a**. (Red line) After the exhaustive oxidation of **2a**.

2.2.3. UV-vis Spectroscopy

In situ electrochemical-UV-vis-NIR experiments were conducted in an optically semi-transparent thin layer electrochemical cell on compounds **1a** – **3a**, with the spectra for $\mathbf{1a}/\mathbf{1a}^{++}$ given in Figure 2.5(a). The starting material showed one band between $200 - 3300 \text{ nm}$ at $\sim 300 \text{ nm}$, while the oxidized compound $\mathbf{1a}^{++}$, displayed a more intense absorbance at 313 nm and an additional band at 482 nm (with a shoulder at 456 nm). No absorbances were detected in the NIR region for **1a** or $\mathbf{1a}^{++}$. The thin-layer operation of the cell meant that exhaustive electrolysis occurred within 2 minutes, therefore, spectra were also obtained for $\mathbf{2a}^{++}$ and $\mathbf{3a}^{++}$ (without any appreciable signs of additional reaction products) that were very similar in appearance to $\mathbf{1a}^{++}$.

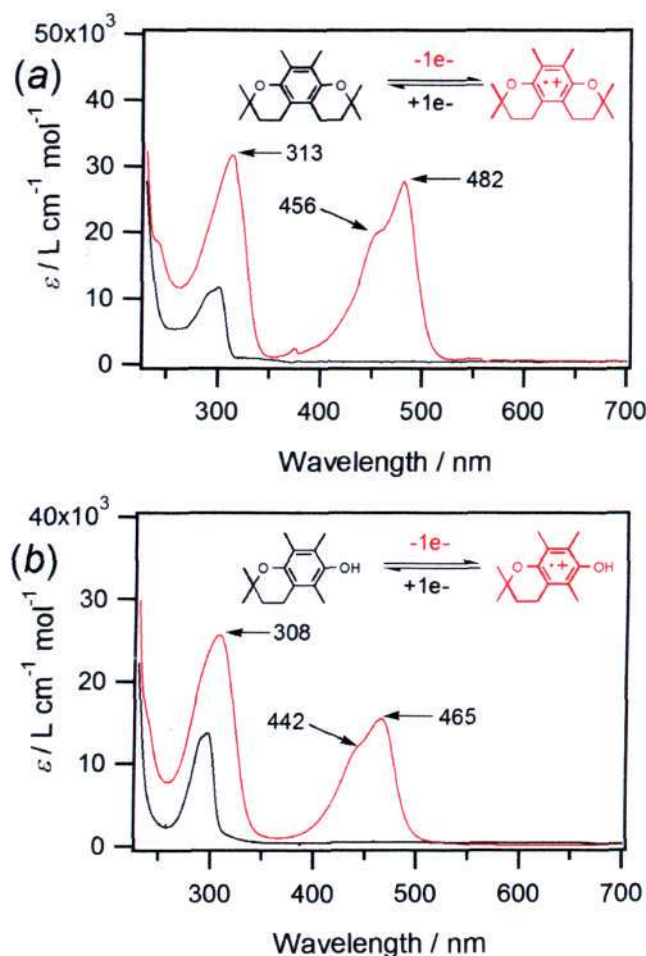


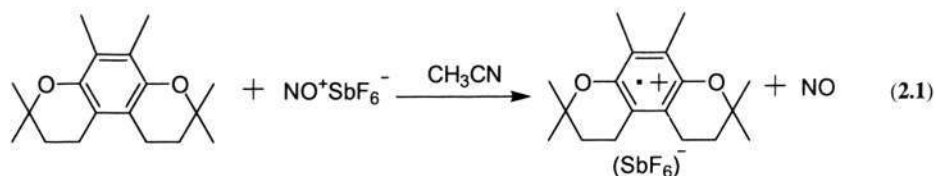
Figure 2.5. *In situ* electrochemical-UV-vis spectra. (a) Obtained during the electrolysis of 0.2 mM **1a** in CH₃CN at 293 K with 0.5 M Bu₄NPF₆. (Black line) **1a**. (Red line) **1a**⁺. (b) Obtained in CH₂Cl₂ containing 0.5 M Bu₄NPF₆ and 1 M CF₃COOH at 253 K during the sequential one-electron oxidation of 1 mM α-TOH. (Black line) α-TOH. (Red line) α-TOH⁺. Data in (b) were modified from reference 6c.

Figure 2.5(b) showed the UV-vis spectrum of $[(\text{CH}_3)\alpha\text{-TOH}]^{++}$ that was obtained by oxidizing $[(\text{CH}_3)\alpha\text{-TOH}]$ in an organic solvent containing a very strong acid, thereby preventing the deprotonation of the phenol.^{6d} The UV-vis spectrum of $[(\text{CH}_3)\alpha\text{-TOH}]^{++}$ is very similar to the spectrum of $1a^{++}$, which provides good evidence that the electronic transitions observed in the UV-vis spectrum of $[(\text{CH}_3)\alpha\text{-TOH}]^{++}$ are independent of the hydroxyl group (Figure 2.5).

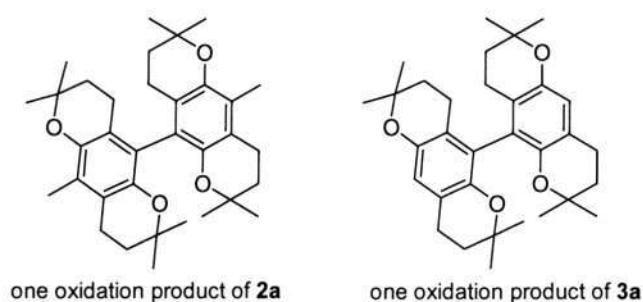
2.2.4. Chemical Oxidation Experiments

Compounds **1a** – **3a** were reacted chemically with equivalent molar amounts of NOSbF_6 in CH_3CN at 20 ± 2 °C. The one-electron chemical oxidation of **1a** produced **1a⁺** quantitatively that

survived in solution for at least several weeks. Removal of the solvent under vacuum allowed the isolation of a solid sample of $\mathbf{1a}^{++}(\text{SbF}_6^-)$ (the byproduct, $\text{NO}^\bullet(\text{g})$, is easily removed with the solvent) (eq 2.1).



In contrast to the simple oxidation of $\mathbf{1a}$, the one-electron oxidation of $\mathbf{2a}$ and $\mathbf{3a}$ led to the formation of a range of reaction products. Two products that were identified by NMR (^1H and ^{13}C) and high resolution mass spectrometry (HRMS) experiments in 20 – 25 % yield from the chemical oxidations of $\mathbf{2a}$ and $\mathbf{3a}$ were the cross-coupled products given in Scheme 2.3. The mechanism for the formation of the products can most simply be rationalized by dimerization of the cation radicals followed by the loss of two protons. In fact, cross-coupling of aromatic cations (or anions) have been reported in organic electrochemistry.⁸ An ECEC mechanism is also possible, where one cation radical reacts with the starting material to form a dimer cation radical, which subsequently undergoes further one-electron oxidation and proton loss processes. A range of other scenarios are possible depending on the order of the electron transfer and the homogeneous chemical steps. TLC and NMR experiments indicated that a number of other products were also produced (which were not identified), which were likely to be the result of other cross-coupling reactions.



Scheme 2.3. Cross-coupling products obtained *via* the oxidation of $\mathbf{2a}$ and $\mathbf{3a}$ with one mol equivalent of NOSbF_6 in CH_3CN .

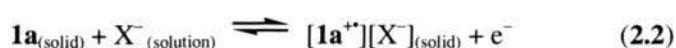
The chemical oxidation and electrolysis experiments indicate that $\mathbf{1a}^{++}$ is long-lived in solution because of the steric hindrance introduced by its fully methylated aromatic ring

preventing irreversible dimerization reactions, while **2a**⁺⁺ and **3a**⁺⁺ with fewer methyl groups have less steric hindrance at the aromatic ring and are able to undergo additional reactions.

2.2.5. Electrochemistry of Films Attached to GC Electrodes

In order to allow experiments to be performed on the compounds in an aqueous environment, solid state electrochemical experiments were conducted by allowing a 2 μ L droplet of a 2 mM solution of **1a** in CH₃CN to evaporate from the surface of a 5 mm diameter GC electrode. The electrode was then immersed in an aqueous solution at different pH-values. At a fixed scan rate and pH-value, 5 – 10 voltammetric cycles were recorded. Similar experiments were conducted with Au and Pt electrodes, but the voltammograms showed only very small and poorly reproducible oxidation processes, so the discussion is limited to the GC surface.

Figure 2.6 shows representative voltammetric data obtained at two scan rates (0.1 V s⁻¹ and 50 V s⁻¹) and three pH values (pH = 1, 7, and 13) for films of **1a** on the electrode surface. At a scan rate of 0.1 V s⁻¹, a clear oxidation process was evident with an E_p^{ox} at $\sim +0.8$ V vs. Ag/AgCl associated with the one-electron oxidation of **1a** to **1a**⁺⁺. At a pH of 1, a reductive peak was detected when the scan direction was reversed, with the separation between the E_p^{ox} and E_p^{red} values equal to 70 mV, which is similar to the value observed under diffusion-controlled solution phase conditions (Figure 2.2). The general mechanism for the oxidation of **1a** adhered to an electrode surface involves incorporation of the supporting electrolyte anion (X⁻) into the solid material according to equation (2.2).



The close similarity between the voltammetry of the solution phase compound (Figure 2.2) and that of the solid compound (Figure 2.6) indicates that the coupled electron and ion transport within the adhered compound are rate determining.⁹ Therefore, the supporting electrolyte anion is readily able to diffuse into and out of the solid material during the potential cycling experiments.

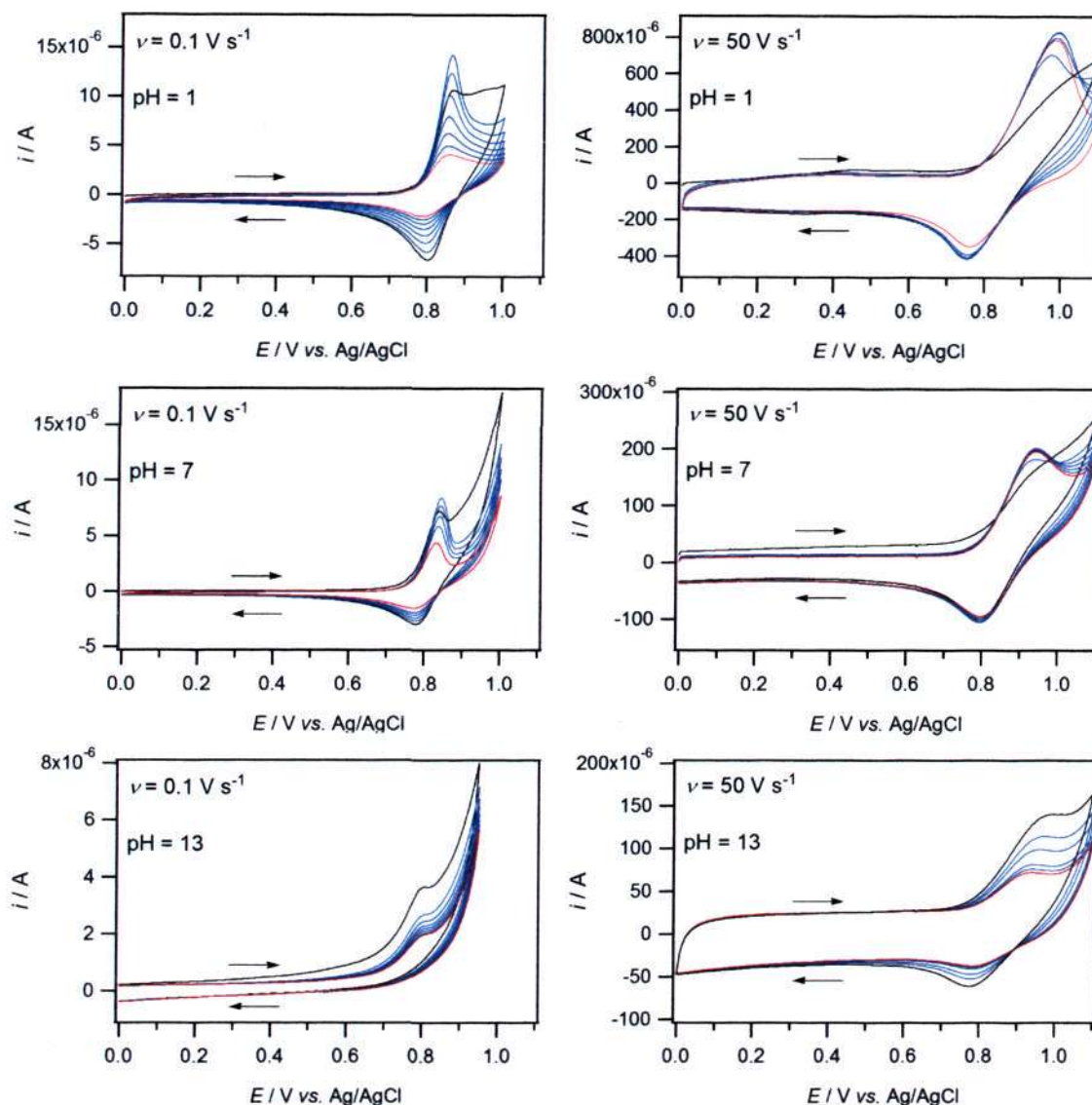


Figure 2.6. Multiple cycle solid state voltammograms of **1a** recorded at two scan rates (ν) at a 5 mm diameter planar GC electrode at 25 °C. The surface of the electrode was prepared by allowing a 2 μ L droplet from a 2 mM solution of **1a** (in CH₃CN) to evaporate, then immersing the electrode in an aqueous solution at different pH-values. (Black line) First scan. (Blue lines) Sequential intermediate scans. (Red line) Final scan.

At pH 1, the first scan often showed a higher current response after the oxidation process than the second and subsequent scans, which is likely to be due to an alteration of the electro-active material on the electrode surface during the first scan. The solid material can exist attached to the electrode in a number of forms (thin films, thick films, microcrystalline particles or as a combination of morphologies) and an applied potential can alter the structure of the solid.^{9b} By measuring the charge passed during the first and subsequent scans and knowing the amount of

solid material adhered to the electrode, it was possible to calculate that amount of material that was oxidized during any one scan. It was estimated that only around 1 – 2% of material underwent oxidation during a CV experiment.

At all pH values, apart from the first scan, the second and subsequent scans always showed a diminishing peak current with repetitive cycling, caused by material being lost (dissolving) from the electrode with each scan. It is likely that **1a**⁺⁺ is at least partly soluble in water, therefore, with each cycle a percentage is removed from the electrode surface. A further feature of the voltammograms that supports some material being removed from the electrode surface with repetitive cycling is that within any one cycle, the peak current for the reverse scan is always smaller than the forward scan. Furthermore, at faster scan rates (50 V s⁻¹), the diminishing current observed with repetitive cycling was less than at slower scan rates, due to less material being lost because less time was available for dissolution. The ΔE_{pp} -values obtained at 50 V s⁻¹ were greater than those obtained at slower scan rates but quite similar to the ΔE_{pp} -values obtained at an equivalent scan rate when the experiments were performed with the compound dissolved in CH₃CN. Therefore, the increasing ΔE_{pp} -values with increasing scan rate are likely to be caused by the effects of uncompensated solution resistance, rather than slow heterogeneous electron or ion transfer.

At a scan rate of 0.1 V s⁻¹, the voltammograms became progressively less chemically reversible as the pH was increased (Figure 2.6), so that at pH 13, only a forward oxidation process was observed and a relatively large decrease in current was seen between the first and second scans. The reason for the decrease in current could be two-fold. In one instance, the increase in pH could favor the dissolution of the positively charged solid compound. This is supported by the experiments at faster scan rates which show that the chemical reversibility begins to return (Figure 2.6), although there is still a large decrease in current between cycles, suggesting that dissolution is a major process. The alternative mechanism could be if the cationic compound was more reactive at high pH and underwent a hydrolysis type reaction to form a hydroxylated compound. The exact identity of the supporting electrolyte anion (other than hydroxide) is not considered to be critical to the chemical reversibility, since the change observed in the reversibility of the

voltammograms at pH values of 1, 3, 5, 7, 9, 11 and 13 were systematic, despite different buffers used at pH 1, pH 3 – 7 and pH 9 – 13.

2.2.6. Computational Section

Computational calculations were performed on **1a** and **1a⁺⁺** in order to determine the structure of the cation radical and to calculate the infrared spectrum. The results were compared with the theoretical results already reported for the cationic forms of the α -tocopherol model compound, (CH₃) α -TOH, with the values summarized in Table 2.1 (and figure 2.7). Previously it was found that the structures (bond lengths and bond angles) predicted by computational calculations were very close to the structural data obtained by X-ray crystallographic studies,^{6d} and it is therefore reasonable to expect that the computational values for **1a** and **1a⁺⁺** are accurate. For ease of comparison, the same atomic numbering system was used for the vitamin E model compounds as for **1a/1a⁺⁺** (Figure 2.7) even though the higher symmetry of **1a/1a⁺⁺** clearly made some bond lengths coincident.

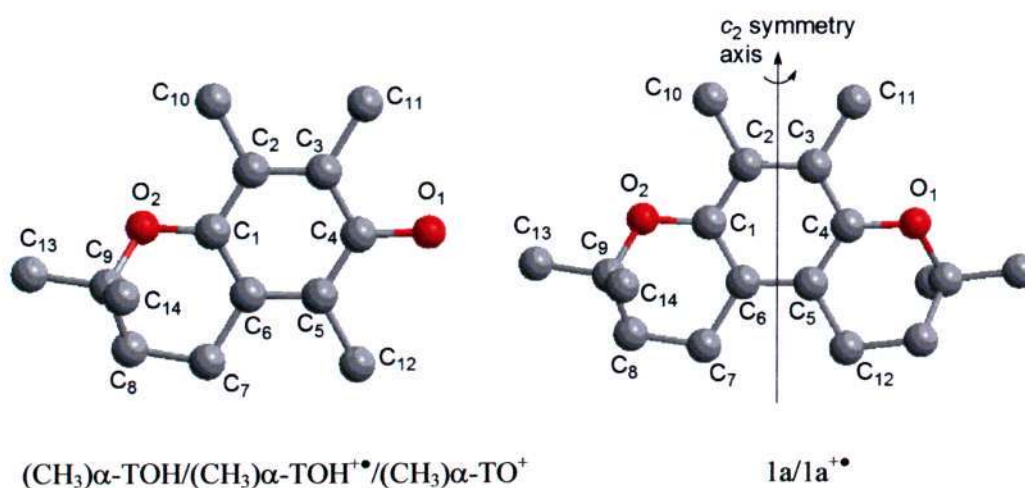


Figure 2.7. Atomic numbering system for the computational values given in Table 2.1.^a

^a Hydrogen atoms are omitted for clarity.

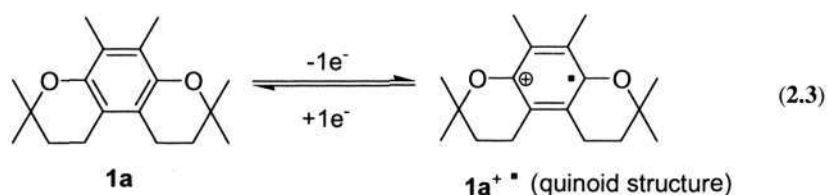
Table 2.1. A selection of bond lengths from computational (EDF2/6-31+G*) calculations.^{a,b}

Bond	Bond Length / Å				
	(CH ₃) α -TOH ^{c,e}	1a	(CH ₃) α -TOH ⁺⁺ ^d	1a⁺⁺	(CH ₃) α -TO ⁺ ^{c,e}
C ₁ –C ₂	1.404 <i>1.4055(14)</i>	1.405	1.437	1.438	1.454 <i>1.455(4)</i>
C ₂ –C ₃	1.398 <i>1.3954(14)</i>	1.398	1.378	1.377	1.360 <i>1.355(4)</i>
C ₃ –C ₄	1.399 <i>1.3974(15)</i>	1.405	1.424	1.438	1.498 <i>1.488(4)</i>
C ₄ –C ₅	1.397 <i>1.3929(15)</i>	1.396	1.429	1.426	1.501 <i>1.491(4)</i>
C ₅ –C ₆	1.406 <i>1.4012(15)</i>	1.407	1.378	1.381	1.359 <i>1.355(4)</i>
C ₆ –C ₁	1.400 <i>1.3934(14)</i>	1.396	1.435	1.426	1.447 <i>1.447(4)</i>
C ₆ –C ₇	1.511 <i>1.5132(14)</i>	1.508	1.506	1.503	1.504 <i>1.505(4)</i>
C ₇ –C ₈	1.526 <i>1.5202(16)</i>	1.527	1.526	1.525	1.525 <i>1.518(4)</i>
C ₈ –C ₉	1.526 <i>1.5217(16)</i>	1.528	1.519	1.521	1.519 <i>1.515(4)</i>
C ₉ –C ₁₃	1.521 <i>1.5159(16)</i>	1.521	1.518	1.518	1.516 <i>1.518(5)</i>
C ₉ –C ₁₄	1.529 <i>1.5207(16)</i>	1.529	1.524	1.524	1.521 <i>1.511(5)</i>
C ₂ –C ₁₀	1.504 <i>1.5084(14)</i>	1.503	1.487	1.499	1.498 <i>1.499(4)</i>
C ₃ –C ₁₁	1.508 <i>1.5113(15)</i>	1.503	1.498	1.499	1.490 <i>1.493(4)</i>
C ₅ –C ₁₂	1.508 <i>1.5097(15)</i>	1.508	1.502	1.503	1.487 <i>1.495(4)</i>
C ₄ –O ₁	1.377 <i>1.3950(13)</i>	1.374	1.329	1.318	1.217 <i>1.214(3)</i>
C ₁ –O ₂	1.374 <i>1.3827(12)</i>	1.374	1.314	1.318	1.289 <i>1.282(3)</i>
C ₉ –O ₂	1.440 <i>1.4566(12)</i>	1.441	1.487	1.483	1.510 <i>1.520(4)</i>

^aResults from X-ray crystallographic measurements are in italics. ^bAtomic numbering system is given in Figure 2.7. ^cValues from reference 6b. ^dValues from reference 6c. ^eValues from reference 6d.

The results in Table 2.1 illustrated that the analogous calculated bond lengths for (CH₃) α -TOH and compound **1a** were very close (in most instances within 0.005 Å). Furthermore, the comparable calculated bond lengths for the one-electron oxidized compounds [(CH₃) α -TOH⁺⁺ and

$1a^{+ \bullet}$] were also very close indicating that the structure and positive charge distribution within $1a^{+ \bullet}$ is similar to $(CH_3)\alpha\text{-TOH}^{+ \bullet}$. Both $1a^{+ \bullet}$ and $(CH_3)\alpha\text{-TOH}^{+ \bullet}$ undergo a shortening of the $C_2\text{-}C_3$ and $C_5\text{-}C_6$ bonds compared to the uncharged starting material, indicating that the charged compounds begin to take on the structure expected for a quinoid type compound (eq 2.3). The results in Table 2.1 indicate that the structure of the phenoxonium cation $[(CH_3)\alpha\text{-TO}^+]$ is even closer to that expected for a quinone, with relatively short $C_2\text{-}C_3$ and $C_5\text{-}C_6$ (double) bonds and elongated $C_1\text{-}C_2$, $C_3\text{-}C_4$, $C_4\text{-}C_5$ and $C_6\text{-}C_1$ (single) bonds, compared to the neutral starting material.



2.2.7. IR spectroscopy

The infrared spectra of **1a** (black line) and $1a^{+ \bullet}(\text{SbF}_6^-)$ (red line) prepared by one-electron chemical oxidation of **1a** with NOSbF_6 are given in Figure 2.8. The IR spectrum of **1a** is very similar to $1a^{+ \bullet}$ showing a number of absorbances at identical wavenumbers. However, notable differences in the IR spectrum of $1a^{+ \bullet}(\text{SbF}_6^-)$ compared to **1a** are the appearance of relatively weak absorbances at 1624 cm^{-1} and 1649 cm^{-1} , which are associated with the "asymmetric and symmetric ring stretching modes" respectively, that result as the cation radical approaches a quinoid structure (eq 2.3). The symmetric ring stretching mode originates from the $C_2\text{-}C_3$ and $C_5\text{-}C_6$ (Figure 2.7) bonds symmetrically stretching and contracting, while the carbon-oxygen bonds simultaneously stretch and contract. The asymmetric ring stretching mode is associated with the $C_2\text{-}C_3$ and $C_5\text{-}C_6$ bonds contracting and stretching not in unison (coupled with other atoms undergoing bond stretching and contraction). The theoretical calculations predicted the asymmetric and symmetric ring stretching modes at 1638 cm^{-1} and 1696 cm^{-1} respectively, which is up to 50 cm^{-1} higher than that observed experimentally, but of a similar level of accuracy previously found for the infrared vibrations of the phenoxonium cation.^{6b}

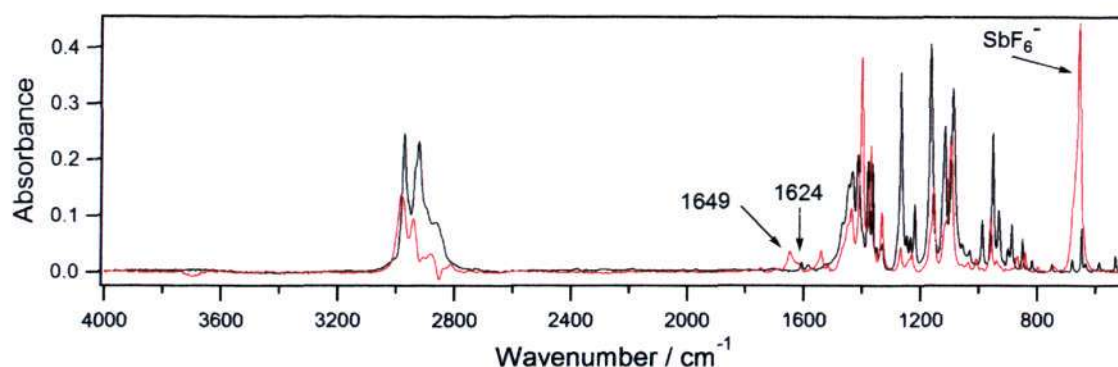


Figure 2.8. FTIR spectra of (black line) **1a** and (red line) **1a⁺·(SbF₆⁻)** obtained by oxidizing **1a** with 1 mol equivalent of NOSbF₆.

These asymmetric and symmetric ring stretching modes were not previously detected in the infrared spectrum of (CH₃) α -TOH⁺,^{6c} but this is likely to be because of their relatively weak intensity and because of the difficulty in handling solutions of (CH₃) α -TOH⁺ for infrared spectroscopic analysis [(CH₃) α -TOH⁺ has not to date been isolated as a solid compound].

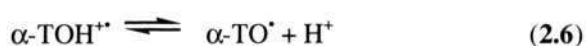
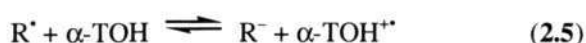
2.3. Discussion and Conclusions

A series of experiments (CV, CPE, theoretical calculation, and IR spectroscopy) have demonstrated that compounds **1a** – **3a** can be oxidized to their respective radical cations in simple one-electron chemically reversible electron transfer processes; either heterogeneously at solid electrodes or homogeneously using NOSbF₆ as the oxidant. Compound **1a** contains a fully methylated aromatic ring and is hence the most closely related to α -TOH. The reduction potential of **1a⁺·** and its spectroscopic and structural properties are very similar to those of α -TOH⁺. However, the lifetime of **1a⁺·** is considerably longer than the lifetime of α -TOH⁺ in aqueous and non-aqueous solvents for the following reasons: firstly, it contains an aprotic cyclic ether linkage in place of a hydroxyl group; secondly, the methyl groups in the aromatic ring provide steric hindrance from coupling reactions to other cation radicals (as occurs for the less methyl substituted **2a⁺·** and **3a⁺·**). Therefore, it can be concluded that **1a⁺·** is a good "model" compound for examining aspects of the reductive properties of α -TOH⁺.

It is generally thought that the biological antioxidant function of vitamin E occurs *via* a hydrogen atom transfer (HAT) mechanism where a reactive free radical (R^\bullet) reacts with the phenolic hydrogen atom (eq 2.4).^{4,10}



Detailed kinetic experiments have demonstrated that the HAT mechanism involves strong interactions with the solvent molecules.⁴ In theory it is possible that the reactive free radicals can also react with vitamin E through electron transfer (ET) and proton transfer (PT) reactions, which would lead to the radical cation ($\alpha\text{-TOH}^{+\bullet}$) (eq 2.5) and phenoxyl radical ($\alpha\text{-TO}^\bullet$) (eq 2.6) intermediates.



Whether reaction (2.4) or reaction (2.5) occurs depends on the oxidizing ability of the R^\bullet group. The role of $\alpha\text{-TOH}^{+\bullet}$ in the antioxidant chemistry of vitamin E has not been ascertained,^{4,10} although it is logical that under certain conditions reaction (2.5) should occur if the free radical is a strong enough oxidant. It has been proposed that $\alpha\text{-TOH}^{+\bullet}$ is able to react with carotenoids (CAR) in a ET mechanism subsequently regenerating vitamin E and thereby giving the carotenoids synergistic antioxidant properties (eq 2.7).¹¹



Electron paramagnetic resonance (EPR) experiments have shown that $\alpha\text{-TO}^\bullet$ does not undergo an ET reaction to produce the carotenoid cation radicals,¹² most likely because it is not a powerful enough oxidant ($\alpha\text{-TO}^\bullet$ is reduced at approximately +0.15 V *vs.* Fc/Fc⁺ in CH₃CN compared to +0.5 V *vs.* Fc/Fc⁺ for $\alpha\text{-TOH}^{+\bullet}$).^{6g} A major difficulty in studying reaction (2.7) is that the cation radical of vitamin E is very acidic and not long-lived (except in organic solvents containing strong acids^{6,13} or in CH₂Cl₂ at low temperatures¹⁴), therefore, the phenoxyl radical will immediately form (eq 2.6). Thus, **1a**⁺ is potentially useful as a model compound to determine the oxidizing efficiency of α -tocopherol under homogeneous oxidizing conditions, especially in low dielectric constant solvents where the formal reduction potentials are difficult to determine experimentally. The replacement of one of the methyl groups at the quaternary carbons (C₁₃ or C₁₄

in Figure 2.7) with a "phytyl chain" ($C_{16}H_{33}$) would give a lipid soluble species suitable for *in vivo* or *in vitro* studies. Previously it was found that the phytyl chain in the natural compound is unimportant to the electrochemical properties of α -TOH, and is unlikely to affect the lifetime of $1a^{+}$ (or oxidation potential of $1a$).

In conclusion, compound $1a^{+}$ is a suitable long-lived model for testing the oxidizing abilities of the radical cation of vitamin E (α -TOH $^{+}$) under homogeneous conditions, without the additional complication of a deprotonation reaction. Electrochemical and spectroscopic experiments combined with theoretical calculations, indicate that the formal reduction potential, the structure and the charge distribution of $1a^{+}$ are similar to α -TOH $^{+}$, despite the absence of a hydroxyl group.

2.4. Experimental Section

2.4.1. Chemicals

HPLC grade CH_3CN (Tedia) was used as received and Bu_4NPF_6 was prepared and purified by standard methods.¹⁵ Water, with a resistivity of no less than 18 M Ω cm was used for experiments at different pH-values. Sulfuric acid was used for experiments at pH 1. Citric acid–phosphate buffer solutions (pH 3, 5, and 7) were prepared from disodium hydrogen phosphate (Merck) and citric acid (Amresco). Britton–Robinson buffer solutions (pH 9, 11, and 13) were prepared using 0.04 M acetic, phosphoric, and boric acids (Merck), and adjusted to the required pH using KOH (Merck).

2.4.2. Synthetic Experiments. The synthesis of compounds $1a$ – $3a$ was based on a modified version of literature reports.¹⁶

Compound 1a: 2, 3-Dimethylbenzene-1, 4-diol (276 mg, 2.0 mmol) and TsOH (38 mg, 0.2 mmol) were placed in a flask, and dry toluene (5 mL) was added under argon. 2-Methyl-but-3-en-2-ol (189 mg, 4.1 mmol) was injected dropwise into the flask by syringe, and the mixture was stirred for 18 h at 100 °C. After cooling, ethyl acetate was added to dilute the solution, and the organic layer was washed with water and brine, and dried with Na_2SO_4 . After the solvent was

removed, the residue was separated by column chromatography to give a white solid (482 mg, 1.8 mmol, 88%). ^1H NMR (CDCl_3 , 300 MHz) δ 2.55 (t, 4H, $J = 13.6$ and 6.8 Hz), 2.10 (s, 6H), 1.78 (t, 4H, $J = 13.7$ and 6.8 Hz), 1.29 (s, 12H); ^{13}C $\{^1\text{H}\}$ NMR (CDCl_3 , 75 MHz) δ 144.7 ($\text{C}_{\text{aromatic}}$), 123.4 ($\text{C}_{\text{aromatic}}$), 115.5 ($\text{C}_{\text{aromatic}}$), 72.4 (OCCH_3), 33.0 (CH_2), 26.9 (OCCH_3), 20.1 (Ar-CH_2), 11.8 (Ar-CH_3).

Compound 2a (obtained as two isomers): 2-Methylbenzene-1, 4-diol (248 mg, 2.0 mmol) and TsOH (38 mg, 0.2 mmol) were placed in a flask, and dry toluene (5 mL) was added under argon. 2-Methyl-but-3-en-2-ol (206 mg, 2.4 mmol) was injected dropwise into the flask by syringe, and the mixture was stirred for 18 h at 100°C . The same procedure as used for **1a** was used to work up this reaction, and the product was obtained as a white solid (143 mg, 46%).

Compound 3a (obtained as two isomers): Hydroquinone (220 mg, 2.0 mmol) and TsOH (38 mg, 0.2 mmol) were placed in a flask, and dry toluene (5 mL) was added under argon. 2-Methyl-but-3-en-2-ol (189 mg, 2.2 mmol) was injected dropwise into the flask by syringe, and the mixture was stirred for 18 h at 80°C . The same procedure as used for **1a** was used to work up this reaction, and the product was obtained as a white solid (135 mg, 50%).

Chemical oxidation of compound 1a: In a glove box, to a solution of **1a** in 1 mL acetonitrile was added NOSbF_6 (1 equiv) in one pot, and the solution became black immediately. After the mixture was stirred for ten minutes, the solvent was removed to give a dark yellow solid [**1a** $^{++}(\text{SbF}_6^-)$], which was analyzed by infrared spectroscopy, UV-vis spectroscopy and elemental analysis. Anal. Calc for $\text{C}_{18}\text{H}_{26}\text{F}_6\text{O}_2\text{Sb}$ (510.15): C, 42.38; H, 5.14%. Found: C, 42.71; H, 4.94%.

Chemical oxidation of compound 2a: In a glove box, to a solution of **2a** (52 mg, 0.20 mmol) in 1 mL acetonitrile was added NOSbF_6 (1 equiv) in one pot, and the solution became black immediately. After the mixture was stirred for ten minutes, the solution was removed from the glove box and stirred in air for 12 h. After the solvent was removed, the residue was chromatographed on silica gel using hexane : ethyl acetate = 10:1 as eluent to give the cross-coupled product as a yellow solid (13 mg, 0.025 mmol, 24%). ^1H NMR (CDCl_3 , 400 MHz) δ 2.56 (t, 4H, $J = 13.6$ and 6.8 Hz), 2.06 (s, 3H, Ar-CH_3), 1.86-1.79 (m, 4H), 1.29 (s, 12H); ^{13}C $\{^1\text{H}\}$ NMR (CDCl_3 , 100 MHz) δ 144.6 ($\text{C}_{\text{aromatic}}$), 140.9, 137.8, 121.0, 118.3, 116.9, 74.4 (OCCH_3),

73.5 (OCCH₃), 32.32 (CH₂), 32.29 (CH₂), 26.64(OCCH₃), 26.27 (OCCH₃), 20.24(Ar-CH₂), 19.81 (Ar-CH₂), 10.4 (Ar-CH₃). **HRMS (ESI)** calcd for C₃₄H₄₇O₄ 519.3474; found 519.3456.

Chemical oxidation of compound 3a: In a glove box, to a solution of **3a** (50 mg, 0.20 mmol) in 1 mL acetonitrile was added NOSbF₆ (1 equiv) in one pot, and the solution became black immediately. After the mixture was stirred for ten minutes, the solution was removed from the glove box and stirred in air for 12 h. After the solvent was removed, the residue was chromatographed on silica gel using hexane : ethyl acetate = 10:1 as eluent to give the cross-coupled product as a yellow solid (10 mg, 0.02 mmol, 20%). ¹H NMR (CDCl₃, 400 MHz) δ 6.63 (s, 1H, Ar-CH), 2.73 (t, 2H, *J* = 13.6 and 6.8 Hz), 2.65 (t, 2H, *J* = 13.2 and 6.8 Hz), 1.81 (t, 2H, *J* = 13.2 and 6.4 Hz), 1.76 (t, 2H, *J* = 13.6 and 6.4 Hz), 1.31 (s, 12H); ¹³C {¹H} NMR (CDCl₃, 100 MHz) δ 146.2, 140.3, 139.2, 122.3, 119.0, 112.2, 75.5 (OCCH₃), 74.1 (OCCH₃), 32.4 (CH₂), 31.7 (CH₂), 26.5 (Ar-CH₂), 22.2 (Ar-CH₂), 18.2 (CH₃). **HRMS (ESI)** calcd for C₃₂H₄₃O₄ 491.3161; found 491.3138.

2.4.3. Electrochemical Measurements.

Cyclic voltammetry (CV) experiments were conducted with a computer controlled Eco Chemie Autolab PGSTAT 100 with an ADC fast scan generator. Working electrodes were 1 mm or 5 mm diameter planar Au, Pt or glassy carbon (GC) disks, used in conjunction with a Pt auxiliary electrode. For non-aqueous experiments, an Ag wire reference electrode was connected to the test solution *via* a salt bridge containing 0.5 M Bu₄NPF₆ in CH₃CN, with accurate potentials obtained by using ferrocene (Fc) as an internal standard. An Ag/AgCl reference electrode containing 3 M KCl was used for experiments in aqueous systems.

Bulk oxidation experiments were performed in a divided controlled potential electrolysis (CPE) cell separated with a porosity no. 5 (1.0 – 1.7 μm) sintered glass frit.¹⁷ The working and auxiliary electrodes were identically sized Pt mesh plates symmetrically arranged with respect to each other with an Ag wire reference electrode (isolated by a salt bridge) positioned to within 2 mm of the surface of the working electrode. The volumes of both the working and auxiliary electrode compartments were approximately 10 mL each. The solution in the working electrode compartment was simultaneously deoxygenated and stirred using bubbles of argon gas. The

number of electrons transferred during the bulk oxidation process was calculated from $N = Q/nF$, where N = no. of moles of starting compound, Q = charge (coulombs), n = no. of electrons and F is the Faraday constant (96485 C mol^{-1}).

2.4.4. UV-vis-NIR and FTIR Measurements.

In situ UV-vis spectra were obtained with a Perkin-Elmer Lambda 750 spectrophotometer in an optically semi-transparent thin layer electrochemical (OSTLE) cell (pathlength = 0.05 cm) using a Pt mesh working electrode.¹⁸ FTIR experiments were conducted with a Thermo Electron Nicolet 6700 spectrometer mainframe with a Continuum infrared microscope.

2.4.5. Computational Procedures.

Molecular orbital calculations were performed using a development version of the Q-Chem 3.1 software package¹⁹ and the Spartan '04 software package.²⁰ Harmonic vibrational frequencies were calculated by Q-Chem using the EDF2/6-31+G* density functional model²¹ and the SG-1 quadrature grid²² and no empirical scale factors were applied. (The EDF2/6-31+G* model was used because it was previously found to give a high level of accuracy in predicting the structures of cations.)^{6b,6d}

2.5. References

1. (a) Burton, G. W.; Ingold, K. U. *J. Am. Chem. Soc.* **1981**, *103*, 6472. (b) Burton, G. W.; Ingold, K. U. *Acc. Chem. Res.* **1986**, *19*, 194.
2. Finkel, T.; Holbrook, N. J. *Nature* **2000**, *408*, 239, and references therein.
3. S  nchen-Moreno, C. *Food. Sci. Tech. Int.* **2002**, *8*, 121.
4. Litwinienko, G.; Ingold, K. U. *Acc. Chem. Res.* **2007**, *40*, 222.
5. Hammerich, O.; Svensmark, B. In *Organic Electrochemistry*, 3rd ed.; Lund, H., Baizer, M. M., Eds.; Marcel Dekker: New York, **1991**; Chapter 16.
6. (a) Williams, L. L.; Webster, R. D. *J. Am. Chem. Soc.* **2004**, *126*, 12441. (b) Lee, S. B.; Lin, C. Y.; Gill, P. M. W.; Webster, R. D. *J. Org. Chem.* **2005**, *70*, 10466. (c) Wilson, G. J.; Lin, C. Y.; Webster, R. D. *J. Phys. Chem. B* **2006**, *110*, 11540. (d) Lee, S. B.; Willis, A. C.; Webster, R. D. *J. Am. Chem. Soc.* **2006**, *128*, 9332. (e) Webster, R. D. *Acc. Chem. Res.* **2007**, *40*, 251. (f) Peng, H. M.; Webster, R. D. *J. Org. Chem.* **2008**, *73*, 2169. (g) Yao, W. W.; Peng, H. M.; Webster, R. D. *J. Phys. Chem. B* **2008**, *112*, 6847.
7. (a) Rudolph M. J. *J. Electroanal. Chem.* **2003**, *543*, 23. (b) Rudolph M. J. *J. Electroanal. Chem.* **2004**, *571*, 289. (c) Rudolph M. J. *J. Electroanal. Chem.* **2003**, *558*, 171. (d) Rudolph M. J. *Comput. Chem.* **2005**, *26*, 619. (e) Rudolph M. J. *Comput. Chem.* **2005**, *26*, 633. (f) Rudolph M. J. *Comput. Chem.* **2005**, *26*, 1193.
8. (a) Hammerich, O.; Parker, V. D. *Acta Chem. Scand., Ser. B*, 1981, **35**, 341. (b) Amatore, C.; Pinson, J.; Sav  ant, J. M. *J. Electroanal. Chem.*, 1982, **137**, 143. (c) Smie, A.; Heinze, J. *Angew. Chem., Int. Ed.* 1997, **36**, 363. (d) Tschuncky, P.; Heinze, J.; Smie, A.; Engelmann, G.; Ko  mehl, G. *J. Electroanal. Chem.*, 1997, **433**, 223.
9. (a) Marken, F.; Webster, R. D.; Bull, S. D.; Davies, S. G. *J. Electroanal. Chem.* **1997**, *437* (1-2), 209. (b) Bond, A. M. In *Broadening Electrochemical Horizons*; Oxford University Press: Oxford, **2002**; Chapter 5. (c) Banks, C. E.; Davies, T. J.; Evans, R. G. Hignett, G.; Wain, A. J.; Lawrence, N. S.; Wadhawan, J. D.; Marken, F.; Compton, R. G. *Phys. Chem. Chem. Phys.* **2003**, *5*, 4053.
10. (a) Traber, M. G.; Atkinson, J. *Free Rad. Bio. Med.* **2007**, *43*, 4. (b) Bowry, V. W.; Ingold, K. U. *Acc. Chem. Res.* **1999**, *32*, 27.

11. Edge, R.; Land, E. J.; McGarvey, D.; Mulroy, L.; Truscott, T. G. *J. Am. Chem. Soc.* **1998**, *120*, 4087.
12. Valgimigli, L.; Lucarini, M.; Pedulli, G. F.; Ingold, K. U. *J. Am. Chem. Soc.* **1997**, *119*, 8095.
13. (a) Parker, V. D. *J. Am. Chem. Soc.* **1969**, *91*, 5380. (b) Svanholm, U.; Bechgaard, K.; Parker, V. D. *J. Am. Chem. Soc.* **1974**, *96*, 2409.
14. Lehtovuori, P.; Joela, H. *Phys. Chem. Chem. Phys.* **2002**, *4*, 1928.
15. Fry, A. J.; Britton, W. E. In *Laboratory Techniques in Electroanalytical Chemistry*; Kissinger, P. T., Heineman, W. R., Eds.; Marcel Dekker: New York, **1984**; Chapter 13.
16. (a) Dean, F. M.; France, S. N.; Oyman, U. *Tetrahedron* **1988**, *44*, 4857. (b) Patel, A.; Liebner, F.; Netscher, T.; Mereiter, K.; Rosenau, T. *J. Org. Chem.* **2007**, *72*, 6504.
17. Webster, R. D.; Bond, A. M.; Schmidt, T. *J. Chem. Soc., Perkin Trans. 2* **1995**, 1365.
18. (a) Webster, R. D.; Heath, G. A.; Bond, A. M. *J. Chem. Soc., Dalton Trans.* **2001**, 3189. (b) Webster, R. D.; Heath, G. A. *Phys. Chem. Chem. Phys.* **2001**, *3*, 2588.
19. Shao, Y.; Fusti Molnar, L.; Jung, Y.; Kussmann, J.; Ochsenfeld, C.; Brown, S. T.; Gilbert, A. T. B.; Slipchenko, L. V.; Levchenko, S. V.; O'Neill, D. P.; DiStasio Jr., R. A.; Lochan, R. C.; Wang, T.; Beran, G. J. O.; Besley, N. A.; Herbert, J. M.; Lin, C. Y.; Van Voorhis, T.; Chien, S. H.; Sodt, A.; Steele, R. P.; Rassolov, V. A.; Maslen, P. E.; Korambath, P. P.; Adamson, R. D.; Austin, B.; Baker, J.; Byrd, E. F. C.; Dachsel, H.; Doerksen, R. J.; Dreuw, A.; Dunietz, B. D.; Dutoi, A. D.; Furlani, T. R.; Gwaltney, S. R.; Heyden, A.; Hirata, S.; Hsu, C.-P.; Kedziora, G.; Khalliulin, R. Z.; Klunzinger, P.; Lee, A. M.; Lee, M. S.; Liang, W.; Lotan, I.; Nair, N.; Peters, B.; Proynov, E. I.; Pieniazek, P. A.; Rhee, Y. M.; Ritchie, J.; Rosta, E.; Sherrill, C. D.; Simmonett, A. C.; Subotnik, J. E.; Woodcock III, H. L.; Zhang, W.; Bell, A. T.; Chakraborty, A. K.; Chipman, D. M.; Keil, F. J.; Warshel, A.; Hehre, W. J.; Schaefer III, H. F.; Kong, J.; Krylov, A. I.; Gill, P. M. W.; Head-Gordon, M. *Phys. Chem. Chem. Phys.* **2006**, *8*, 3172.
20. Spartan 04 for Macintosh, Wavefunction Inc.: Irvine CA, **2004**.
21. Lin, C. Y.; George, M. W.; Gill, P. M. W. *Aust. J. Chem.* **2004**, *57*, 365.
22. Gill, P. M. W.; Johnson, B. G.; Pople, J. A. *Chem. Phys. Lett.* **1993**, *209*, 506.

PART II

Quinoline-functionalized N-heterocyclic Carbenes

(NHCs) Metal Complexes:

Synthesis, Structures, and Catalysis

CHAPTER 3

Palladium Complexes of Quinoline-Tethered N-Heterocyclic Carbenes (NHCs):

Synthesis, Structures, Solution Dynamics, and Catalysis

3.1. Introduction

3.1.1. General Properties of N-Heterocyclic Carbenes (NHCs)

Carbene is a highly reactive organic molecule containing a divalent carbon atom with only six valence electrons, and the high reactivity comes from its electronic unsaturation. In general, there are two types of carbenes: singlet and triplet carbenes (Figure 3.1). If two electrons occupy one orbital leaving the fourth orbital empty, it is termed a singlet carbene. Triplet carbenes have two unpaired electrons. Usually, singlet carbenes are more stable than triplet carbenes, particularly when substituted by heteroatoms at the α -position. However, both of them are too reactive to be isolated. For over a century, tremendous efforts have been made to isolate free carbenes, but most of them have been unsuccessful. It was not until 1991 that Arduengo and co-workers reported the first imidazole-based free carbene, which was confirmed by X-ray crystallography (Scheme 3.1).¹ The bulky adamantyl substituent played an important role in stabilizing carbenes in this free state, although it was later demonstrated that the steric hindrance is not the only factor to explain the stability of this type of carbene. From then on, the chemistry of N-heterocyclic carbenes (NHCs) was ignited rapidly, especially by the pioneering research works of Herrmann,² Grubbs,³ Nolan,⁴ and others⁵. In recent years, various reviews have been published detailing the applications of NHCs from essentially every possible angle of view, including preparation, structures, electronic properties, coordination modes, and catalytic applications. On the one hand, they can be directly applied as organo-catalysts in homogeneous catalysis.⁶ On the other hand, they can be incorporated into metal systems that can be further applied to coordination chemistry and catalysis.⁷ Up to now, Ru(I)-NHCs represent the most important applications of metal-NHCs in olefin metathesis, which was pioneered by Grubbs.⁸ In addition, Pd(II)-NHCs-catalyzed cross-coupling reactions are other noticeable successful

examples.⁹ These discoveries almost revolutionized the area of catalysis. In comparison to phosphine ligands, NHCs exhibit higher electron-donating capacity, and their σ -donor characters can be roughly estimated by the pK_a values of the corresponding azolium salts.¹⁰ Moreover, NHCs possess several other advantages. On the one hand, the electronic and steric effects are tunable with the modification of the substituents attached to the nitrogen substituents or with the modification of the carbene backbone.¹¹ On the other hand, strong metal-NHC bonds and greater thermal stability are especially important to efficient catalysis.^{7b} Furthermore, NHCs complexes tend to be more air and moisture stable than their related phosphine analogues.

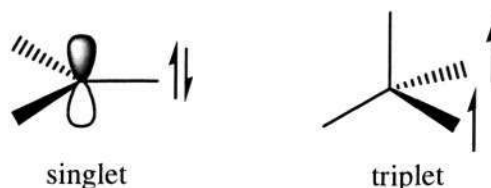
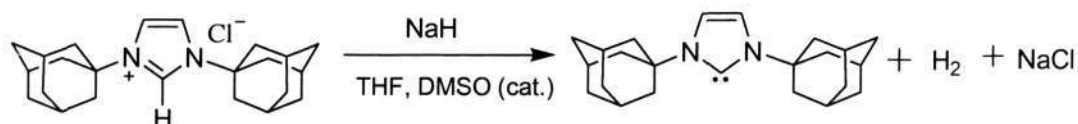


Figure 3.1. Singlet and triplet carbenes.



Scheme 3.1. Formation of the first isolable free carbene.

In terms of the ring size of the carbene backbone, until now, reported NHCs include four-,¹² five-, six-,¹³ and seven-membered¹⁴ ring systems. The first four-membered NHC ligand was reported by Grubbs and co-workers.¹² However, among them, the vast majority of NHCs are still based on five-membered ring backbones (Figure 3.2), and some of them have been supplied commercially, such as the first stable free carbene and imidazol-2-ylidenes IMes and IPr (Figure 3.3). The most common way to prepare NHCs is the deprotonation of the corresponding imidazolium salts by bases such as NaH, KOBu^t, LDA or KHMDS.

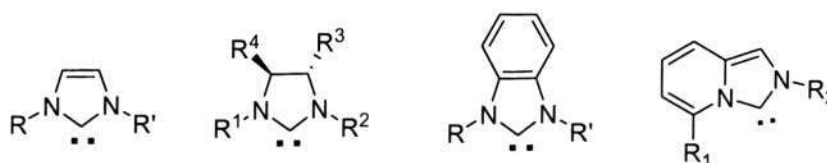


Figure 3.2. Representative five-membered NHCs.

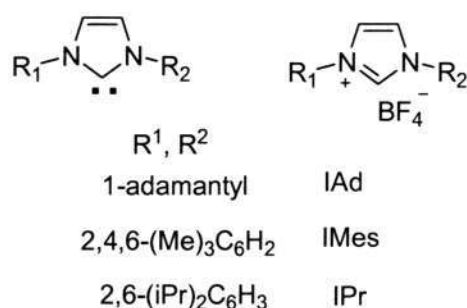
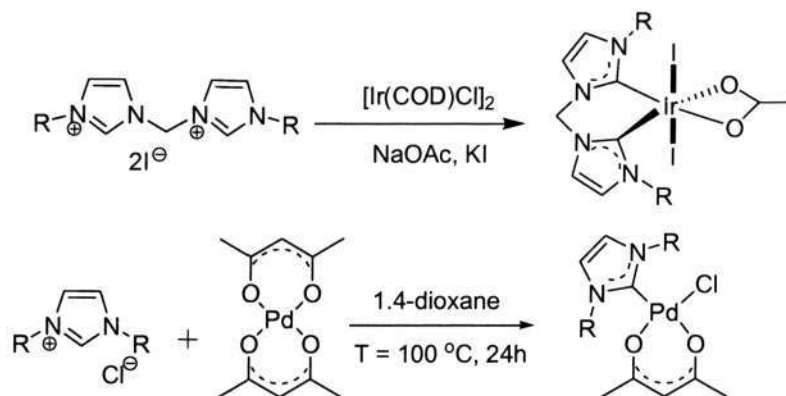


Figure 3.3. Commercially available NHCs and their precursors.

3.1.2. Synthesis and Properties of N-Heterocyclic Carbene Metal Complexes

Many synthetic strategies and protocols have been developed to prepare NHC-metal complexes, and those typical methods are summarized as following.

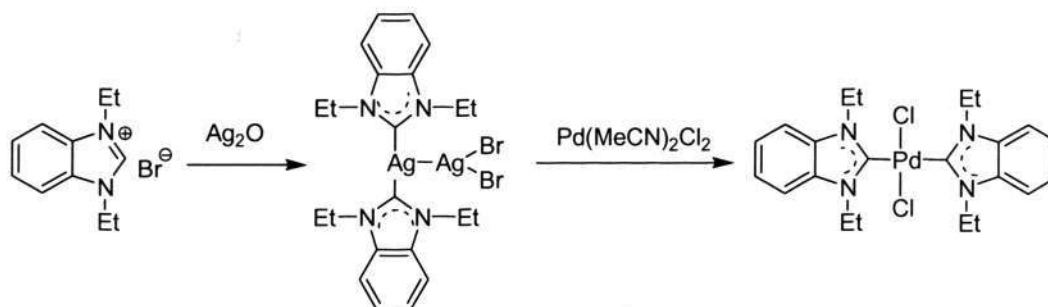
1. Deprotonation of Imidazolium Salts: Deprotonation of the corresponding imidazolium salts is a very straightforward method to prepare NHC-metal complexes, and two strategies can be employed in this method. A weak or strong base (such as NaOAc, NEt₃, or KOBu^t, KH) can be added to a reaction mixture that contains a metal source.¹⁵ Alternatively, a basic metal complex can be directly used as a precursor (such as Pd(OAc)₂ and [Ir(COD)(OEt)]₂), where the anionic ligand serves as an internal base (Scheme 3.2).¹⁶



Scheme 3.2. Formation of NHC-metal complexes *via* deprotonation.

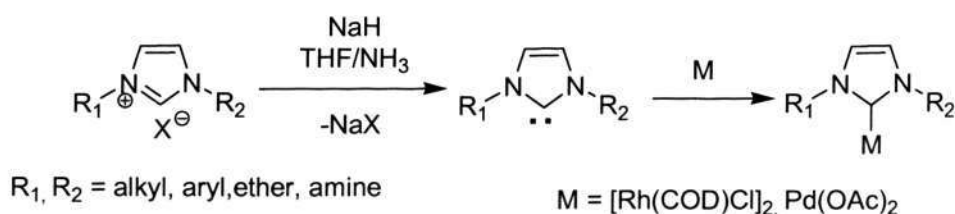
2. Transmetalation from Silver Complexes: In 1998, Lin et al. reported a very useful method that has been explored to prepare NHC-metal complexes (Scheme 3.3).^{17a} They found that NHC-silver(I) halide complexes are consecutive precursors to prepare other metal complexes, and further research results proved that some NHC-silver complexes had potential application in medical studies.^{17d} During transmetalation reactions, the carbon-silver bond is broken, giving

solid silver(I) halide, and the carbene is transferred to a more electronegative metal. By following this procedure, many NHC-metal complexes (including palladium, rhodium, iridium, ruthenium, and gold) have been synthesized in excellent yields with no side-reactions.^{17c,d}



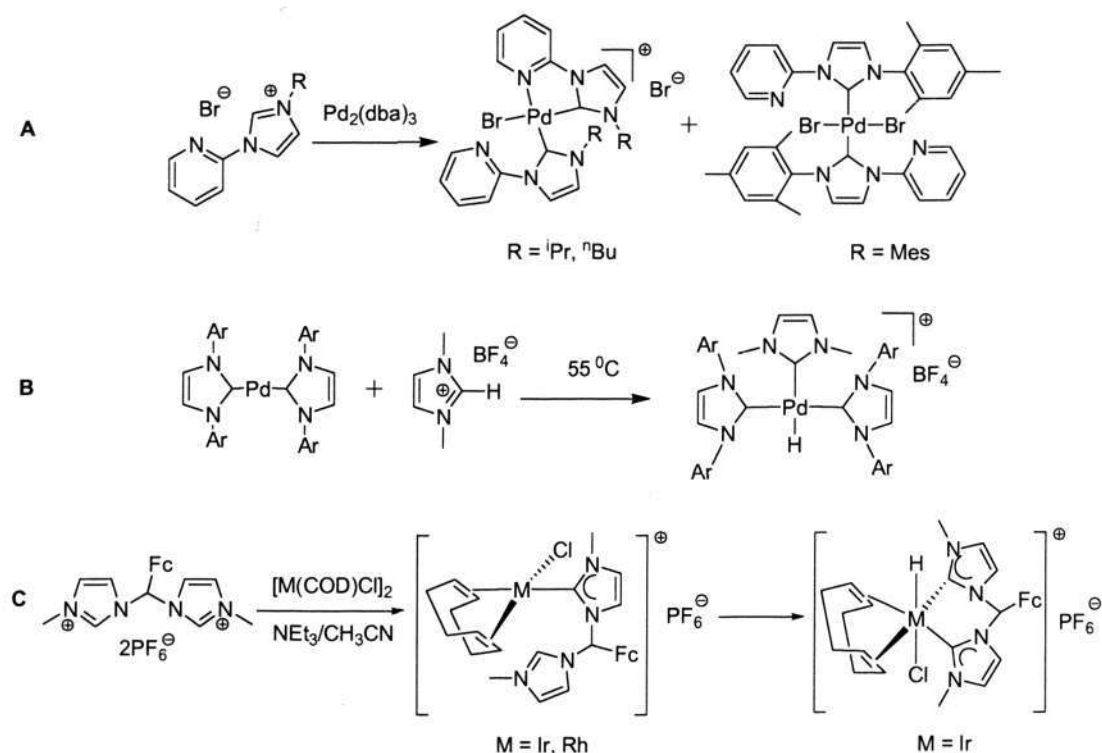
Scheme 3.3. The synthesis of NHC-Pd complexes by silver-transmetalation.

3. Metalation of Free Carbenes:¹⁸ Following this method, the first step is the generation of a free carbene using a strong base (e.g. ⁿBuLi, NaH, KOBu^t), followed by a metalation process (Scheme 3.4). However, this method has limitations since it is not always possible to isolate free NHCs.



Scheme 3.4. The preparation of NHC-metal complexes *via* proton abstraction.

4. Oxidative Addition: The oxidative addition method is especially important for zero-valent Group 10 metals (Ni, Pd, Pt) (Scheme 3.5 **A, B**).^{19a,b} Importantly, Peris et al. successfully extended this strategy to Group 9 metals with the synthesis of an Ir(III) hydride complex from the oxidative addition of a ferrocenyl-linked bisimidazolium salt,^{19c} where the first incipient carbene acts as a directing group for the C-H activation of the 2nd imidazolium (Scheme 3.5 **C**). Another interesting aspect of this approach is the formation of metal hydride complexes (Scheme 3.5 **B, C**).^{19b,c}



Scheme 3.5. Formation of NHC-metal complexes *via* oxidative addition.

With the applications of the above strategies, various NHC-metal complexes have been synthesized and studied, especially late transition-metal complexes. In most cases, C2-metallated complexes have been obtained, which are named normal or classical carbenes. However, in some instances, abnormal carbenes will be formed through metalation of the C4 or C5 carbon (Figure 3.4).²⁰ In addition, other unconventional classes of carbenes have been discovered, such as remote carbenes,²¹ acyclic carbenes,²² and carbocyclic carbenes²³ (Figure 3.5). These structures are beyond the scope of this work and are not discussed here. Unless otherwise noted, all N-heterocyclic carbenes refer to normal five-membered ring NHCs in this thesis.

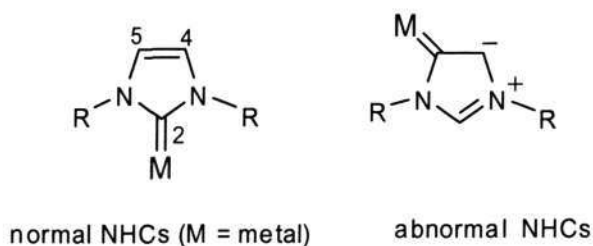


Figure 3.4. The carbon labelling of generic carbenes.

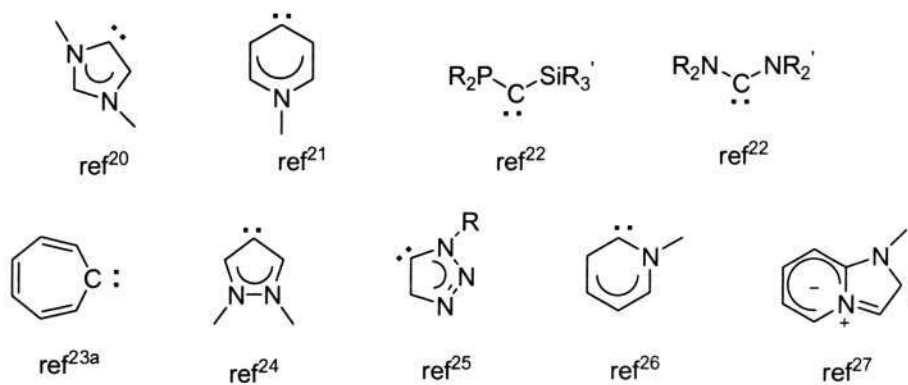
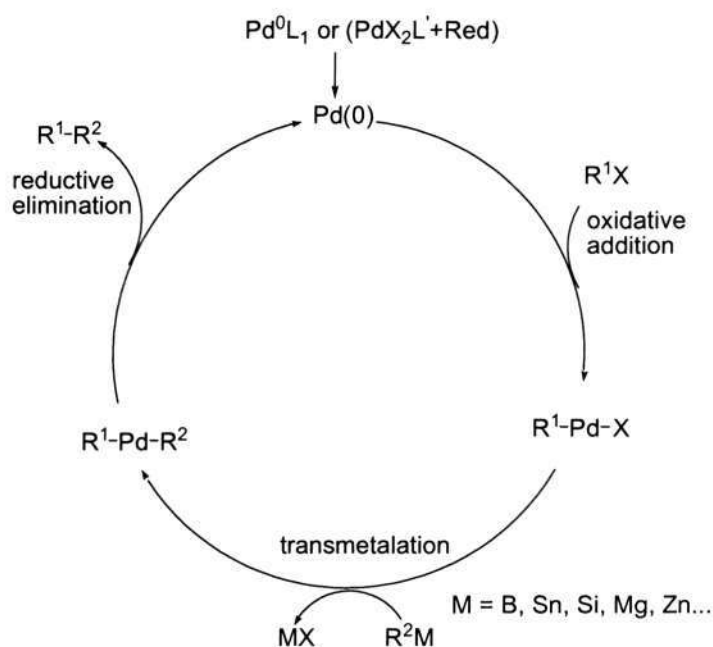


Figure 3.5. Some examples of beyond conventional NHCs.

3.1.3. NHC-Palladium Complexes

In the history of transition-metal-catalyzed reactions, palladium complexes played a decisive role.²⁸ They were successfully applied to cross-coupling reactions, such as the Mizoroki-Heck reaction²⁹, Miyaura-Suzuki reaction³⁰, and Sonogashira reaction³¹. The general mechanism involves three key steps (Scheme 3.6): oxidative addition, transmetalation, and reductive elimination.^{28a-b} In the catalytic cycle, the oxidative addition step is often considered as the rate-determining step. The strength of the C-X bond (X = halide or pseudo-halide) has an important effect on the reactivity which follows the order $\text{Cl} \ll \text{Br} < \text{OTf} < \text{I}$.^{30a}



Scheme 3.6. The proposed mechanism for cross-coupling reactions.

In recent years, with the widespread development of N-heterocyclic carbene ligands, NHC-palladium complexes represent a new type of catalyst owing to their easy accessibility, high thermal stability, and remarkable catalytic activities.^{9a,32} Herrmann et al. reported the first well-defined palladium carbene catalyst that has been applied to Heck reaction giving impressive results.³³ From that time on, a rapidly growing research field of NHC-metal-catalyzed reactions was ignited, and many of these catalysts displayed remarkable activities in various C-C, C-O, and C-N coupling reactions.³² Although literature reports have shown that most monodentate NHCs give highly effective results in catalysis, concurrent efforts have also been devoted to the construction of multidentate NHC ligands.³⁴ Rösch et al. have shown that a palladium complex with NHC-phosphine ligand was a suitable catalyst for Heck reaction based on theoretical calculations, and during the course of this reaction, the Pd—P bond could be reversibly broken.³⁵ More importantly, a recent result which was reported by Schmidt and co-workers experimentally demonstrated the hemilability of the 3-iminophosphine ligand class.^{36a} The chelation effect imparted on the metals offered extra stability desirable for the design of catalysts with both high stability and activity. Palladium complexes with mixed-donor ligands include those containing NHC-nitrogen,³⁶ NHC-alkoxy/phenoxy,³⁷ NHC-sulfur,³⁸ NHC-phosphine,³⁹ and some of them show increased catalytic activity (Figure 3.6).^{39b,c,g} Among these chelating systems, the NHC-pyridine ligands were investigated most widely, but many reports were of tridentate systems (Figure 3.7).^{28a,40,41}

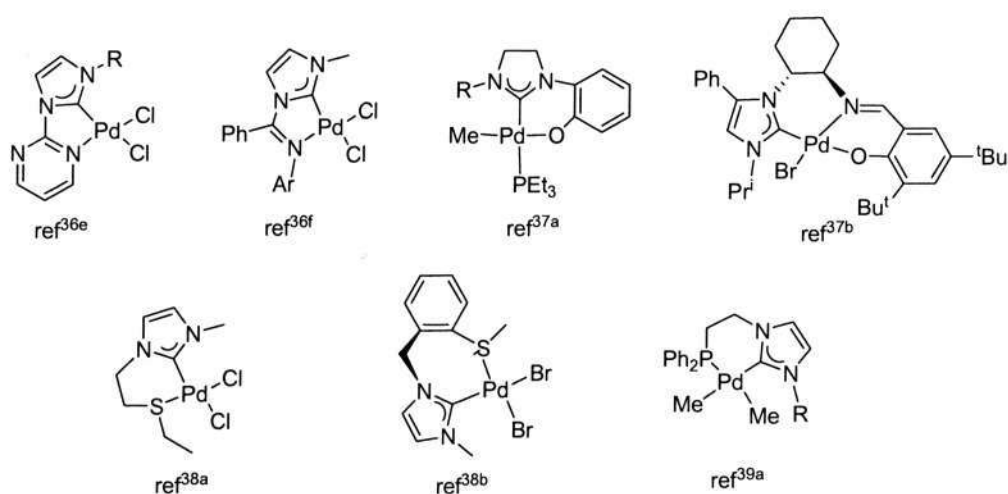


Figure 3.6. Some examples of chelating NHC-palladium systems.

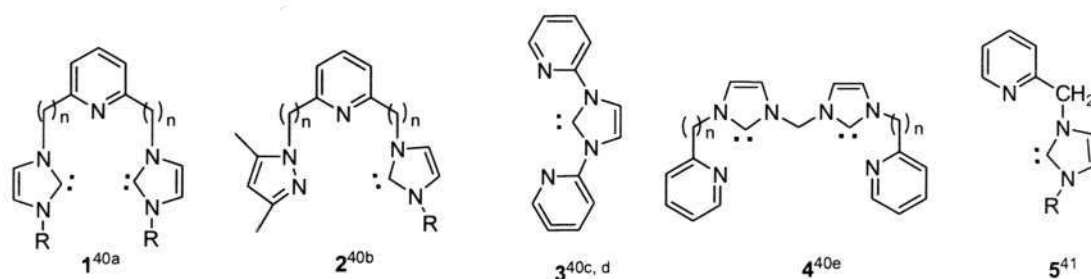
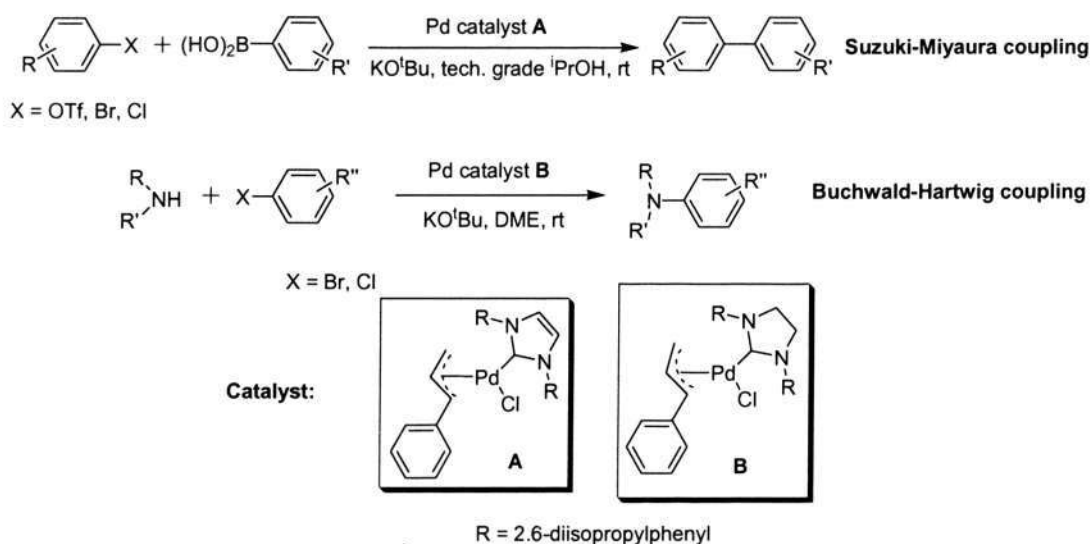


Figure 3.7. Examples of functionalized NHC-pyridine ligands ($n = 0, 1$).

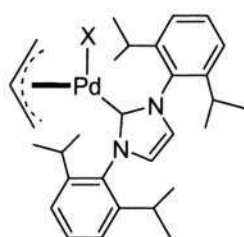
In various palladium complexes, palladium π -allyl complexes have been witnessed as efficient catalysts in the allylic alkylation reaction.⁴² The Nolan group recently demonstrated that air and moisture stable complexes (NHC)Pd(allyl)Cl are efficient catalysts for Suzuki-Miyaura and Buchwald-Hartwig reactions. These reactions can be performed at room temperature with extremely low catalyst loadings (Scheme 3.7).^{43,9a} They found that the substituent at the terminal position of the allyl moiety played an important role towards the catalytic activity, and it was rationalized that the increasing asymmetry of the allyl scaffold gave a more facile activation step of Pd(II) to Pd(0) conversion.^{43a}



Scheme 3.7. NHC-Pd-Allyl complexes catalyzed coupling reactions.

In addition, several groups have studied the dynamic behavior of Pd N-heterocyclic carbene allyl complexes, and the $\eta^3\text{-}\eta^1\text{-}\eta^3$ interchange mechanism is generally accepted.⁴⁴ For example, Pregosin, Albinati, and co-authors prepared a series of $[\text{PdX}(\eta^3\text{-C}_3\text{H}_5)(\text{IPr})]$ complexes (Figure

3.8). The following conclusions have been drawn for this system: (1) the *trans* influence of the carbene carbon seems to be smaller than phosphine-donor ligands (such as PPh_3); (2) the X ligand can affect the rates of η^3 - η^1 allyl isomerization, which is achieved *via* a dissociative rather than an associative mechanism.^{44b} In contrast, reported NHC-Pd-allyl complexes mostly contain monodentate NHC ligands, although there are some examples of hemilabile bidentate ligands (Figure 3.9).⁴⁵ Herein, we are interested in the functionalized bidentate NHC ligands with new nitrogen donors. In this thesis work, a series of palladium complexes bearing new quinoline-tethered NHC ligands (NHC^N) have been synthesized, and the solution dynamics of these complexes have also been studied.



X = Cl (a); Br (b); I (c); N_3 (d); NCO (e); SCN (f); CN (g); OAc (h); OTf (i); 4-Me-pyridine (j).

Figure 3.8. A series of $[\text{PdX}(\eta^3\text{-C}_3\text{H}_5)(\text{IPr})]$ complexes.

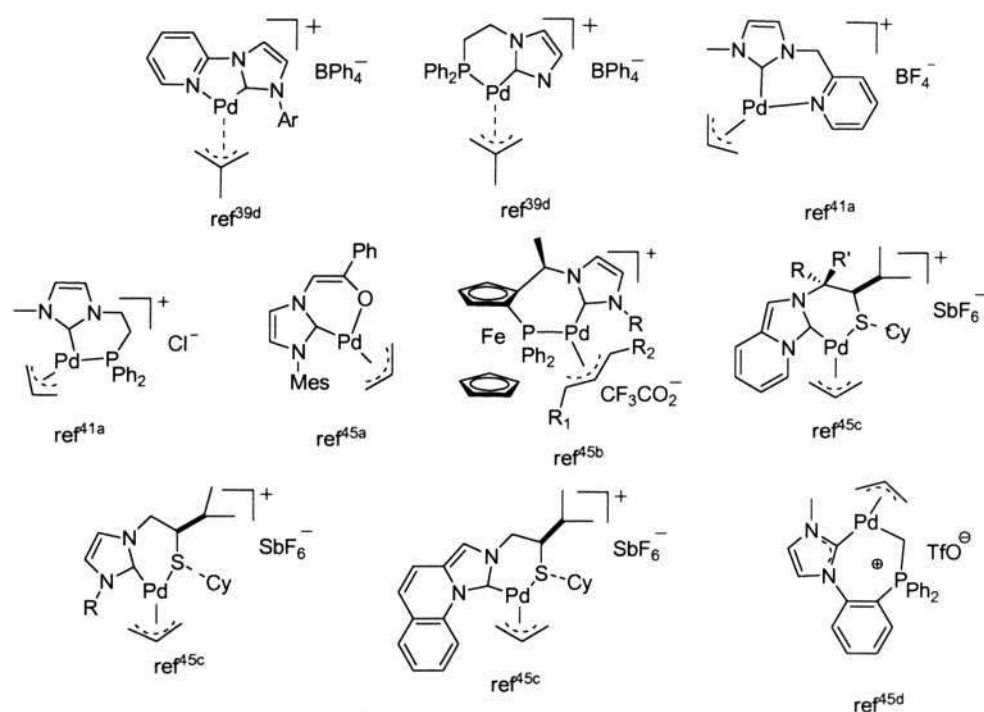
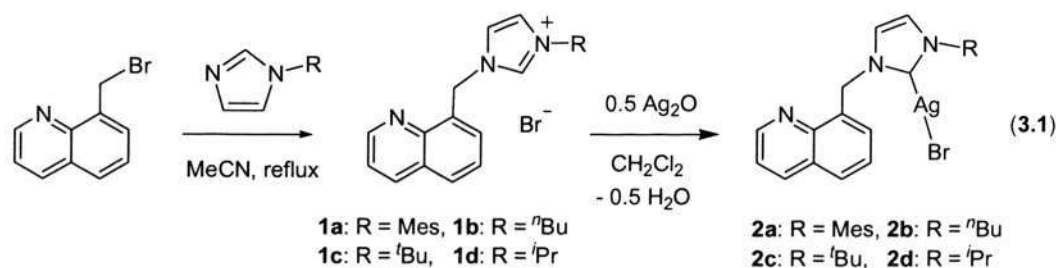


Figure 3.9. Reported well-characterized hemilabile NHC-Pd-Allyl complexes.

3.2. Results and Discussions

3.2.1. Ligand Synthesis and the Corresponding Silver Complexes

Imidazolium salts **1a-d** with a (8-quinolinyl)methyl group were synthesized in high yields by the quaternization of 8-(bromomethyl)quinoline tethered to imidazoles in MeCN. Stirring a mixture of **1a-d** and Ag₂O in CH₂Cl₂ gave a clear solution of silver carbene complexes **2a-d**, which were isolated with yields ranging from 84 to 92% (eq 3.1). All these silver complexes can be kept in the solution for at least two days without appreciable decomposition, and the structure of complex **2a** was confirmed by X-ray crystallography (Figure 3.10), which shows that it is a neutral complex with silver linearly bound to a carbene moiety and a bromide. The reported coordination mode of NHC-silver complexes, as deduced from X-ray crystallography, can be divided into five forms in the solid state: coordinating (C-Ag-X/Y), bridging (C-Ag-X₂), staircase (C-Ag-X₃), halogeno-counterion of type [AgX₂]⁻, and silver NHCs with silver-silver interactions C₂-Ag-Ag(X/Y)₃ (Figure 3.11).^{17c} Figure 3.12 gives examples analogous to **2a**, and all of them were structurally characterized by X-ray crystallography. The silver-carbene bond distances for these complexes are 2.075(7), 2.093(4), 2.09(2), and 2.087(3) Å respectively.⁴⁶⁻⁴⁸ The Ag-Br distances range from 2.401(3) to 2.4584(4) Å, and the C-Ag-Br bond angles are within the range of 169.4(1) (for **B**) to 176.1(2) (for **A**).



Imidazolium salt **4** without any linker was synthesized by N-propylation of **3** using an excess amount of 1-iodopropane (eq 3.2). This quaternization is highly selective and compound **4** was obtained as the only product. The quinoline nitrogen remained intact on the basis of ¹H NMR spectroscopy (CDCl₃) and a low field signal at δ 10.40 (s, 1H) was assigned to the C(2)-H of **4**.

The difference of the reactivity of the two nitrogen atoms likely originates from a combination of electronic and steric effects, where the imidazole nitrogen is favored for both reasons. Compound **4** can also react as a carbene precursor with Ag_2O and complex **5** was isolated in 88% yield.

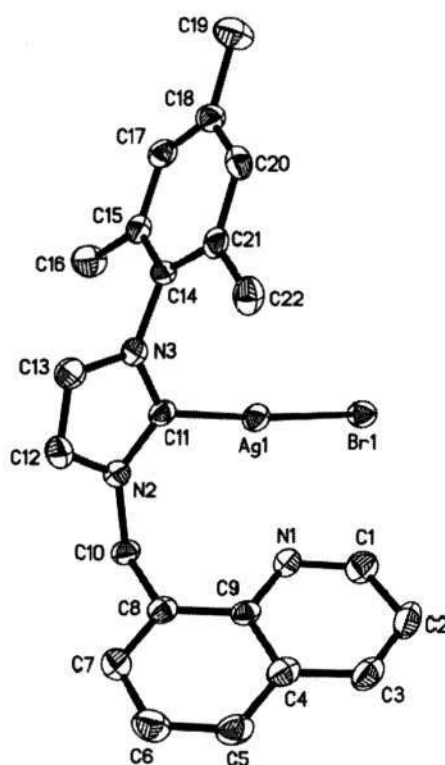
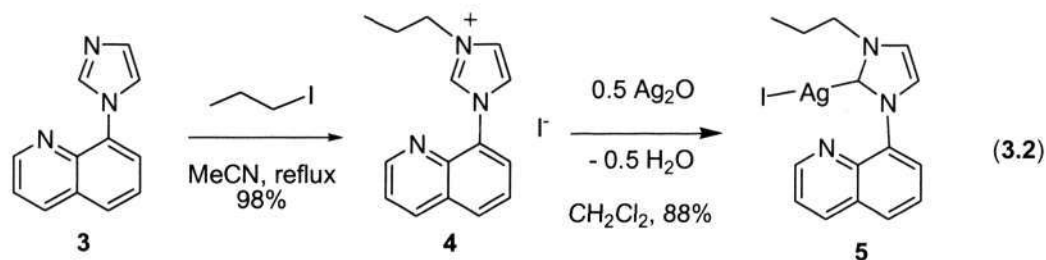


Figure 3.10. Oak Ridge Thermal Ellipsoid Plot (ORTEP) diagram of the molecular structure of complex **2a** at 50% probability level. Selected lengths (\AA) and angles (deg): $\text{Ag}(1)\text{-C}(11)$ 2.087(3), $\text{Ag}(1)\text{-Br}(1)$ 2.4584(4), $\text{C}(11)\text{-Ag}(1)\text{-Br}(1)$ 175.93(8). Temperature 173(2) K, $F(000) = 2048$, orthorhombic, space group Pbca , $a = 14.8533(5)$ \AA , $b = 16.3649(6)$ \AA , $c = 16.9100(7)$ \AA , $\alpha = 90^\circ$, $\beta = 90^\circ$, $\gamma = 90^\circ$, $V = 4110.4(3)$ \AA^3 , $Z = 8$, $d = 1.665$ Mg/m^3 , $\mu = 2.936$ mm^{-1} , Goodness-of-fit on $F^2 = 1.031$.

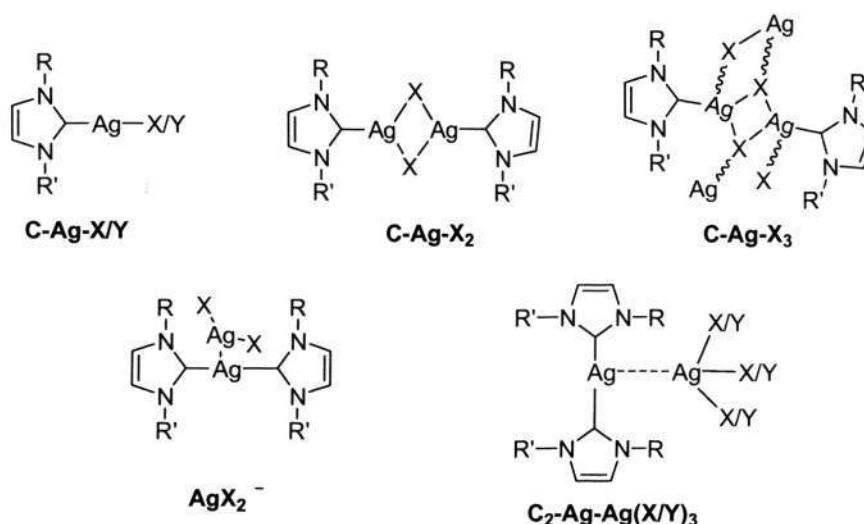


Figure 3.11. Coordination modes of NHC-Ag complexes (X = halide, and Y = non-halide).

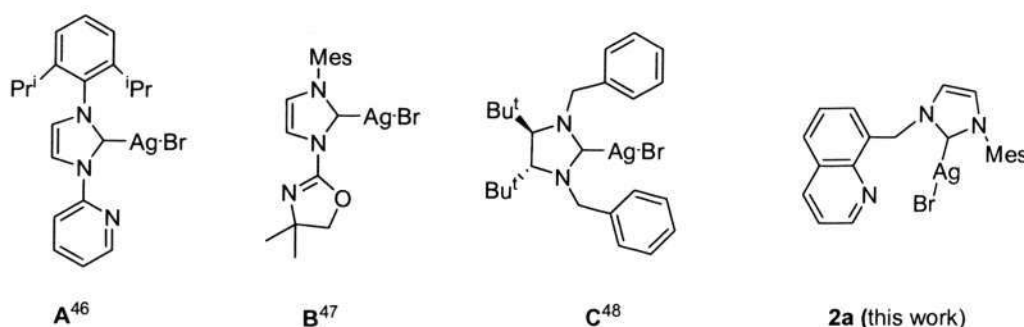


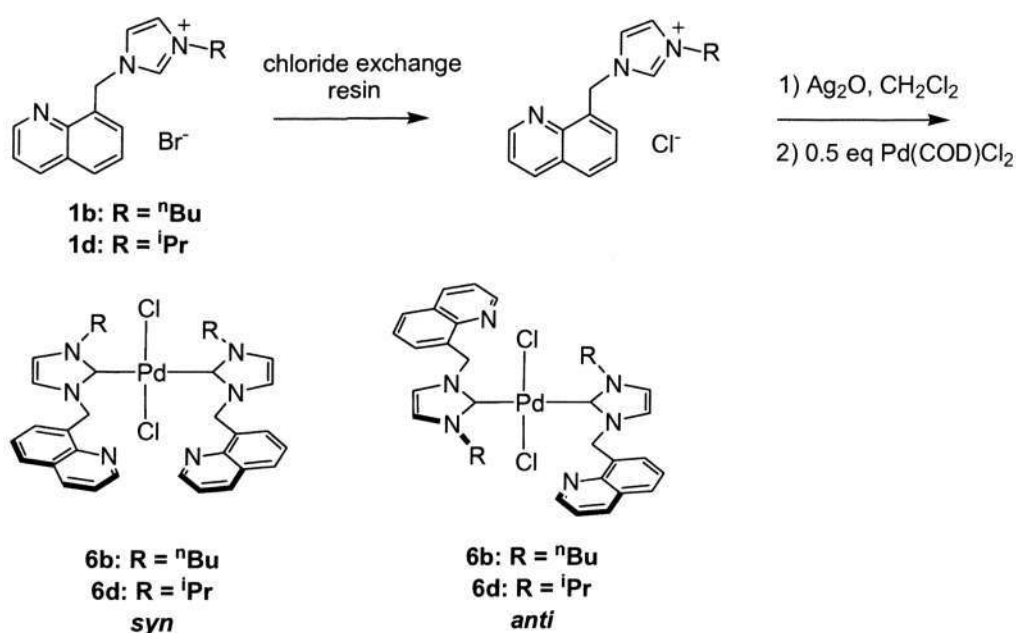
Figure 3.12. Well-characterized NHC-silver complexes with coordinating halide mode.

3.2.2. Neutral NHC-Palladium Dichlorides

Silver complexes **2a-d** and **5** are precursors to prepare other transition-metal-carbene complexes by following the well-established silver transmetalation method.^{17a,40a,49} Addition of an equal molar amount of Pd(COD)Cl₂ to a CH₂Cl₂ solution of silver carbene **2b** immediately afforded a precipitate. ¹H NMR analysis showed that only half of the Pd(COD)Cl₂ was consumed and hence the ratio of the NHC unit to Pd atom is likely 2:1 in the product. This stoichiometry was further confirmed by ESI-MS, which also showed that the product was a mixture of palladium halides [(NHC)₂PdCl₂, (NHC)₂PdClBr, and (NHC)₂PdBr₂], instead of a simple (NHC)₂PdCl₂ complex. ¹H NMR spectroscopy also gave various overlapping peaks contributed from different *iso*-structural halide complexes. Although halide scrambling has been noted in the synthesis of NHC rhodium and iridium complexes *via* silver transmetalation,⁵⁰ there are few reports of halide scrambling in the synthesis of NHC palladium halide complexes. Therefore, it is

advisable to use the same halide during the transmetalation process. On the basis of these results, we optimized the conditions by using the silver carbene chloride to avoid any halide exchange (Scheme 3.8). Furthermore, the ratio of the silver carbene chloride and Pd(COD)Cl₂ was adjusted to 2:1. Thus palladium complexes **6b** and **6d** were synthesized, which could also be obtained from Pd(MeCN)₂Cl₂ or Pd(PhCN)₂Cl₂ in similar yields.

X-ray quality crystals of **6b** were obtained by the slow diffusion of Et₂O into its CH₂Cl₂ solution. X-ray crystallographic analysis of **6b** revealed the *trans* square planar geometry of the palladium center (Figure 3.13). Complex **6b** is C_i symmetrical in the solid state and the two imidazole rings are essentially perpendicular to the Pd coordination plane, giving an *anti* conformer. The Pd-carbene distances [2.020(4) Å] agree well with the distances found for similar bis-carbene Pd complexes with the range from 2.015(2) to 2.037(1) Å.^{19b,38a,b, 51}



Scheme 3.8. The synthesis of neutral palladium complexes.

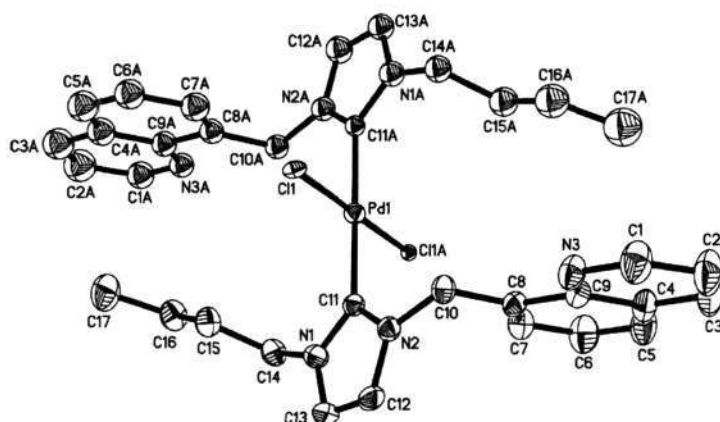


Figure 3.13. ORTEP diagram of the molecular structure of complex **6b** at 50% probability level. Selected lengths (Å) and angles (deg): Pd(1)-C(11) 2.020(4), Pd(1)-Cl(1) 2.3744(8), C(11)-Pd(1)-C(11A) 180.0(3), Cl(1)-Pd(1)-Cl(1A) 180.00(6), C(11)-Pd(1)-Cl(1) 90.71(12). Temperature 173(2) K, F(000) = 728, monoclinic, space group P2(1)/n, $a = 12.1693(5)$ Å, $b = 8.4018(4)$ Å, $c = 16.8050(7)$ Å, $\alpha = 90^\circ$, $\beta = 106.463(3)^\circ$, $\gamma = 90^\circ$, $V = 1647.77(12)$ Å³, $Z = 2$, $d = 1.427$ Mg/m³, $\mu = 0.758$ mm⁻¹, Goodness-of-fit on $F^2 = 1.074$.

Information on the solution structure of **6b** was obtained from its NMR spectra. Here two sets of signals were observed in the ¹H NMR spectrum with 1.0 to 0.97 ratio in CDCl₃. The presence of two sets of peaks was also evidenced by the ¹³C NMR spectrum (acetone-*d*₆) with two characteristic Pd-C_{carbene} signals (δ 171.6 and 171.3). In either set the methylene protons are equivalent and resonate as a singlet in the ¹H NMR spectrum, indicating that the imidazole plane represents a plane of symmetry on the time average. It follows that there is a free rotation about the C(8)-C(10) bond in the quinoline substituent. While one set of signals is explained by the approximately C_{2h} symmetrical structure in solution evident from the X-ray analysis (*anti* conformer), the second set is attributed to the C_{2v} symmetrical conformational isomer (*syn* conformer). Hence, the barrier of the rotation about the Pd-C_{carbene} bond must be high in the NMR time scale. Indeed, while all lines are sharp at ambient temperature, they are broadened (but not coalesced) at 50 °C, so that a slow exchange between the *anti* and *syn* conformers proceeds by the Pd-C_{carbene} rotation. The presence of any *cis*-(NHC)₂PdCl₂ structure is unlikely since here the methylene protons should be diastereotopic so long as the NHC planes are perpendicular to the coordination plane, a reasonable assumption based on closely related reports.^{36b,c,41e} It is indicated

that the rotation barriers of Pd-C(carbene) bond and the relative abundance of the two orientations might be changed with the N-substituents, which affect the orientation of two substituents in the same or the opposite directions (Figure 3.14).^{36b} Similar spectra were also observed for **6d** (R = ⁱPr).

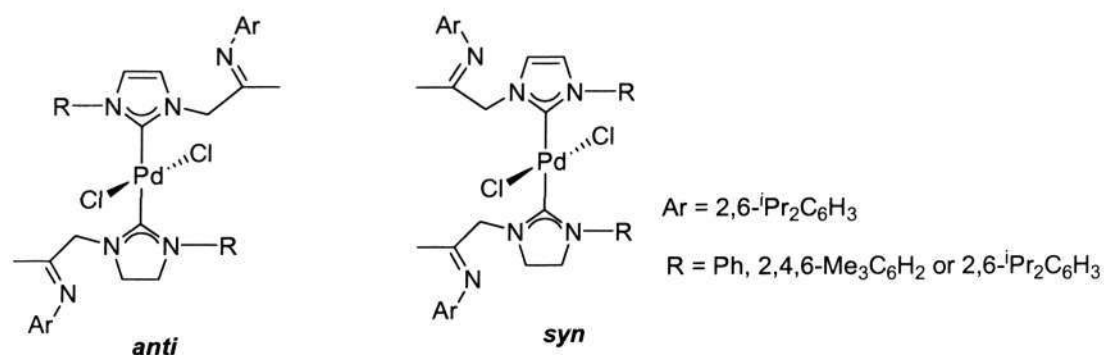
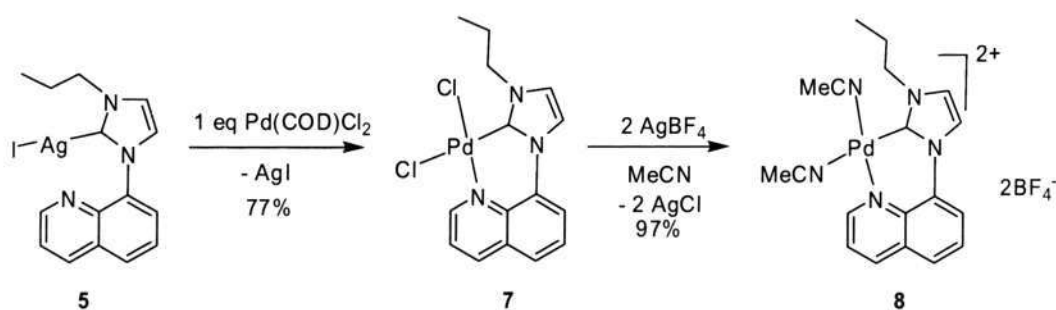


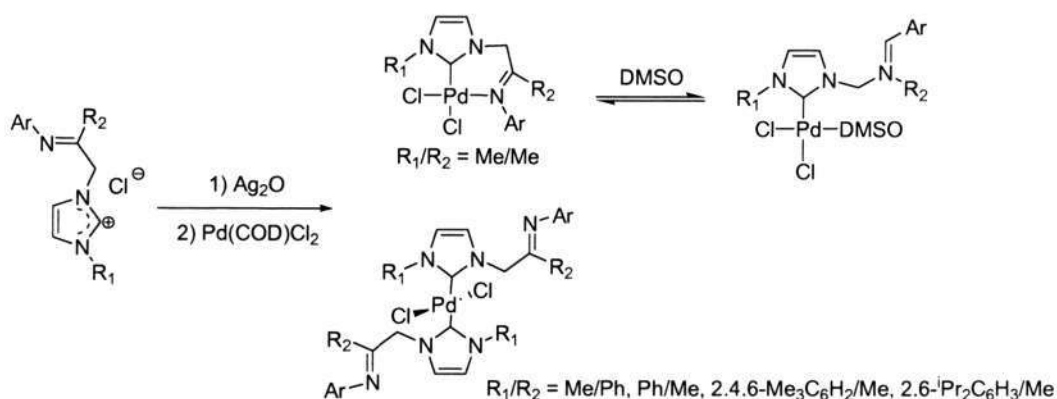
Figure 3.14. Structure analogous to complexes **6b**, **6d**.^{36b}

When Pd(COD)Cl₂ was treated with 1 equiv of **5** in CH₂Cl₂, the COD ligand was easily displaced by the carbene to afford *cis*-(NHC)PdCl₂ (**7**) in 77% yield, bearing a chelating NHC-quinoline ligand (Scheme 3.9). It should be noted that in this reaction, maintaining the *cis*-PdCl₂ entity, no halide exchange was observed. In the ¹³C NMR spectrum of **7**, the carbene resonates at δ 149.2 and is thus more shielded than that in complexes **6b** and **6d**. Treatment of **7** with 2 equiv of AgBF₄ in quantitatively yield gave complex **8**. In the ¹H and ¹³C NMR spectra of **8** (CD₃CN), the signal of free CH₃CN [δ 1.90 (¹H) and 1.76 (¹³C)] was found with the expected intensity, indicating exchange between the CH₃CN ligands and the CD₃CN solvent.

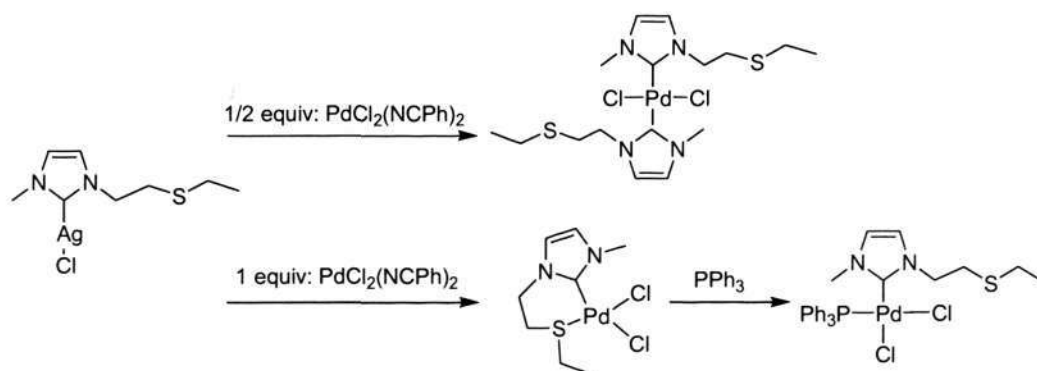


Scheme 3.9. Routes to synthesize palladium complexes.

As demonstrated in the above hemilabile N⁺NHC systems, the coordination mode of the ligands was dramatically affected by the identity of the ligand. With a CH₂ linker in the N⁺NHC systems, the formation of seven-membered chelation ring is probably not favorable. This was supported by related examples from the literature.^{36b,c,41e} Tilset et al. studied a series of iminocarbene ligands and their coordination modes in the corresponding palladium complexes.^{36b,c} It is pointed out that the steric requirements of the ligand system and solvent effects are two important factors that strongly influence the interconversion between chelating κ^2 -C, N and monodentate κ^1 -C species (Scheme 3.10). In 2000, Cavell and co-workers reported palladium bidentate carbene complexes bearing pyridine or carbonyl functional groups. In these examples, the coordination mode and the conformation of the products vary with different palladium precursors giving rise to *cis*- or *trans*-, mono- or *bis*-carbene palladium complexes. They also proved that these hemilabile carbene palladium complexes are active catalysts for C-C coupling reactions.^{41e} Two recent examples showed that the coordination modes of the products could be adjusted by molar ratio of carbene to palladium precursor. If a phosphine ligand such as PPh₃ was added to the chelating product, Pd-S bond could be cleaved with the formation of a monodentate NHC-phosphine complex (Scheme 3.11).^{38a,b}



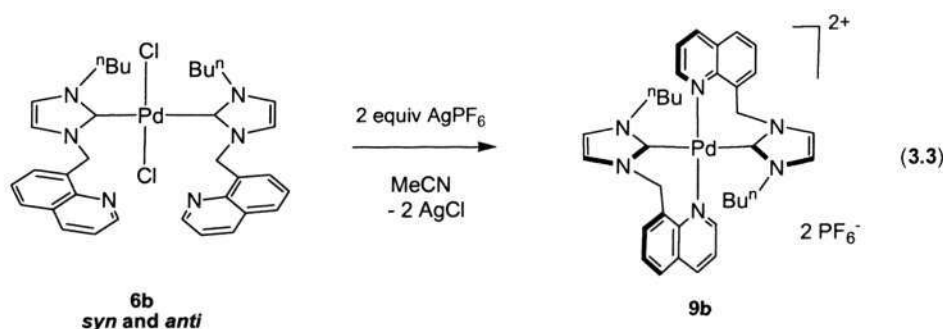
Scheme 3.10. Substituents and solvent effects to the formation of palladium complexes.



Scheme 3.11. Molar ratio effects (carbene ligand to palladium precursor) to the formation of chelating or non-chelating palladium complexes.

3.2.3. Cationic NHC-Quinoline Palladium Complexes

Complexes with chelating NHC-N ligands can be obtained by chloride abstraction of **6b** using 2 equiv of AgPF_6 in MeCN (eq 3.3). Thus dicationic palladium complex **9b** was obtained in 98% yield and was spectroscopically and crystallographically characterized. Only one set of peaks was observed in the ^1H NMR spectrum. The methylene linker protons are diastereotopic ($2J_{\text{HH}} = 15.6$ Hz) and so are all the methylene protons in the $\text{N-CH}_2\text{CH}_2\text{CH}_2\text{Me}$ unit, indicating that the imidazole ring is no longer a plane of symmetry. X-ray crystallography further confirmed the identity of the C_i symmetrical **9b** (Figure 3.15). This rigid boat-type conformation is the only one the ring can attain. While the individual palladacycle is chiral, a *meso* structure is obtained for the whole complex because of the C_i point group symmetry. Indicative of some ring strain, the two aromatic rings in the quinoline moiety are slightly twisted, and the palladium atom is not positioned exactly along the C(11)-N(3)-C(15) bisector, but it is oriented away from the NHC unit. Related 7-membered NHC-containing metallacycles have been reported for palladium and iridium.⁵²



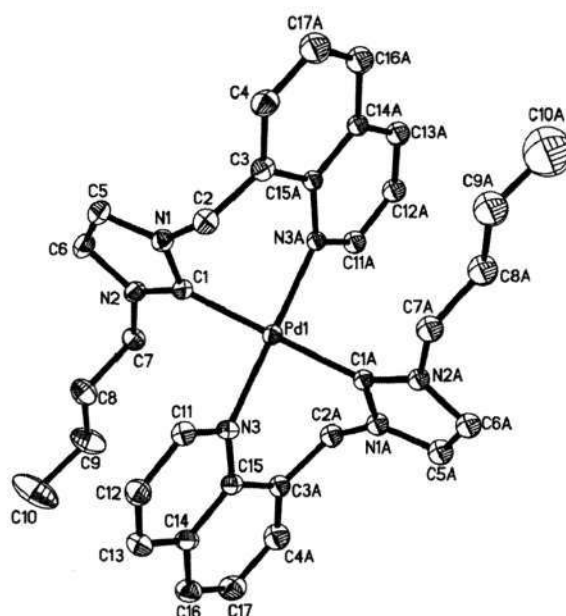
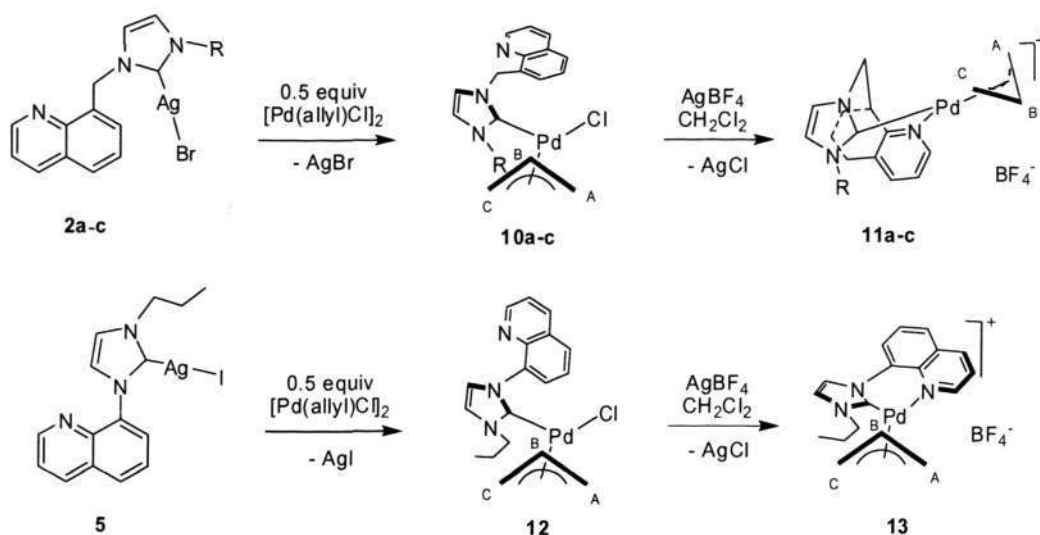


Figure 3.15. ORTEP diagram of the molecular structure of complex **9b** (cation only) at 50% probability level. Selected lengths (Å) and angles (deg): Pd(1)-C(1) 2.016(2), Pd(1)-N(3) 2.0634(19), N(3A)-Pd(1)-N(3) 180.000(1), C(1)-Pd(1)-C(1A) 180.000(1), N(1)-C(1)-N(2) 105.66(19), N(1)-C(1)-Pd(1) 118.71(16). Temperature 173(2) K, F(000) = 468, Triclinic, space group P-1, $a = 10.0533(4)$ Å, $b = 10.6877(8)$ Å, $c = 10.7290(5)$ Å, $\alpha = 108.459(3)^\circ$, $\beta = 108.014(2)^\circ$, $\gamma = 107.082(2)^\circ$, $V = 936.75(9)$ Å³, $Z = 1$, $d = 1.643$ Mg/m³, $\mu = 0.676$ mm⁻¹, Goodness-of-fit on $F^2 = 1.108$.

3.2.4. Neutral NHC-Pd-Allyl Complexes

Synthesis and Molecular Structures of Neutral Palladium NHC η^3 -Allyl Complexes

Silver transmetalation method was also applied to the preparation of NHC-Pd-allyl complexes (Scheme 3.12). Silver carbene complexes **2a-c** rapidly reacted with 0.5 equiv of $[\text{Pd}(\eta^3\text{-allyl})\text{Cl}]_2$ in CH_2Cl_2 to give the corresponding $\text{Pd}(\text{NHC})(\text{allyl})\text{Cl}$ complexes **10a-c**. Monodentate complex **12** was also synthesized following the same method (scheme 3.12) and no halide scrambling was observed.



Scheme 3.12. Routes for the synthesis of cationic NHC-palladium-allyl complexes.

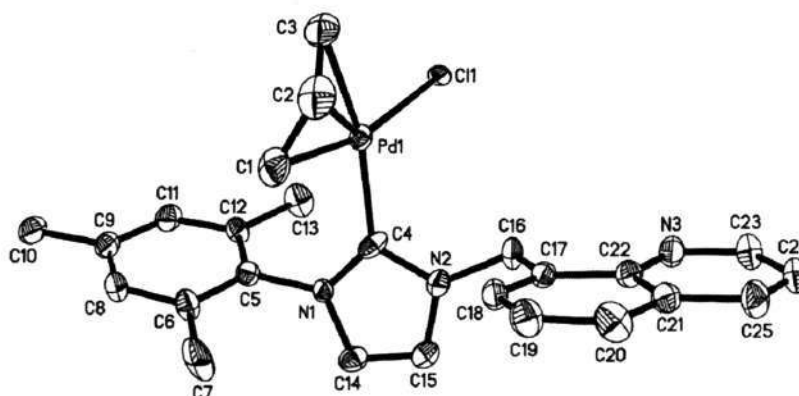


Figure 3.16. ORTEP diagram of the molecular structure of complex **10a** at 50% probability level. Selected lengths (Å) and angles (deg): Pd(1)-C(1) 2.116(6), Pd(1)-C(2) 2.126(5), Pd(1)-C(3) 2.202(5), Pd(1)-C(4) 2.054(5), Pd(1)-Cl(1) 2.4163(10), N(1)-C(4)-Pd(1) 129.7(3), N(2)-C(4)-Pd(1) 124.9(4). Temperature 173(2) K, F(000) = 520, monoclinic, space group P2(1), $a = 7.9796(2)$ Å, $b = 12.7023(4)$ Å, $c = 11.7635(4)$ Å, $\alpha = 90^\circ$, $\beta = 106.5800(10)^\circ$, $\gamma = 90^\circ$, $V = 1142.76(6)$ Å³, $Z = 2$, $d = 1.483$ Mg/m³, $\mu = 0.945$ mm⁻¹, Goodness-of-fit on $F^2 = 1.055$.

X-ray crystallography unambiguously confirmed the structures of complexes **10a** (Figure 3.16) and **10c** (Figure 3.17). For **10c**, two molecules with enantiomeric relation cocrystallized, and here only one of them is discussed. The Pd-C_{carbene} distances in **10a** [2.054(5) Å] and **10c** [2.069(4) Å] are similar. The trihapticity of the allyl group follows from the three Pd-C(allyl) distances ranging from 2.116(6) to 2.202(5) Å for **10a** and from 2.121(5) to 2.198(5) Å for **10c**. The Pd(1)-C(3) bond in **10a** and the Pd(1)-C(3) bond in **10c** are slightly longer because of the

imbalance of the *trans* influence of NHC and Cl, resulting in shortening of the Pd-C bond *trans* to Cl and lengthening of the bond *trans* to the NHC. In both structures C(2) of the allyl group and the *tert*-Bu or Mes substituent are oriented in an *anti* fashion with respect to the palladium coordination plane. In comparison with palladium NHC allyl complexes bearing symmetric substituent in the literature, nothing particular was noted for the structures of **10a** and **10c**.^{43a,44a,53}

Solution Dynamics of 10a and 10b: NMR spectroscopy shows that complexes **10a-c** all have fluxionality to different extents on the NMR time scale depending on the bulk of the substituents (wing tip groups). The following common features were observed for the ¹H and ¹³C spectra (room temperature, CDCl₃) of **10a** (R = Mes) and **10b** (R = ⁿBu): (1) there is simply one set of signals in both the ¹H and ¹³C spectra; (2) the protons of the methylene linkers resonate as a singlet, which has been reported for other Pd(allyl)(NHC) complexes;^{41a} and (3) three sharp signals and two broad signals are observed for the five allyl protons, with the broad signals attributed to the *syn* and *anti* protons at the allyl terminus *trans* to the chloride (C_c, see Scheme 3.7 for the labelling scheme and Table 3.1 for signal assignment). Exactly the same pattern was also observed for complex **12** (see Figure 3.18 for the selective broadening of signals). The broadening pattern of the allyl groups in complexes **10a** and **10b** suggests that there is *syn/anti* exchange only between two protons in germinal orientation. This is consistent with a selective η^3 to η^1 rearrangement of the allyl ligand, possibly under electronic control. The η^1 -allyl intermediate then undergoes C-C single bond rotation followed by re-formation of the η^3 complex (Scheme 3.13). The fact that the CH₂ linker protons are equivalent in solution can be accounted for by this selective η^3 to η^1 rearrangement together with the free Pd-C_{carbene} rotation. If only the NHC ring rotates, the complex remains chiral and the CH₂ remain diastereotopic. However, the concurrent η^3 - η^1 - η^3 rearrangement process should lead to enantiomerization of this complex and to the equivalence of the CH₂ protons. This type of selective *syn/anti* exchange has been observed on many occasions and this process could be associative or dissociative in mechanism.^{43a,b,53-55}

Pörschke et al. recently reported selective line-broadening of allyl protons of Pd(allyl)(IPr)Cl [IPr = *N,N*-bis(2,6-diisopropylphenyl)imidazol-2-ylidene] only in donor solvents such as THF, whereas no solvent dependence of the ¹H and ¹³C NMR spectra was observed for Pd(allyl)(IPr)Me.^{44a} Here, the lability of the anionic ligand (Cl vs Me) plays an important role.

Moreover, Albinati and Pregosin analyzed the selective *syn/anti* exchange of Pd(allyl)(IPr)Br using phase-sensitive ^1H NOESY spectroscopy and have concluded that the conversion is dissociative in CD_2Cl_2 . The rate constant of the allyl proton exchange was determined to be $0.8 \pm 0.1 \text{ s}^{-1}$ at 298 K, although all the allyl proton signals are seemingly sharp.^{44b}

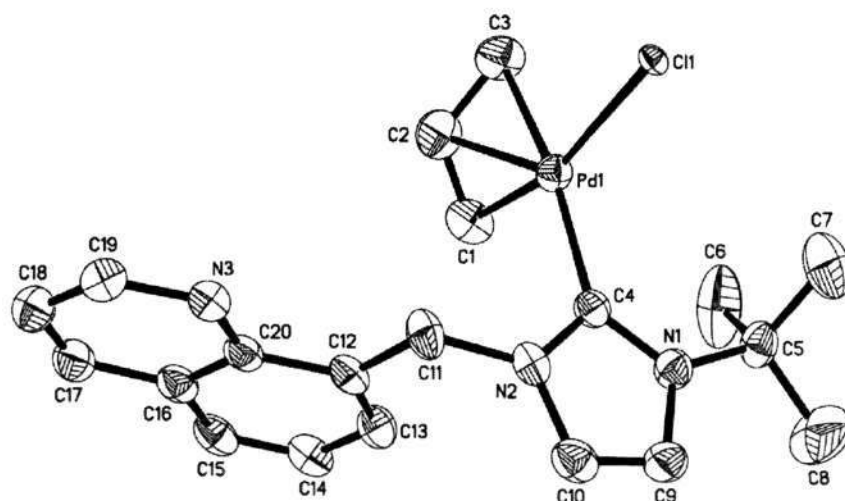
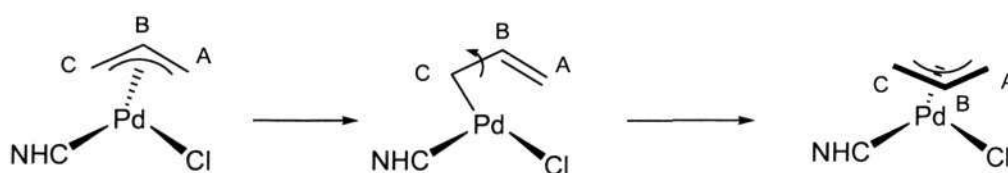


Figure 3.17. ORTEP diagram of the molecular structure of complex **10c** at 50% probability level. Selected lengths (\AA) and angles (deg): Pd(1)-C(1) 2.121(5), Pd(1)-C(2) 2.121(5), Pd(1)-C(3) 2.198(5), Pd(1)-C(4) 2.069(4), Pd(1)-Cl(1) 2.4209(9), Cl(1)-Pd(1)-C(4) 98.59(12), N(1)-C(4)-Pd(1) 133.4(3), N(2)-C(4)-Pd(1) 122.6(3). Temperature 173(2) K, $F(000) = 912$, Triclinic, space group P-1, $a = 11.3527(5) \text{ \AA}$, $b = 11.5964(5) \text{ \AA}$, $c = 17.1348(7) \text{ \AA}$, $\alpha = 85.099(2)^\circ$, $\beta = 77.932(2)^\circ$, $\gamma = 63.716(2)^\circ$, $V = 1977.81(15) \text{ \AA}^3$, $Z = 4$, $d = 1.505 \text{ Mg/m}^3$, $\mu = 1.080 \text{ mm}^{-1}$, Goodness-of-fit on $F^2 = 1.062$.



Scheme 3.13. η^3 - η^1 - η^3 rearrangement process.

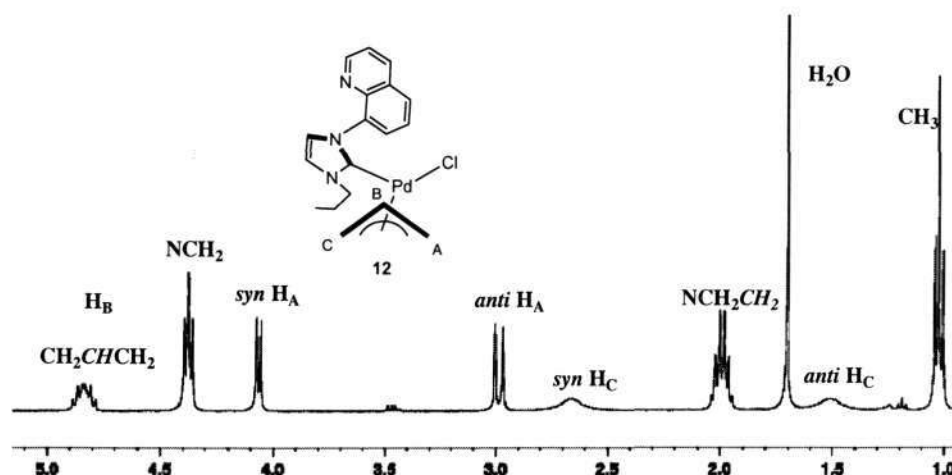


Figure 3.18. Part of the ^1H NMR spectrum of complex **12**.

Solution Dynamics of 10c: The solution dynamic behavior for **10c** ($R = ^i\text{Bu}$), however, is different from that of **10a** and **10b**. Both ^1H and ^{13}C NMR spectra at room temperature give two sets of peaks with a ratio of 1:1.13 (CDCl_3) based on proton signal integration. In either set of proton peaks, the linker CH_2 protons are diastereotopic. We note that while there are two independent molecules in the crystals comprising an enantiomeric pair, these are not distinguishable by solution NMR. However, solution NMR does show that two different C_1 symmetrical molecules are present, so they must have a different origin, most likely contributed by different rotamers in solutions. These two rotamers are caused by hindered rotation of the NHC ligand about the $\text{Pd-C}_{\text{carbene}}$ bond, which puts the quinolynyl group of one rotamer closer to the *syn* proton at C_C (the conformation displayed by the molecules in the solid-state as determined by X-ray crystallography, Figure 3.17), but away from it in the second rotamer. As a contrast, only the *syn* proton on C_C is broadened and this signal is attributed to the quinolynyl group in one isomer, but not in the other (Table 3.1). The selective broadening pattern here likely originates from a partially hindered rotation along the $\text{Pd-C}_{\text{carbene}}$ bond in this conformer, and only the chemical environment of this *syn* proton on C_C is more affected when the NHC ligand undergoes local motion.

Table 3.1. Collective ^1H and ^{13}C data for palladium allyl complexes in CDCl_3

complex	allyl ^1H and ^{13}C								^1H (CH_2)	^{13}C (CH_2)	^{13}C (carbene)
	A_{syn}	A_{anti}	B	C_{syn}	C_{anti}	$^{13}\text{C}_A$	$^{13}\text{C}_B$	$^{13}\text{C}_C$			
10a	4.06	2.95	4.87	2.9	1.64	72.2	114.4	48.3	6.29	50.4	181.3
				(br)	(br)						
10b	4.26	3.24	5.24	3.30	2.23	72.7	114.6	48.1	6.07	51.0	179.6
				(br)	(br)						
10c (set a)	4.18	3.28	5.22	3.41	2.26	71.1 ^b	113.8 ^b	50.3	6.20, 6.30	58.1	179.0
10c (set b)	4.18	3.18	5.21	3.26	2.19	70.9 ^b	113.4 ^b	50.2	5.91, 6.53	58.0	178.7
				(br)							
11b^a	4.48	3.73	5.84	3.70	2.89	78.1	119.3	46.2	6.88	52.4	174.8
	(br)	(br)	(br)	(br)	(br)				(br)		(br)
11c (set a)	4.20	3.64	5.86	3.74	2.94	75.3 ^b	118.9 ^b	51.3 ^b	[5.62 (<i>endo</i>) + 7.35 (<i>exo</i>)] ^b	57.9 ^b	173.8 ^b
11c (set b)	4.42	3.55	5.70	3.91	2.83	74.7 ^b	117.4 ^b	50.7 ^b		54.1 ^b	173.2 ^b
									[5.40 (<i>endo</i>) + 7.00 (<i>exo</i>)] ^b		
12	4.07	2.98	4.83	2.67	1.51	71.6	114.3	49.0	-	52.8	180.7
				(br)	(br)						
13^c	4.36	3.80	5.82	4.04	3.05	- ^d	- ^d	- ^d	-	- ^d	- ^d
14^c	4.22	3.65	5.69	3.93	2.94	76.6	121.5	48.2	-	-	174.6
				(br)	(br)						

^a 55 °C, ^b unable to assign to set a or set b, ^c in acetone- d_6 , ^d poor solubility in acetone for ^{13}C NMR analysis, ^e in CD_3CN

3.2.5. Cationic NHC-Pd-Allyl Complexes

The chloride complexes **10a-c** and **12** readily undergo halide abstraction by AgBF_4 to afford ionic complexes **11a-c** and **13**, respectively (Scheme 3.12). The isolated products were fully characterized by elemental analysis and NMR spectroscopy, and X-ray crystallography further confirmed the structures of complexes **11a**, **11b**, and **11c** (Figure 3.19-3.21). In all cases, a chelating NHC-N ligand and an η^3 -allyl group complete the coordination sphere of the Pd(II) center. The Pd-NHC distances are in the normal range from 2.024(4) to 2.051(6) Å (Table 3.2). The allyl ligands adopt an *endo* structure and the seven-membered palladacycles exhibit boat

conformations analogous to that in **9b**. Both the NHC ring and the quinoline plane are nearly perpendicular to the Pd coordination plane as a result of the twist in a boat conformation. The Pd is in plane with the NHC ring, indicated by the summation of the three angles around C(14) being 360.0°. However, an in-plane distortion is quite obvious. This type of yaw distortion was recently described by Crabtree⁵⁶ and the extent of distortion was defined by $\theta = \frac{1}{2}(\alpha - \beta)$ (Figure 3.22). θ values ranging up to 15 deg were previously observed for carbene complexes.⁵⁷ Here θ is 6.9, 10.55, and 14.4 deg for **11a**, **11b**, and **11c** respectively, and $\theta = 14.4^\circ$ for complex **11c** is close to the upper limit.³⁴

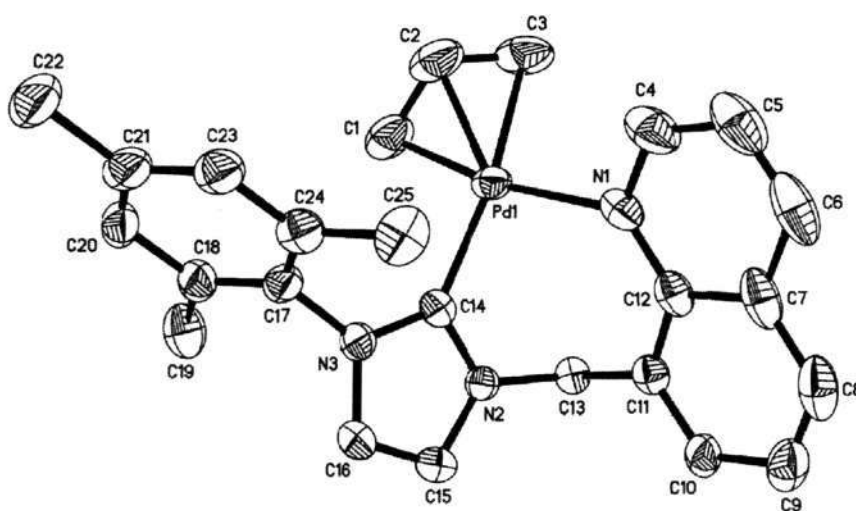


Figure 3.19. ORTEP diagram of the molecular structure of complex **11a**•CH₂Cl₂ (cation only) at 50% probability level. Temperature 173(2) K, F(000) = 652, Triclinic, space group P-1, $a = 9.0457(5)$ Å, $b = 10.8883(5)$ Å, $c = 15.0034(8)$ Å, $\alpha = 79.179(2)^\circ$, $\beta = 78.479(3)^\circ$, $\gamma = 75.660(2)^\circ$, $V = 1387.87(12)$ Å³, $Z = 2$, $d = 1.547$ Mg/m³, $\mu = 0.908$ mm⁻¹, Goodness-of-fit on $F^2 = 1.125$.

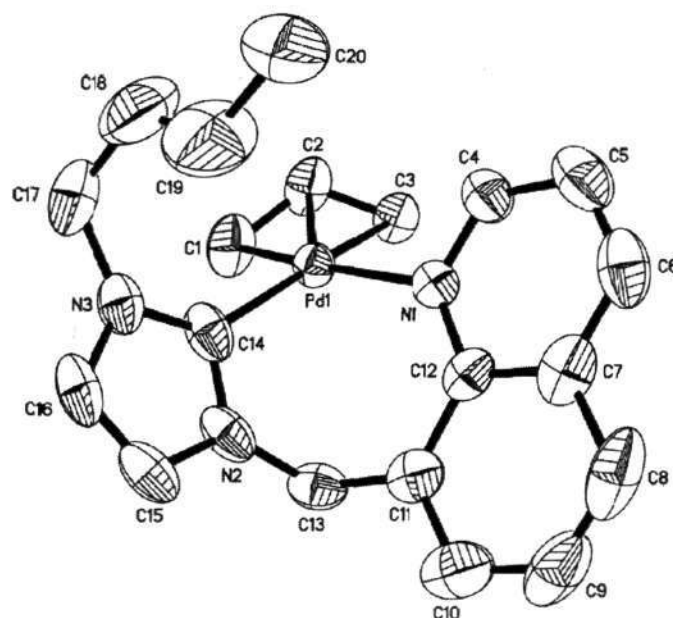


Figure 3.20. ORTEP diagram of the molecular structure of complex **11b** (cation only) at 50% probability level. Temperature 173(2) K, $F(000) = 1008$, orthorhombic, space group $P2(1)2(1)2(1)$, $a = 10.9692(3)$ Å, $b = 13.67242(4)$ Å, $c = 14.1572(4)$ Å, $\alpha = \beta = \gamma = 90.0^\circ$, $V = 2123.51(10)$ Å³, $Z = 4$, $d = 1.563$ Mg/m³, $\mu = 0.919$ mm⁻¹, Goodness-of-fit on $F^2 = 1.043$.

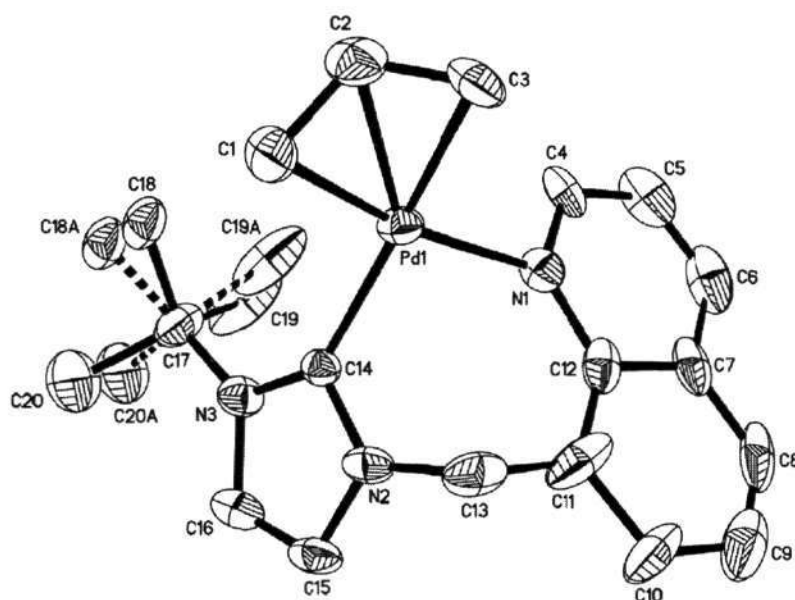


Figure 3.21. ORTEP diagram of the molecular structure of complex **11c** (cation only) at 50% probability level (the t-Bu group is disorder). Temperature 173(2) K, $F(000) = 1008$, orthorhombic, space group $P2(1)2(1)2(1)$, $a = 10.9198(5)$ Å, $b = 12.8986(6)$ Å, $c = 14.6494(7)$ Å, $\alpha = \beta = \gamma = 90.0^\circ$, $V = 2063.37(17)$ Å³, $Z = 4$, $d = 1.608$ Mg/m³, $\mu = 0.945$ mm⁻¹, Goodness-of-fit on $F^2 = 1.089$.

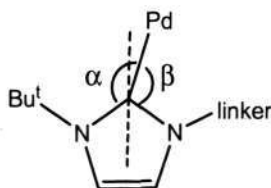


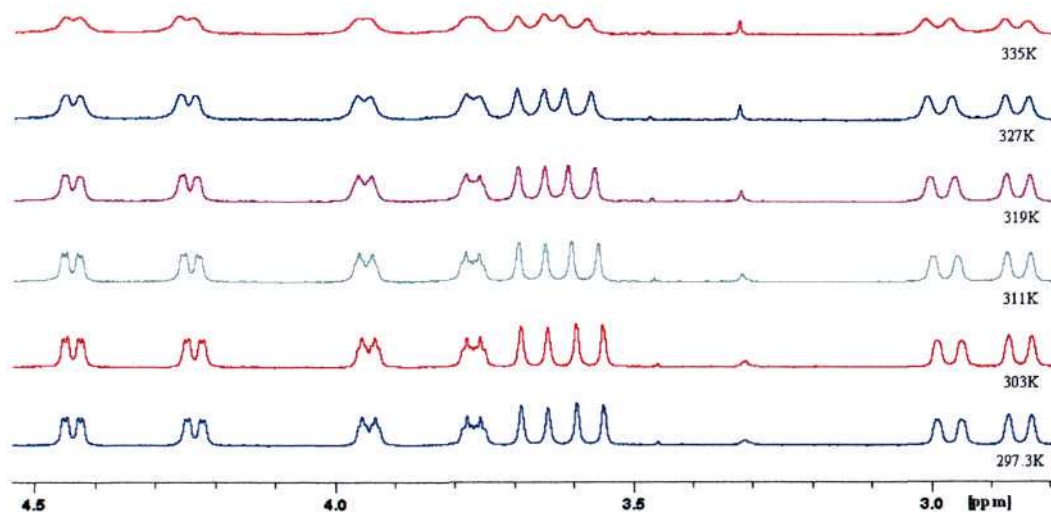
Figure 3.22. In-plane distortion of the carbene in complex **11a-c**.

Complexes **11a-c** all show dynamic behavior in the NMR time scale in their solutions. For complex **11a**, significant line broadening of exchangeable protons, such as the allyl protons and the N-CH in the quinoline moiety, was observed at room temperature in ^1H NMR spectroscopy and there is only one set of proton peaks. These results suggest that room temperature is above the coalescence temperature and the exchange is in the fast regime of dynamic NMR spectroscopy. For both complexes **11b** and **11c**, two sets of proton peaks with 1:1 ratio were observed at ambient temperature (Table 3.1). The signals of **11b** showed significant line broadening and poor resolution of virtually all signals. Coalescence of the allyl protons was achieved at 55 °C in the ^1H NMR spectrum (Table 3.1). $^{13}\text{C}\{^1\text{H}\}$ NMR spectrum of **11b** also showed two broad exchanging carbene signals (δ 174.9 and 174.3) at room temperature, but they coalesced at 55 °C (δ 174.9).

The dynamics of **11c** were studied in more detail. Here, the two sets of proton peaks were observed together with diastereotopic CH_2 linker protons in each conformer. They showed essentially no line-broadening at ambient temperature, but line-broadening occurred at elevated temperatures (Figure 3.23). Two sets of peaks were also observed in the ^{13}C NMR spectra. Different solvents (CDCl_3 , CD_2Cl_2 , and $\text{DMSO}-d_6$) have no significant effects on the relative amounts of these two species. The lack of solvent effects suggests that the two species are probably not examples of $\kappa^2\text{-C,N}$ (bidentate) versus $\kappa^1\text{-C}$ (monodentate) isomers.^{36b} The five allyl protons and the methylene linker protons were all well resolved in ^1H NMR spectroscopy, and the kinetic parameters were measured by VT NMR line-width analysis (Figure 3.23). The Eyring plot gave $\Delta H^\ddagger = 19.0$ kcal/mol and $\Delta S^\ddagger = 3.2$ eu for this exchange process (average of two measurements, Table 3.3-3.4 and Figure 3.24-3.25).

Table 3.2. Selected bond distances (Å) and angles (deg) for compound **11a**, **11b**, and **11c**

Param	11a	11b	11c
Pd-C _{carbene}	2.024(4)	2.028(6)	2.051(6)
Pd-C(1)	2.094(5)	2.067(6)	2.123(6)
Pd-C(2)	2.147(5)	2.102(6)	2.145(7)
Pd-C(3)	2.206(5)	2.200(6)	2.169(7)
C _{carbene} -Pd-N(1)	93.00(5)	89.5(3)	88.8(2)
N(2)-C _{carbene} -Pd	120.6(3)	116.4(5)	113.2(4)
N(3)-C _{carbene} -Pd	134.4(3)	137.5(6)	142.0(5)

**Figure 3.23.** Part of the VT NMR spectra of **11c** in CDCl₃.**Table 3.3.** Spectroscopic data based on the signal at δ 3.66

T (K)	1/T (1/K)	$W_{1/2}$ (Hz)	$\kappa = \pi \times \Delta W_{1/2}$ (Hz)	$\ln(\kappa/T)$
263	0.003802	2.494		
303	0.003300	2.671	0.556	-6.3006
311	0.003215	2.921	1.34	-5.4460
319	0.003135	3.424	2.92	-4.6930
327	0.003058	4.486	6.26	-3.9561
335	0.002985	6.537	12.7	-3.2724

Figure 3.24. Eyring Plot of complex **11c** at $\delta 3.66$.

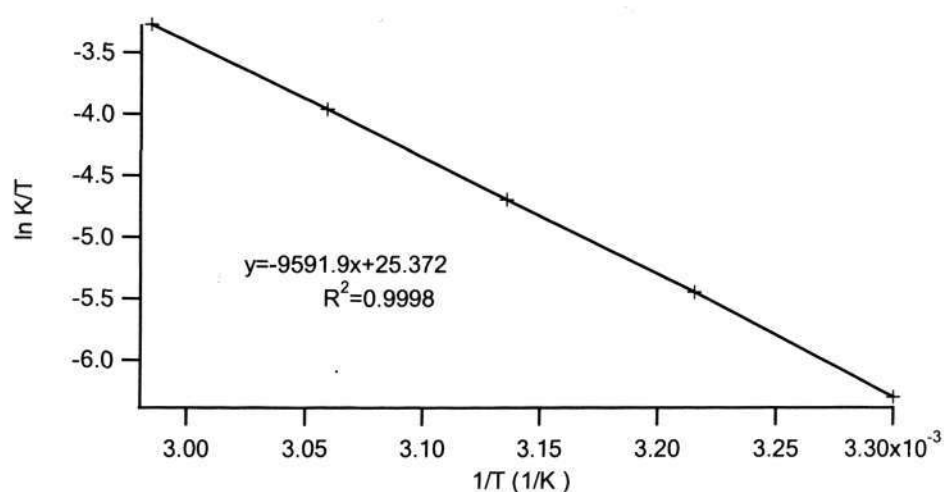
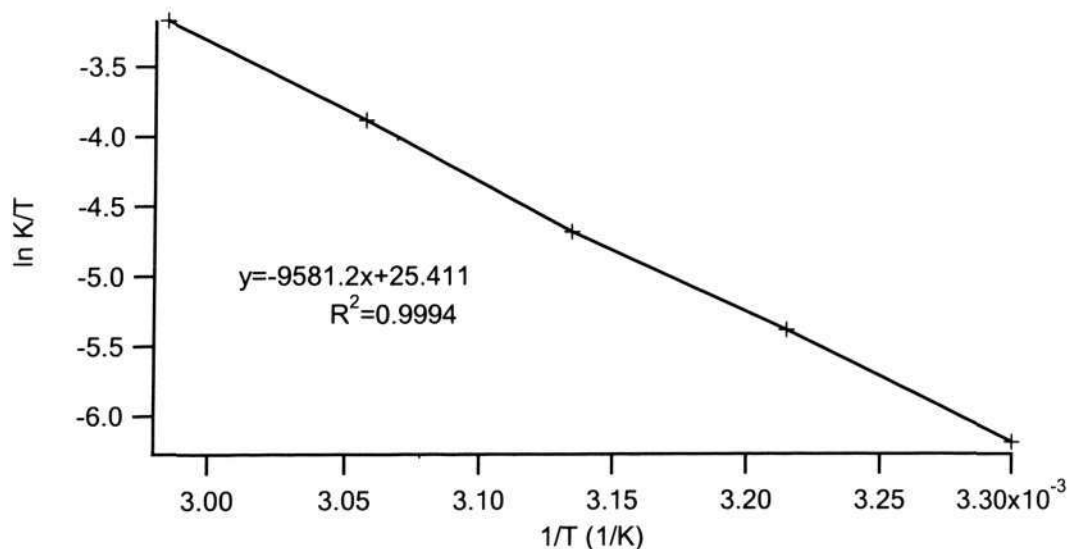


Table 3.4. Spectroscopic data based on the signal at $\delta 3.56$.

T (K)	1/T (1/K)	$W_{1/2}$ (Hz)	$\kappa = \pi \times \Delta W_{1/2}$ (Hz)	$\ln (\kappa/T)$
263	0.003802	2.258		
303	0.003300	2.507	0.622	-6.1885
311	0.003215	2.712	1.43	-5.3847
319	0.003135	3.202	2.97	-4.6781
327	0.003058	4.409	6.76	-3.8793
335	0.002985	6.741	14.1	-3.1691

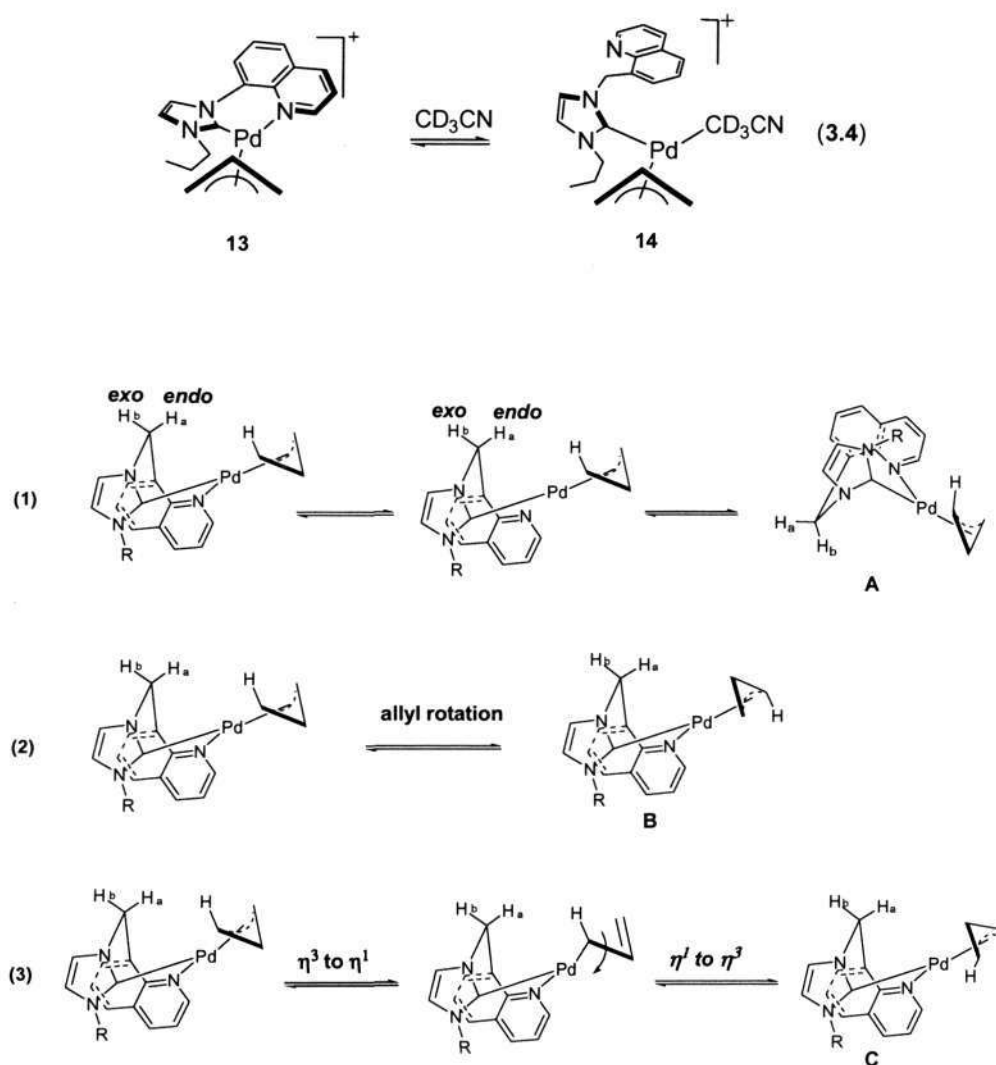
Figure 3.25. Eyring Plot of complex **11c** at $\delta 3.56$.



There are three possible mechanisms that can account for the fluxionality in **11c** (Scheme 3.14). Path (1) is overall a boat-to-boat conversion of the palladacycle which will lead to an *anti* (set **a**) to *anti* (set **b**) exchange in the allyl group and also an exchange between *endo* (set **a**) and *exo* (set **b**) protons of the methylene linker. Path (2) involves the partially hindered π -allyl rotation with NHC-N ligand being a spectator.⁵⁸ This process will lead to an *anti-anti* exchange for the allyl protons but an *endo-endo* exchange for the methylene protons. Path (3) is the $\eta^3\text{-}\eta^1\text{-}\eta^3$ ($\pi\text{-}\sigma\text{-}\pi$) rearrangement process and will lead to a *syn-anti* exchange for the allyl protons together with an *endo-endo* exchange for the methylene protons.

The rotating-frame overhauser enhancement spectroscopy (ROESY) spectrum of **11c** in CDCl₃ was obtained to elucidate the mechanism of this exchange. Correlations of signals (cross peaks) in ROESY can be exchange-derived (colored in red here) or overhauser-derived (colored in black here) and they are distinguishable.⁵⁹ It clearly shows exchange-derived correlation of the *anti-anti* (and also *syn-syn* and *meso-meso*) allyl protons and also *endo-exo* exchange for the CH₂ linker protons in these two sets of peaks (Figure 3.26). The conclusion that these exchanging signals are contributed by different molecules was safely drawn on the basis of the ¹H-¹H correlation spectroscopy (COSY) spectrum of **11c** (Figure 3.27). The fact that exchange between *endo* and *exo* protons of the CH₂ linker was observed suggests that pathways (2) and (3) are unlikely, therefore pathway (1) is the most likely mechanism. Modelling shows that this 7-membered metalacycle is highly rigid, and it is not very likely for it to undergo boat-to-boat ring flip with the 7-membered ring staying intact, although this type of ring flip has been known in 6-membered carbene palladacycles.⁶⁰⁻⁶² Instead, boat-to-boat conversion *via* the dissociation of the labile quinoline N atom seems more likely. A simple Pd-C_{carbene} bond rotation is not likely here since the tethering effect of the quinoline nitrogen would significantly raise the rotation barrier around the Pd-C_{carbene} bond. Complex **13** was synthesized by an analogous method (Scheme 3.4). The BF₄ salt is insoluble in chloroform, but it is sparingly soluble in acetone-*d*₆, where it shows well-resolved allyl proton signals with no indication of line-broadening at ambient temperature, in agreement with a stable chelate coordination of the NHC-quinoline ligand. No ¹³C NMR spectrum could be obtained for **13** in either acetone-*d*₆ or CD₂Cl₂ because of poor solubility.

Complex **13** is more soluble in acetonitrile. However, the NMR spectra are significantly different. The ambient temperature ^1H NMR spectrum shows line-broadening for the *syn* and *anti* protons on C_6 , reminiscent of the likewise monodentate complexes **10a-b** and **12** and suggesting that the species present in solution undergo selective $\eta^3\text{-}\eta^1\text{-}\eta^3$ isomerization. In the ^{13}C NMR spectrum, in addition to the signal of solvent CD_3CN (δ 1.32, septet), a new signal is found (δ 1.18, septet) which is attributed to coordinated CD_3CN , so the exchange must be slow. We conclude that solvation of **13** with CD_3CN leads to the opening of the NHC-quinoline chelate ring so that the ligand becomes monodentate, affording the ionic complex **14** in solution (eq 3.4). Attempts to isolate **14** by removal of CH_3CN from the corresponding solutions have been unsuccessful, and only the starting material **13** was recovered, indicating that the $\kappa^2\text{-(C, N)}$ to $\kappa^1\text{-(C)}$ conversion is reversible.



Scheme 3.14. Three possible mechanisms leading to the fluxionality of complex **11c**.

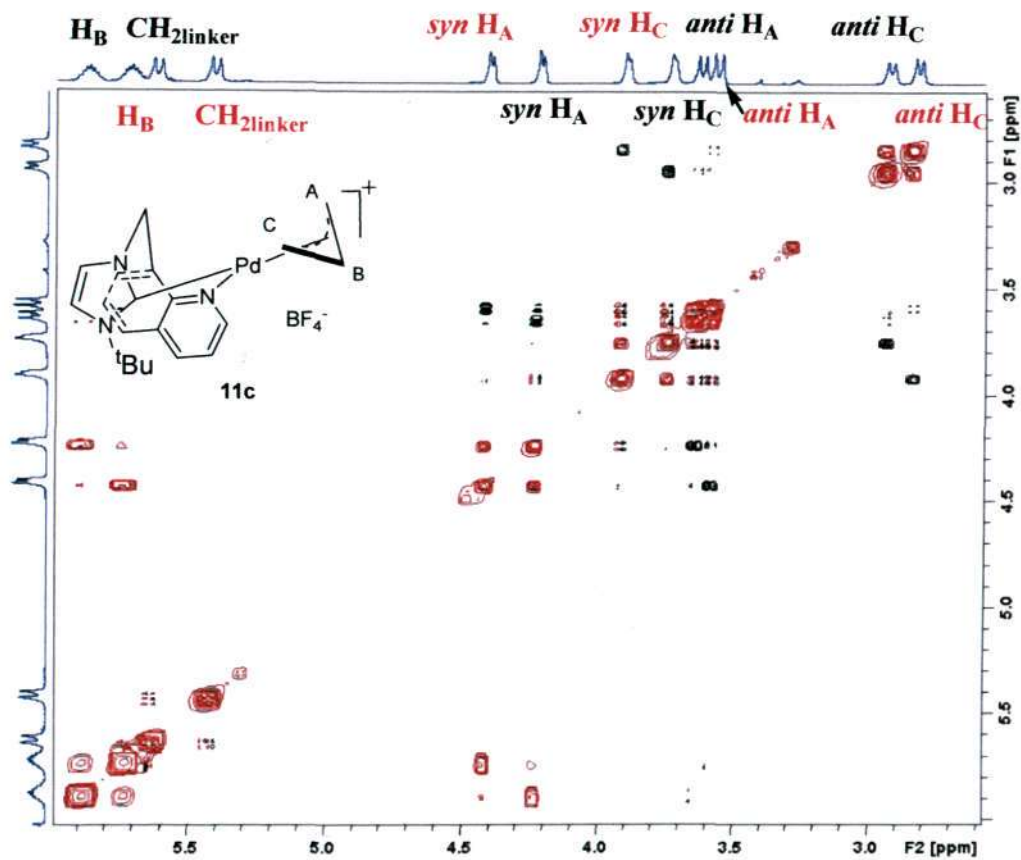


Figure 3.26. Part of the ROESY spectrum of **11c** in CDCl_3 .

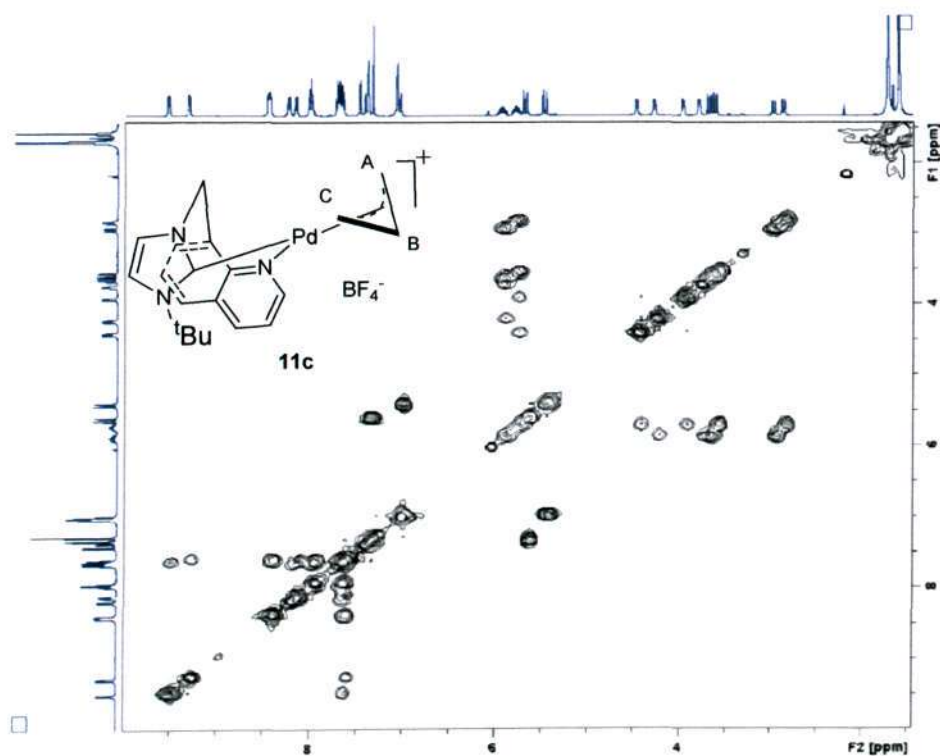
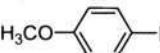

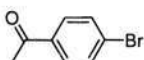
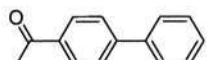
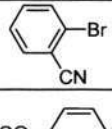
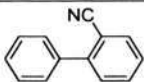
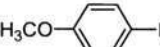

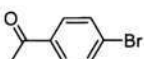
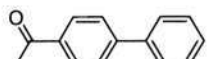
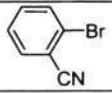
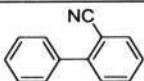
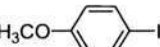
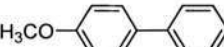

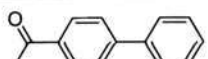
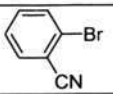
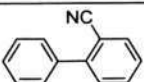


Figure 3.27. ^1H - ^1H COSY spectrum of complex **11c** in CDCl_3 .

3.2.6. Catalytic Applications

Representative Pd allyl complexes were applied as catalysts for the Suzuki coupling reactions. Neutral complex **10a**, cationic complexes **11a**, and **13** were studied and all showed good activity in this C-C coupling reaction with 1 mol% loading. The catalytic activities are roughly the same for activated or deactivated aryl bromides or iodides in the reaction with phenylboronic acid. For a fixed coupling reaction, cationic complex **13** shows a slightly lower activity. The use of Cs₂CO₃ proved to be a better choice than KOBu^t, which afforded slightly more homo-coupling products. These catalysts showed little or no activity for the coupling between chlorobenzene and phenylboronic acid, with only 10% coupling product obtained under the same conditions (80 °C, 4 h, dioxane). Representative results are summarized in Table 3.5.

Table 3.5. Palladium-catalyzed Suzuki coupling between phenylboronic acid and arylhalides ^a

entry	catalyst	substrate	product	Isolated yield (%)
1	10a			90
2				89
3				94
4	11a			87
5				80
6				89
7	13			73
8				77
9				74

^a Reaction conditions: 0.5 mmol of ArX; 0.6 mmol of phenylboronic acid; 0.6 mmol of Cs₂CO₃; 1.0 ml of 1,4-dioxane; 1 mmol % catalyst; 80 °C; 4 h.

3.3. Conclusions

We have described the synthesis a series of new neutral and cationic quinoline functionalized Pd NHC complexes *via* silver transmetalation. The quinoline moiety could be directly attached to the imidazole or linked by a methylene group. NHCs with a methylene linker tend to form *trans* biscarbene complexes with pendent quinoline groups in the reaction of Pd(COD)Cl₂, while NHCs without CH₂ linker form chelating palladium NHC-quinoline complexes. These two types of carbenes also react with [Pd(allyl)Cl]₂ to give monodentate NHC palladium η^3 -allyl chlorides [Pd(NHC)(allyl)Cl]. Fluxionality on the NMR time scale was observed for most complexes and the solution dynamics depend on the carbene wing tip and the coordination mode. For Pd(NHC)(allyl)Cl with a Mes or *n*-Bu wing tip, the fluxionality originates from selective η^3 - η^1 - η^3 rearrangement. While selective broadening was also observed for Pd(NHC)(allyl)Cl with a *tert*-Bu wing tip, the fluxionality is proposed to originate from the partially hindered Pd-carbene bond rotation. In cationic complex [Pd(NHC^{^N})(allyl)]BF₄, boat-to-boat conversion of the 7-membered ring *via* dissociative mechanism is proposed as the mechanism of the solution dynamics on the basis of ROESY spectroscopy. Crystal structures were obtained for complexes in each category. Representative Palladium allyl complexes were shown to be active catalysts for the Suzuki reactions between aryl bromides or aryl iodides and phenylboronic acid.

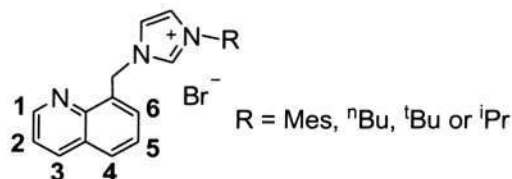
3.4. Experimental Section

3.4.1. General Information

All the manipulations were performed under nitrogen using the standard shlenk technique, although most of the products proved to be air stable. One-dimensional NMR spectra were recorded on a Bruker ACF 300 (300 MHz) or a Bruker DPX 400 (400 MHz) NMR spectrometer. ROESY spectrum was recorded on a Bruker AMX 500 (500 MHz) NMR spectrometer. Unless otherwise indicated, NMR spectra were recorded at room temperature (23 °C) and were internally referenced relative to the residual protio-solvent (¹H) or the solvent (¹³C). Chemical shifts referenced to $\delta = 0$ for tetramethylsilane. Microanalyses were performed in-house. Pd(PhCN)₂Cl₂

and $[\text{Pd}(\text{allyl})\text{Cl}]_2$ were purchased from the Strem Co.. $\text{Pd}(\text{COD})\text{Cl}_2$ was prepared following a published procedure.⁶³ Solvents and all remaining reagents were purchased from Aldrich and were used without further purification.

3.4.2. Synthetic Procedures



Synthesis of 8-(bromomethyl)quinoline: 8-(bromomethyl)quinoline was synthesized based on a literature report,⁶⁴ as follows: N-bromosuccinimide (2.94 g, 16.5 mmol) and benzoyl peroxide (182 mg, 0.752 mmol) were added to a cyclohexane solution (50 mL) of 8-methylquinoline (2.15 g, 15.0 mmol). The mixture was stirred under reflux and under light for 10 h. White precipitates were observed. The mixture was filtered, and the solution was washed with aq NaHCO_3 (2×8 mL) and dried over anhydrous Na_2SO_4 . Removal of the solvent gave a pale brown solid which was recrystallized from hot aqueous ethanol to give white crystals. 2.26 g, 10.2 mmol, 68%. ^1H NMR (CDCl_3 , 400 MHz): δ 9.02 (dd, 1H, $J = 3.9$ and 1.5 Hz, N- $\text{CH}_{\text{quinoline}}$), 8.17 (dd, 1H, $J = 8.2$ and 1.4 Hz), 7.85-7.80 (m, 2H), 7.54-7.44 (m, 2H), 5.25 (s, 2H, CH_2). The NMR spectrum matches that in a literature report.⁶⁴

General Procedure for Synthesis of Imidazolium Salts (1a-d): A substituted imidazole was added to a solution of 8-(bromomethyl)quinoline in acetonitrile. The solution was heated under reflux for 16 h (1a) and 3 h (1b-d). Removal of MeCN followed by addition of ether gave a solid or an oil, which was further washed with ether (2×5 mL) and dried under vacuum.

Synthesis of 1a: 1-mesitylimidazole (440 mg, 2.36 mmol) and 8-(bromomethyl)quinoline (500 mg, 2.25 mmol) were heated under reflux in MeCN (10 mL) for 16 h. A white solid was obtained following removal of MeCN and addition of ether, which was dried in vacuum to give an analytically pure white powder (912 mg, 2.2 mmol, 99%). ^1H NMR (CDCl_3 , 400 MHz): δ 10.40 (s, 1H, NCHN), 8.93 (dd, 1H, $J = 4.2$ and 1.5 Hz, H-1), 8.66 (d, 1H, $J = 6.9$ Hz), 8.22 (dd, 1H, $J = 8.2$ and 1.5 Hz, H-3), 8.16 (s, 1H, $\text{CH}_{\text{imidazole}}$), 7.89 (d, 1H, $J = 8.0$ Hz), 7.61 (t, 1H, $J = 7.4$ Hz, H-5), 7.50 (dd, 1H, $J = 8.3$ and 4.2 Hz, H-2), 6.99 (s, 1H, $\text{CH}_{\text{imidazole}}$), 6.95 (s, 2H, $2\text{CH}_{\text{mesityl}}$), 6.53

(s, 2H, CH₂ linker), 2.30 (s, 3H, CH₃ mesityl), 1.98 (s, 6H, CH₃ mesityl); ¹³C{¹H} NMR (CDCl₃, 100 MHz): δ 150.2 (N-CH₂ quinoline), 146.3 (N-C quinoline), 141.2 (C mesityl), 138.0 (C mesityl), 136.8, 134.3, 133.1, 131.7, 130.8, 130.0, 129.8, 128.5, 127.2, 124.1, 122.2 (imidazole), 121.7 (imidazole), 49.2 (CH₂ linker), 21.1 (CH₃), 17.6 (2CH₃). Anal. Calc for C₂₂H₂₂N₃Br (408.33): C, 64.71; H, 5.43; N, 10.29%. Found: C, 64.46; H, 5.32; N, 10.37%.

Synthesis of 1b: 1-*n*-Butylimidazole (409 mg, 3.30 mmol) and 8-(bromomethyl)quinoline (666 mg, 3.00 mmol) were heated under reflux in MeCN (10 mL) for 3 h. Product **1b** was obtained as an oil (1.00 g, 2.89 mmol, 99%). ¹H NMR (CDCl₃, 400 MHz): δ 10.74 (s, 1H, NCHN), 8.98 (d, 1H, *J* = 2.8 Hz, H-1), 8.43 (d, 1H, *J* = 6.8 Hz), 8.21 (d, 1H, *J* = 8.1 Hz, H-3), 7.88 (d, 1H, *J* = 7.9 Hz), 7.78 (s, 1H, CH₂ imidazole), 7.60 (t, 1H, *J* = 7.6 Hz, H-5), 7.50 (dd, 1H, *J* = 8.1 and 4.2 Hz, H-2), 7.20 (s, 1H, CH₂ imidazole), 6.22 (s, 2H, CH₂ linker), 4.28 (t, 2H, *J* = 7.4 Hz, NCH₂), 1.93-1.85 (m, 2H, NCH₂CH₂), 1.40-1.31 (m, 2H, NCH₂CH₂CH₂), 0.93 (t, 3H, *J* = 7.2 Hz, CH₃); ¹³C{¹H} NMR (CDCl₃, 100 MHz): δ 150.4 (N-CH₂ quinoline), 146.1 (N-C quinoline), 137.4, 136.7, 132.5, 131.6, 130.0, 128.5, 127.0, 123.2, 121.8 (imidazole), 120.8 (imidazole), 49.8, 49.0 (CH₂ linker), 32.1, 19.5, 13.4 (CH₃). Anal. Calcd for C₁₇H₂₀N₃Br (346.26): C, 58.97; H, 5.82; N, 12.14%. Found: C, 58.78; H, 5.72; N, 12.23%. The chloride analogue of **1b** was obtained by chloride exchange between **1b** and Dowex® 21K chloride exchange resin in methanol for 12 h.⁵⁰

Synthesis of 1c: 1-*tert*-Butylimidazole (273 mg, 2.20 mmol) and 8-(bromomethyl)quinoline (444 mg, 2.00 mmol) in MeCN (10 mL) were heated under reflux for 3 h. **1c** was obtained as a white solid (680 mg, 1.97 mmol, 98%). ¹H NMR (CDCl₃, 400 MHz): δ 10.88 (s, 1H, NCHN), 8.97-8.95 (m, 1H, H-1), 8.60 (d, 1H, *J* = 6.9 Hz), 8.21 (d, 1H, *J* = 8.2 Hz, H-3), 7.88-7.86 (m, 2H, CH₂ imidazole + CH₂ quinoline), 7.62 (t, 1H, *J* = 7.5 Hz, H-5), 7.50 (dd, 1H, *J* = 8.2 and 4.2 Hz, H-2), 7.29 (s, 1H, CH₂ imidazole), 6.31 (s, 2H, CH₂ linker), 1.69 (s, 9H, C(CH₃)₃); ¹³C{¹H} NMR (CDCl₃, 100 MHz): δ 150.2 (N-CH₂ quinoline), 146.0 (N-C quinoline), 136.6, 135.6, 132.7, 131.8, 129.7, 128.3, 126.9, 123.4, 121.6 (imidazole), 118.5 (imidazole), 60.1 (C(CH₃)₃), 48.5 (CH₂ linker), 30.0 (C(CH₃)₃). Anal. Calcd for C₁₇H₂₀N₃Br (346.26): C, 58.97; H, 5.82; N, 12.14%. Found: C, 58.69; H, 5.94; N, 12.17%.

Synthesis of *Id*: 1-*iso*-Propylimidazole (363 mg, 3.30 mmol) and 8-(bromomethyl)quinoline (666 mg, 3.00 mmol) were heated under reflux in MeCN (10 mL) for 3 h. **Id** was obtained as a white solid (968 mg, 2.92 mmol, 97%). ^1H NMR (CDCl_3 , 400 MHz): δ 10.78 (s, 1H, NCHN), 8.96 (d, 1H, $J = 4.0$ Hz, H-1), 8.45 (d, 1H, $J = 6.7$ Hz), 8.20 (d, 1H, $J = 8.0$ Hz, H-3), 7.86 (d, 1H, $J = 8.0$ Hz), 7.80 (s, 1H, CH_{imidazole}), 7.58 (t, 1H, $J = 7.2$ Hz, H-5), 7.49 (dd, 1H, $J = 8.2$ and 4.2 Hz, H-2), 7.37 (s, 1H, CH_{imidazole}), 6.22 (s, 2H, CH₂ linker), 4.82-4.78 (m, 1H, CH(CH₃)₂), 1.58 (d, 6H, $J = 6.6$ Hz, 2CH₃); $^{13}\text{C}\{^1\text{H}\}$ NMR (CDCl_3 , 100 MHz): δ 150.3 (N-CH_{quinoline}), 145.9 (N-C_{quinoline}), 136.6, 135.8, 132.2, 131.6, 129.8, 128.3, 126.7, 123.2, 121.7 (imidazole), 119.4 (imidazole), 53.0 (CH(CH₃)₂), 48.6 (CH₂ linker), 23.0 (CH(CH₃)₂). Anal. Calcd for C₁₆H₁₈N₃Br (332.24): C, 57.84; H, 5.46; N, 12.65%. Found: C, 57.50; H, 5.62; N, 12.77%. The chloride analogue of **Id** was obtained by chloride exchange between **Id** and Dowex® 21K chloride exchange resin in methanol for 12 h.⁵⁰

General Procedure for Synthesis of Silver Complexes 2a-d: Ag₂O was added to a CH₂Cl₂ solution of imidazolium salts, and the mixture was stirred for 30 min in the dark to give an almost homogeneous solution. The mixture was then filtered to remove a small amount of insolubles, and removal of the solvent gave a white solid.

Synthesis of Complex 2a: Ag₂O (86 mg, 0.37 mmol) was added to a CH₂Cl₂ solution of imidazolium **1a** (275 mg, 0.674 mmol). Compound **2a** was obtained as an analytically pure product (307 mg, 0.60 mmol, 89%). ^1H NMR (CDCl_3 , 400 MHz): δ 8.98 (d, 1H, $J = 2.5$ Hz, H-1), 8.23 (dd, 1H, $J = 8.3$ and 1.7 Hz, H-3), 7.88 (d, 1H, $J = 7.6$ Hz), 7.78 (d, 1H, $J = 5.6$ Hz), 7.60-7.49 (m, 3H), 6.94 (s, 2H, 2CH_{mesityl}), 6.87 (d, 1H, $J = 1.6$ Hz, CH_{imidazole}), 6.00 (s, 2H, CH₂ linker), 2.28 (s, 3H), 1.90 (s, 6H, 2CH₃); $^{13}\text{C}\{^1\text{H}\}$ NMR (CDCl_3 , 100 MHz): δ 182.6 (carbene), 150.4 (N-CH_{quinoline}), 146.0 (N-C_{quinoline}), 139.4, 136.4, 135.5, 134.7, 134.2, 129.8, 129.4, 129.1, 128.5, 126.6, 122.3, 122.1, 121.8, 51.6 (CH₂ linker), 21.1 (CH₃), 17.8 (2CH₃). Anal. Calcd for C₂₂H₂₁AgBrN₃ (515.19): C, 51.29; H, 4.11; N, 8.16%. Found: C, 51.01; H, 4.28; N, 8.05%.

Synthesis of Complex 2b: Ag₂O (193 mg, 0.833 mmol) was added to a CH₂Cl₂ solution of **1b** (524 mg, 1.51 mmol). Compound **2b** was obtained as an analytically pure product (576 mg, 1.27 mmol, 84%). ^1H NMR (CDCl_3 , 400 MHz): δ 9.06 (d, 1H, $J = 2.9$ Hz, H-1), 8.20 (d, 1H, $J =$

8.3 Hz), 7.86 (d, 1H, $J = 8.3$ Hz), 7.78 (d, 1H, $J = 7.0$ Hz), 7.54 (t, 1H, $J = 7.4$ Hz, H-5), 7.48 (dd, 1H, $J = 8.2$ and 4.2 Hz, H-2), 7.36 (s, 1H, CH_{imidazole}), 6.92 (s, 1H, CH_{imidazole}), 5.95 (s, 2H, CH₂ linker), 4.08 (t, 2H, $J = 7.3$ Hz, NCH₂), 1.76 (quintet, 2H, $J = 7.2$ Hz, NCH₂CH₂), 1.35 (sextet, 2H, $J = 7.3$ Hz, CH₂CH₃), 0.94 (t, 3H, $J = 7.3$ Hz, CH₃); $^{13}\text{C}\{^1\text{H}\}$ NMR (CDCl₃, 100 MHz): δ 180.9 (carbene), 150.4 (N-CH_{quinoline}), 145.7 (N-C_{quinoline}), 136.3, 134.0, 129.7, 128.9, 128.3, 126.3, 122.0, 121.6, 120.4, 51.7 (NCH₂), 51.2 (NCH₂), 33.3 (CH₂CH₂CH₃), 19.6 (CH₂CH₂CH₃), 13.5 (CH₃). Anal. Calcd for C₁₇H₁₉AgBrN₃ (453.13): C, 45.06; H, 4.23; N, 9.27%. Found: C, 44.87; H, 3.95; N, 9.36%.

Synthesis of Complex 2c: Ag₂O (77 mg, 0.33 mmol) was added to a CH₂Cl₂ solution of imidazolium **1c** (208 mg, 0.630 mmol). **2c** was obtained as an analytically pure product (251 mg, 0.55 mmol, 92%). ^1H NMR (CDCl₃, 400 MHz): δ 9.00 (dd, 1H, $J = 4.2$ and 1.7 Hz, H-1), 8.13 (dd, 1H, $J = 8.3$ and 1.7 Hz, H-3), 7.79-7.69 (m, 2H), 7.48 (t, 1H, $J = 7.2$ Hz, H-5), 7.42 (dd, 1H, $J = 8.2$ and 4.2 Hz, H-2), 7.29 (d, 1H, $J = 1.8$ Hz, CH_{imidazole}), 7.08 (s, 1H, $J = 1.7$ Hz, CH_{imidazole}), 5.94 (s, 2H, CH₂ linker), 1.65 (s, 9H, C(CH₃)₃). $^{13}\text{C}\{^1\text{H}\}$ NMR (CDCl₃, 100 MHz): δ 179.6 (carbene), 150.4 (N-CH_{quinoline}), 145.8 (N-C_{quinoline}), 136.3, 134.1, 129.7, 128.9, 128.4, 126.4, 121.6, 120.5, 118.5, 57.6 (C(CH₃)₃), 52.4 (CH₂ linker), 31.7 (3CH₃). Anal. Calc for C₁₇H₁₉AgBrN₃ (453.13): C, 45.06; H, 4.23; N, 9.27%. Found: C, 44.91; H, 4.31; N, 9.42%.

Synthesis of Complex 2d: Ag₂O (192 mg, 0.829 mmol) was added to a CH₂Cl₂ solution of imidazolium **1d** (500 mg, 1.51 mmol). **2d** was obtained as an analytically pure product (612 mg, 1.39 mmol, 92%). ^1H NMR (CDCl₃, 400 MHz): δ 9.08 (dd, 1H, $J = 4.2$ and 1.7 Hz, H-1), 8.20 (dd, 1H, $J = 8.3$ and 1.7 Hz, H-3), 7.83 (d, 1H, $J = 8.2$ Hz), 7.77 (d, 1H, $J = 7.0$ Hz), 7.54 (t, 1H, $J = 7.4$ Hz, H-5), 7.47 (dd, 1H, $J = 8.2$ and 4.2 Hz, H-2), 7.38 (d, 1H, $J = 1.7$ Hz, CH_{imidazole}), 6.95 (d, 1H, $J = 1.7$ Hz, CH_{imidazole}), 5.93 (s, 2H, CH₂ linker), 4.73 (septet, 1H, $J = 6.9$ Hz, CH(CH₃)₂), 1.44 (d, 6H, $J = 6.8$ Hz, 2CH₃); $^{13}\text{C}\{^1\text{H}\}$ NMR (CDCl₃, 100 MHz): δ 180.2 (carbene), 150.6, (N-CH_{quinoline}) 145.9, (N-C_{quinoline}) 136.4, 134.2, 130.0, 129.0, 128.5, 126.5, 122.3, 121.7, 116.8, 54.1 (CH(CH₃)₂), 51.5 (CH₂ linker), 23.8 (2CH₃). Anal. Calcd for C₁₆H₁₇AgBrN₃ (439.10): C, 43.76; H, 3.90; N, 9.57%. Found: C, 43.57; H, 3.82; N, 9.68%.

Synthesis of Imidazole 3: Imidazole **3** was synthesized based on a literature report.⁶⁵ ¹H NMR (CDCl₃, 300 MHz): δ 8.98 (dd, 1H, J = 5.6 and 2.3 Hz), 8.25 (dd, 1H, J = 11.1 and 2.3 Hz), 8.11 (s, 1H), 7.86 (dd, 1H, J = 10.8 and 2.0 Hz), 7.70 (dd, 1H, J = 9.9 and 2.0 Hz), 7.64-7.49 (m, 3H), 7.28 (s, 1H). The ¹H NMR spectrum of **3** matches that in reported.⁶⁵

Synthesis of 4: Compound **3** (302 mg, 1.55 mmol) and 1-iodopropane (1.05 g, 6.18 mmol) were dissolved in acetonitrile (10 mL). The solution was heated under reflux for 24 h. All the volatiles were removed under reduced pressure and dichloromethane (1 mL) was added to dissolve the residue. Diethyl ether (10 mL) was then added to the solution to give a yellow solid, which was filtered and washed with diethyl ether to give an analytically pure product (556 mg, 1.52 mmol, 98%). ¹H NMR (CDCl₃, 300 MHz): δ 10.40 (s, 1H, NCHN), 8.99 (dd, 1H, J = 4.2 and 1.7 Hz, N-CH_{quinoline}), 8.43 (dd, 1H, J = 7.5 and 1.1 Hz), 8.37 (dd, 1H, J = 8.4 and 1.8 Hz), 8.09 (dd, 1H, J = 8.3 and 1.1 Hz), 7.98 (t, 1H, J = 1.7 Hz, CH_{imidazole}), 7.81-7.75 (m, 1H), 7.67-7.59 (m, 2H, CH_{imidazole} + CH_{quinoline}), 4.64 (t, 2H, J = 7.3 Hz, NCH₂), 2.19-2.09 (m, 2H, NCH₂CH₂), 1.12 (t, 3H, J = 7.4 Hz, CH₃); ¹³C{¹H} NMR (CDCl₃, 75 MHz): δ 151.8 (N-CH_{quinoline}), 140.7 (N-C_{quinoline}), 137.4, 136.8, 131.0, 130.8, 129.3, 126.8, 126.1, 124.4, 122.9, 121.5, 52.1 (NCH₂), 23.7 (NCH₂CH₂), 10.8 (CH₃). Anal. Calcd for C₁₅H₁₆IN₃ (365.21): C, 49.33; H, 4.42; N, 11.51%. Found: C, 49.21; H, 4.32; N, 11.67%.

Synthesis of Complex 5: Ag₂O (105 mg, 0.453 mmol) was added to a dichloromethane (5 mL) solution of imidazolium salt **3** (300 mg, 0.822 mmol). The mixture was stirred for half an hour in the dark. Following the same workup procedure for **2a**, **5** was obtained as a white or light yellow solid (339 mg, 0.72 mmol, 88%). ¹H NMR (CDCl₃, 400 MHz): δ 8.89 (dd, 1H, J = 4.0 and 1.3 Hz, N-CH_{quinoline}), 8.29 (dd, 1H, J = 8.4 and 1.4 Hz), 7.98 (d, 1H, J = 7.2 Hz), 7.93 (d, 1H, J = 8.4 Hz), 7.62-7.58 (t, 1H, J = 7.8 Hz), 7.52-7.48 (m, 2H), 7.18 (d, 1H, J = 1.6 Hz, CH_{imidazole}), 4.13 (t, 2H, J = 7.3 Hz, NCH₂), 1.90 (sextet, 2H, J = 7.2 Hz, CH₂CH₃), 0.95 (t, 3H, J = 7.4 Hz, CH₃); ¹³C{¹H} NMR (CDCl₃, 75 MHz): δ 183.9 (carbene), 151.3 (N-CH_{quinoline}), 142.5 (N-C_{quinoline}), 136.7, 136.6, 129.5, 129.3, 127.2, 126.3, 124.7, 122.3, 120.2, 53.8 (NCH₂), 24.7 (NCH₂CH₂), 11.3 (CH₃). Anal. Calc for C₁₅H₁₅AgIN₃ (472.07): C, 38.16; H, 3.20; N, 8.90%. Found: C, 37.85; H, 3.25; N, 8.97%.

Synthesis of Complex 6b: The chloride analogue of silver complex **2b** (300 mg, 0.734 mmol) was dissolved in CH₂Cl₂ (10 mL), followed by addition of Pd(COD)Cl₂ (104 mg, 0.364 mmol) in one portion. White precipitates appeared immediately. This mixture was stirred at room temperature for 1 h, then filtered and the solvent was quickly removed to afford a white solid, which was dried under vacuum. Recrystallization using CH₂Cl₂-ether gave an analytically pure **6b** (235 mg, 0.33 mmol, 91% yield). Two sets of peaks were observed in the ¹H NMR spectrum of **6b** and no attempt can be made to disentangle these two sets of signals since the ratio of these two species is 1:1. ¹H NMR (CDCl₃, 400 MHz): δ 9.03 (dd, 1H, *J* = 4.0 and 1.4 Hz, N-CH_{quinoline}), 8.83 (dd, 1H, *J* = 4.0 and 1.4 Hz, N-CH_{quinoline}), 8.23 (d, 1H, *J* = 7.0 Hz), 8.10 (d, 1H, *J* = 7.0 Hz), 7.96 (d, 1H, *J* = 8.1 Hz), 7.82 (m, 2H), 7.46-7.62 (m, 3H), 7.35-7.25 (m, 2H), 6.94-6.97 (m, 2H), 6.82 (d, 1H, *J* = 1.5 Hz, CH_{imidazole}), 6.79 (d, 1H, *J* = 1.6 Hz, CH_{imidazole}), 6.61 (s, 2H, CH₂ linker), 6.34 (s, 2H, CH₂ linker), 4.62 (t, 2H, *J* = 7.2 Hz, NCH₂CH₂CH₃), 4.43 (t, 2H, *J* = 7.3 Hz, NCH₂CH₂CH₃), 2.18 (quintet, 2H, *J* = 7.3 Hz), 1.90 (quintet, 2H, *J* = 7.4 Hz), 1.50-1.59 (m, 2H), 1.02-1.10 (m, 5H, CH₂ + CH₃), 0.68 (t, 3H, *J* = 7.4 Hz, CH₃). ¹³C{¹H} NMR (acetone-*d*₆, 75 MHz): δ 171.6 (carbene), 171.3 (carbene), 149.9, 149.5, 146.0, 145.6, 136.3, 135.9, 135.7, 135.1, 129.1, 128.9, 128.2, 127.7, 127.4, 127.2, 126.4, 126.1, 121.5, 121.44, 121.37, 121.25, 121.22, 121.0, 50.1 (CH₂ linker), 50.0 (CH₂ linker), 49.4 (NCH₂), 49.0 (NCH₂), 33.3 (CH₂), 33.1 (CH₂), 19.9 (CH₂), 19.4 (CH₂), 13.3 (CH₃), 13.0 (CH₃); Anal. Calcd for C₃₄H₃₈PdCl₂N₆ (708.03): C, 57.68; H, 5.41; N, 11.87%. Found: C, 57.32; H, 5.49; N, 11.82%.

Synthesis of Complex 6d: Complex **6d** was synthesized following the same method as for **6b**. Complex **6d** was obtained as a white solid (199 mg, 0.29 mmol, 93%). Two sets of peaks were observed in the ¹H NMR spectrum of **6d** and no attempt was made to disentangle these two sets of resonance signals since the ratio of these two species approximates 1:1. ¹H NMR (CDCl₃, 300 MHz): δ 8.99 (dd, 1H, *J* = 4.1 and 1.6 Hz, N-CH_{quinoline}), 8.80 (dd, 1H, *J* = 4.1 and 1.7 Hz, N-CH_{quinoline}), 8.20 (dd, 1H, *J* = 8.1 and 1.5 Hz), 8.10 (d, 1H, *J* = 6.8 Hz), 7.94-7.91 (m, 1H), 7.84-7.77 (m, 2H), 7.58-7.44 (m, 3H), 7.32-7.20 (m, 1H), 6.98 (d, 1H, *J* = 1.7 Hz, CH_{imidazole}), 6.94 (d, 1H, *J* = 1.7 Hz, CH_{imidazole}), 6.85 (d, 1H, *J* = 1.8 Hz, CH_{imidazole}), 6.80 (d, 1H, *J* = 1.8 Hz, CH_{imidazole}), 6.52 (s, 2H, CH₂ linker), 6.31 (s, 2H, CH₂ linker), 5.78 (septet, 1H, *J* = 6.9 Hz, CH(CH₃)₂),

5.54 (septet, 1H, $J = 6.9$ Hz, $\text{CH}(\text{CH}_3)_2$), 1.64 (d, 6H, $J = 6.8$ Hz, 2CH_3), 1.31 (d, 6H, $J = 6.8$ Hz, 2CH_3); $^{13}\text{C}\{^1\text{H}\}$ NMR (CDCl_3 , 75 MHz): δ 169.8 (carbene), 169.7 (carbene), 149.7, 149.5, 146.2, 145.9, 136.2, 135.9, 135.1, 134.8, 130.5, 130.3, 128.1, 127.8, 127.6, 127.4, 126.9, 126.7, 121.74, 121.71, 121.2, 120.8, 116.32, 116.26, 52.00 (CH_2 linker), 51.6 (CH_2 linker), 49.5 (NCH_2), 49.3 (NCH_2), 23.6 (CH_3), 23.3 (CH_3); Anal. Calcd for $\text{C}_{32}\text{H}_{34}\text{PdCl}_2\text{N}_6$ (679.98): C, 56.52; H, 5.04; N, 12.36%. Found: C, 56.34; H, 5.13; N, 12.43%.

Synthesis of Complex 7: To a CH_2Cl_2 (5 mL) solution of silver complex **5** (175 mg, 0.371 mmol) was added $\text{Pd}(\text{COD})\text{Cl}_2$ (106 mg, 0.371 mmol). A solution was obtained after filtration and it was concentrated to 0.5 mL. Addition of ether (20 mL) to the solution gave a light yellow solid (118 mg, 0.29 mmol, 77%). ^1H NMR (CDCl_3 , 400 MHz): δ 9.71 (d, 1H, $J = 4.1$ Hz, N-CH quinoline), 8.49 (d, 1H, $J = 8.0$ Hz), 8.02 (d, 1H, $J = 7.6$ Hz), 7.92 (d, 1H, $J = 8.0$ Hz), 7.79-7.75 (m, 1H), 7.58-7.55 (m, 1H), 7.46 (d, 1H, $J = 2.1$ Hz, CH imidazole), 7.21 (d, 1H, $J = 1.9$ Hz, CH imidazole), 4.72 (br, 2H, NCH_2), 2.10-2.05 (m, 2H, CH_2CH_3), 1.07 (t, 3H, $J = 7.4$ Hz, CH_3); $^{13}\text{C}\{^1\text{H}\}$ NMR (CDCl_3 , 100 MHz): δ 159.1, 149.2 (carbene), 140.4, 137.3, 133.5, 129.8, 128.3, 127.7, 124.7, 122.4, 121.9, 120.4, 53.2 (NCH_2), 24.7 (NCH_2CH_2), 11.1 (CH_3). Anal. Calc for $\text{C}_{15}\text{H}_{15}\text{Cl}_2\text{N}_3\text{Pd}$ (414.63): C, 43.45; H, 3.65; N, 10.13%. Found: C, 43.91; H, 3.76; N, 10.25%.

Synthesis of Complex 8: To a MeCN (5 mL) solution of palladium complex **7** (75 mg, 0.18 mmol) was added AgBF_4 (71 mg, 0.36 mmol). The mixture was stirred for 3 h in the dark. The precipitate (AgCl) generated was removed by filtration to give a clear solution. Removal of all the volatiles afforded **8** as a white powder (105 mg, 0.88 mmol, 97%). ^1H NMR (CD_3CN , 400 MHz): δ 9.12 (d, 1H, $J = 4.5$ Hz, N-CH quinoline), 8.85 (d, 1H, $J = 7.9$ Hz), 8.36 (d, 1H, $J = 7.6$ Hz), 8.20 (d, 1H, $J = 8.1$ Hz), 7.98-7.92 (m, 2H), 7.85-7.83 (m, 1H), 7.61 (d, 1H, $J = 2.1$ Hz, CH imidazole), 4.34 (t, 2H, $J = 7.3$ Hz, NCH_2), 2.09-2.00 (m, 2H, NCH_2CH_2), 1.96 (s, 6H, CH_3CN), 1.03 (t, 3H, $J = 7.3$ Hz, CH_3); $^{13}\text{C}\{^1\text{H}\}$ NMR (CD_3CN , 100 MHz): δ 159.4 (carbene), 144.3, 136.8, 135.4, 133.4, 131.6, 130.5, 129.7, 127.1, 124.6, 124.4, 123.4, 118.3 (CH_3CN), 53.8 (NCH_2), 24.7 (NCH_2CH_2), 11.1 (CH_3), 1.76 (CH_3CN). The resonance of coordinated MeCN is masked by the solvent signal. Anal. Calcd for $\text{C}_{19}\text{H}_{21}\text{B}_2\text{F}_8\text{N}_5\text{Pd}$ (599.43): C, 38.07; H, 3.53; N, 11.68%. Found: C, 37.88; H, 3.45; N, 11.79%.

Complex 9b: AgPF₆ (23 mg, 0.091 mmol) was quickly weighted and added to a flask charged with CH₃CN (2 mL), to which was added palladium complex **6b** (32 mg, 0.045 mmol) in one portion. The mixture was stirred for 3 h in the dark. The workup procedure is the same as for complex **8**. 41 mg, 0.44 mmol, 98%. ¹H NMR (CD₃CN, 500 MHz): δ 9.30 (dd, 1H, *J* = 5.4 and 1.6 Hz, N-CH_{quinoline}), 8.68 (dd, 1H, *J* = 8.2 and 1.4 Hz), 8.34-8.32 (m, 1H), 8.22 (d, 1H, *J* = 8.3 and 1.3 Hz), 8.10 (d, 1H, *J* = 15.6 Hz, CH_{2 linker}), 7.91-7.88 (m, 1H), 7.60-7.57 (m, 1H), 7.41 (d, 1H, *J* = 1.8 Hz, CH_{imidazole}), 6.95 (d, 1H, *J* = 1.9 Hz, CH_{imidazole}), 5.81 (d, 1H, *J* = 15.7 Hz, CH_{2 linker}), 3.87-3.81 (m, 1H, diastereotopic NCH₂), 3.65-3.59 (m, 1H, diastereotopic NCH₂), 1.31-1.24 (m, 1H, NCH₂CH₂), 0.62-0.58 (m, 1H, NCH₂CH₂), 0.57-0.52 (m, 2H, NCH₂CH₂CH₂), 0.41 (t, 3H, *J* = 7.1 Hz, CH₃); ¹³C{¹H} NMR (CD₃CN, 125 MHz): δ 163.2 (carbene), 158.3, 144.9, 142.9, 136.1, 132.6, 132.0, 129.1, 128.1, 122.3, 122.2, 121.7, 52.2 (CH_{2 linker}), 49.8 (NCH₂), 32.3 (CH₂), 19.0 (CH₂), 12.4 (CH₃). Anal. Calcd for C₃₄H₃₈F₁₂N₆P₂Pd (927.05): C, 44.05; H, 4.13; N, 9.07%. Found: C, 43.81; H, 4.33; N, 9.34%.

General Procedure for Synthesis of Palladium Allyl complexes 10a-c: In a glove box filled with nitrogen, silver carbene complexes were dissolved in dichloromethane, to which was added [Pd(allyl)Cl]₂ in one portion. The mixture was stirred at room temperature for 1 h. The precipitates generated were removed by filtration. Removal of all the solvent gave a white solid as an analytically pure product.

Complex 10a: [Pd(allyl)Cl]₂ (103 mg, 0.280 mmol) was added to a CH₂Cl₂ solution of silver complex **2a** (290 mg, 0.563 mmol). Product **10a** was obtained as a white solid (272 mg, 0.53 mmol, 95%). ¹H NMR (CDCl₃, 400 MHz): δ 8.95-8.94 (m, 1H, N-CH_{quinoline}), 8.16 (dd, 1H, *J* = 8.2 and 1.4 Hz), 8.07 (d, 1H, *J* = 5.7 Hz), 7.80 (d, 1H, *J* = 8.0 Hz), 7.53-7.44 (m, 2H), 7.35 (d, 1H, *J* = 1.6 Hz, CH_{imidazole}), 6.92 (s, 1H), 6.88 (s, 1H), 6.81 (d, 1H, *J* = 1.4 Hz, CH_{imidazole}), 6.27 (s, 2H, CH_{2 linker}), 4.88 (m, 1H, H_B), 4.06 (d, 1H, *J* = 7.0 Hz, *syn* H_A), 2.95 (d, 1H, *J* = 13.1 Hz, *anti* H_A), 2.93 (br s, 1H, *syn* H_C), 2.30 (s, 3H, CH₃), 2.16 (s, 3H, CH₃), 2.02 (s, 3H, CH₃), 1.64 (br d, 1H, *J* = 11.4 Hz, *anti* H_C); ¹³C{¹H} NMR (CDCl₃, 100 MHz): δ 181.3 (carbene), 149.9, 146.5, 138.6, 136.5, 136.3, 135.8, 135.3, 135.2, 131.0, 129.0, 128.7, 128.3, 126.4, 122.9, 121.6, 121.3, 114.4 (C_B), 72.2 (br, C_A), 50.4 (CH_{2 linker}), 48.3 (br, C_C), 21.1 (CH₃), 18.5 (CH₃), 18.1

(CH₃). Anal. Calcd for C₂₅H₂₆ClN₃Pd (510.37): C, 58.83; H, 5.13; N, 8.23%. Found: C, 58.56; H, 5.16; N, 8.16%.

Complex 10b: [Pd(allyl)Cl]₂ (128 mg, 0.348 mmol) was added to a CH₂Cl₂ solution of silver complex **2b** (316 mg, 0.698 mmol). Complex **10b** was obtained as a white foamy solid (283 mg, 0.63 mmol, 91%). ¹H NMR (CDCl₃, 400 MHz): δ 8.94-8.92 (m, 1H, N-CH_{quinoline}), 8.18-8.16 (m, 1H), 7.80-7.76 (m, 2H), 7.52-7.43 (m, 2H), 7.13 (d, 1H, *J* = 1.5 Hz, CH_{imidazole}), 6.88 (d, 1H, *J* = 1.5 Hz, CH_{imidazole}), 6.07 (s, 2H, CH₂ linker), 5.24 (m, 1H, H_B), 4.26 (d, 1H, *J* = 7.5 Hz, *syn* H_A), 4.20-4.16 (br m, 2H, NCH₂), 3.30 (br s, 1H, *syn* H_C), 3.24 (d, 1H, *J* = 13.6 Hz, *anti* H_A), 2.23 (br d, 1H, *J* = 11.6 Hz, *anti* H_C), 1.81 (m, 2H, NCH₂CH₂), 1.36 (m, 2H, CH₂CH₃), 0.94 (t, 3H, *J* = 7.3 Hz, CH₃); ¹³C{¹H} NMR (CDCl₃, 100 MHz): δ 179.6 (carbene), 149.9, 146.1, 136.4, 134.9, 130.1, 128.2, 128.1, 126.4, 122.2, 121.4, 120.5, 114.6 (C_B), 72.7 (br, C_A), 51.0 (CH₂ linker), 50.4 (NCH₂), 48.1 (br, C_C), 33.1 (NCH₂CH₂), 19.9 (NCH₂CH₂CH₂), 13.8 (CH₃). Anal. Calcd for C₂₀H₂₄ClN₃Pd (448.30): C, 53.58; H, 5.40; N, 9.37%. Found: C, 53.32; H, 5.33; N, 9.52%.

Complex 10c: [Pd(allyl)Cl]₂ (100 mg, 0.272 mmol) was added to a CH₂Cl₂ solution of silver complex **2c** (247 mg, 0.545 mmol). Complex **10c** was obtained as a white foamy solid (231 mg, 0.52 mmol, 96%). Two sets of peaks (set **a** and set **b** in 1.13 to 1.00 ratio) were observed in the ¹H NMR spectrum. ¹H NMR (CDCl₃, 400 MHz): δ 8.94-8.93 (m, 2H, set a and set b, N-CH_{quinoline}), 8.16 (d, 2H, *J* = 8.1 Hz, set a and set b), 7.81-7.75 (m, 3H, set a and set b), 7.67 (d, 1H, *J* = 7.0 Hz, set a or b), 7.53-7.45 (m, 4H, set a and set b), 7.10 (d, 1H, *J* = 1.5 Hz, CH_{imidazole}), 7.07 (d, 1H, *J* = 1.5 Hz, CH_{imidazole}), 7.04-7.01 (m, 2H, 2CH_{imidazole}), 6.53 (d, 1H, *J* = 14.9 Hz, CH₂ linker), 6.30 (d, 1H, *J* = 14.9 Hz, CH₂ linker), 6.20 (d, 1H, *J* = 15.3 Hz, CH₂ linker), 5.91 (d, 1H, *J* = 15.3 Hz, CH₂ linker), 5.25-5.18 (m, 2H, H_B set a and H_B set b), 4.18 (m, 2H, *syn* H_A set a and set b), 3.41 (br, 1H, *syn* H_C set a), 3.28 (d, 1H, *J* = 13.1 Hz, *anti* H_A set a), 3.26 (br s, 1H, *syn* H_C set b), 3.18 (d, 1H, *J* = 13.4 Hz, *anti* H_A set b), 2.26 (d, 1H, *J* = 11.5 Hz, *anti* H_C set a), 2.19 (d, 1H, *J* = 12.0 Hz, *anti* H_C set b), 1.86 (s, 9H, set a or set b), 1.70 (s, 9H, set a or b); ¹³C{¹H} NMR (CDCl₃, 100 MHz): δ 179.0 (carbene), 178.7 (carbene), 149.9, 149.8, 146.2, 146.0, 136.37, 136.35, 134.8, 134.7, 130.5, 130.1, 128.2, 128.1, 126.6, 126.5, 121.35, 121.33, 120.9, 120.8, 119.1, 119.0, 113.8 (C_B set a), 113.4 (C_B set b), 71.1 (br, C_A set a and set b), 58.1 (C(CH₃)₃, set a), 58.0 (C(CH₃)₃, set b).

b), 51.7 (CH₂ linker, set a), 51.3 (CH₂ linker, set b), 50.3 (br, C_C set a and set b), 31.7 (3CH₃), 31.6 (3CH₃). Anal. Calcd for C₂₀H₂₄ClN₃Pd (448.30): C, 53.58; H, 5.40; N, 9.37%. Found: C, 53.17; H, 5.62; N, 9.49%.

Synthesis of Complex 11a: Palladium complex **10a** (95 mg, 0.19 mmol) was dissolved in CH₂Cl₂, and AgBF₄ (37 mg, 0.19 mmol) was added quickly. Then, the mixture was stirred for 3 h under dark. After filtration, the solvent was removed in vacuo to give a white solid product (102 mg, 0.18 mmol, 95%). ¹H NMR (CDCl₃, 300 MHz): δ 9.40 (br, 1H), 8.46 (dd, 1H, *J* = 8.3 and 1.5 Hz), 8.35 (d, 1H, *J* = 6.9 Hz), 8.00 (dd, 1H, *J* = 8.3 and 1.3 Hz), 7.74-7.62 (m, 3H), 6.99-6.97 (m, 2H), 6.83 (d, 1H, *J* = 1.85 Hz), 5.61-5.52 (m, 1H), 4.42 (d, 1H, *J* = 7.7 Hz), 3.51-3.18 (m, 2H), 2.36 (s, 3H), 1.98-1.70 (br, 7H). ¹³C{¹H} NMR (CDCl₃, 75 MHz): δ 176.5 (carbene), 156.5 (N-CH_{quinoline}), 145.7 (N-C_{quinoline}), 140.8, 139.4, 135.5, 135.1, 134.7, 131.6, 130.5, 129.3, 129.2, 128.0, 123.1, 121.8, 119.5, 52.3 (CH₂), 30.9, 21.1 (CH₃), 17.64 (CH₃), 17.60 (CH₃). Anal. Calc for C₂₅H₂₆BF₄N₃Pd (561.72): C, 53.46; H, 4.67; N, 7.48%. Found: C, 53.02; H, 4.62; N, 7.45%.

Complex 11b: The synthetic procedure is the same as for **11a** using palladium complex **10b** (66 mg, 0.15 mmol) and AgBF₄ (29 mg, 0.15 mmol). Complex **11b** was obtained as a white solid (72 mg, 0.14 mmol, 96%). ¹H NMR (CDCl₃, 300 MHz, 328 K): δ 9.49 (br, 1H, N-CH_{quinoline}), 8.37 (dd, 1H, *J* = 8.3 and 1.6 Hz), 8.14 (d, 1H, *J* = 6.5 Hz), 7.92 (dd, 1H, *J* = 8.2 and 1.4 Hz), 7.61-7.56 (m, 2H), 7.41 (d, 1H, *J* = 1.6 Hz, CH_{imidazole}), 6.90 (br s, 2H, CH₂ linker), 6.88 (d, 1H, *J* = 1.9 Hz, CH_{imidazole}), 5.84 (br, 1H, H_B), 4.48 (br d, 1H, *J* = 7.0 Hz, *syn* H_A), 4.00-3.96 (br m, 2H, NCH₂CH₂), 3.73 (br s, 1H, *anti* H_A), 3.70 (br, 1H, *syn* H_C), 2.89 (br, 1H, *anti* H_C), 1.75-1.65 (m, 2H, NCH₂CH₂), 1.28-1.19 (m, 2H, NCH₂CH₂CH₂), 0.84 (t, 3H, *J* = 7.3 Hz, CH₃); ¹³C{¹H} NMR (CDCl₃, 75 MHz, 328 K): δ 174.8 (br, carbene), 156.7 (N-CH_{quinoline}), 145.7 (N-C_{quinoline}), 140.5, 134.8, 131.4, 131.3, 130.7, 127.5, 121.8, 121.3, 121.2, 119.3 (C_B), 78.1 (br, C_A), 52.4 (CH₂ linker), 50.4 (NCH₂), 46.2 (br, C_C), 33.0 (CH₂), 19.5 (CH₂), 13.4 (CH₃). Anal. Calcd for C₂₀H₂₄N₃BF₄Pd (499.65): C, 48.08; H, 4.84; N, 8.41%. Found: C, 47.70; H, 4.92; N, 8.52%.

Complex 11c: The synthetic procedure of **11c** is the same as that for **11a** using palladium complex **10c** (145 mg, 0.324 mmol) and AgBF₄ (64 mg, 0.33 mmol). Complex **11c** was obtained as a white solid (158 mg, 0.32 mmol, 96%). The ¹H NMR spectrum of **11c** shows two sets of

peaks in a ratio of 1:1 and they were disentangled by the ^1H - ^1H COSY spectroscopy. ^1H NMR (CDCl_3 , 400 MHz): δ 9.48-9.46 (m, 1H, set a or set b, N-CH_{quinoline}), 9.25 (dd, 1H, J = 4.8 and 1.0 Hz, set a or set b, N-CH_{quinoline}), 8.39-8.37 (m, 2H, set a and set b), 8.17 (d, 1H, J = 6.7 Hz, set a or set b), 8.11 (d, 1H, J = 6.7 Hz, set a or set b), 7.96-7.92 (m, 2H, set a and set b), 7.68-7.56 (m, 4H, set a and set b), 7.40 (d, 1H, J = 1.4 Hz, CH_{imidazole}), 7.35 (d, 1H, J = 15.0 Hz, set a or set b, *exo* diastereotopic CH₂ linker), 7.32 (d, 1H, J = 1.4 Hz, CH_{imidazole}), 7.01-6.97 (m, 3H, 2 imidazole CH + 1 *exo* diastereotopic CH₂ linker), 5.86 (m, 1H, H_B set a), 5.70 (m, 1H, H_B set b), 5.62 (d, 1H, J = 14.9 Hz, *endo* diastereotopic CH₂ linker, coupled with the signal at 7.35), 5.40 (d, 1H, J = 15.0 Hz, *endo* diastereotopic CH₂ linker, coupled with a signal in 7.01-6.97), 4.42 (d, 1H, J = 7.4 Hz, *syn* H_A set b), 4.20 (d, 1H, J = 7.6 Hz, *syn* H_A set a), 3.91 (d, 1H, J = 6.6 Hz, *syn* H_C set b), 3.74 (d, 1H, J = 6.6 Hz, *syn* H_C set a), 3.64 (d, 1H, J = 13.6 Hz, *anti* H_A set a), 3.55 (d, 1H, J = 13.5 Hz, *anti* H_A set b), 2.94 (d, 1H, J = 12.3 Hz, *anti* H_C set a), 2.83 (d, 1H, J = 11.8 Hz, *anti* H_C set b), 1.69 (s, 9H, 3CH₃), 1.57 (s, 9H, 3CH₃); $^{13}\text{C}\{^1\text{H}\}$ NMR (CDCl_3 , 100 MHz): δ 173.8 (carbene), 173.2 (carbene), 155.9, 155.4, 145.7, 145.6, 140.35, 140.31, 135.0, 134.9, 131.4, 131.3, 131.0, 130.9, 127.82, 127.80, 121.8, 121.7, 120.5, 120.2, 120.0, 119.3, 118.9 (C_B), 117.4 (C_B), 75.3 (C_A), 74.7 (C_A), 57.9 (CH₂ linker), 54.1 (CH₂ linker), 53.9 (NC(CH₃)₃), 53.4 (NC(CH₃)₃), 51.3 (C_C), 50.7 (C_C), 31.4 (CH₃), 31.3 (CH₃). Anal. Calcd for C₂₀H₂₄BF₄N₃Pd (499.65): C, 48.08; H, 4.84; N, 8.41%. Found: C, 48.01; H, 4.87; N, 8.54%.

Complex 12: The synthetic procedure is directly analogous to that for **10a** using **5** (0.34 mmol) and [Pd(allyl)Cl]₂ (64 mg, 0.17 mmol). Compound **12** was obtained as a yellow air sensitive solid (124 mg, 0.30 mmol, 84%). ^1H NMR (CDCl_3 , 400 MHz): δ 8.96-8.94 (m, 1H), 8.58 (d, 1H, J = 7.2 Hz), 8.26 (d, 1H, J = 8.2 Hz), 7.90 (d, 1H, J = 8.1 Hz), 7.67-7.63 (m, 1H), 7.54-7.50 (m, 2H), 7.16 (d, 1H, J = 1.5 Hz, CH_{imidazole}), 4.83 (m, 1H, H_B), 4.38 (t, 2H, J = 7.4 Hz, NCH₂), 4.07 (d, 1H, J = 7.4 Hz, *syn* H_A), 2.98 (d, 1H, J = 13.5 Hz, *anti* H_A), 2.67 (br s, 1H, *syn* H_C), 2.04-1.97 (m, 2H, NCH₂CH₂), 1.51 (br, 1H, *anti* H_C), 1.04 (t, 3H, J = 7.4 Hz, CH₃); $^{13}\text{C}\{^1\text{H}\}$ NMR (CDCl_3 , 100 MHz): δ 180.8 (carbene), 151.0, 142.4, 137.0, 136.6, 129.2, 128.8, 128.6, 126.2, 124.4, 121.8, 120.5, 114.3 (C_B), 71.6 (C_A), 52.8 (NCH₂), 49.0 (C_C), 24.3 (NCH₂CH₂), 11.4

(CH₃). Anal. Calcd for C₁₈H₂₀ClN₃Pd (420.24): C, 51.44; H, 4.80; N, 10.00%. Found: C, 51.32; H, 4.91; N, 10.21%.

Complex 13: Palladium complex **12** (80 mg, 0.19 mmol) was dissolved in dichloromethane (5 mL), to which was quickly added AgBF₄ (37 mg, 0.19 mmol). The mixture was stirred for 3 h in the dark. The precipitates generated were filtered off to give a clear solution. The solvent was removed in vacuo to give a light yellow solid (94 mg, 0.20 mmol, 97%). ¹H NMR (acetone-*d*₆, 400 MHz): δ 9.59 (dd, 1H, *J* = 4.9 and 1.4 Hz), 8.92 (dd, 1H, *J* = 4.9 and 1.4 Hz), 8.40 (d, 1H, *J* = 7.8 Hz), 8.26 (d, 1H, *J* = 8.2 Hz), 8.13 (d, 1H, *J* = 2.0 Hz, CH_{imidazole}), 7.95 (t, 1H, *J* = 7.9 Hz), 7.84-7.90 (m, 2H), 5.82 (m, 1H, H_B), 4.37-4.33 (m, 3H, NCH₂ + allyl *syn* H_A), 4.04 (d, 1H, *J* = 6.8 Hz, *syn* H_C), 3.80 (d, 1H, *J* = 13.8 Hz, *anti* H_A), 3.05 (d, 1H, *J* = 12.0 Hz, *anti* H_C), 1.06 (t, 3H, *J* = 7.3 Hz, CH₃). The NCH₂CH₂CH₃ signals overlap with the solvent residue peaks at δ 2.05. The ¹³C NMR spectrum of complex **13** could not be obtained due to its poor solubility in acetone-*d*₆ or CDCl₃. Anal. Calcd for C₁₈H₂₀BF₄N₃Pd (471.60): C, 45.84; H, 4.27; N, 8.91%. Found: C, 45.47; H, 4.31; N, 8.78%.

The mixture of complex 13 and complex 14: ¹H NMR (CD₃CN, 300 MHz): δ 9.30-9.32 (m, 1H), 8.72-8.70 (m, 1H), 8.16-8.09 (m, 2H), 7.84 (t, 1H, *J* = 8.0 Hz), 7.76 (d, 1H, *J* = 1.8 Hz, CH_{imidazole}), 7.72-7.69 (m, 1H), 7.52 (d, 1H, *J* = 1.9 Hz, CH_{imidazole}), 5.69 (m, 1H, H_B), 4.20-4.17 (m, 3H, NCH₂ + *syn* H_A), 3.93 (br, 1H, *syn* H_C), 3.65 (d, 1H, *J* = 13.8 Hz, *anti* H_A), 2.94 (br d, 1H, *anti* H_C), 1.96-1.94 (m, 2H, CH₂CH₃), 1.02 (t, 3H, *J* = 7.34 Hz, CH₃); ¹³C{¹H} NMR (CD₃CN, 75 MHz): δ 175.6 (carbene), 161.1, 141.7, 139.1, 135.3, 132.0, 129.8, 128.7, 125.4, 124.4, 123.1, 122.5, 121.7 (C_B), 77.6 (C_A), 54.1 (NCH₂), 49.2 (C_C), 25.4 (NCH₂CH₂), 11.2 (CH₃), 1.32 (septet, ¹*J*_{DC} = 20.6 Hz, CD₃CN-Pd). The resonance signal of CD₃CN-Pd overlaps with that of the solvent peak (δ 118.2).

General Procedure for Suzuki Reaction: Under an atmosphere of argon, phenylboronic acid (0.6 mmol), Cs₂CO₃ (0.6 mmol) and catalyst (1 mmol%) were added to the bottle, then, 1,4-dioxane (1 mL) was injected. After it was stirred for ten minutes, aryl halide (0.5 mmol) was added. The mixture was stirred for additional 4 h at 80 °C. After addition of ethyl acetate (20 mL),

it was filtered and washed with excess ethyl acetate. The solvent was removed, and the residue was purified by column.

X-ray Crystallographic Analyses of Complexes 6b, 9b, 10a, 10c, 11a, 11b, and 11c:

Colorless crystals of each compound suitable for X-ray structure studies were obtained by the slow diffusion of ether to their dichloromethane solutions at room temperature for two or three days. A single crystal of each complex of suitable size was mounted on a glass fiber using glue. Intensity data were collected on a Bruker-AXS X8 Kappa diffractometer equipped with an Apex-II CCD detector, using a graphite monochromator $\lambda(\text{Mo K}_{\alpha 1}) = 0.71073 \text{ \AA}$ radiation. The structures were solved by direct methods and refined against all F^2 data by full-matrix least-squares techniques. All the non-hydrogen atoms were refined with anisotropic displacement parameter. The hydrogen atoms were introduced into the geometrically calculated position and refined riding on the corresponding parent atoms.

3.5. References

1. (a) Arduengo, A. J., III; Harlow, R. L.; Kline, M. *J. Am. Chem. Soc.* **1991**, *113*, 361. (b) Arduengo, A. J., III. *Acc. Chem. Res.* **1999**, *32*, 913.
2. Hermann, W. A. *Angew. Chem., Int. Ed.* **2002**, *41*, 1290, and references therein.
3. Trnka, T. M.; Grubbs, R. H. *Acc. Chem. Res.* **2001**, *34*, 18, and references therein.
4. Hillier, A. C.; Grasa, G. A.; Viciu, M. S.; Lee, H. M.; Yang, C.; Nolan, S. P. *J. Organomet. Chem.* **2002**, *653*, 69, and references therein.
5. (a) Perry, M. C.; Burgess, K. *Tetrahedron Asymmetry* **2003**, *14*, 951. (b) Peris, E.; Crabtree, R. H. *Coord. Chem. Rev.* **2004**, *248*, 2239.
6. (a) Enders, D.; Niemeier, O.; Henseler, A. *Chem. Rev.* **2007**, *107*, 5606. (b) Marion, N.; Díez-González, S.; Nolan, S. P. *Angew. Chem., Int. Ed.* **2007**, *46*, 2988. (c) Phillips, E. M.; Wadamoto, M.; Chan, A.; Scheidt, K. A. *Angew. Chem., Int. Ed.* **2007**, *46*, 3107.
7. Some books and reviews about NHC-metals: (a) Nolan, S. P., Ed. *N-Heterocyclic Carbenes in Synthesis*, Wiley-VCH **2006**. (b) Glorius, F., Ed. *N-Heterocyclic Carbenes in Transition Metal Catalysis*, Springer **2007**. (c) Lee, H. M.; Lee, C. C.; Cheng, P. Y. *Curr. Org. Chem.* **2007**, *11*, 1491. (d) Hahn, F. E.; Jahnke, M. C. *Angew. Chem., Int. Ed.* **2008**, *47*, 3122. On coinage metals (Cu, Ag, Au): (e) Lin, J. C. Y.; Huang, R. T. W.; Lee, C. S.; Bhattacharyya, A.; Hwang, W. S.; Lin, I. J. B. *Chem. Rev.* **2009**, *109*, 3561. (f) Marion, N.; Nolan, S. P. *Chem. Soc. Rev.* **2008**, *37*, 1776.
On F-block metals: (g) Arnold, P. L.; Casely, I. J. *Chem. Rev.* **2009**, *109*, 3599.
On Ruthenium: (h) Colacino, E.; Martinez, J.; Lamaty, F. *Coord. Chem. Rev.* **2007**, *251*, 726. (i) Dragutan, V.; Dragutan, I.; Delaude, L.; Demonceau, A. *Coord. Chem. Rev.* **2007**, *251*, 765.
8. Grubbs, R. H. *Tetrahedron*. **2004**, *60*, 7117.
9. (a) Marion, N.; Nolan, S. P. *Acc. Chem. Res.* **2008**, *41*, 1440. (b) Wuerztz, S.; Glorius, F. *Acc. Chem. Res.* **2008**, *41*, 1523.
10. Magill, A. M.; Cavell, K. J.; Yates, B. F. *J. Am. Chem. Soc.* **2004**, *126*, 8717.
11. Dorta, R.; Stevens, E. D.; Scott, N. M.; Costabile, C.; Cavallo, L.; Hoff, C. D.; Nolan, S. P. *J. Am. Chem. Soc.* **2005**, *127*, 2485.
12. Despagnet-Ayoub, E.; Grubbs, R. H. *J. Am. Chem. Soc.* **2004**, *126*, 10198.

13. (a) Prasang, C.; Donnadiou, B.; Bertrand, G. *J. Am. Chem. Soc.* **2005**, *127*, 10182. (b) Bazinet, P.; Yap, G. P. A.; Richeson, D. S. *J. Am. Chem. Soc.* **2003**, *125*, 13314.
14. (a) Scarborough, C. C.; Grady, M. J. W.; Guzei, I. A.; Gandhi, B. A.; Bunel, E. E.; Stahl, S. S. *Angew. Chem., Int. Ed.* **2005**, *44*, 5269. (b) Iglesias, M.; Beetstra, D. J.; Knight, J. C.; Ooi, L.-L.; Stasch, A.; Coles, S.; Male, L.; Hursthouse, M. B.; Cavell, K. J.; Dervisi, A.; Fallis, I. A. *Organometallics* **2008**, *27*, 3279. (c) Scarborough, C. C.; Popp, B. V.; Guzei, I. A.; Stahl, S. S. *J. Organomet. Chem.* **2005**, *690*, 6143.
15. (a) Albrecht, M.; Miecznikowski, J. R.; Samuel, A.; Faller, J. W.; Crabtree, R. H. *Organometallics* **2002**, *21*, 3596. (b) Mas-Marzá, E.; Poyatos, M.; Sanaú, M.; Peris, E. *Inorg. Chem.* **2004**, *43*, 2213. (c) Chianese, A. R.; Crabtree, R. H. *Organometallics* **2005**, *24*, 4432.
16. (a) Marion, N.; Ecarnot, E. C.; Navarro, O.; Amoroso, D.; Bell, A.; Nolan, S. P. *J. Org. Chem.* **2006**, *71*, 3816. (b) Peris, E.; Loch, J. A.; Mata, J.; Crabtree, R. H. *Chem. Commun.* **2001**, 201.
17. (a) Wang, H. M. J.; Lin, I. J. B. *Organometallics* **1998**, *17*, 972. (b) Lin, I. J. B.; Vasam, C. S. *Coord. Chem. Rev.* **2007**, *251*, 642, and references therein. (c) Garrison, J. C.; Youngs, W. J. *Chem. Rev.* **2005**, *105*, 3978, and references therein. (d) Kascatan-Nebioglu, A.; Panzner, M. J.; Tessier, C. A.; Cannon, C. L.; Youngs, W. J. *Coord. Chem. Rev.* **2007**, *251*, 884.
18. (a) Herrmann, W. A.; Gooßen, L. J.; Spiegler, M. *J. Organomet. Chem.* **1997**, *547*, 357. (b) Danopoulos, A. A.; Winston, S.; Motherwell, W. B. *Chem. Commun.* **2002**, 1376.
19. (a) Grundemann, S.; Albrecht, M.; Kovacevic, A.; Faller, J. W.; Crabtree, R. H. *J. Chem. Soc., Dalton Trans.* **2002**, 2163. (b) Clement, N. D.; Cavell, K. J.; Jones, C.; Elsevier, C. J. *Angew. Chem., Int. Ed.* **2004**, *43*, 1277. (c) Viciano, M.; Mas-Marzá, E.; Poyatos, M.; Sanaú, M.; Crabtree, R. H.; Peris, E. *Angew. Chem., Int. Ed.* **2005**, *44*, 444.
20. (a) Schuster, O.; Yang, L.; Raubenheimer, H. G.; Albrecht, M. *Chem. Rev.* **2009**, *109*, 3445. (b) Arnold, P. L.; Pearson, S. *Coord. Chem. Rev.* **2007**, *251*, 596.
21. Raubenheimer, H. G.; Cronje, S. *Dalton Trans.* **2008**, 1265.
22. Vignolle, J.; Cattoen, X.; Bourissou, D. *Chem. Rev.* **2009**, *109*, 3333.
23. (a) Herrmann, W. A.; Ofele, K.; Schneider, S. K.; Herdtweck, E.; Hoffmann, S. D. *Angew. Chem., Int. Ed.* **2006**, *45*, 3859. (b) Wass, D. F.; Haddow, M. F.; Hey, T. W.; Orpen, A. G.; Russell, C. A.; Wingad, R. L.; Green, M. *Chem. Commun.* **2007**, 2704. (c) Wass, D. F.; Hey,

- T. W.; Rodriguez-Castro, J.; Russel, C. A.; Shishkov, I. V.; Wingand, R. L.; Green, M. *Organometallics* **2007**, 26, 4702. (d) öfele, K.; Tosh, E.; Taubmann, C.; Herrmann, W. A. *Chem. Rev.* **2009**, 109, 3408.
24. (a) Lavallo, V.; Dyker, C. A.; Donnadieu, B.; Bertrand, G. *Angew. Chem., Int. Ed.* **2008**, 47, 5411. (b) Han, Y.; Huynh, H. V.; Tan, G. K. *Organometallics* **2007**, 26, 6581. (c) Han, Y.; Huynh, H. V. *Chem. Commun.* **2007**, 1089.
25. (a) Wiedemann, S. H.; Lewis, J. C.; Ellman, J. A.; Bergman, R. G. *J. Am. Chem. Soc.* **2006**, 128, 2452. (b) Conejero, S.; Lara, P.; Paneque, M.; Petronilho, A.; Poveda, M. L.; Serrano, O.; Vattier, F.; Álvarez, E.; Moya, C.; Salazar, V.; Carmona, E. *Angew. Chem., Int. Ed.* **2008**, 47, 4380. (c) Buil, M. L.; Esteruelas, M. A.; Garcés, K.; Oliván, M.; Oñate, E. *J. Am. Chem. Soc.* **2007**, 129, 10998. (d) Song, G.; Li, Y.; Chen, S.; Li, X. *Chem. Commun.* **2008**, 3558.
26. Schuster, E. M.; Botoshansky, M.; Gandelman, M. *Angew. Chem., Int. Ed.* **2008**, 47, 4555.
27. Song, G.; Zhang, Y.; Li, X. *Organometallics* **2008**, 27, 1936.
28. (a) Yin, L. X.; Liebscher, J. *Chem. Rev.* **2007**, 107, 133. (b) Lightowler, S.; Hird, M. *Chem. Mater.* **2004**, 16, 3963. (c) Beccalli, E. M.; Broggini, G.; Martinelli, M.; Sottocornola, S. *Chem. Rev.* **2007**, 107, 5318.
29. (a) Beletskaya, I. P.; Cheprakov, A. V. *Chem. Rev.* **2000**, 100, 3009. (b) Amatore, C.; Jutand, A. *Acc. Chem. Res.* **2000**, 33, 314. (c) Phan, N. T. S.; Sluys, M. V. D.; Jones, C. W. *Adv. Synth. Catal.* **2006**, 348, 609.
30. (a) Miyaura, N.; Suzuki, A. *Chem. Rev.* **1995**, 95, 2457. (b) Suzuki, A. *J. Organomet. Chem.* **1999**, 576, 147. (c) Martin, R.; Buchwald, S. L. *Acc. Chem. Res.* **2008**, 41, 1461.
31. Chinchilla, R.; Nájera, C. *Chem. Rev.* **2007**, 107, 874.
32. Some reviews about palladium NHCs in catalysis, see: (a) Kantchev, E. A. B.; O'Brien, C. J.; Organ, M. G. *Angew. Chem., Int. Ed.* **2007**, 46, 2768. (b) Crudden, C. M.; Allen, D. P. *Coord. Chem. Rev.* **2004**, 248, 2247.
33. Herrmann, W. A.; Elison, M.; Fisher, J.; Köcher, C.; Artus, G. R. J. *Angew. Chem., Int. Ed.* **1995**, 34, 2371.
34. (a) Poyatos, M.; Mata, J. A.; Peris, E. *Chem. Rev.* **2009**, 109, 3677. (d) Mata, J. A.; Poyatos, M.; Peris, E. *Coord. Chem. Rev.* **2007**, 251, 841.

35. Albert, K.; Gisdakis, P.; Rösch, N. *Organometallics* **1998**, *17*, 1608.
36. (a) Shaffer, A. R.; Schmidt, J. A. R. *Organometallics* **2009**, *28*, 2494. (b) Frøseth, M.; Netland, K. A.; Törnroos, K. W.; Dhindsa, A.; Tilset, M. *Dalton Trans.* **2005**, 1664. (c) Frøseth, M.; Dhindsa, A.; Røise, H.; Tilset, M. *Dalton Trans.* **2003**, 4516. (d) Coleman, K. S.; Chamberlayne, H. T.; Tuberville, S.; Green, M. L. H.; Cowley, A. R. *Dalton Trans.* **2003**, 2917. (e) Meyer, D.; Taige, M. A.; Zeller, A.; Hohlfeld, K.; Ahrens, S.; Strassner, T. *Organometallics* **2009**, *28*, 2142. (f) Netland, K. A.; Krivokapic, A.; Schröder, M.; Boldt, K.; Lundvall, F.; Tilset, M. *J. Organomet. Chem.* **2008**, 693, 3703. (g) Bonnet, L. G.; Douthwaite, R. E.; Kariuki, B. M. *Organometallics* **2003**, *22*, 4187.
37. (a) Waltman, A. W.; Grubbs, R. H. *Organometallics* **2004**, *23*, 3105. (b) Dyson, G.; Frison, J.; Simonovic, S.; Whitwood, A. C.; Douthwaite, R. E. *Organometallics* **2008**, *27*, 281.
38. (a) Fliedel, C.; Schnee, G.; Braunstein, P. *Dalton Trans.* **2009**, 2474. (b) Huynh, H. V.; Yeo, C. H.; Tan, G. K. *Chem. Commun.* **2006**, 3833.
39. (a) Tsoureas, N.; Danopoulos, A. A.; Tulloch, A. A. D.; Light, M. E. *Organometallics* **2003**, *22*, 4750. (b) Wang, A.-E.; Zhong, J.; Xie, J.-H.; Li, K.; Zhou, Q.-L. *Adv. Synth. Catal.* **2004**, *346*, 595. (c) Yang, C.; Lee, H. M.; Nolan, S. P. *Org. Lett.* **2001**, *3*, 1511. (d) Danopoulos, A. A.; Tsoureas, N.; Macgregor, S. A.; Smith, C. *Organometallics* **2007**, *26*, 253. (e) Hahn, F. E.; Jahnke, M. C.; Pape, T. *Organometallics* **2006**, *25*, 5927. (f) Song, G.; Wang, X.; Li, Y.; Li, X. *Organometallics* **2008**, *27*, 1187. (g) Shaghafi, M. B.; Kohn, B. L.; Jarvo, E. R. *Org. Lett.* **2008**, *10*, 4743.
40. (a) Simons, R. S.; Custer, P.; Tessier, C. A.; Youngs, W. J. *Organometallics* **2003**, *22*, 1979. (b) Zeng, F. L.; Yu, Z. K. *J. Org. Chem.* **2006**, *71*, 5274. (c) Xi, Z.; Zhang, X.; Chen, W.; Fu, S.; Wang, D. *Organometallics* **2007**, *26*, 6636. (d) Chiu, P. L.; Lai, C.-L.; Chang, C.-F.; Hu, C.-H.; Lee, H. M. *Organometallics* **2005**, *24*, 6169. (e) Chen, J. C. C.; Lin, I. J. B. *Organometallics* **2000**, *19*, 5113.
41. (a) Barczak, N. T.; Grote, R. E.; Jarvo, E. R. *Organometallics* **2007**, *26*, 4863. (b) Wang, X.; Liu, S.; Weng, L.-H.; Jin, G.-X. *Organometallics* **2006**, *25*, 3565. (c) Zhang, X.; Xi, Z.; Liu, A.; Chen, W. *Organometallics* **2008**, *27*, 4401. (d) Loch, J. A.; Albrecht, M.; Peris, E.; Mata, J.; Faller, J. W.; Crabtree, R. H. *Organometallics* **2002**, *21*, 700. (e) McGuinness, D. S.; Cavell, K. J. *Organometallics* **2000**, *19*, 741. (f) Cheng, Y.; Sun, J.-F.; Yang, H.-L.; Xu, H.-J.; Li, Y.-Z.; Chen, X.-T.; Xue, Z.-L. *Organometallics* **2009**, *28*, 819.
42. (a) Trost, B. M. *Acc. Chem. Res.* **1996**, *29*, 355. (b) Pregosin, P. S.; Salzmänn, R. *Coord. Chem. Rev.* **1996**, *155*, 35.

43. (a) Marion, N.; Navarro, O.; Mei, J.; Stevens, E. D.; Scott, N. M.; Nolan, S. P. *J. Am. Chem. Soc.* **2006**, *128*, 4101. (b) Viciu, M. S.; Germaneau, R. F.; Navarro-Fernandez, O.; Stevens, E. D.; Nolan, S. P. *Organometallics* **2002**, *21*, 5470. (c) Navarro, O.; Kaur, H.; Mahjoor, P.; Nolan, S. P. *J. Org. Chem.* **2004**, *69*, 3173.
44. (a) Chernyshova, E. S.; Goddard, R.; Pörschke, K-R. *Organometallics* **2007**, *26*, 3236, and references therein. (b) Filipuzzi, S.; Pregosin, P. S.; Albinati, A.; Rizzato, S. *Organometallics* **2008**, *27*, 437.
45. (a) Ketz, B. E.; Cole, A. P.; Waymouth, R. M. *Organometallics* **2004**, *23*, 2835. (b) Visentin, F.; Togni, A. *Organometallics* **2007**, *26*, 3746. (c) Roseblade, S. J.; Ros, A.; Monge, D.; Alcarazo, M.; Álvarez, E.; Lassaletta, J. M.; Fernández, R. *Organometallics* **2007**, *26*, 2570. (d) Canac, Y.; Duhayon, C.; Chauvin, R. *Angew. Chem., Int. Ed.* **2007**, *46*, 6313.
46. Tulloch, A. A. D.; Danopoulos, A. A.; Winston, S.; Kleinhenz, S.; Eastham, G. *J. Chem. Soc., Dalton Trans.* **2000**, 4499.
47. César, V.; Bellemin-Lapponnaz, S.; Gade, L. H. *Organometallics* **2002**, *21*, 5204.
48. Pytkowicz, J.; Roland, S.; Mangeney, P. *J. Organomet. Chem.* **2001**, *631*, 157.
49. Chianese, A. R.; Li, X.; Janzen, M. C.; Faller, J. W.; Crabtree, R. H. *Organometallics* **2003**, *22*, 1663.
50. Chianese, A. R.; Kovacevic, A.; Zeglis, B. M.; Faller, J. W.; Crabtree, R. H. *Organometallics* **2004**, *23*, 2461.
51. (a) Tulloch, A. A. D.; Winston, S.; Danopoulos, A. A.; Eastham, G.; Hursthouse, M. B. *Dalton Trans.* **2003**, 699. (b) Danopoulos, A. A.; Tulloch, A. A. D.; Winston, S.; Eastham, G.; Hursthouse, M. B. *Dalton Trans.* **2003**, 1009. (c) Ray, L.; Shaikh, M. M.; Ghosh, P. *Organometallics* **2007**, *26*, 958. (d) Ray, L.; Barman, S.; Shaikh, M. M.; Ghosh, P. *Chem. Eur. J.* **2008**, *14*, 6646.
52. (a) Wanniarachchi, Y. A.; Kogiso, Y.; Slaughter, L. M. *Organometallics* **2008**, *27*, 21. (b) Viciano, M.; Feliz, M.; Corberan, R.; Mata, J. A.; Clot, E.; Peris, E. *Organometallics* **2007**, *26*, 5304.
53. (a) Xu, L.; Shi, Y. *J. Org. Chem.* **2008**, *73*, 749. (b) Roland, S.; Audouin, M.; Mangeney, P. *Organometallics* **2004**, *23*, 3075.

54. (a) Vriez, K. In *Dynamic Nuclear Magnetic Resonance Spectroscopy*; Jackman, L. M.; Cotton, F. A., Eds.; Academic Press: New York, **1975**; p 44-483. (b) Breutel, C.; Pregosin, P. S.; Salzmann, R.; Togni, A. *J. Am. Chem. Soc.* **1994**, *116*, 4067. (c) Kumar, P. G. A.; Dotta, P.; Hermatschweiler, R.; Pregosin, P. S.; Albinati, A.; Rizzato, S. *Organometallics* **2005**, *24*, 1306. (d) Faller, J. W.; Sarantopoulos, N. *Organometallics* **2004**, *23*, 2008.
55. Gogoll, A.; örnebro, J.; Grennberg, H.; Bäckvall, J.-E. *J. Am. Chem. Soc.* **1994**, *116*, 3631.
56. Leung, C. H.; Incarvito, C. D.; Crabtree, R. H. *Organometallics* **2006**, *25*, 6099.
57. (a) Douthwaite, R. E.; Haüssinger, D.; Green, M. L. H.; Silcock, P. J.; Gomes, P. T.; Martins, A. M.; Danopoulos, A. A. *Organometallics* **1999**, *18*, 4584. (b) Caddick, S.; Cloke, F. G. N.; Hitchcock, P. B.; Lewis, A. K. de K. *Angew. Chem., Int. Ed.* **2004**, *43*, 5824.
58. Canal, J. M.; Gómez, M.; Jiménez, F.; Rocamora, M.; Muller, G.; Duañch, E.; Franco, D.; Jiménez, A.; Cano, F. H. *Organometallics* **2000**, *19*, 966.
59. Anderson, D. R.; Hickstein, D. D.; ÓLeary, D. J.; Grubbs, R. H. *J. Am. Chem. Soc.* **2006**, *128*, 8386.
60. Gardiner, M. G.; Herrmann, W. A.; Reisinger, C.-P.; Schwarz, J.; Spiegler, M. *J. Organomet. Chem.* **1999**, *572*, 239.
61. Bertrand, G.; Díez-Barra, E.; Fernández-Baeza, J.; Gornitzka, H.; Moreno, A.; Otero, A.; Rodríguez-Curiel, R. I.; Tejeda, J. *Eur. J. Inorg. Chem.* **1999**, 1965.
62. (a) Tulloch, A. A. D.; Danopoulos, A. A.; Tizzard, G. J.; Coles, S. J.; Hursthouse, M. B.; Hay-Motherwell, R. S.; Motherwell, W. B. *Chem. Commun.* **2001**, 1270. (b) Magill, A. M.; McGuinness, D. S.; Cavell, K. J.; Britovsek, G. J. P.; Gibson, V. C.; White, A. J. P.; Williams, D. J.; White, A. H.; Skelton, B. W. *J. Organomet. Chem.* **2001**, *617*, 546. (c) Gründemann, S.; Albrecht, M.; Loch, J. A.; Faller, J. W.; Crabtree, R. H. *Organometallics* **2001**, *20*, 5485. (d) Miecznikowski, J. R.; Gründemann, S.; Albrecht, M.; Mégret, C.; Clot, E.; Faller, J. W.; Eisenstein, O.; Crabtree, R. H. *Dalton Trans.* **2003**, 831.
63. Drew, D.; Doyle, J. R. *Inorg. Syn.* **1990**, *28*, 346.
64. Dwyer, A. N.; Grossel, M. C.; Horton, P. N. *Supramol. Chem.* **2004**, *16*, 405.
65. Liu, J.; Chen, J.; Zhao, J.; Zhao, Y.; Li, L.; Zhang, H. *Synthesis* **2003**, *17*, 2661.

CHAPTER 4

Quinoline-Tethered N-heterocyclic Carbenes (NHCs) Complexes of Rhodium and Iridium: Synthesis, Catalysis, and Electrochemistry

4.1. Introduction

Among various transition-metal catalysts, rhodium and iridium catalysts show some unique and complementary reactivity in comparison with other catalyst systems. Notable examples include rhodium-catalyzed cycloaddition,¹ asymmetric addition,² hydroacylation,³ and iridium-catalyzed asymmetric hydrogenation.^{4,13b} In contrast to the commonly used Group 10 metal catalysts (nickel, palladium, and platinum) which function between valence zero and plus two oxidation states in many catalytic cycles, it is generally believed that both rhodium and iridium shuttle between (I) and (III) oxidation states. Therefore, they possess some distinctive catalytic reactivity. Recently, N-heterocyclic carbene (NHC) complexes of rhodium and iridium have been widely studied. Several review articles summarized the structure properties and catalytic applications of poly(N-heterocyclic carbene) metal complexes.⁵ Bidentate and tridentate chelating NHC ligands are well-known as poly(N-heterocyclic carbene) ligands (Figure 4.1), which can coordinate to metals in different modes affording structure versatility. For rhodium and iridium, different valences (+I or +III) and structures can be obtained depending on the reaction conditions. Ligand A (Figure 4.1.) is taken as an example to discuss in further detail.

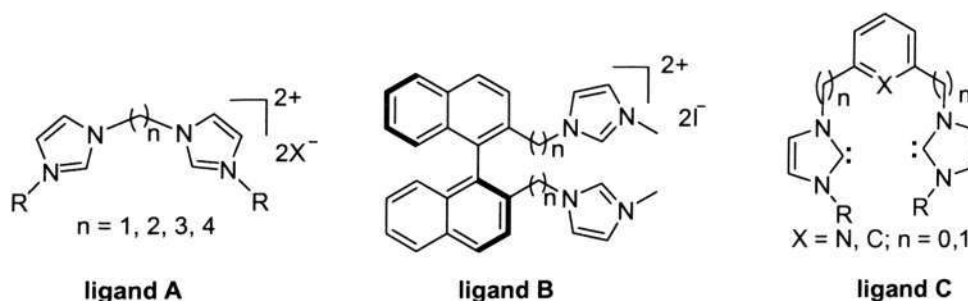
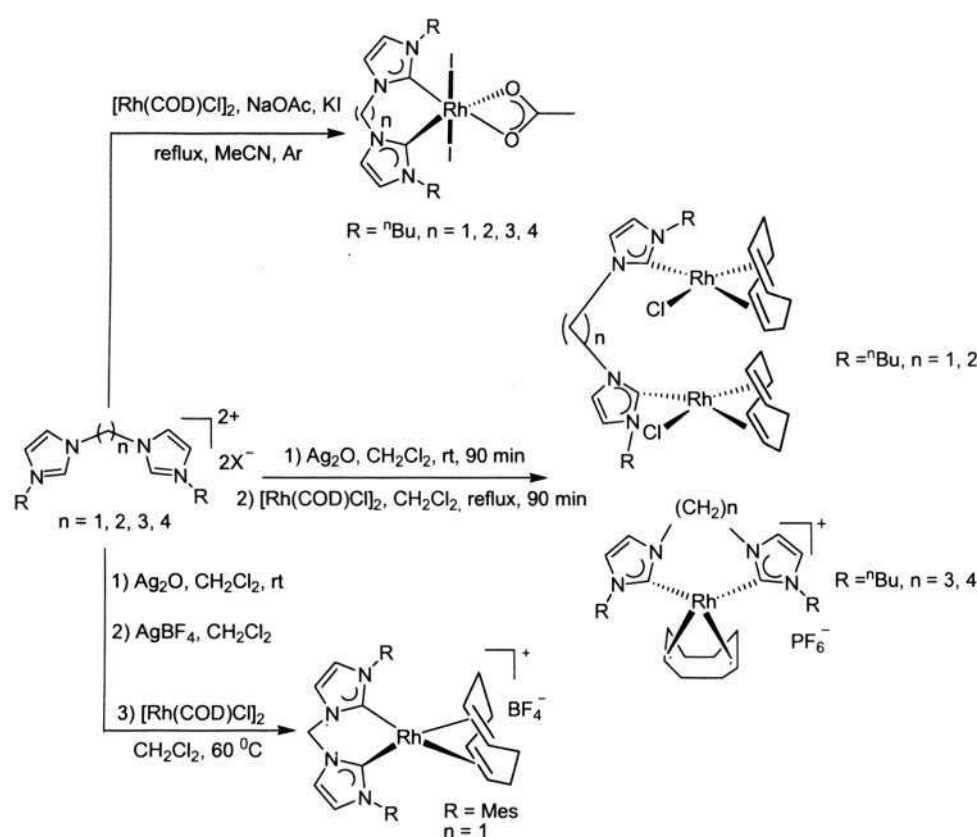


Figure 4.1. Several commonly used poly(N-heterocyclic carbene) ligands.

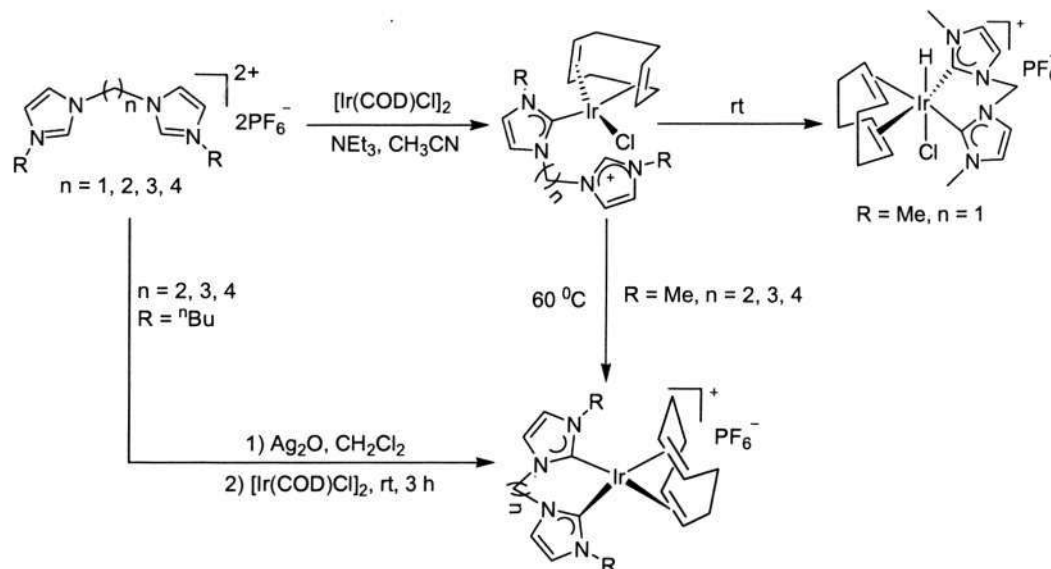
In 2003, Crabtree and co-workers gave detailed studies of the reactivity of chelating NHCs derived from bis-imidazolium salts having $(\text{CH}_2)_n$ ($n = 1-4$) linkers.⁶ They found that short linkers ($n = 1-2$) prefer to form monodentate bimetallic compounds, while long linkers ($n = 3-4$) favor a chelating square-planar Rh(I) product. Meanwhile, they point out that the origin of the effect comes from the restricted rotation of the diazole rings and orientations of these rings as n changes. The N-substituents also have a pronounced influence on the reaction product, as was demonstrated by Slaughter and co-workers who introduced a bulky mesityl group to this type ligand, which switched the coordination mode of the methylene-linker ligand ($n = 1$) to afford a chelating complex (Scheme 4.1).⁷



Scheme 4.1. Routes to synthesize various structure NHC-rhodium complexes.

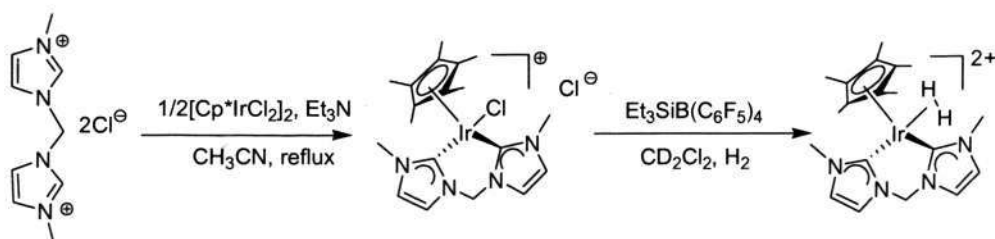
In the case of iridium, lengths of the linker and the substituent R also have great influences.⁸ For instance, using a silver transmetalation method ($n = 2-4$), bis-chelating products can be obtained from imidazolium ions, although with low yields (5-10%). If a base such as NEt_3 was added to the reaction mixture, $[\text{Ir}(\text{COD})\text{Cl}]_2$ can react with imidazolium salts affording

monometalated species at 60 °C (4 h, $n = 2, 3, 4$). Longer reaction times (12 h) give double-metalated products directly. However, when the linker is shorter ($n = 1$), monometalated intermediates cannot be isolated even at room temperature, as they further quickly evolve to their oxidative addition products: NHC-Ir(III)-hydride complexes (Scheme 4.2).^{8a}

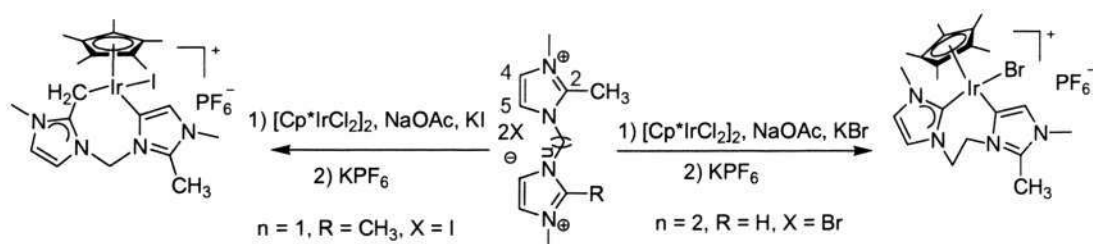


Scheme 4.2. Routes to prepare NHC-iridium complexes.

These bis-chelating NHC ligands have also been employed to prepare iridium(III) Cp* complexes, which can be synthesized by following either deprotonation of imidazolium salts⁹ or the silver-transmetalation method.^{10,13a} For example, Heinekey et al. reported the first dihydrogen bis-carbene complex, which was obtained from the reaction of a chelation iridium Cp* complex and $\text{Et}_3\text{SiB}(\text{C}_6\text{F}_5)_4$ under a hydrogen atmosphere (Scheme 4.3).^{9a} Later, Peris and co-workers extended the scope of this ligand,^{9b} and a series of iridium Cp* complexes were synthesized *via* double metalation processes, and experimental results showed that the reaction patterns were influenced by electronic and steric factors (Scheme 4.4). The following conclusion was drawn from DFT calculations: the first metalation is kinetically preferred at the aliphatic position, but it is not discriminable whether this step is a direct deprotonation by base or metalation through C-H activation. The second metalation has been proven as a kinetically chelation-assisted C-H activation at the C4/C5 position.



Scheme 4.3. Routes to synthesize the first NHC-iridium dihydrogen complex.



Scheme 4.4. Formation of abnormal iridium carbene complexes.

In addition to these bis-carbene ligands, another type of bidentate hemilabile ligand has also attracted much attention.¹¹ This kind of ligand combines a relatively weak donor and an NHC moiety, and has the advantages of both the strong NHC-metal bond and the labile heteroatom (O, N, S, or P) adjusting coordination modes, since ligand lability is crucial for many active catalysts that rely on ligand dissociation in the catalytic cycle.¹² However, in comparison with palladium compounds, these systems are less studied for rhodium and iridium complexes (Figure 4.2),^{12a,13} although reported results indicated that some of them could be efficient catalysts in different catalytic reactions. For instance, well-characterized iridium complexes based on oxazoline-carbene ligands have been employed in highly enantio-selective hydrogenation.¹⁴ Therefore, we incorporate our hemilabile quinoline-functionalized NHC ligand to prepare a series of rhodium and iridium complexes. In addition, catalytic activity and electrochemical properties of representative complexes have been investigated.

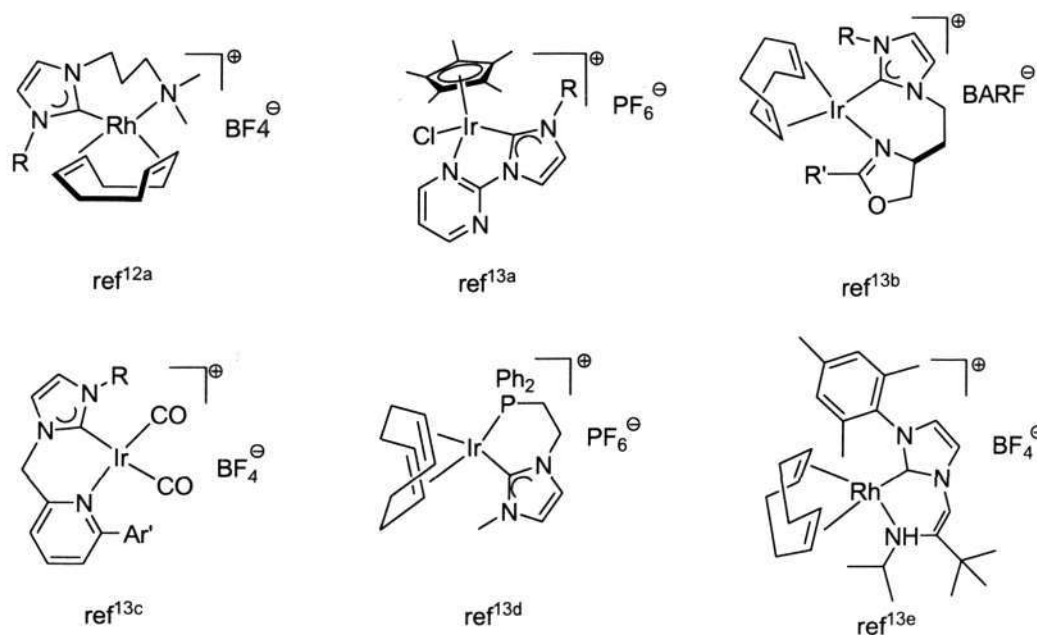
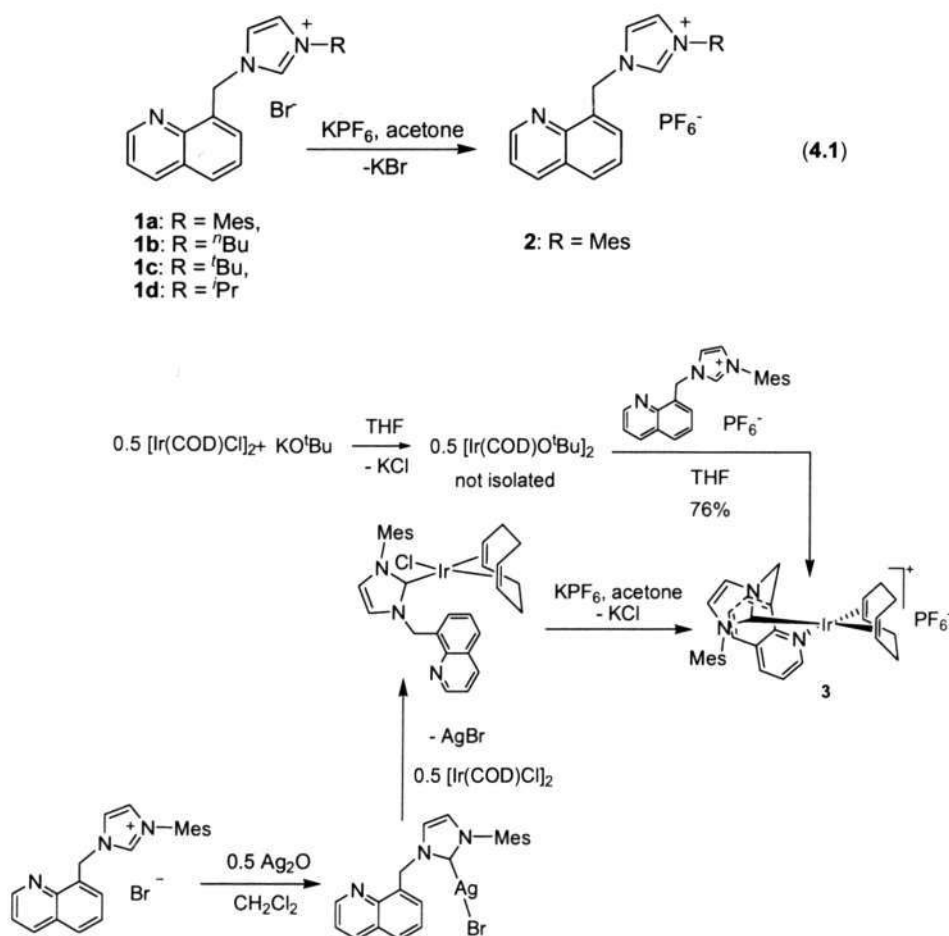


Figure 4.2. Reported examples of hemilabile NHC rhodium and iridium complexes.

4.2. Results and Discussion

4.2.1. Preparation of Rhodium and Iridium Complexes

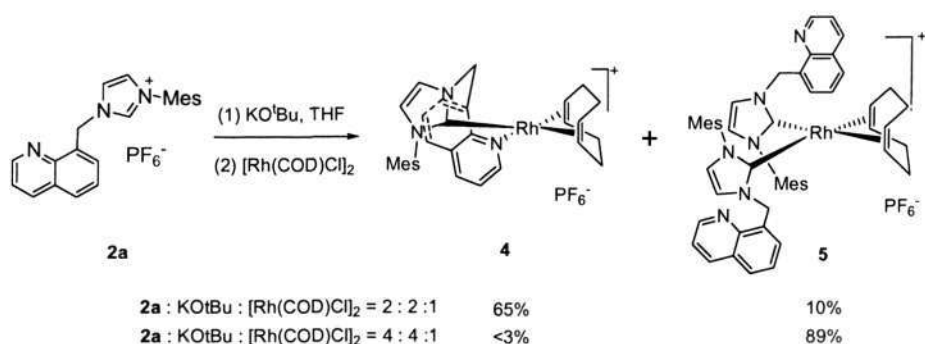
Cyclooctadiene Complexes of Rhodium and Iridium: Compound **2** can be prepared from imidazolium salt **1a** via anion exchange using KPF₆ (eq 4.1). Metalation of this carbene was performed first via two general methods starting from the corresponding imidazolium ions: direct metalation^{5a,15} and silver transmetalation (Scheme 4.5).¹⁶ In the direct metalation route, treatment of [Ir(COD)Cl]₂ with 2 equiv of KOBu^t gave [Ir(COD)OBu^t]₂ *in situ*, which further reacted with imidazolium **2** to afford a chelating carbene complex **3** in 76% overall yield. We also noted that complex **3** could be obtained in similar yield when **2** was first treated with KOBu^t to generate the corresponding carbene *in situ*, followed by metalation with [Ir(COD)Cl]₂. Alternatively, a silver carbene complex was obtained when **1a** was stirred with Ag₂O (0.5 equiv) in CH₂Cl₂. Subsequent addition of [Ir(COD)Cl]₂ (0.5 equiv) afforded the corresponding monodentate Ir(COD)(NHC)Cl complex and chloride abstraction by KPF₆ eventually gave product **3** in 94% yield (Scheme 4.5).



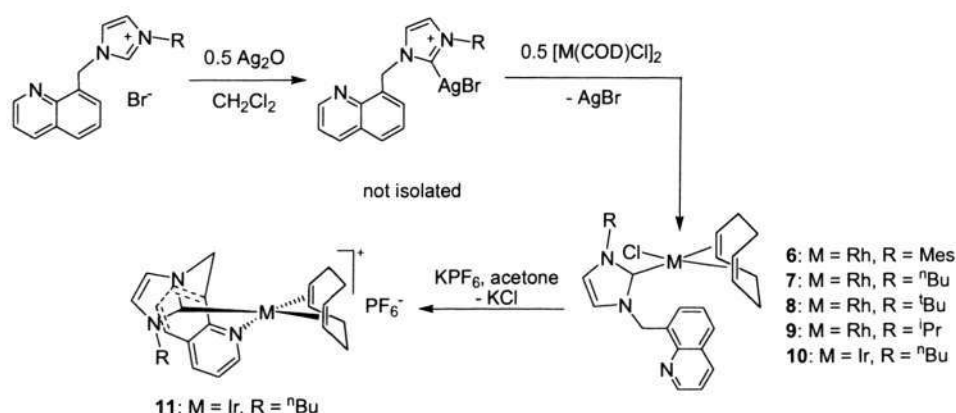
Scheme 4.5. Strategies to synthesize NHC-iridium complexes.

However, when we applied the direct metalation method to the synthesis of the rhodium analogue of **3**, we obtained both **4** and **5** in 65% and 10% yield, respectively (Scheme 4.6). The ^1H NMR spectrum of **5** shows that the ratio of carbene to COD is 2:1 and the identity of product **5** was confirmed by X-ray crystallography and mass spectrometry. We reason that the yield of biscarbene **5** can be maximized by increasing the ratio of carbene to rhodium. Indeed, when we used **2**, KO^tBu , and $[\text{Rh}(\text{COD})\text{Cl}]_2$ in 4:4:1 ratio, the yield of **5** was improved to 89%, with essentially no monocarbene product **4**. Herein, the difference between $[\text{Rh}(\text{COD})\text{Cl}]_2$ and $[\text{Ir}(\text{COD})\text{Cl}]_2$ in this direct metalation reaction likely originates from the strength of the $\text{M}_{\text{quinoline}}$ bond ($\text{M} = \text{Ir}$ or Rh). The quinoline N ligand in complex **4** is more labile when it is bound to Rh and can be readily substituted by the second incoming NHC, while no such substitution took place for the iridium analogue. It is also noted that it is relatively less common to have rhodium complexes of biscarbene in a monodendate mode,¹⁷ and there are even less examples of

bis-chelating ligands. In contrast, iridium or rhodium cyclooctadiene complexes (**6-10**) obtained from silver transmetalation are consistently neutral monodentate NHC complexes with a pendent quinoline moiety, from which chloride abstraction by KPF_6 can cleanly give the corresponding ionic chelating complexes (Scheme 4.7). ^1H NMR spectra (CDCl_3 or CD_3COCD_3) of complex **11** shows poorly resolved signals for virtually every peak, even at $-40\text{ }^\circ\text{C}$. Those signals appear significantly improved in CD_3CN , although the CH_2 linker signal is still slightly broadened in comparison with that of the analogous complex **3**. In the ^{13}C NMR spectrum in CD_3CN , however, we can only observe one sharp peak (δ 83.7) and one broad peak (δ 53.1) for the COD olefinic CH groups, although four COD methylene signals are well-resolved. Furthermore, in the ^{13}C NMR spectrum, in addition to the signal of solvent CD_3CN (δ 1.32, septet), a new signal can be found (δ 1.20, septet) that is attributed to coordinated CD_3CN . It is likely that the quinoline arm of the NHC-quinoline ligand is reversibly substituted by CD_3CN , which is probably the origin of the dynamic process responsible for signal broadening in ^1H and ^{13}C NMR spectra.



Scheme 4.6. Strategies to prepare NHC-rhodium complexes.



Scheme 4.7. Routes to synthesize cationic NHC rhodium and iridium complexes.

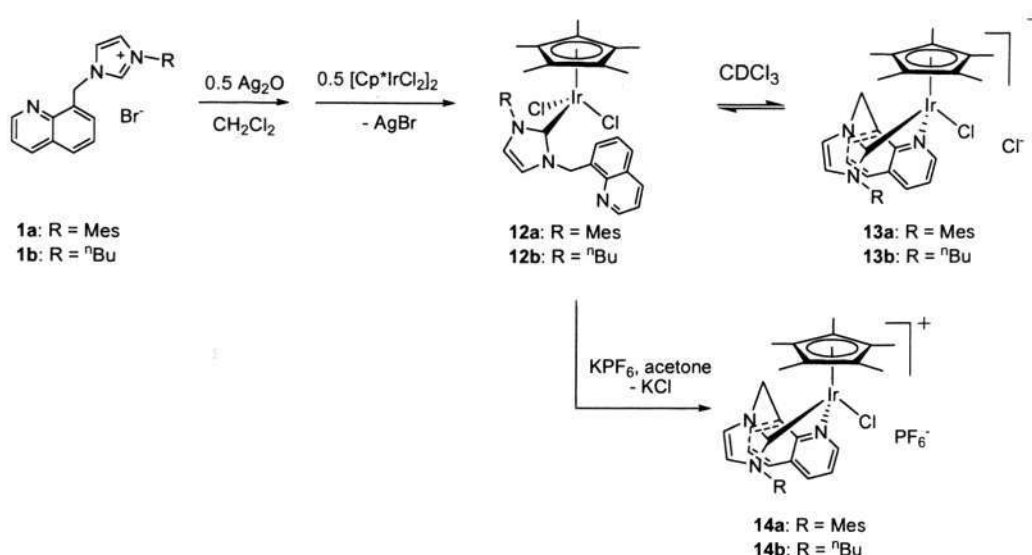
All these iridium and rhodium cyclooctadiene complexes were characterized by NMR spectroscopy and characteristic signals were listed in Table 4.1. In the ^1H NMR spectra, all the linker CH_2 protons are diastereotopic, indicating that there is a hindered rotation along the $\text{M}-\text{C}_{\text{carbene}}$ bond and complexes **3**, **4**, **6-11** are all C_1 symmetrical. ^1H NMR spectra also showed that the differences in the chemical shifts of these two diastereotopic protons are more significant in chelating $\text{NHC}^{\wedge}\text{N}$ complexes (**3** and **4**) possibly due to the *endo* and *exo* orientation of these two protons with respect to the seven-membered metalacycle. The carbene C atoms resonate characteristically ranging from δ 172 to 183.

Table 4.1. Selected NMR signals (CDCl_3) of iridium and rhodium COD complexes

complex	3	4	5	6	7	8	9	10	11^a
$\text{CH}_2(\text{diastereotopic})$	5.90/6.97	5.86/8.54	5.30/7.12	6.38/6.95	6.40/6.57	6.83/7.08	6.40/6.57	6.27/6.44	6.08/6.53
$\text{C}_{\text{carbene}}$	172.8	175.4	183.0	182.4	181.7	180.6	181.4	179.9	179.5

^a in CD_3CN

Iridium Cp^* Complexes via Silver Transmetalation: We then applied silver transmetalation of this type of carbenes to $[\text{Cp}^*\text{IrCl}_2]_2$ to determine whether these NHCs can be chelating ligands in this different Ir(III) environment.¹⁸ Transmetalation readily took place from the silver carbene bromide complexes (Scheme 4.8). However, ^1H NMR spectroscopy shows two sets of peaks for the transmetalation products obtained from **1a** or **1b** and these two species are ascribed to the neutral monodentate NHC complexes **12a, b** and the corresponding chelating ionic complexes **13a, b**. In fact, they are in equilibrium in CD_2Cl_2 or CDCl_3 . Addition of KPF_6 to an acetone solution of **12b** and **13b** completely shifted the equilibrium to the right side with anion exchange and **14b** was isolated in 95% yield. Complex **14a** could be synthesized analogously. The CH_2 protons in **14a, b** are diastereotopic; the carbene carbon atoms resonate at δ 164.8 and 161.7, respectively, and they are more shielded than those in the iridium(I) cyclooctadiene complexes.



Scheme 4.8. Routes to the synthesis of NHC-iridium complexes.

Equilibrium between 12b and 13b: The equilibrium between **12b** and **13b** has been studied in detail by NMR spectroscopy in CDCl_3 . Addition of tetra-*n*-butylammonium chloride to a mixture of **12b** and **13b** led to a decrease in the signal intensity of one component, unambiguously ascribed to **13b**, and an increase in that of the other, which was ascribed to **12b**, on the basis of the common ion effect. The equilibrium constants at various temperatures were then measured with 1,3,5-trimethoxybenzene as an internal standard by ^1H NMR spectroscopy. These data are shown in Table 4.2 and the van't Hoff plot based on these data gives $\Delta H^\circ = 32.1 \text{ kJ mol}^{-1}$ and $\Delta S^\circ = 70.1 \text{ J mol}^{-1} \text{ K}^{-1}$ ($R^2 = 0.9979$). This intramolecular chloride substitution is endothermic, possibly due to the ring strain in combination with the charge separation in **13b**. The large positive value of ΔS° is also consistent with the more disordered structure of complex **13b**. Although experiments were not attempted to apply this equilibrium to catalysis, it is possibly a good system to study the function of the ligand lability in the catalytic cycle. The reason is that the ratio of these two species is tuneable by varying the temperature. If the temperature is increased, the equilibrium will shift towards the ionic complex. However, it is difficult to differentiate the effect of the temperature on the catalytic reaction from the effect of changing the coordination of the ligand, since both occur simultaneously.

Table 4.2. Measurement of the K_{eq} between **12b** and **13b** at different temperatures

T (K)	[12b] (M)	[13b], [Cl] (M)	K_{eq} ($[\mathbf{13b}]^2/[\mathbf{12b}]$)
297.1	0.02241	0.01535	0.0105
303.1	0.02117	0.01716	0.0139
313.1	0.01885	0.01922	0.0196
318.1	0.01750	0.02084	0.0248
323.1	0.01644	0.02224	0.0301
328.1	0.01522	0.02351	0.0363

X-ray Structures: Single crystals of **4** and **5** were obtained by layering their CH_2Cl_2 solution with diethyl ether (Table 4.3). Complex **4** co-crystallized with one equivalent of ether and it has a square planar geometry (Figure 4.3). The Rh-C_{carbene} distance [2.0288(19) Å] is within the normal range for rhodium NHC complexes.^{15b,19} The seven-membered rhodacycle adopts a boat conformation and is highly twisted. Indicative of the ring strain, the imidazole and the pyridine rings are nearly perpendicular to each other and the rhodium atom is not positioned exactly along the C(1)-N(1)-C(9) bisector, but it is displaced away from the pyridine ring. The Rh-C(27) and Rh-C(28) bond distances are at least 0.05 Å longer than those of Rh-C(23) and Rh-C(24), undoubtedly due to the high trans effect of the NHC ligand. Complex **5** is also square planar in geometry and is nearly C_2 symmetrical in the solid state (Figure 4.4). The two Rh-C_{carbene} distances [2.072(5) and 2.091(5) Å] are similar and are at least 0.04 Å longer than that in complex **4**, possibly due to the increased steric bulk rendered by the introduction of the second NHC ligand or due to the *cis* effect of these NHC ligands. The two NHC rings offset each other by 78.79° and each is nearly perpendicular to the rhodium coordination plane. The solution structure elucidated by NMR spectroscopy is consistent with the solid analysis, where C_2 symmetrical solution structure should exist in the time average. For example, the number of resonance signals in the ^{13}C NMR spectrum (26) is half of the total number of C atoms (52), suggestive of the C_2 symmetry.

Single crystals of **14a** were obtained by slow diffusion of diethyl ether into a CH_2Cl_2 solution and a half equivalent of CH_2Cl_2 was co-crystallized. X-ray crystallography confirmed the proposed structure of complex **14a** (Figure 4.5). This seven-membered iridacycle also has a boat conformation and, suggestive of the ring strain and the steric bulk of the Mes group, there is a

strong in-plane distortion of the NHC ligand. Consequently, the iridium atom is not positioned along the bisector of the N(2)-C(21)-N(3), as indicated by the large difference between the N(2)-C(21)-Ir(1) [119.8(3)°] and the N(3)-C(21)-Ir(1) [136.0(3)°] angles.

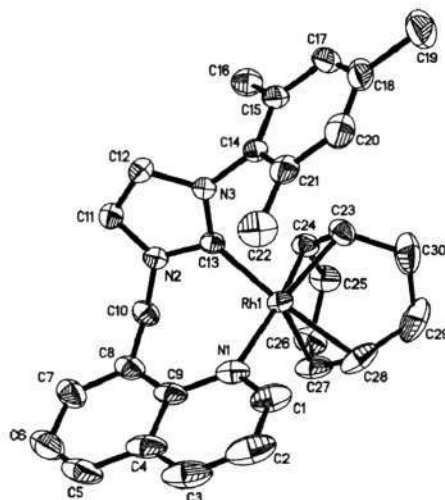


Figure 4.3. Molecular structure of **4** with the thermal ellipsoid at 50% probability. Hydrogen atoms and anion are omitted for clarity. Selected lengths (Å) and angles (deg): Rh(1)-C(13), 2.0288(19); Rh(1)-N(1), 2.1677(18); Rh(1)-C(23), 2.124(2); Rh(1)-C(24), 2.135(2); Rh(1)-C(27), 2.183(2); Rh(1)-C(28), 2.217(2); C(23)-C(24), 1.401(3); C(27)-C(28), 1.380(4); N(1)-Rh(1)-C(13), 86.41(7); N(2)-C(13)-N(3), 104.37(16).

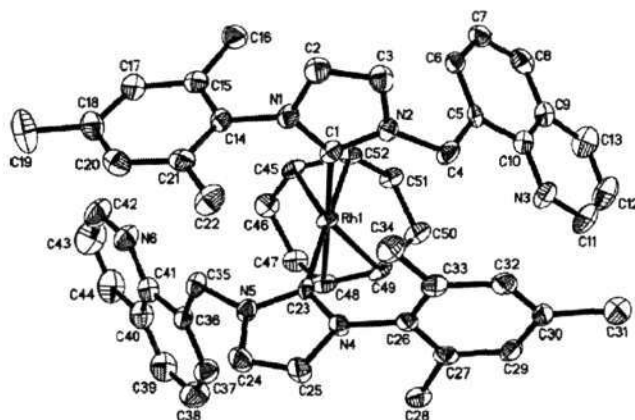


Figure 4.4. Molecular structure of **5** with the thermal ellipsoid at 50% probability. Hydrogen atoms and anion are omitted for clarity. Selected lengths (Å) and angles (deg): Rh(1)-C(1), 2.091(5); Rh(1)-C(23), 2.072(5); Rh(1)-C(45), 2.165(5); Rh(1)-C(48), 2.218(5); Rh(1)-C(49), 2.175(5); Rh(1)-C(52), 2.226(5); C(45)-C(52), 1.372(8); C(48)-C(49), 1.385(8); C(1)-Rh(1)-C(23), 93.94(18); N(1)-C(1)-N(2), 104.3(4); N(4)-C(23)-N(5), 103.6(4).

Table 4.3. Crystallographic data for complexes **4**, **5**, and **14a**

	4 •Et ₂ O	5	14a •0.5CH ₂ Cl ₂
empirical formula	C ₃₀ H ₃₃ F ₆ N ₃ PRh•Et ₂ O	C ₅₂ H ₅₄ F ₆ N ₆ PRh	C ₃₂ H ₃₆ ClF ₆ IrN ₃ P•0.5 CH ₂ Cl ₂
molecular weight (g mol ⁻¹)	757.59	1010.89	877.72
radiation, λ(Å)	Mo K _α (monochr), 0.71073 Å		
T (K)	173(2)		
cryst syst	monoclinic	monoclinic	triclinic
space group	<i>P</i> 2 ₁ / <i>n</i>	<i>P</i> 2 ₁ / <i>n</i>	<i>P</i> -1
<i>a</i> (Å)	11.2937(3)	17.9389(6)	8.6792(4)
<i>b</i> (Å)	27.1335(8)	15.8145(7)	14.4528(6)
<i>c</i> (Å)	11.4634(3)	18.7496(5)	14.4654(6)
α(deg)	90	90	110.965(2)
β(deg)	105.052(1)	117.490(2)	95.119(1)
γ(deg)	90	90	92.420(1)
<i>V</i> (Å ³)	3392.29(16)	4718.6(3)	1682.27(13)
<i>Z</i>	4	4	2
<i>D</i> _{calcd} (g cm ⁻³)	1.483	1.423	1.773
μ (mm ⁻¹)	0.615	0.463	4.236
cryst size (mm)	0.30 × 0.20 × 0.20	0.25 × 0.15 × 0.10	0.30 × 0.25 × 0.15
total, unique no. of rflns	96133, 10259	35106, 8205	30719, 10112
<i>R</i> _{int}	0.0412	0.0799	0.0246
data, restraints, parameters	10259, 0, 420	8205, 0, 602	10112, 2, 429
<i>R</i> , <i>R</i> _w	0.0361, 0.0900	0.0664, 0.175	0.0370, 0.1053
GOF	1.068	1.027	1.101
min., max. resid dens (eÅ ⁻³)	-0.603, 0.842	-0.0909, 1.483	-3.04, 1.857

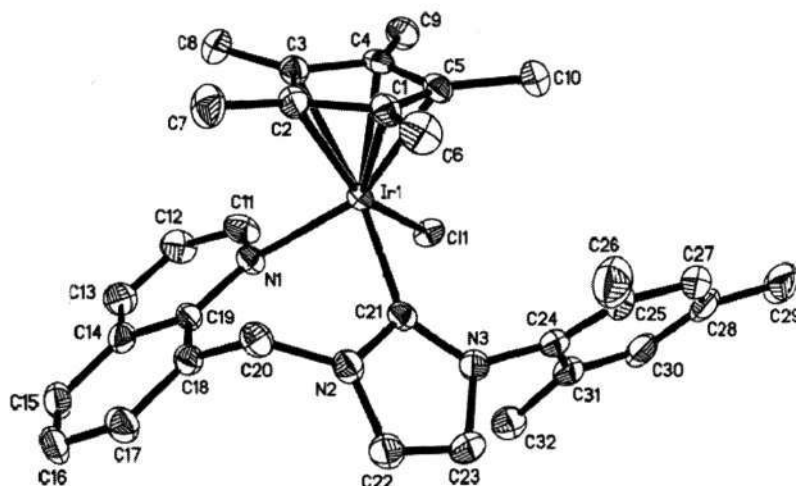


Figure 4.5. Molecular structure of **14a** with the thermal ellipsoid at 50% probability. Hydrogen atoms and anion are omitted for clarity. Selected lengths (Å) and angles (deg): Ir(1)-C(21), 2.058(5); Ir(1)-Cl(1), 2.4098(10); Ir(1)-N(1), 2.190(4); N(1)-Ir(1)-C(21), 89.95(16); N(2)-C(21)-Ir(1), 119.8(3); N(3)-C(21)-Ir(1), 136.0(3); N(2)-C(21)-N(3), 104.2(4).

4.2.2. Rh(I) Catalyzed [3+2] Cycloaddition Reactions

Rhodium can mediate a variety of organic transformations, including hydroformylation,²⁰ hydrosilylation,²¹ hydroboration,²² cyclotrimerization²³ and asymmetric hydrogenation.²⁴ In recent years, with the development of metal complexes containing N-heterocyclic carbenes, Rh(I) NHC complexes have been successfully applied to hydroformylation,²⁵ hydrosilylation,^{12a,26} intramolecular hydroamination²⁷ and carbocyclization.²⁸ However, to our best knowledge, there were only two reports on cycloaddition reaction using well-characterized NHC-rhodium catalysts (Figure 4.6).²⁹

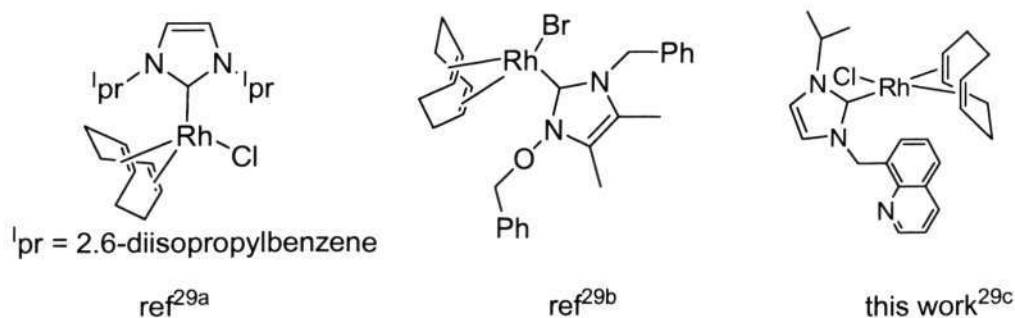


Figure 4.6. Reported well-characterized NHC-rhodium catalysts.

In 2006, Wender and co-authors reported that $[\text{RhCl}(\text{CO})_2]_2$ could catalyze the [3+2] cycloaddition of diphenylcyclopropenone and alkynes (eq 4.2).³⁰ In view of the high cost and sensitivity of $[\text{RhCl}(\text{CO})_2]_2$, we examined this reaction using $\text{Rh}(\text{COD})(\text{NHC})\text{Cl}$ complexes as catalysts. Heating (110 °C) diphenylcyclopropenone and 1-phenyl-1-propyne in the presence of 5 mol% compound **6** rapidly led to a dark purple solution, and the desired product was isolated in 77% yield. Other rhodium catalysts were then screened, and the results were displayed in Table 4.4. Complex **9**, which has an ⁱPr substituent, shows the highest catalytic activity (entry 2, Table 4.4). Surprisingly, changing the substituent to a Mes, ^tBu, or ⁿBu group gave rise to significant drop of the catalytic activity in every case. The ionic rhodium carbene complexes **4** and **5** all showed poor activity for this reaction.

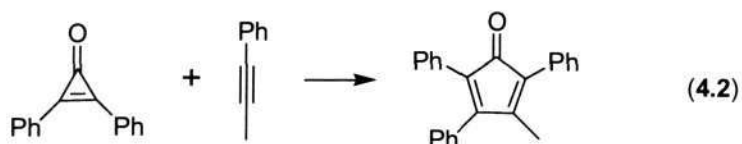


Table 4.4. Screening of rhodium catalysts for equation 4.2

entry	catalyst	conditions	isolated yield
1	6 (5%)	18 h, 110 °C	77 %
2	9 (2%)	2 h, 110 °C	84 %
3	7 (2%)	6 h, 110 °C	24 %
4	8 (2%)	6 h, 110 °C	12 %
5	4 (5%)	18 h, 110 °C	27%
6	5 (5%)	18 h, 110 °C	---

We then retained complex **9** to further study the scope of this catalytic reaction (eq 4.3) and the results were shown in Table 4.5. Electron-donating substituents in the aromatic ring favor this reaction (entries 1 and 2, Table 4.5). Furthermore, catalyst **9** can also tolerate other functional

groups such as a ketone (entry 5), an ester (entry 6), and a hydroxyl group (entry 7). Diphenylacetylene only gave 8% yield after 18 h at 110 °C (entry 8) and *o*-CH₃(C₆H₄)C≡CSiMe₃ failed to react (entry 9), where the steric hindrance might be accountable. In addition, PhC≡CH and MeO₂C-C≡C-CO₂Me failed to give any product under the same conditions, which is consistent with Wender's report.³⁰

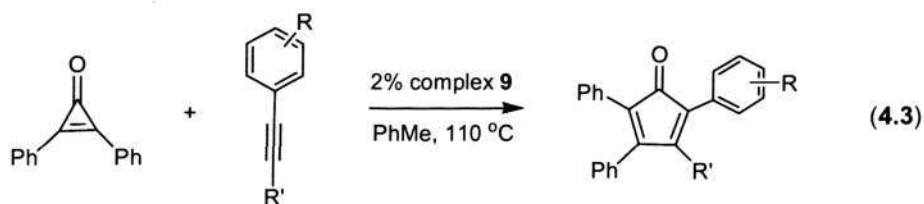


Table 4.5. Substrate scope of equation 4.3

entry	R, R'	conditions	product	Isolated yield
1	<i>p</i> -CH ₃ , CH ₃ (15)	2 h, 110 °C	16	86%
2	<i>p</i> -OCH ₃ , CH ₃ (17)	2 h, 110 °C	18	86%
3	<i>p</i> -CF ₃ , CH ₃ (19)	6 h, 110 °C	20	68%
4	<i>o</i> -Br, CH ₃ (21)	17 h, 110 °C	22	40%
5	H, COCH ₃	18 h, 110 °C	23	80%
6	H, COOEt	18 h, 110 °C	24	74%
7	H, CH ₂ OH (25)	12 h, 110 °C	26	38%
8	H, Ph	18 h, 110 °C	27	8%
9	<i>o</i> -Me, Si(CH ₃) ₃ (28)	18 h, 110 °C	---	---

4.2.3. Electrochemistry

Cyclic voltammograms (CVs) of compounds **4** – **11** were obtained at a scan rate of 0.1 V s^{-1} at a GC electrode in CH_2Cl_2 and were shown in Figure 4.7. The compounds were all able to undergo a one-electron oxidation process with the anodic peak potential (E_p^{ox}) ranging from +0.1 to +0.7 V vs. Fc/Fc^+ . For all compounds measured, the peak current for the anodic reaction (i_p^{ox}) was greater than the cathodic peak current (i_p^{red}) detected when the scan direction was reversed. The large $i_p^{\text{ox}}/i_p^{\text{red}}$ ratio is caused by chemical instability of the oxidized compounds, indicating that they undergo an EC mechanism (where E is an electron transfer and C is a chemical step) on the time-scale of the experiment.

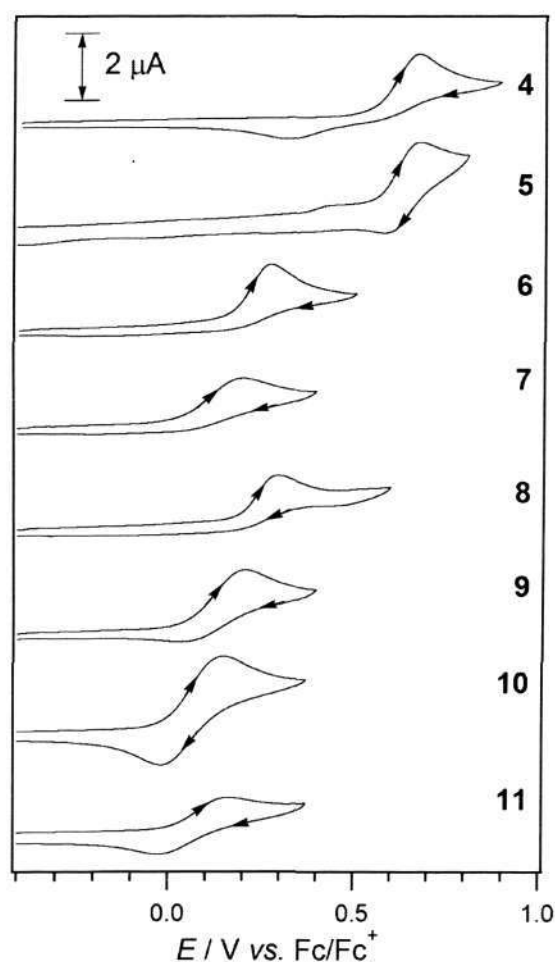


Figure 4.7. Cyclic voltammograms of 1 mM solutions of compounds **4** – **11** performed at a 1 mm diameter planar GC electrode in CH_2Cl_2 (containing 0.2 M Bu_4NPF_6) at a scan rate of 100 mV s^{-1} at $20 \pm 0.2^\circ\text{C}$.

As the scan rate was increased towards 5 V s^{-1} , the $i_p^{\text{ox}}/i_p^{\text{red}}$ ratio became closer to unity, indicating that the chemical step could be outrun at intermediate voltammetric scan rates. Nevertheless, increasing the scan rate also resulted in the E_p^{ox} and E_p^{red} separation (ΔE_{pp}) increasing for all of the compounds, significantly more than could be accounted for by the effects of uncompensated solution resistance. The increase in ΔE_{pp} with increasing scan rate is illustrated in Figure 4.8a for compound **9**, which also shows the $i_p^{\text{ox}}/i_p^{\text{red}}$ ratio increasing with increasing scan rate. Therefore, it can be concluded that the compounds display relatively slow rates of heterogeneous electron transfer. The effect is particularly pronounced on Pt surfaces where the oxidation processes were shifted to more positive potentials (Figure 4.8b).

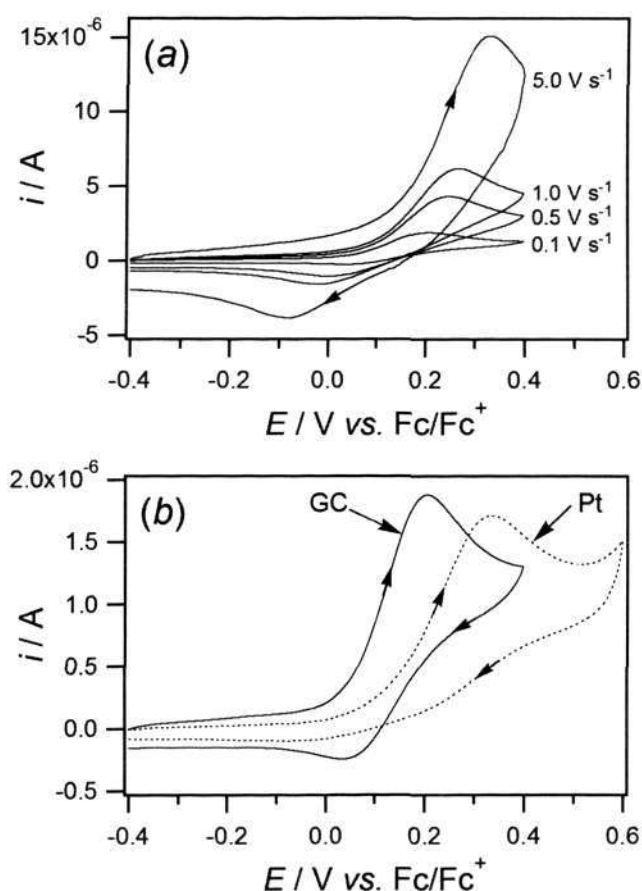


Figure 4.8. Cyclic voltammograms of a 1 mM solution of compound **9** performed at a 1 mm diameter planar electrode in CH_2Cl_2 (containing 0.2 M Bu_4NPF_6) at $20 \pm 0.2^\circ\text{C}$. (a) Voltammograms recorded at variable scan rates at a GC electrode. (b) Voltammograms recorded at a scan rate of 0.1 V s^{-1} at GC (solid line) and Pt (dashed line) electrodes.

The slow heterogeneous electron transfer rates and the chemical instability of the oxidized states make it difficult to accurately calculate the formal one-electron oxidation potentials. It can be observed in Figure 4.7 that the E_p^{ox} values for compounds **4** and **5** are more positive than those observed for the other compounds, which can be accounted for by their formal positive charge (**4** and **5** exist as cations) making them more difficult to oxidize. However, compound **11** also has a positive charge but it is oxidized at a very similar potential to the closely related neutral compound **10**.

The i_p^{ox} values observed for compounds at the same concentration and scan rate were similar, suggesting that the oxidation process occurred by the same number of electrons (although the peak current relationship depends on the diffusion coefficient of the molecules and is complicated by the slow rates of heterogeneous electron transfer). Controlled potential electrolysis and coulometry experiments conducted on compound **10** (the compound that appeared the most chemically reversible at slow scan rates) led to the transfer of 1.1 electrons per molecule, supporting the notion that the oxidation processes all occur *via* one-electron. Under electrolysis conditions the oxidized form of **10** was not long-lived, such that the starting material could not be regenerated when a reducing potential was applied.

4.3. Conclusions

A series of rhodium and iridium complexes of quinoline-tethered hemilabile N-heterocyclic carbenes (NHC^N) have been synthesized *via* either deprotonation of imidazolinium salts or silver transmetalation. Deprotonation of imidazolinium ions using KOBu^t in the presence of [Rh(COD)Cl]₂ afforded a mixture of chelating [Rh(COD)(NHC^N)]⁺ and monodentate [Rh(COD)(NHC)₂]⁺ complexes, while only the chelating complexes were obtained for the iridium analogues. Silver transmetalation of this type of carbene to [M(COD)Cl]₂ (M = Rh or Ir) consistently afforded monodentate carbene complexes M(NHC)(COD)Cl maintaining the pendant quinoline entity. Silver transmetalation of these carbene to (Cp^{*}IrCl₂)₂ gave an equilibrium mixture of neutral Cp^{*}Ir(NHC)Cl₂ and ionic [Cp^{*}Ir(NHC^N)Cl]Cl complexes. Rh(COD)(NHC)Cl proved to be active in catalyzing the [3+2] cycloaddition reactions of

diphenylcyclopropanone and internal alkynes. The carbene N-substituent has significant effects on the catalytic activity and the ⁱPr substituent gives the highest activity among those screened. Crystal structures of metal complexes in each category have been reported.

Electrochemical experiments performed on compounds **4** – **11** indicate that they can all undergo one-electron oxidation. The variable scan rate cyclic voltammetry experiments indicate that these compounds undergo relatively slow heterogeneous electron transfer and that the oxidized form of compound **9** is the most long-lived among compounds **6** – **9**. The oxidation potentials of these compounds appear to be very similar but it is not clear whether the oxidative behavior is important to their catalytic properties.

4.4. Experimental Section

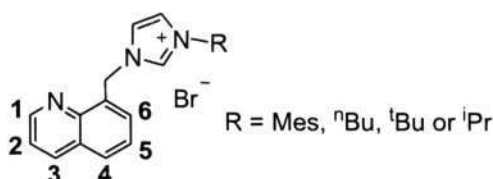
4.4.1. General Information

General Procedure: All reactions were carried out at room temperature without exclusion of air unless otherwise noted. NMR spectra were recorded on Bruker Avance DPX 300 or Bruker AMX 400 MHz (¹H) and 75 or 100 MHz (¹³C), respectively, and were referenced to tetramethylsilane. Microanalyses were performed in-house. X-ray crystallographic data were collected on a Bruker X8 APEX X-Ray diffractometer.

Electrochemistry: Voltammetric experiments were conducted with a computer controlled Eco Chemie Autolab III potentiostat with 1 mm diameter glassy carbon (GC) and Pt disk working electrodes. The miniature non-aqueous reference electrode was from Cypress Systems (EE008) and consisted of a silver wire inside a salt bridge containing 0.5 M Bu₄NPF₆ in CH₃CN. Fc/Fc⁺ (Fc = ferrocene) was measured as ~ +0.4 V versus the Ag/Bu₄NPF₆/CH₃CN reference electrode. Accurate potentials were obtained for each compound by adding ferrocene during the final scans and recording the potential of the analyte directly against ferrocene using square-wave (SWV) and cyclic voltammetry (CV). The formal potential (E^0_f) measured for the oxidation of ferrocene (either the peak potential from SWV or the $E'_{1/2}$ from CV) was then digitally subtracted from the potential scale of each voltammogram. Voltammograms containing only the solvent and electrolyte showed no processes in the range over which the voltammetric scans were performed

(± 1 V vs. Fc/Fc⁺), confirming that there were no interferences within the solvent/electrolyte. Coulometry experiments were performed in a divided controlled potential electrolysis (CPE) cell separated with a porosity no. 5 (1.0 - 1.7 μ m) sintered glass frit. The working and auxiliary electrodes were identically sized Pt mesh plates symmetrically arranged with respect to each other with an Ag wire reference electrode (isolated by a salt bridge) positioned to within 2 mm of the surface of the working electrode. The electrolysis cell was jacketed in a glass sleeve and cooled to 253 K using a Thermo Electron Neslab RTE 740 circulating bath with isopropyl alcohol. The volumes of both the working and auxiliary electrode compartments were approximately 10 mL each. The solution in the working electrode compartment was simultaneously deoxygenated and stirred using bubbles of argon gas. The number of electrons transferred during the bulk oxidation process was calculated from $N = Q/nF$, where N = no. of moles of starting compound, Q = charge (coulombs), n = no. of electrons and F is the Faraday constant (96485 C mol⁻¹).

4.4.2. Synthetic procedures



Synthesis of 2: Imidazolium **1a** (650 mg, 1.59 mmol) was dissolved in acetone (10 mL), to which was added an acetone solution (5 mL) of KPF₆ (2.90 g, 15.9 mmol). The mixture was stirred for 3 h at room temperature. All the volatiles were then removed, followed by addition of CH₂Cl₂ (10 mL). Filtration gave a clear solution. Product **2** was isolated as a white solid after the solvent was removed under vacuum (720 mg, 1.52 mmol, 96%). ¹H NMR (CDCl₃, 400 MHz): δ 10.40 (s, 1H, NCHN), 8.93 (dd, 1H, J = 4.2 and 1.5 Hz, H-1), 8.66 (d, 1H, J = 7.0 Hz), 8.23 (dd, 1H, J = 8.2 and 1.4 Hz, H-3), 8.16 (s, 1H, CH_{imidazole}), 7.88 (d, 1H, J = 7.8 Hz), 7.61 (t, 1H, J = 7.5 Hz, H-5), 7.50-7.47 (dd, 1H, J = 8.3 and 4.2 Hz, H-2), 6.99 (s, 1H, CH_{imidazole}), 6.95 (s, 2H, 2CH_{mesityl}), 6.53 (s, 2H, CH₂ linker), 2.30 (s, 3H, CH₃ mesityl), 1.98 (s, 6H, 2CH₃ mesityl); ¹³C {¹H} NMR (CDCl₃, 100 MHz): δ 150.2 (N-CH_{quinoline}), 146.3 (N-C_{quinoline}), 141.2 (C_{mesityl}), 138.0 (C_{mesityl}), 136.8, 134.3, 133.1, 131.7, 130.8 (C_{mesityl}), 130.0, 129.8 (CH_{mesityl}), 128.5, 127.2, 124.1,

122.2 (imidazole), 121.7 (imidazole), 49.2 (CH_2 linker), 21.1 (CH_3 aromatic), 17.6 (2CH_3 aromatic). Anal. Calcd for $\text{C}_{22}\text{H}_{22}\text{N}_3\text{F}_6\text{P}$ (473.39): C, 55.82; H, 4.68; N, 8.88%. Found: C, 55.75; H, 4.77; N, 8.85%.

Synthesis of 3: A THF solution of KOBu^t (1.0 M, 0.26 mL) was added dropwise to a mixture of $[\text{Ir}(\text{COD})\text{Cl}]_2$ (84 mg, 0.13 mmol) and THF (3 mL). After 30 min, a THF solution of **2** (119 mg, 0.252 mmol) was added to this mixture and was stirred overnight. The solution was concentrated to ca. 1 mL, which was chromatographed on silica gel with 10/1 CH_2Cl_2 /acetone to give **3** as a yellow solid (146 mg, 0.19 mmol, 76%). ^1H NMR (CDCl_3 , 400 MHz): δ 9.38 (d, 1H, $J = 4.4$ Hz, H-1), 8.42 (d, 1H, $J = 8.0$ Hz, H-3), 8.33 (d, 1H, $J = 6.6$ Hz), 8.03-8.00 (m, 2H), 7.76 (t, 1H, $J = 7.6$ Hz, H-5), 7.63 (dd, 1H, $J = 8.1$ and 5.3 Hz, H-2), 7.50 (d, 1H, $J = 1.7$ Hz, CH imidazole), 6.97 (m, 2H, diastereotopic CH_2 linker + CH aromatic), 6.61 (d, 1H, $J = 1.7$ Hz, CH imidazole), 5.90 (d, 1H, $J = 15.0$ Hz, diastereotopic CH_2 linker), 4.15-4.12 (m, 1H, COD-CH), 3.79-3.71 (m, 2H, COD-2CH), 3.48-3.43 (m, 1H, COD-CH), 2.43-2.27 (m+s, 5H, COD- CH_2 + CH_3 mesityl), 2.10-1.99 (m, 4H, COD- 2CH_2), 1.95 (s, 3H, CH_3 mesityl), 1.61 (s, 3H, CH_3 mesityl), 1.38-1.28 (m, 2H, COD- CH_2); $^{13}\text{C}\{^1\text{H}\}$ NMR (CDCl_3 , 100 MHz): δ 172.8 (carbene), 153.5 (N-CH quinoline), 145.6 (N-C quinoline), 140.4, 139.6, 135.9, 134.91, 134.86, 134.2, 131.8, 131.5, 130.3, 129.4, 129.1, 128.4, 123.3, 121.6 (imidazole), 121.5 (imidazole) 85.0 (COD-CH), 83.6 (COD-CH), 63.9 (COD-CH), 60.5 (COD-CH), 53.6 (CH_2 linker), 36.4 (COD- CH_2), 33.1 (COD- CH_2), 29.4 (COD- CH_2), 26.5 (COD- CH_2), 21.1 (CH_3 mesityl), 17.8 (CH_3 mesityl), 17.6 (CH_3 mesityl). Anal. Calcd for $\text{C}_{30}\text{H}_{33}\text{F}_6\text{IrN}_3\text{P}$ (772.78): C, 46.63; H, 4.30; N, 5.44%. Found: C, 46.23; H, 4.45; N, 5.29%.

Synthesis of 4 and 5: A THF solution of KOBu^t (1.0 M, 0.25 mL) was added dropwise to a stirred suspension of imidazolium salt **2** (118 mg, 0.250 mmol) in dry THF at room temperature. After the mixture was stirred for 30 min, $[\text{Rh}(\text{COD})\text{Cl}]_2$ (62 mg, 0.13 mmol) was added in one portion. The reaction mixture was stirred overnight. Removal of the solvent gave a residue, which was chromatographed on silica gel with 25/1 CH_2Cl_2 /acetone to give yellow solid products **4** (88 mg, 0.13 mmol, 65%) and **5** (22 mg, 0.02 mmol, 10%).

Compound 4: ^1H NMR (CDCl_3 , 400 MHz): δ 9.43 (d, 1H, $J = 4.7$ Hz, H-1), 8.54 (d, 1H, $J = 14.7$ Hz, diastereotopic CH_2 linker), 8.40 (d, 1H, $J = 8.1$ Hz, H-3), 8.33 (d, 1H, $J = 6.9$ Hz), 7.98

(d, 1H, $J = 8.2$ Hz), 7.74 (t, 1H, $J = 7.4$ Hz, H-5), 7.63 (dd, 1H, $J = 8.2$ and 5.1 Hz, H-2), 7.45 (d, 1H, $J = 1.9$ Hz, CH_{imidazole}), 7.08 (s, 1H, CH_{mesityl}), 6.99 (s, 1H, CH_{mesityl}), 6.62 (d, 1H, $J = 1.8$ Hz, CH_{imidazole}), 5.86 (d, 1H, $J = 14.7$ Hz, diastereotopic CH₂ linker), 4.61-4.58 (m, 1H, COD-CH), 4.01-3.98 (m, 2H, COD-CH), 3.81- 3.79 (m, 1H, COD-CH), 2.75-2.65 (m, 1H), 2.40 (s, 3H, CH₃ mesityl), 2.38-2.11 (m, 6H, COD-CH₂), 1.91 (s, 3H, CH₃ mesityl), 1.71-1.64 (s + m, 4H); $^{13}\text{C}\{^1\text{H}\}$ NMR (CDCl₃, 100 MHz): δ 175.4 (d, $J_{\text{C-Rh}} = 51.9$ Hz, C_{N₃}), 153.2 (N-CH_{quinoline}), 145.6 (N-C_{quinoline}), 140.1, 139.5, 135.1, 134.9, 134.7, 134.4, 131.3, 130.9, 130.8, 129.5, 129.1, 128.1, 123.8, 121.4 (imidazole), 121.3 (imidazole), 98.4 (d, $J_{\text{C-Rh}} = 7.6$ Hz, COD-CH), 73.8 (d, $J_{\text{C-Rh}} = 13.2$ Hz, COD-CH), 53.4 (CH₂ linker), 35.3 (COD-CH₂), 31.7 (COD-CH₂), 29.2 (COD-CH₂), 26.3 (COD-CH₂), 21.1 (CH₃ mesityl), 17.9 (CH₃ mesityl), 17.6 (CH₃ mesityl). Anal. Calcd for C₃₀H₃₃F₆N₃PRh•C₄H₁₀O (757.59): C, 53.90; H, 5.72; N, 5.55%. Found: C, 53.43; H, 5.91; N, 5.62%.

Compound 5: ^1H NMR (CDCl₃, 400 MHz): δ 8.86 (dd, 2H, $J = 4.1$ and 1.5 Hz, H-1), 8.20 (dd, 2H, $J = 8.2$ and 1.3 Hz, H-3), 7.83 (d, 2H, $J = 8.3$ Hz), 7.56-7.49 (m, 4H, H-5 + H-2), 7.26-7.22 (m, 8H, overlapping with solvent residue), 7.12 (d, 2H, $J = 17.1$ Hz, diastereotopic CH₂ linker), 6.94 (d, 2H, $J = 1.6$ Hz, CH_{imidazole}), 5.33 (d, 2H, $J = 16.9$ Hz, diastereotopic CH₂ linker), 5.01 (br, 2H, 2COD-CH), 3.61-3.56 (m, 2H, 2COD-CH), 2.54 (s, 6H, 2CH₃ mesityl), 1.95 (s, 6H, 2CH₃ mesityl), 1.70 (s, 6H, 2CH₃ mesityl), 1.59-1.56 (m, 4H, 2COD-CH₂), 1.02-0.97 (m, 2H, 2COD-CH₂), 0.65-0.60 (m, 2H, 2COD-CH₂); $^{13}\text{C}\{^1\text{H}\}$ NMR (CDCl₃, 100 MHz): δ 183.0 (d, $J_{\text{C-Rh}} = 54.2$ Hz, C_{N₃}), 149.7 (N-CH_{quinoline}), 145.7 (N-C_{quinoline}), 140.2, 136.3, 135.6, 135.5, 135.1, 135.0, 130.0, 129.6, 128.2, 128.1, 126.4, 126.3, 124.6, 123.2, 121.9 (imidazole), 92.6 (d, $J_{\text{C-Rh}} = 9.1$ Hz, COD-CH), 83.3 (d, $J_{\text{C-Rh}} = 7.0$ Hz, COD-CH), 52.3 (CH₂ linker), 33.9 (COD-CH₂), 26.2 (COD-CH₂), 21.4 (CH₃), 17.75 (CH₃), 17.72 (CH₃). Anal. Calcd for C₅₂H₅₄F₆N₆PRh (1010.90): C, 61.78; H, 5.38; N, 8.31%. Found: C, 61.70; H, 5.42; N, 8.27%.

Synthesis of 6: Ag₂O (60 mg, 0.26 mmol) was added to a CH₂Cl₂ solution of complex **1a** (204 mg, 0.500 mmol), and this mixture was stirred for 1 h in the dark. Filtration of this mixture gave a clear solution, to which was added [Rh(COD)Cl]₂ (123 mg, 0.250 mmol) in one portion. The mixture was stirred for another 1 h. After filtration, the solvent was removed and the residue was washed with hexane twice to give **6** as a yellow solid product (278 mg, 0.48 mmol, 97%). ^1H

NMR (CDCl₃, 400 MHz): δ 8.98 (dd, 1H, J = 4.0 and 1.2 Hz, H-1), 8.23-8.17 (m, 2H), 7.85 (d, 1H, J = 8.0 Hz), 7.60 (t, 1H, J = 7.7 Hz, H-5), 7.47 (dd, 1H, J = 8.2 and 4.1 Hz, H-2), 7.10 (s, 1H), 7.03 (s, 1H), 6.95 (d, 1H, J = 14.3 Hz, diastereotopic CH₂ linker), 6.91 (s, 1H), 6.65 (d, 1H, J = 1.5 Hz, CH_{imidazole}), 6.38 (d, 1H, J = 14.2 Hz, diastereotopic CH₂ linker), 4.92-4.83 (m br, 2H, COD-2CH), 3.68 (br, 1H, COD-CH), 3.05 (br, 1H, COD-CH), 2.49 (s, 3H), 2.38 (s, 3H), 2.28-2.24 (m, 1H, COD-CH₂), 2.18-2.09 (m, 1H, COD-CH₂), 2.09-1.96 (m, 1H, COD-CH₂), 1.82-1.67 (s + m, 6H, CH₃ mesityl + COD-CH₂), 1.56-1.48 (m, 2H, COD-CH₂); ¹³C{¹H} NMR (CDCl₃, 100 MHz): δ 182.4 (d, J_{C-Rh} = 49.7 Hz, C_{NCCN}), 149.9 (N-CH_{quinoline}), 146.7 (N-C_{quinoline}), 138.5, 137.2, 136.4, 135.2, 134.4, 131.3, 129.6, 128.4, 128.1, 126.6, 122.8, 121.6 (imidazole), 121.4 (imidazole), 96.8 (br, m, COD-CH), 68.7 (br, COD-CH), 67.6 (br, COD-CH), 51.1 (CH₂ linker), 33.8 (COD-CH₂), 31.6 (COD-CH₂), 29.2 (COD-CH₂), 28.1 (COD-CH₂), 21.1 (CH₃), 19.9 (CH₃), 17.8 (CH₃). Anal. Calcd for C₃₀H₃₃ClN₃Rh (573.96): C, 62.78; H, 5.80; N, 7.32%. Found: C, 62.38; H, 5.87; N, 7.23%.

The same procedure for complex **6** was followed in the preparation of complexes **7**, **8** and **9**.
Complex 7 (246 mg, 0.48 mmol, 96%): ¹H NMR (CDCl₃, 400 MHz): δ 8.97 (dd, 1H, J = 4.1 and 2.6 Hz, H-1), 8.21 (dd, 1H, J = 8.4 and 1.4 Hz, H-3), 7.97 (d, 1H, J = 7.0 Hz), 7.80 (d, 1H, J = 8.0 Hz), 7.55 (t, 1H, J = 7.6 Hz, H-5), 7.46 (dd, 1H, J = 8.3 and 4.2 Hz, H-2), 6.81 (s, 1H, CH_{imidazole}), 6.77 (s, 1H, CH_{imidazole}), 6.57 (d, 1H, J = 14.6 Hz, diastereotopic CH₂ linker), 6.40 (d, 1H, J = 14.6 Hz, diastereotopic CH₂ linker), 5.05 (br, 2H, COD-2CH), 4.59-4.51 (m, 2H, NCH₂), 3.53 (br, 1H, COD-CH), 3.36 (br, 1H, COD-CH), 2.43-2.34 (m, 4H, COD-2CH₂), 2.07-1.88 (m, 6H, NCH₂CH₂ + COD-2CH₂), 1.58-1.49 (m, 2H, NCH₂CH₂CH₂), 1.05 (t, 3H, J = 7.3 Hz, CH₃); ¹³C{¹H} NMR (CDCl₃, 75 MHz): δ 181.7 (d, J_{C-Rh} = 50.1 Hz, C_{NCCN}), 149.8 (N-CH_{quinoline}), 146.3 (N-C_{quinoline}), 136.4, 134.9, 131.0, 128.7, 128.2, 128.1, 126.9, 121.2, 120.1 (imidazole), 98.3 (d, J_{C-Rh} = 6.9 Hz, COD-CH), 98.1 (d, J_{C-Rh} = 7.0 Hz, COD-CH), 68.5 (d, J_{C-Rh} = 14.6 Hz, COD-CH), 68.2 (d, J_{C-Rh} = 14.6 Hz, COD-CH), 50.6 (CH₂ linker), 49.6 (NCH₂), 33.0, 32.9, 30.9, 28.9, 28.0, 20.2, 13.9 (CH₃). Anal. Calcd for C₂₅H₃₁ClN₃Rh (511.89): C, 58.66; H, 6.10; N, 8.21%. Found: C, 58.46; H, 6.07; N, 8.29%.

Complex 8 (241 mg, 0.47 mmol, 94%): ^1H NMR (CDCl_3 , 400 MHz): δ 8.99 (d, 1H, $J = 2.8$ Hz, H-1), 8.21 (d, 1H, $J = 8.2$ Hz, H-3), 8.07 (d, 1H, $J = 6.9$ Hz), 7.80 (d, 1H, $J = 8.0$ Hz), 7.55 (t, 1H, $J = 7.6$ Hz, H-5), 7.46 (dd, 1H, $J = 8.2$ and 4.1 Hz, H-2), 7.08 (d, 1H, $J = 14.7$ Hz, diastereotopic CH_2 linker), 6.94 (s, 1H, CH imidazole), 6.83 (d, 1H, $J = 14.3$ Hz, diastereotopic CH_2 linker), 6.77 (s, 1H, CH imidazole), 5.00 (br, 2H, COD-CH), 3.62 (br, 1H, COD-CH), 3.37 (br, 1H, COD-CH), 2.46-2.39 (m, 4H, COD-2 CH_2), 2.00-1.81 (s + m, 13H); $^{13}\text{C}\{^1\text{H}\}$ NMR (CDCl_3 , 100 MHz): δ 180.6 (d, $J_{\text{C-Rh}} = 49.9$ Hz, C_{NCN}), 149.9 (N-CH quinoline), 146.3 (N-C quinoline), 136.5, 135.0, 131.3, 128.2, 128.0, 127.1, 121.2, 120.5 (imidazole), 119.7 (imidazole), 96.5 (d, $J_{\text{C-Rh}} = 7.5$ Hz, COD-CH), 94.2 (d, $J_{\text{C-Rh}} = 7.2$ Hz, COD-CH), 70.6 (d, $J_{\text{C-Rh}} = 15.0$ Hz, COD-CH), 67.2 (d, $J_{\text{C-Rh}} = 14.3$ Hz, COD-CH), 58.3 ($\text{C}(\text{CH}_3)_3$), 51.2 (CH_2 linker), 33.3 (COD- CH_2), 32.4 ($\text{C}(\text{CH}_3)_3$), 31.9 (COD- CH_2), 29.4 (COD- CH_2), 28.4 (COD- CH_2). Anal. Calcd for $\text{C}_{25}\text{H}_{31}\text{ClN}_3\text{Rh}$ (511.89): C, 58.66; H, 6.10; N, 8.21%. Found: C, 58.39; H, 6.07; N, 8.26%.

Complex 9 (242 mg, 0.49 mmol, 97%): ^1H NMR (CDCl_3 , 400 MHz): δ 8.98 (dd, 1H, $J = 4.2$ and 1.7 Hz, H-1), 8.21 (dd, 1H, $J = 8.2$ and 1.6 Hz, H-3), 7.96 (d, 1H, $J = 6.8$ Hz), 7.80 (d, 1H, $J = 8.2$ Hz), 7.55 (t, 1H, $J = 7.9$ Hz, H-5), 7.46 (dd, 1H, $J = 8.2$ and 4.2 Hz, H-2), 6.85 (s, 1H, CH imidazole), 6.80 (s, 1H, CH imidazole), 6.57 (d, 1H, $J = 14.6$ Hz, diastereotopic CH_2 linker), 6.40 (d, 1H, $J = 14.8$ Hz, diastereotopic CH_2 linker), 5.88-5.81 (m, 1H, $\text{CH}(\text{CH}_3)_2$), 5.10 (br, 1H, COD-CH), 5.00 (br, 1H, COD-CH), 3.50 (br, 2H, COD-CH), 2.50-2.30 (m, 4H, COD-2 CH_2), 2.01-1.88 (m, 4H, COD-2 CH_2), 1.52-1.49 (m, 6H, 2 CH_3); $^{13}\text{C}\{^1\text{H}\}$ NMR (CDCl_3 , 100 MHz): δ 181.4 (d, $J_{\text{C-Rh}} = 52.5$ Hz, C_{NCN}), 149.8 (N-CH quinoline), 146.3 (N-C quinoline), 136.5, 134.9, 130.9, 128.2, 128.1, 126.9, 121.6 (imidazole), 121.3, 116.4 (imidazole), 98.5 (d, $J_{\text{C-Rh}} = 6.3$ Hz, COD-CH), 97.8 (br, COD-CH), 68.3 (d, $J_{\text{C-Rh}} = 13.9$ Hz, COD-CH), 67.9 (d, $J_{\text{C-Rh}} = 15.5$ Hz, COD-CH), 52.5 (CH_2 linker), 49.6 ($\text{CH}(\text{CH}_3)_2$), 33.5 (COD- CH_2), 32.3 (COD- CH_2), 29.4 (COD- CH_2), 28.4 (COD- CH_2), 23.3 ($\text{CH}(\text{CH}_3)_2$, accidentally equivalent). Anal. Calcd for $\text{C}_{24}\text{H}_{29}\text{ClN}_3\text{Rh}$ (497.87): C, 57.90; H, 5.87; N, 8.44%. Found: C, 57.78; H, 5.93; N, 8.36%.

Synthesis of 10 (285 mg, 0.47 mmol, 95%): The synthetic method for complex **6** was followed to prepare complex **10**, except that $[\text{Ir}(\text{COD})\text{Cl}]_2$ was used. ^1H NMR (CDCl_3 , 400 MHz): δ 8.97-8.96 (m, 1H, H-1), 8.18 (d, 1H, $J = 8.4$ Hz), 7.94 (d, 1H, $J = 7.1$ Hz), 7.78 (d, 1H, $J = 8.1$

Hz), 7.54 (t, 1H, $J = 7.6$ Hz, H-5), 7.46 (dd, 1H, $J = 8.2$ and 4.2 Hz, H-2), 6.88 (d, 1H, $J = 1.0$ Hz, CH_{imidazole}), 6.77 (s, 1H, CH_{imidazole}), 6.44 (d, 1H, $J = 14.6$ Hz, diastereotopic CH₂ linker), 6.27 (d, 1H, $J = 14.6$ Hz, diastereotopic CH₂ linker), 4.62 (s, 2H, COD-2CH), 4.42-4.38 (m, 2H, NCH₂), 3.10 (br, 1H, COD-CH), 2.99 (br, 1H, COD-CH), 2.22-2.18 (m, 4H, COD-2CH₂), 2.03-1.73 (m, 6H, COD-2CH₂ + NCH₂CH₂CH₂), 1.53-1.45 (m, 2H, NCH₂CH₂CH₂), 1.01 (t, 3H, $J = 7.3$, CH₃); ¹³C{¹H} NMR (CDCl₃, 100 MHz): δ 179.9 (carbene), 149.8 (N-CH_{quinoline}), 146.3 (N-C_{quinoline}), 136.5, 134.8, 130.8, 128.2, 128.1, 126.8, 121.3, 121.1, 119.9 (imidazole), 84.1 (COD-CH), 83.9 (COD-CH), 51.9 (COD-CH), 51.8 (COD-CH), 50.3, 49.2, 33.7, 33.5, 33.0, 29.7, 29.5, 20.1 (NCH₂CH₂CH₂), 13.8 (CH₃). Anal. Calcd for C₂₅H₃₁ClIrN₃ (601.20): C, 49.94; H, 5.20; N, 6.99%. Found: C, 49.75; H, 5.21; N, 6.93%.

Synthesis of 11 (341 mg, 0.48 mmol, 96%): Complex **11** was prepared from complex **10** by following the same method of the synthesis of **2**. ¹H NMR (CD₃CN, 300 MHz): δ 9.00 (dd, 1H, $J = 4.2$ and 1.7 Hz, H-1), 8.35 (dd, 1H, $J = 8.3$ and 1.6 Hz, H-3), 7.92 (d, 1H, $J = 8.1$ Hz), 7.66-7.53 (m, 3H), 7.10 (d, 1H, $J = 1.9$ Hz, CH_{imidazole}), 7.08 (d, 1H, $J = 2.0$ Hz, CH_{imidazole}), 6.53 (d, 1H, $J = 15.5$ Hz, diastereotopic CH₂ linker), 6.08 (d, 1H, $J = 15.6$ Hz, diastereotopic CH₂ linker), 4.51-4.23 (m, 4H, COD-2CH + NCH₂), 3.06 (br, 2H, COD-2CH), 2.21-2.03 (m, 4H, COD-2CH₂), 1.86-1.82 (m, 2H, COD-CH₂), 1.69-1.61 (m, 2H, NCH₂CH₂), 1.50-1.40 (m, 4H, COD-CH₂ + NCH₂CH₂CH₂), 1.05 (t, 3H, $J = 7.3$ Hz, CH₃); ¹³C{¹H} NMR (CD₃CN, 75 MHz): δ 179.5 (carbene), 151.1 (N-CH_{quinoline}), 146.8 (N-C_{quinoline}), 137.5, 136.4, 129.9, 129.2, 129.1, 127.3, 122.7 (imidazole), 122.6, 121.8 (imidazole), 83.7 (COD-CH), 53.1 (br, COD-CH), 50.9 (CH₂ linker), 50.7 (NCH₂), 34.2, 34.0, 33.7, 30.2, 30.1, 20.6 (NCH₂CH₂CH₂), 14.1 (CH₃), 1.20 (septet, $^1J_{\text{DC}} = 20.7$ Hz, CD₃CN-Ir). The resonance signal of CD₃CN-Ir overlaps with that of the solvent peak (δ 118.2). Anal. Calcd for C₂₅H₃₁F₆IrN₃P (710.71): C, 42.25; H, 4.40; N, 5.91%. Found: C, 42.11; H, 4.47; N, 5.85%.

Synthesis of mixture 12b and 13b: Ag₂O (32 mg, 0.14 mmol) was added to a CH₂Cl₂ solution of imidazolium salt **1b** (93 mg, 0.27 mmol). The mixture was stirred for 1 h in the dark. After filtration, [IrCp*Cl₂]₂ (108 mg, 0.136 mmol) was added in one portion to the solution, and was stirred for another 1 h. The solvent was removed and the residue was washed with hexane to give yellow solid products (141 mg, 0.21 mmol, 97%). Compound **12b**: ¹H NMR (CDCl₃, 400

MHz): δ 8.94 (dd, 1H, $J = 4.1$ and 1.6 Hz, H-1), 8.23-8.21 (m, 2H), 7.83-7.81 (m, 1H), 7.58-7.54 (m, 1H), 7.48-7.45 (m, 1H), 6.88 (d, 1H, $J = 2.1$ Hz, CH_{imidazole}), 6.66 (d, 1H, $J = 2.0$ Hz, CH_{imidazole}), 6.48 (d, 1H, $J = 14.2$ Hz, CH_{2 linker}), 6.18 (d, 1H, $J = 14.0$ Hz, CH_{2 linker}), 4.73-4.66 (m, 1H, NCH₂), 3.96-3.88 (m, 1H, NCH₂), 1.68 (s, 15H, 5CH₃), 1.55-1.44 (m, 2H, NCH₂CH₂), 1.42-1.37 (m, 2H, NCH₂CH₂CH₂), 1.01-0.93 (m, 3H, CH₃). Compound **13b**: ¹H NMR (CDCl₃, 400 MHz): δ 9.60 (dd, 1H, $J = 5.6$ and 1.7 Hz, H-1), 8.85-8.83 (m, 1H), 8.50 (d, 1H, $J = 1.9$ Hz, CH_{imidazole}), 8.32 (dd, 1H, $J = 8.2$ and 1.5 Hz, H-3), 7.92-7.90 (m, 1H), 7.74-7.70 (m, 1H), 7.41-7.38 (m, 1H), 6.98 (d, 1H, $J = 2.0$ Hz, CH_{imidazole}), 6.41 (d, 1H, $J = 14.0$ Hz, CH_{2 linker}), 6.00 (d, 1H, $J = 14.2$ Hz, CH_{2 linker}), 4.38-4.31 (m, 1H, NCH₂), 3.87-3.80 (m, 1H, NCH₂), 2.07-1.99 (m, 1H, NCH₂CH₂), 1.87-1.79 (m, 1H, NCH₂CH₂), 1.61 (s, 15H, 5CH₃), 1.44-1.37 (m, 2H, NCH₂CH₂CH₂), 1.00-0.93 (m, 3H, CH₃). Anal. Calcd for C₂₇H₃₄Cl₂IrN₃ (663.70): C, 48.86; H, 5.16; N, 6.33%. Found: C, 48.74; H, 5.13; N, 6.38%.

Synthesis of 14a: The procedure for the synthesis of the mixture **12b** and **13b** was followed to prepare the mixture **12a** and **13a**, but no attempt was made to disentangle them, since almost each of the resonance signals is broadened to a certain extent in the ¹H NMR spectrum. Then, the mixture of **12a** and **13a** (91 mg, 0.13 mmol) were dissolved in CH₂Cl₂, and KPF₆ (230 mg, 1.25 mmol) was added quickly. The mixture was stirred for 3 h. After filtration, the solvent was evaporated under vacuum to give **14a** as a yellow solid (99 mg, 0.12 mmol, 95%). ¹H NMR (CDCl₃, 400 MHz): δ 9.71 (dd, 1H, $J = 5.5$ and 1.7 Hz, H-1), 8.33 (dd, 1H, $J = 8.1$ and 1.6 Hz, H-3), 8.25-8.23 (m, 1H), 8.01-7.97 (m, 1H), 7.72 (s, 2H, 2CH_{mesityl}), 7.42-7.38 (m, 1H), 6.88 (s, 1H), 6.80 (s, 1H), 6.65 (d, 1H, $J = 1.8$ Hz, CH_{imidazole}), 6.50 (d, 1H, $J = 15.0$ Hz, diastereotopic CH_{2 linker}), 5.88 (d, 1H, $J = 14.9$ Hz, diastereotopic CH_{2 linker}), 2.31 (s, 3H, CH_{3 mesityl}), 2.08 (s, 3H, CH_{mesityl}), 1.58 (s, 3H, CH_{mesityl}), 1.45 (s, 15H, 5CH₃); ¹³C{¹H} NMR (CD₃CN, 100 MHz): δ 161.7 (carbene), 152.8 (N-CH_{quinoline}), 145.7 (N-C_{quinoline}), 141.6, 139.1, 138.5, 136.3, 135.9, 132.9, 132.7, 130.9, 128.7, 128.5, 127.7, 126.2, 122.8, 122.0, 91.5 (C₅(Me)₅), 53.5 (CH_{2 linker}), 21.2 (CH_{3 mesityl}), 19.1 (CH_{3 mesityl}), 18.6 (CH_{3 mesityl}), 9.1 (C₅(Me)₅). Anal. Calcd for C₃₂H₃₆ClF₆N₃PIr (835.28): C, 46.01; H, 4.34; N, 5.03%. Found: C, 46.14; H, 4.58; N, 5.30%.

Synthesis of 14b: The same method for **14a** was followed to prepare **14b**. 95 mg, 0.12 mmol, 95%. ^1H NMR (CD_3CN , 400 MHz): δ 9.59 (d, 1H, $J = 4.7$ Hz, H-1), 8.50 (dd, 1H, $J = 8.2$ and 1.5 Hz, H-3), 8.07-8.01 (m, 2H), 7.70-7.66 (m, 1H), 7.59-7.52 (m, 2H), 7.26 (d, 1H, $J = 2.0$ Hz, CH_{imidazole}), 6.14 (d, 1H, $J = 14.4$ Hz, diastereotopic CH₂ linker), 5.26 (d, 1H, $J = 14.5$ Hz, diastereotopic CH₂ linker), 4.38-4.31 (m, 1H, NCH₂), 3.93-3.86 (m, 1H, NCH₂), 1.98-1.96 (m, 2H, NCH₂CH₂), 1.61 (s, 15H, 5CH₃), 1.45-1.29 (m, 2H, NCH₂CH₂CH₂), 0.92 (t, 3H, $J = 7.4$ Hz, CH₃); $^{13}\text{C}\{^1\text{H}\}$ NMR (CD_3CN , 100 MHz): δ 164.8 (carbene), 155.6 (N-CH_{quinoline}), 146.0 (N-C_{quinoline}), 141.7, 134.8, 132.4, 130.4, 129.7, 127.0, 123.4, 122.7, 121.4, 91.4 (C₅(Me)₅), 50.7 (CH₂ linker), 49.8 (NCH₂), 33.2 (NCH₂CH₂), 19.6 (NCH₂CH₂CH₂), 13.1 (CH₃), 8.3 (C₅(Me)₅). Anal. Calcd for C₂₇H₃₄ClF₆N₃PIr (773.21): C, 41.94; H, 4.43; N, 5.43%. Found: C, 41.68; H, 4.48; N, 5.24%.

Catalytic [3+2] Coupling: A rhodium catalyst (2%) and diphenylcyclopropanone (1.5 equiv) were weighed into a 20 mL flask. Dry toluene (1 mL) and alkyne (0.25 mmol) were added *via* syringe sequentially. The mixture was heated for 2-18 h at 110 °C (see Table 4.4 and Table 4.5). Removal of volatiles gave a residue and was then purified by silica gel column chromatography using hexane and ether as eluents. The coupling product was isolated as a purple or red product. The identity of products **18**, **20**, **23** and **27** has been confirmed by comparison with the reported NMR spectra.³⁰ Products **16**, **22**, **24** and **26** are new compounds. Substrates **15**,³¹ **17**,³¹ **19**,³² **21**,³³ **25**³⁴ and **28**³⁵ were prepared following reported methods.

Product 16: 72 mg, 0.21 mmol, 86%. ^1H NMR (CDCl_3 , 300 MHz): δ 7.43-7.22 (m, 14H), 2.42 (s, 3H), 2.12 (s, 3H); $^{13}\text{C}\{^1\text{H}\}$ NMR (CDCl_3 , 75 MHz): δ 200.7 (CO), 154.7, 153.4, 137.3, 133.9, 130.8, 129.9, 129.5, 129.1, 128.7, 128.6, 128.54, 128.48, 128.0, 127.3, 125.7, 124.6, 21.4, 14.6. IR (film): 3017 (w), 2922 (w), 1709 (m), 1510 (w), 1443 (w), 1379 (w), 1298 (w), 1215 (m), 1113 (w), 993 (w), 846 (w), 756 (s), 669 (m) cm⁻¹. HRMS (EI) for C₂₅H₂₀O calcd: 336.1509, found: 336.1495.

Product 22: 40 mg, 0.10 mmol, 40%. ^1H NMR (CDCl_3 , 400 MHz): δ 7.66 (d, 1H, $J = 7.6$ Hz), 7.41-7.29 (m, 6H), 7.24-7.19 (m, 7H), 1.92 (s, 3H); $^{13}\text{C}\{^1\text{H}\}$ NMR (CDCl_3 , 100 MHz): δ 199.2 (CO), 156.9, 153.2, 133.6, 133.0, 132.0, 130.6, 130.0, 129.4, 128.74, 128.70, 128.6, 128.0, 127.5, 127.2, 127.1, 125.1, 124.6, 15.1. IR (film): 3019 (w), 1713 (m), 1645 (w), 1442 (w), 1378

(w), 1298 (w), 1215 (m), 1028 (w), 928 (w), 768 (s), 752 (s), 669 (m) cm^{-1} . **HRMS (EI)** for $\text{C}_{24}\text{H}_{17}\text{BrO}$ calcd: 400.0457, found: 400.0453.

Product 24: 70 mg, 0.19 mmol, 74%. ^1H NMR (CDCl_3 , 400 MHz): δ 7.57-7.56 (m, 2H), 7.43-7.21 (m, 13H), 4.16-4.10 (m, 2H), 1.02 (t, 3H, $J = 7.1$ Hz); $^{13}\text{C}\{^1\text{H}\}$ NMR (CDCl_3 , 100 MHz): δ 199.4 (CO), 165.7 ($\text{COOCH}_2\text{CH}_3$), 153.0, 144.9, 133.1, 130.2, 130.0, 129.5, 129.4, 129.3, 129.0, 128.6, 128.4, 128.2, 127.9, 124.5, 61.6 ($\text{COOCH}_2\text{CH}_3$), 13.7 ($\text{COOCH}_2\text{CH}_3$). IR (film): 3019 (w), 1717 (m), 1645 (w), 1494 (w), 1445 (w), 1373 (w), 1354 (w), 1215 (m), 1119 (w), 1018 (w), 760 (m), 694 (m) cm^{-1} . **HRMS (EI)** for $\text{C}_{26}\text{H}_{20}\text{O}_3$ calcd: 380.1407, found: 380.1364.

Product 26: 32 mg, 0.10 mmol, 38%. ^1H NMR (CDCl_3 , 400 MHz): δ 7.51-7.36 (m, 10H), 7.21 (br, 5H), 4.53 (d, 2H, $J = 5.8$ Hz), 1.40 (t, 1H, $J = 5.8$ Hz); $^{13}\text{C}\{^1\text{H}\}$ NMR (CDCl_3 , 100 MHz): δ 200.6 (CO), 154.5, 152.4, 133.8, 130.5, 130.3, 129.9, 129.8, 129.1, 129.0, 128.5, 128.33, 128.25, 128.1, 128.0, 127.5, 125.3, 56.6. IR (film): 3483 (w), 3019 (w), 1699 (w), 1494 (w), 1445 (w), 1352 (w), 1215 (s), 1113 (w), 1003 (w), 922 (w), 756 (m), 669 (m) cm^{-1} . **HRMS (EI)** for $\text{C}_{24}\text{H}_{18}\text{O}_2$ calcd: 338.1301, found: 338.1295.

4.5. References

1. (a) Fagnou, K.; Lautens, M. *Chem. Rev.* **2003**, *103*, 169. (b) Wender, P. A.; Gamber, G. G.; Hubbard, R. D.; Zhang, L. *J. Am. Chem. Soc.* **2002**, *124*, 2876. (c) Wender, P. A.; Christy, J. P. *J. Am. Chem. Soc.* **2006**, *128*, 5354. (d) Chopade, P. R.; Louie, J. *Adv. Synth. Catal.* **2006**, *348*, 2307.
2. (a) Hayashi, T.; Yamasaki, K. *Chem. Rev.* **2003**, *103*, 2829. (b) Yu, R. T.; Rovis, T. *J. Am. Chem. Soc.* **2008**, *130*, 3262.
3. (a) Shen, Z.; Khan, H. A.; Dong, V. M. *J. Am. Chem. Soc.* **2008**, *130*, 2916. (b) Tanaka, K.; Fu, G. C. *J. Am. Chem. Soc.* **2001**, *123*, 11492. (c) Park, J.-W.; Park, J.-H.; Jun, C.-H. *J. Org. Chem.* **2008**, *73*, 5598. (d) Tanaka, K.; Shibata, Y.; Suda, T.; Hagiwara, Y.; Hirano, M. *Org. Lett.* **2007**, *9*, 1215. (e) Fu, G. C. In *Modern Rhodium-Catalyzed Reactions*; Evans, P. A., Ed.; Wiley-VCH: New York, 2005; pp 79-91 and references therein.
4. Roseblade, S. J.; Pfaltz, A. *Acc. Chem. Res.* **2007**, *40*, 1402.
5. (a) Mata, J. A.; Poyatos, M.; Peris, E. *Coord. Chem. Rev.* **2007**, *251*, 841. (b) Pugh, D.; Danopoulos, A. A. *Coord. Chem. Rev.* **2007**, *251*, 610. (c) Peris, E.; Crabtree, R. H. *Coord. Chem. Rev.* **2004**, *248*, 2239.
6. Mata, J. A.; Chianese, A. R.; Miecznikowski, J. R.; Poyatos, M.; Peris, E.; Faller, J. W.; Crabtree, R. H. *Organometallics* **2004**, *23*, 1253.
7. Wanniarachchi, Y. A.; Khan, M. A.; Slaughter, L. M. *Organometallics* **2004**, *23*, 5881.
8. (a) Viciano, M.; Poyatos, M.; Sanaú, M.; Peris, E.; Rossin, A.; Ujaque, G.; Lledós, A. *Organometallics* **2006**, *25*, 1120. (b) Albrecht, M.; Miecznikowski, J. R.; Samuel, A.; Faller, J. W.; Crabtree, R. H. *Organometallics* **2002**, *21*, 3596. (c) Viciano, M.; Mas-Marzá, E.; Poyatos, M.; Sanaú, M.; Crabtree, R. H.; Peris, E. *Angew. Chem., Int. Ed.* **2005**, *44*, 444.
9. (a) Vogt, M.; Pons, V.; Heinekey, D. M. *Organometallics* **2005**, *24*, 1832. (b) Viciano, M.; Feliz, M.; Corberán, R.; Mata, J. A.; Clot, E.; Peris, E. *Organometallics* **2007**, *26*, 5304. (c) Miranda-Soto, V.; Grotjahn, D. B.; DiPasquale, A. G.; Rheingold, A. L. *J. Am. Chem. Soc.* **2008**, *130*, 13200.
10. Corberán, R.; Sanaú, M.; Peris, E. *Organometallics* **2007**, *26*, 3492.
11. (a) Normand, A. T.; Cavell, K. J. *Eur. J. Inorg. Chem.* **2008**, 2781. (b) Lee, H. M.; Lee, C.-C.; Cheng, P.-Y. *Curr. Org. Chem.* **2007**, *11*, 1491.

12. (a) Jiménez, M. V.; Pérez-Torrente, J. J.; Bartolomé, M. I.; Gierz, V.; Lahoz, F. J.; Oro, L. A. *Organometallics* **2008**, 27, 224. (b) Gade, L. H.; César, V.; Bellemin-Lapponnaz, S. *Angew. Chem., Int. Ed.* **2004**, 43, 1014. (c) César, V.; Bellemin-Lapponnaz, S.; Wade, H.; Gade, L. H. *Chem. Eur. J.* **2005**, 11, 2862.
13. (a) Gnanamgari, D.; Sauer, E. L. O.; Schley, N. D.; Butler, C.; Incarvito, C. D.; Crabtree, R. H. *Organometallics* **2009**, 28, 321. (b) Perry, M. C.; Cui, X.; Powell, M. T.; Hou, D.-R.; Reibenspies, J. H.; Burgess, K. *J. Am. Chem. Soc.* **2003**, 125, 113. (c) Wang, C.-Y.; Fu, C.-F.; Liu, Y.-H.; Peng, S.-M.; Liu, S.-T. *Inorg. Chem.* **2007**, 46, 5779. (d) Song, G.; Wang, X.; Li, Y.; Li, X. *Organometallics* **2008**, 27, 1187. (e) Coleman, K. S.; Chamberlayne, H. T.; Turberville, S.; Green, M. L. H.; Cowley, A. R. *Dalton Trans.* **2003**, 2917.
14. Gade, L. H.; Bellemin-Lapponnaz, S. *Coord. Chem. Rev.* **2007**, 251, 718.
15. (a) Jin, C.-M.; Twamley, B.; Shreeve, J. M. *Organometallics* **2005**, 24, 3020. (b) Baskakov, D.; Herrmann, W. A.; Herdtweck, E.; Hoffmann, S. D. *Organometallics* **2007**, 26, 626.
16. (a) Wang, H. M. J.; Lin, I. J. B. *Organometallics* **1998**, 17, 972. (b) Chianese, A. R.; Li, X.; Janzen, M. C.; Faller, J. W.; Crabtree, R. H. *Organometallics* **2003**, 22, 1663. (c) Simons, R. S.; Custer, P.; Tessier, C. A.; Youngs, W. J. *Organometallics* **2003**, 22, 1979.
17. (a) Alcarazo, M.; Roseblade, S. J.; Cowley, A. R.; Fernández, R.; Brown, J. M.; Lassaletta, J. M. *J. Am. Chem. Soc.* **2005**, 127, 3290. (b) Herrmann, W. A.; Fischer, J.; Öfele, K.; Artus, G. R. J. *J. Organomet. Chem.* **1997**, 530, 259. (c) Herrmann, W. A.; Frey, G. D.; Herdtweck, E.; Steinbeck, E. *Adv. Synth. Catal.* **2007**, 349, 1677. (d) Huang, J.; Stevens, E. D.; Nolan, S. P. *Organometallics* **2000**, 19, 1194. (e) Martin, H. C.; James, N. H.; Aitken, J.; Gaunt, J. A.; Adams, H.; Haynes, A. *Organometallics* **2003**, 22, 4451. (f) Neveling, A.; Julius, G. R.; Cronje, S.; Esterhuysen, C.; Raubenheimer, H. G. *Dalton Trans.* **2005**, 181. (g) Praetorius, J. M.; Crudden, C. M. *Dalton Trans.* **2008**, 4079.
18. (a) Hanasaka, F.; Fujita, K.-i.; Yamaguchi, R. *Organometallics* **2004**, 23, 1490. (b) Corberán, R.; Sanaú, M.; Peris, E. *J. Am. Chem. Soc.* **2006**, 128, 3974. (c) Wang, X.; Chen, H.; Li, X. *Organometallics* **2007**, 26, 4684.
19. Herrmann, W. A.; Schütz, J.; Frey, G. D.; Herdtweck, E. *Organometallics* **2006**, 25, 2437.
20. (a) Spencer, A. *J. Organomet. Chem.* **1980**, 194, 113. (b) Kuil, M.; Soltner, T.; van Leeuwen, P. W. N. M.; Reek, J. N. H. *J. Am. Chem. Soc.* **2006**, 128, 11344.

21. (a) Yao, S.; Meng, J.-C.; Siuzdak, G.; Finn, M. G. *J. Org. Chem.* **2003**, *68*, 2540. (b) Sato, A.; Kinoshita, H.; Shinokubo, H.; Oshima, K. *Org. Lett.* **2004**, *6*, 2217. (c) Poyatos, M.; Maisse-François, A.; Bellemin-Laponnaz, S.; Gade, L. H. *Organometallics* **2006**, *25*, 2634.
22. (a) Luna, A. P.; Bonin, M.; Micouin, L.; Husson, H.-P. *J. Am. Chem. Soc.* **2002**, *124*, 12098. (b) Kinder, R. E.; Widenhoefer, R. A. *Org. Lett.* **2006**, *8*, 1967. (c) Smith, S. M.; Thacker, N. C.; Takacs, J. M. *J. Am. Chem. Soc.* **2008**, *130*, 3734.
23. (a) Kinoshita, H.; Shinokubo, H.; Oshima, K. *J. Am. Chem. Soc.* **2003**, *125*, 7784. (b) Tanaka, K.; Sagae, H.; Toyoda, K.; Noguchi, K.; Hirano, M. *J. Am. Chem. Soc.* **2007**, *129*, 1522.
24. (a) Hoge, G.; Wu, H.-P.; Kissel, W. S.; Pflum, D. A.; Greene, D. J.; Bao, J. *J. Am. Chem. Soc.* **2004**, *126*, 5966. (b) Liu, Y.; Ding, K. *J. Am. Chem. Soc.* **2005**, *127*, 10488.
25. (a) Chen, A. C.; Ren, L.; Decken, A.; Crudden, C. M. *Organometallics* **2000**, *19*, 3459. (b) Praetorius, J. M.; Kotyk, M. W.; Webb, J. D.; Wang, R.; Crudden, C. M. *Organometallics* **2007**, *26*, 1057.
26. (a) Park, K. H.; Kim, S. Y.; Son, S. U.; Chung, Y. K. *Eur. J. Org. Chem.* **2003**, 4341. (b) Faller, J. W.; Fontaine, P. P. *Organometallics* **2006**, *25*, 5887. (c) Özdemir, I.; Yiğit, M.; Yiğit, B.; Çetinkaya, B.; Çetinkaya, E. *J. Coord. Chem.* **2007**, *60*, 2377.
27. Field, L. D.; Messerle, B. A.; Vuong, K. Q.; Turner, P. *Organometallics* **2005**, *24*, 4241.
28. Evans, P. A.; Baum, E. W.; Fazal, A. N.; Pink, M. *Chem. Comm.* **2005**, 63.
29. (a) Lee, S. I.; Park, S. Y.; Park, J. H.; Jung, I. G.; Choi, S. Y.; Chung, Y. K.; Lee, B. Y. *J. Org. Chem.* **2006**, *71*, 91. (b) Gómez, F. J.; Kamber, N. E.; Deschamps, N. M.; Cole, A. P.; Wender, P. A.; Waymouth, R. M. *Organometallics* **2007**, *26*, 4541. (c) Peng, H. M.; Webster, R. D.; Li, X. *Organometallics* **2008**, *27*, 4484.
30. Wender, P. A.; Paxton, T. J.; Williams, T. J. *J. Am. Chem. Soc.* **2006**, *128*, 14814.
31. Vassilikogiannakis, G.; Orfanopoulos, M. *Tetrahedron Lett.* **1997**, *38*, 4323.
32. Weiss, H. M.; Touchette, K. M.; Angell, S.; Khan, J. *Org. Biomol. Chem.* **2003**, *1*, 2152.
33. Odedra, A.; Wu, C.-J.; Pratap, T. B.; Huang, C.-W.; Ran, Y.-F.; Liu, R.-S. *J. Am. Chem. Soc.* **2005**, *127*, 3406.

34. Lian, J.-J.; Chen, P.-C.; Lin, Y.-P.; Ting, H.-C.; Liu, R.-S. *J. Am. Chem. Soc.* **2006**, *128*, 11372.
35. Che, C.-M.; Yu, W.-Y.; Chan, P.-M.; Cheng, W.-C.; Peng, S.-M.; Lau, K.-C.; Li, W.-K. *J. Am. Chem. Soc.* **2000**, *122*, 11380.

PART III

Rhodium-Catalyzed Alkyne Dimerization and Subsequent Gold-Catalyzed Hydroamination

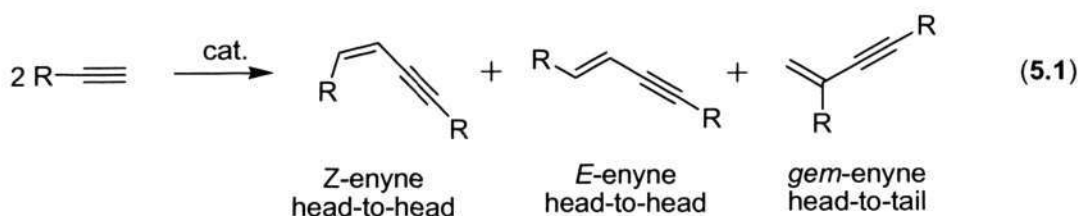
CHAPTER 5

Rhodium-Catalyzed Dimerization of *N*-Functionalized Propargyl Alkynes

5.1. Introduction

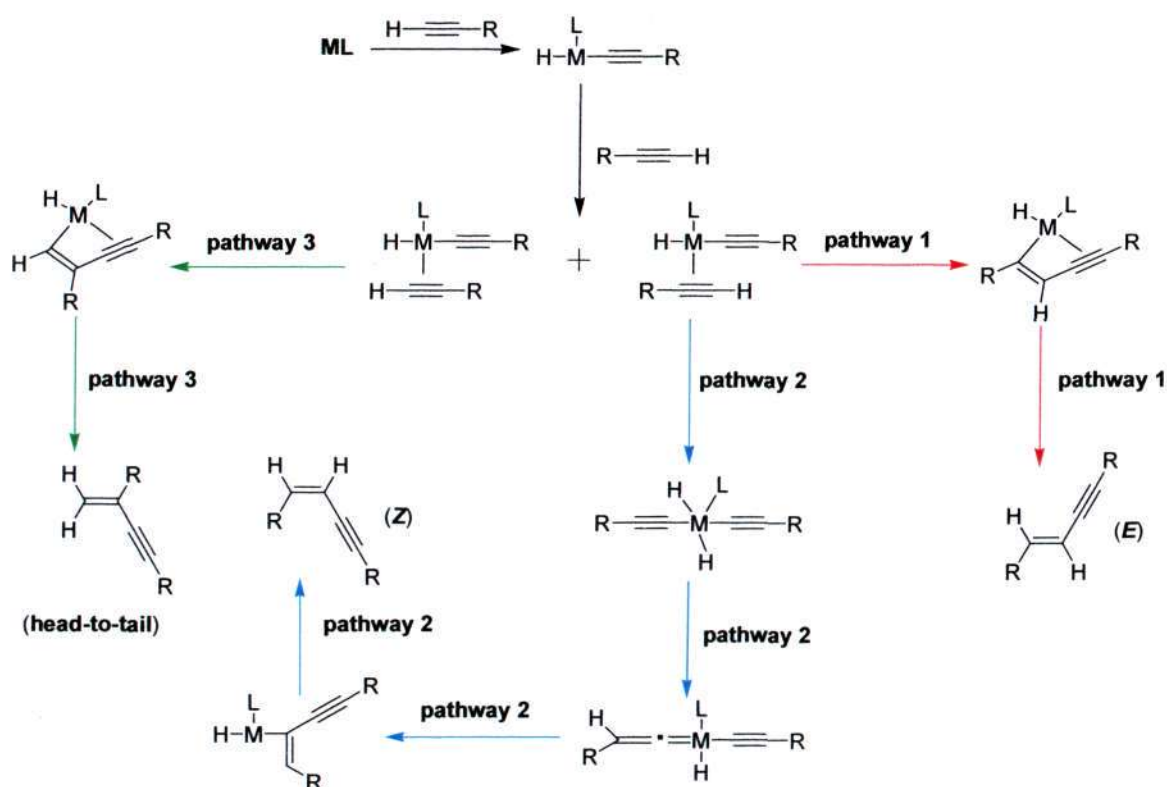
5.1.1. General Considerations of Alkyne Dimerization

Dimerization of 1-alkynes is attractive because it atom-economically affords conjugated enynes which are of great importance in organic synthesis,^{1,2} and as organic materials.³ Three isomeric products in head-to-head (*Z*- or *E*-enyne) and head-to-tail (*gem*-enyne) dimerization modes can be possible as a result of different regio- and stereo-selectivity (eq 5.1), which in principle can be controlled by various factors: such as substrates, ancillary ligands, and the nature of the catalysts. Although selective control of the dimerization product remains a huge challenge, metal vinylidene complexes ($M=C=CHR$) and/or metal alkynyl species [$M(\eta^2-HC\equiv CR)$] are usually considered as intermediates in the proposed mechanisms.^{4-7,19} As shown in the Scheme 5.1, alkyne C-H oxidative addition and subsequent coordination of another alkyne afford two isomeric intermediates [$RC\equiv C-M(\eta^2-HC\equiv CR)$], which undergo three reaction pathways giving different products. An insertion process gives vinyl-metal species leading to (*E*) products or head-to-tail products *via* pathway 1 and pathways 3 respectively. Oxidative addition of the coordination alkyne gives an alkynyl vinylidene metal complex, which affords (*Z*)-selective products through pathway 2.^{15d,16c,17e}



In fact, various metal compounds have been used to achieve this transformation, which include main group elements,⁸ lanthanides,⁹ actinides,¹⁰ and early¹¹ or late¹²⁻²⁰ transition metal complexes. While it has been recognized that the identity of phosphine ligands and the steric

hindrance of alkyne substrates play important roles in regio- and stereo-selectivity, controlling the selectivity to favor *Z*- or *gem*-enynes products remains difficult.^{8b,9d} Only limited review articles have been published including this specific research field,¹⁹ and in the following paragraphs we will discuss the development of this area using transition-metal catalysts from the period of 2002 to early 2009. Reports prior to 2002 will also be reviewed if these references are of great significances.



Scheme 5.1. Proposed mechanisms for the dimerization of terminal alkynes.

Metal-mediated alkyne dimerization was discovered decades ago. However, highly efficient results are quite limited, which are defined as high catalytic activity, high selectivity, and broad substrate scope. In general, organo-lanthanide catalysts tend to favor (*Z*)-enynes products.⁹ For instance, the yield of various (*Z*)-enynes can be even as high as 99% with Lutetium half-metallocene catalysts, and the proposed mechanism involves various dimeric intermediates that lead to the observed selectivity.^{9d} In contrast, late-transition-metal catalysts such as ruthenium, rhodium, palladium, iridium, and nickel complexes tend to give different selectivity, and some of them even show highly efficient catalytic activity towards cross-dimerization of alkynes.

5.1.2. Ruthenium-Catalyzed Alkyne Dimerization

Ruthenium-catalyzed terminal alkyne dimerization reactions usually give head-to-head coupling products, and there is only one known example that gives rise to head-to-tail enynes.^{12g} The Ozawa group reported that ruthenium vinylidene complexes in combination with a basic additive *N*-methylpyrrolidine can effectively give (*Z*)-enynes products for arylacetylenes under mild conditions. It was observed that phosphine ligands played an important role in catalytic activity, and complex **1** (Figure 5.1) bearing bulky and basic triisopropylphosphines exhibited the highest activity.^{19b} The same catalytic system can also be applied in cross-dimerization reactions between arylacetylenes and silylacetylenes, which afford silylated (*Z*)-butenynes (Scheme 5.2).^{12a}

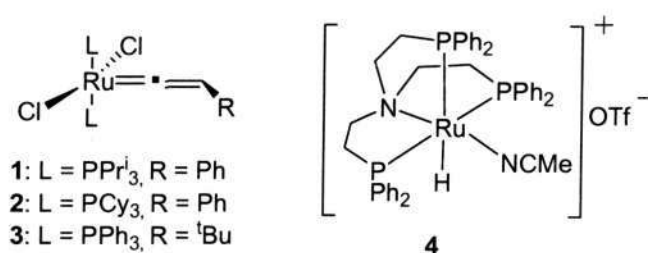
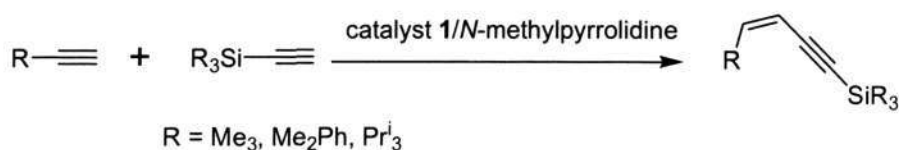


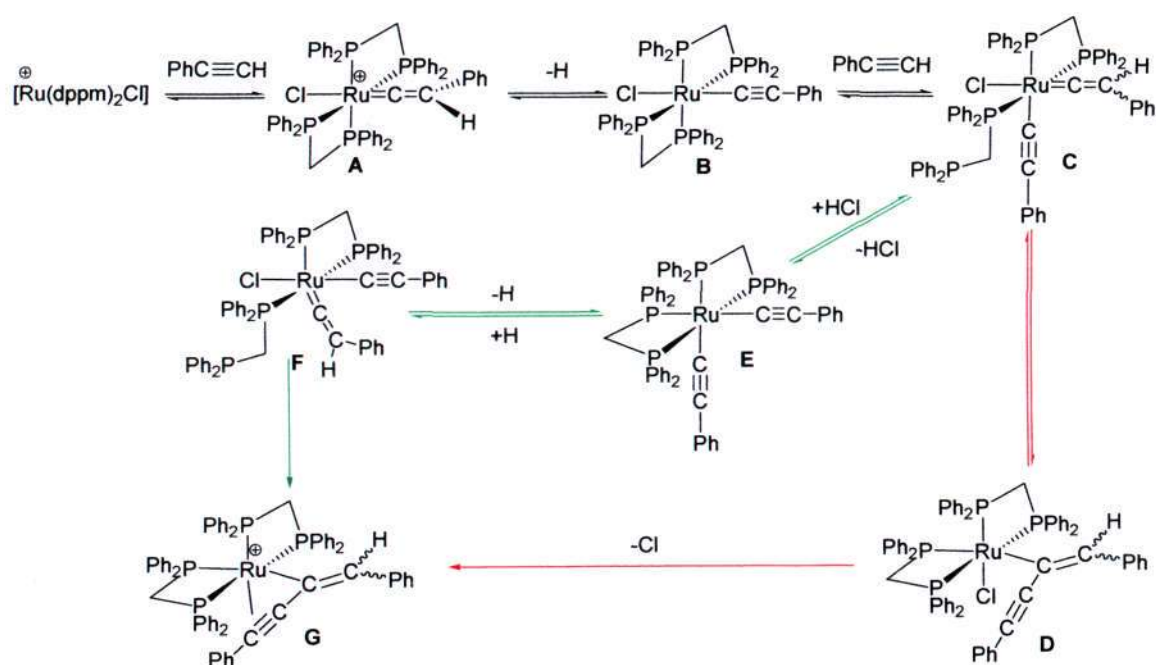
Figure 5.1. Ruthenium catalysts.



Scheme 5.2. Examples for ruthenium-catalyzed cross dimerization.

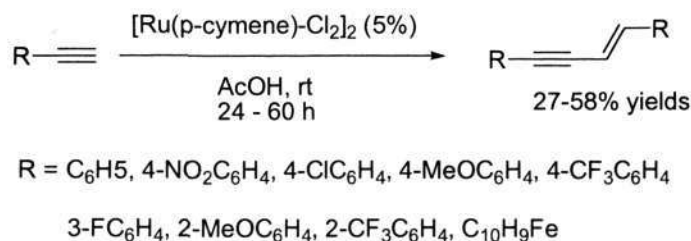
Almost at the same time, Jia, Bianchini, and Peruzzini et al. reported the first example of alkyne dimerization in water using catalyst **4** (Figure 5.1), which are effective for both aromatic and aliphatic alkynes giving (*Z*)-enynes with high regio- and stereo-selectivity.^{12b} Recently, Lynam and co-workers demonstrated that the reaction solvents and the nature of the phosphorus-containing ligands had pronounced influences on the stoichiometric reactions between ruthenium complexes and alkynes.^{12h} Under the conditions of different solvents, reaction time, and phosphine ligands, vinylidene species *trans*-[RuCl(=C=CHR)(P-P)₂]⁺ (complex **A** in Scheme 5.3, P-P = dppe or dppm) and butenynyl species [Ru(η³-RC≡C-C=CHR)(P-P)₂]⁺ (complex **G** in

Scheme 5.3) have been obtained from the reaction of *cis*-[RuCl₂(dppm)₂], PhC≡CH, and NaPF₆. Butenylnyl species have been demonstrated as an effective (*Z*)-selective catalyst for the dimerization of phenylacetylene. The proposed mechanism is shown in Scheme 5.3. Vinylidene complex **A** is formed *via* two steps: coordination of the alkyne to the metal and 1,2-hydrogen shift. Tautomerization of vinylidene complex gives complex **B**, which coordinates with another molecule alkyne affording complex **C** *via* a dissociation step. There is an equilibrium between **C** and **D**, and complex **G** could be formed from **D** by loss of chloride. It is also possible that the final complex **G** is generated from the loss of HCl from complex **C** and subsequent reprotonation.



Scheme 5.3. The proposed mechanism for the reaction between ruthenium complexes and alkynes.

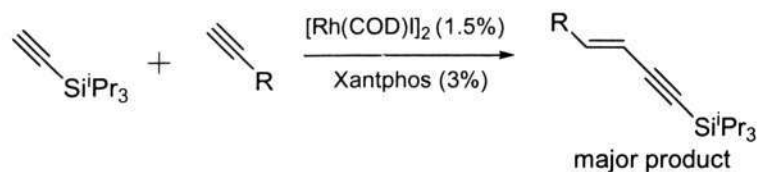
Several examples of (*E*)-selective dimerization have also been reported using ruthenium catalysts.^{12c,12d} For instance, Bassetti et al. gave the first report of arylalkyne dimerization processes promoted by commercially available $[\text{Ru}(p\text{-cymene})\text{Cl}_2]_2$ under phosphine-free conditions. While all previous ruthenium catalysts bear phosphine ligands. However, the isolated yields of this system are not satisfactory (27-58%), although the stereo-selectivity of (*E*)-enynes is high (Scheme 5.4).^{12c}



Scheme 5.4. Examples for ruthenium-catalyzed homo-dimerization.

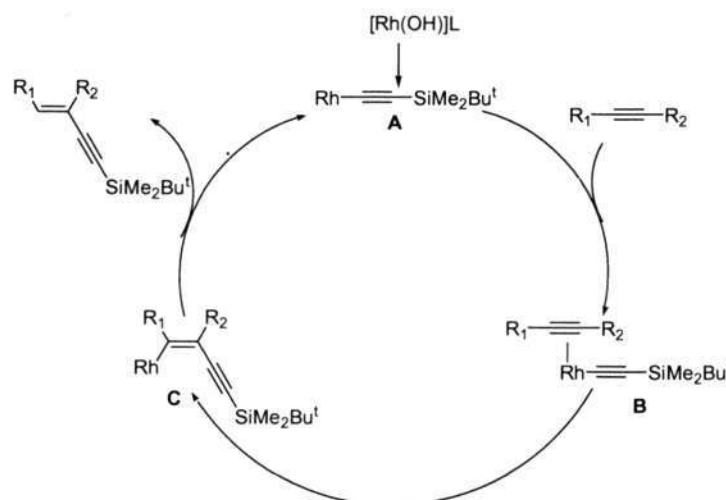
5.1.3. Rhodium-Catalyzed Alkyne Dimerization

The first rhodium catalyst that has been applied in alkyne dimerization is the Wilkinson's catalyst, but the substrates are essentially limited to aliphatic or silyl-substituted alkynes.¹³ In addition, examples of highly selective dimerization are rare using rhodium catalysts although reports in this context span over several decades.^{13,14} Recently, several groups reported successful cross-dimerization using rhodium-phosphine catalysts.^{15a-d} For instance, Miura and co-authors reported $[\text{Rh}(\text{COD})\text{OH}]_2$ /phosphine-catalyzed cross-coupling reactions between internal alkynes and terminal silylacetylenes.^{15c} The proposed mechanism involves three steps (Scheme 5.5). First, the hydroxyl-rhodium catalyst reacted with silyl-substituted acetylenes to form alkynylrhodium **A**. Then, the internal alkyne inserted into alkyne π -complex **B** giving vinylrhodium **C**. Finally, the enyne product was afforded after protonolysis. Later, the same research group described the reaction of various terminal alkynes and bulky silylacetylenes affording *trans*-enyne catalyzed by $[\text{Rh}(\text{COD})\text{X}]_2$ ($\text{X} = \text{I}, \text{Cl}, \text{OH}$) and phosphine ligands (Scheme 5.6).^{15b} This protocol can be applied to various functionalized alkynes such as cyano, ester, hydroxyl, and amino functional groups, but it failed for simple propargyl alcohol or ethyl propiolate.



$\text{R} = \text{CH}_2\text{Ph}, \text{C}_6\text{H}_{12}, (\text{CH}_2)_3\text{CN}, (\text{CH}_2)_3\text{OH}, (\text{CH}_2)_3\text{COOEt}$ and so on

Scheme 5.6. Examples of rhodium-catalyzed cross dimerization.

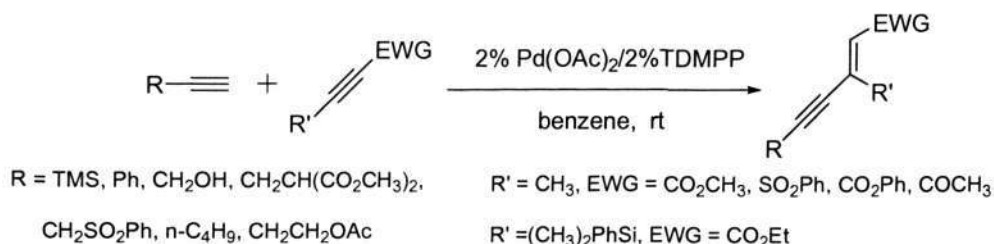


Scheme 5.5. The proposed mechanism for rhodium-catalyzed cross dimerization.

5.1.4. Palladium-Catalyzed Alkyne Dimerization

Palladium catalysts can also be applied in alkyne dimerization. In 1987, Trost et al. made the first great breakthrough in alkyne dimerization using palladium catalysts, which catalyzed the homo- and cross-coupling of various acetylenes in exclusively head-to-tail selectivity. Importantly, this reaction can tolerate esters, sulfones, and hydroxyl groups.^{16a} Extensive studies showed that the C-H bond of terminal alkynes (the donor alkynes) can be added to either terminal alkynes (self-coupling) or activated internal alkynes (cross-coupling) in the presence of a catalytic amount of palladium acetate and tris(2,6-dimethoxyphenyl)phosphine (TDMPP) (Scheme 5.7). Even more remarkably, at 1:1 ratio of donor and acceptor alkynes, only cross-coupling products were observed.^{16b} Under the similar reaction conditions, Gevorgyan et al. reported a highly regio- and stereo-selective (*E*) head-to-head dimerization of terminal arylacetylenes using $[(\pi\text{-allyl})\text{PdCl}]_2/\text{TDMPP}$ ($\text{P}[(2,6\text{-OMe})_2\text{C}_6\text{H}_3]_3$) as catalysts, and one equiv diethylamine was added as a reductant to generate palladium(0) species. In all cases, no other regio- or stereo-isomeric products were detected by GC/MS and NMR analysis of the crude reaction mixtures. It was surprising no head-to-head dimerization products were observed for aliphatic alkynes or arylalkynes without ortho-hydrogen atom. It has been proposed that an agostic interaction between the transition metal and ortho-protons of the aromatic ring resulted in the observed regio-selectivity, which was supported by kinetic isotope effect studies.^{16c} In 2002, Nolan and co-

workers used palladium/imidazolium/base systems to catalyze alkyne dimerization, and it was found that the base had important effects on the distribution of products. (*E*)-selective enynes were the predominant products when Cs_2CO_3 was used, but for K_2CO_3 a significant increase of head-to-tail dimerization was observed. Furthermore, the selectivity was also affected by steric hindrance of the substrates.^{16d}



Scheme 5.7. Examples for cross dimerization using palladium catalysts.

Another example of palladium-catalyzed cross-dimerization was reported by Tsukada, Inoue, and co-workers,^{16e} who demonstrated that both dinuclear and mononuclear palladium complexes (Figure 5.2) are efficient catalysts in the cross-coupling between triisopropylsilylacetylene (TIPSA) and unactivated internal alkynes. If this silyl group was changed to trimethylsilyl, triphenylsilyl or tert-butyldimethylsilyl, the reaction gave a mixture of homo- and cross-dimers.

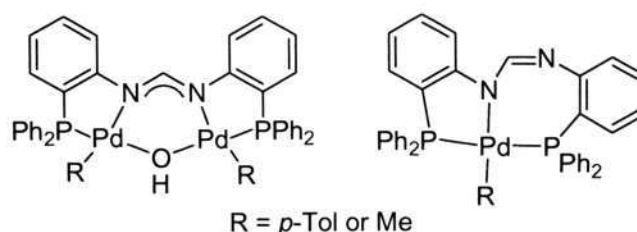


Figure 5.2. Palladium catalysts.

5.1.5. Other Transition-Metal-Catalyzed Alkyne Dimerization

Iridium¹⁷ and nickel¹⁸ complexes have also been investigated as alkyne dimerization catalysts, but they are comparatively less studied. Both of them gave preference to (*E*)-enynes. However, in some cases, the *E/Z* selectivity of resulting enynes can be adjusted by various phosphine ligands.^{17b} For iridium complexes, it is believed that Ir(I)/Ir(III) cycle is involved in this process including three typical steps: oxidative addition, insertion, and reductive

elimination.^{17d} For nickel catalysts, Ni(COD)₂ together with pyridine or phosphine ligands showed highly effective catalytic activity in both homo-dimerization and cross-dimerization, and the ligands have a remarkable impact.¹⁸

5.1.6. Summary

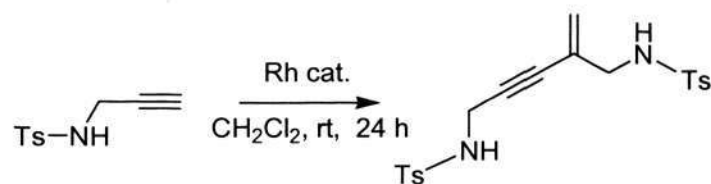
Up to now, some progress has been made in alkyne dimerization leading to conjugated enyne compounds. Importantly, the developments of cross-dimerization reactions in recent years have extended the scope of this type of reaction.^{15a-d,16c,18b} However, head-to-head products are still predominant. In sharp contrast, examples of selective head-to-tail dimerization are highly limited.^{8b,10b,c,11c,12g,16a,20} The few examples of alkyne dimerization in this mode are still limited to aryl-, alkyl- or silyl-substituted 1-alkyne substrates. In addition to the mentioned palladium-catalyzed highly efficient head-to-tail dimerization,^{16a} methylaluminoxane (MAO) has also been shown to catalyze the highly selective head-to-tail dimerization of various aryl or alkyl-substituted terminal alkynes, but it suffers from poor compatibility with heteroatom functional groups.^{8b} Thus it is necessary to develop new efficient methodologies for the head-to-tail dimerization of functionalized alkynes. Herein, we report a selective head-to-tail dimerization of amide- and sulfonamide-functionalized alkynes catalyzed by rhodium-phosphine systems.

5.2. Results and Discussion

We noted that there was a poor reactivity of simple propargyl alcohols or propargyl amines towards dimerization.^{8b,15b} Therefore, sulfonylated propargyl amines such as TsNHCH₂C≡CH were chosen as substrates for the screening of different rhodium catalysts. We reasoned that here the tosyl oxygen might act as a weak donor and, in addition, the introduction of a withdrawing Ts group should inductively change the electronic properties of the alkyne, which might lead to changes in selectivity and reactivity of the dimerization reaction. Indeed, the *gem*-enyne product was obtained in 52% yield (toluene, 24 h, rt) when a combination of [Rh(COD)Cl]₂ (2 mol%) and PPh₃ (4 mol%) was used, although 42% of the starting material remained intact (entry 1, Table 5.1). The yield was improved to 64% when the toluene solvent was replaced by CH₂Cl₂. No appreciable improvement of the reaction yield could be achieved in CH₂Cl₂ under reflux (24 h).

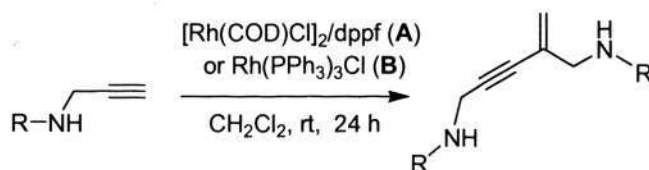
To our surprise, no desired product was obtained when PPh_3 was replaced by $\text{P}(p\text{-FC}_6\text{H}_4)_3$, $\text{P}(p\text{-OMeC}_6\text{H}_4)_3$, or PCy_3 (entries 4, 5, and 10, Table 5.1). We then applied $\text{Rh}(\text{PPh}_3)_3\text{Cl}$ as a catalyst, which was known to catalyze the dimerization of $\text{SiMe}_3\text{C}\equiv\text{CH}$ in (*E*)-selectivity,^{13a} and the isolated yield was improved to 77% (entry 3, Table 5.1). It has been reported that bidentate phosphines have significant effects on the selectivity of alkyne dimerization,^{15b,c} therefore, *dppb*, *dppf*, *dppp*, *dppm*, and *xantphos* were screened together with $[\text{Rh}(\text{COD})\text{Cl}]_2$ in 1:1 ratio,²¹ among which *dppb* and *dppp* gave moderate yields but *dppf* was the best choice (entry 7, Table 5.1). Ionic rhodium complex $[\text{Rh}(\text{COD})(\text{PPh}_3)_2]^+\text{PF}_6^-$, however, showed no activity (entry 12, Table 5.1).

We thus retained $\text{Rh}(\text{PPh}_3)_3\text{Cl}$ and $[\text{Rh}(\text{COD})\text{Cl}]_2/\text{dppf}$ to further explore the scope of this reaction, and the results were given in Table 5.2. Various propargyl carbamates and ureas could also smoothly undergo dimerization under the same conditions. Moderate to good yields were obtained in the dimerization of $\text{BocNHCH}_2\text{C}\equiv\text{CH}$ and $\text{CbzNHCH}_2\text{C}\equiv\text{CH}$ when catalyzed by $\text{Rh}(\text{PPh}_3)_3\text{Cl}$ or $[\text{Rh}(\text{COD})\text{Cl}]_2/\text{dppf}$ (entries 3-5, Table 5.2). $[\text{Rh}(\text{COD})\text{Cl}]_2/\text{dppf}$ system showed activity superior to $\text{Rh}(\text{PPh}_3)_3\text{Cl}$ in the dimerization of $\text{Me}_2\text{NC}(\text{O})\text{NHCH}_2\text{C}\equiv\text{CH}$ (entries 6 and 7, Table 5.2). In addition, both catalysts showed poor activity and selectivity towards phenylacetylene, ethyl propiolate, and trimethylsilylacetylene under the same conditions. Sulfonylated propargyl amines appeared to be the most efficient substrates in this head-to-tail dimerization. We thus extended the substrates to alkynes with different sulfonamide functionalities. As shown in Table 5.3, all of them gave moderate to high yields. It seems that aromatic sulphonamides are more favorable substrates than aliphatic ones.

Table 5.1. Optimization of reaction conditions ^a

entry	cat.	NMR yield ^b (%)	SM ^b (%)
1 ^c	[Rh(COD)Cl] ₂ /PPh ₃	52	42
2	[Rh(COD)Cl] ₂ /PPh ₃	64	31
3	Rh(PPh ₃) ₃ Cl	83 (77 ^d)	10
4	[Rh(COD)Cl] ₂ /P(<i>p</i> -FC ₆ H ₄) ₃	0	75
5	[Rh(COD)Cl] ₂ /P(<i>p</i> -OMeC ₆ H ₄) ₃	0	85
6	[Rh(COD)Cl] ₂ /dppb	64	30
7	[Rh(COD)Cl] ₂ /dppf	90 (83 ^d)	5
8	[Rh(COD)Cl] ₂ /dppp	54	23
9	[Rh(COD)Cl] ₂ /dppm	< 3	75
10	[Rh(COD)Cl] ₂ /PCy ₃	< 3	95
11	[Rh(COD)Cl] ₂ /xantphos	< 3	95
12	[Rh(COD)(PPh ₃) ₂] ⁺ PF ₆ ⁻	< 3	90

^a Unless otherwise noted, the reaction was carried out at rt for 24 h under argon, using TsNHCH₂C≡CH (0.25 mmol), Rh(PPh₃)₃Cl (0.005 mmol) or [Rh(COD)Cl]₂ (0.005 mmol)/phosphine (0.01 mmol), 1,3,5-trimethoxybenzene (internal standard, 0.083 mmol), and CH₂Cl₂ (1.5 mL). ^b Yields and starting material percentage were determined using 1,3,5-trimethoxybenzene as an internal standard by ¹H NMR spectroscopy. ^c Toluene as the solvent. ^d Isolated yield.

Table 5.2. Head-to-tail dimerization of functionalized 1-alkynes^a

entry	R	cat.	Isolated yield (%)	product
1	Ts ^b	A	83	1
2	Ts	B	77	1
3	Boc ^c	A	62	2
4	Cbz ^d	A	68	3
5	Cbz	B	74	3
6	-C(O)NMe ₂	A	67	4
7	-C(O)NMe ₂	B	36	4
8	-C(O)OEt	A	66	5

^a Reaction conditions: alkyne substrate (0.5 mmol), [Rh(COD)Cl]₂ (0.01 mmol)/dppf (0.02 mmol) (**A**) or Rh(PPh₃)₃Cl (0.01 mmol) (**B**), CH₂Cl₂ (1.5 mL), rt, 24 h. ^b Ts = *p*-toluenesulfonyl. ^c Boc = *tert*-butoxycarbonyl. ^d Cbz = carbobenzyloxy.

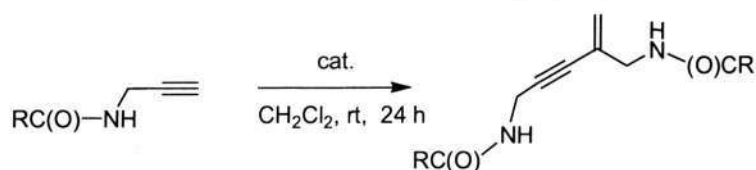
Table 5.3. Head-to-tail dimerization of propargyl sulphonamides^a

entry	R	time	isolated yield (%)	product
1	Me	24	67	6
2		16	79	7
3		16	80	8
4	PhCH ₂	24	64	9
5		24	81	10
6		16	83	11
7	Ph	15	79	12
8	ⁿ Bu	24	72	13

^a Reaction conditions: *N*-propargylamide (0.5 mmol), [Rh(COD)Cl]₂ (0.01 mmol), dppf (0.02 mmol), CH₂Cl₂ (1.5 mL), rt, 24 h.

We then focused on the dimerization of structurally related *N*-propargyl amides. In comparison with propargyl carbamates or ureas, amides with R = aryl or vinyl groups all showed poor activity and only moderate yields were obtained in toluene even at 80 °C using Rh(PPh₃)₃Cl as a catalyst (entry 1 and 3, Table 5.4). This is likely caused by the lower donor capacity of the amide O atom or a weaker inductive effect of amide groups. Interestingly, amide with R = *tert*-butyl can dimerize with 78% isolated yield using [Rh(COD)Cl]₂/dppf as a catalyst at room temperature (entry 7, Table 5.4). Although the steric effect of *tert*-butyl group is a disadvantage, the stronger donor capacity of the amide oxygen atom likely plays an important role.

Table 5.4. Head-to-tail dimerization of *N*-propargyl amides ^a



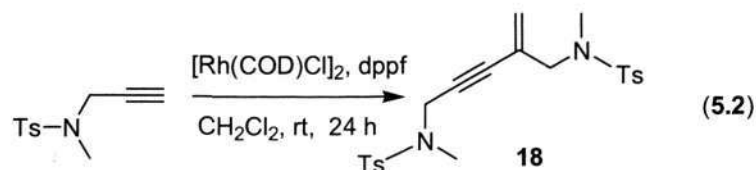
entry	R	solvent	temp (°C)	yield (%)	product
1	Ph	CH ₂ Cl ₂	25	27 ^b	14
2	Ph	toluene	80	46 ^c	14
3		CH ₂ Cl ₂	25	25 ^b	16
4		toluene	80	64 ^c	16
5	^t Bu	CH ₂ Cl ₂	25	31 ^b	17
6	^t Bu	toluene	80	59 ^c	17
7	^t Bu	CH ₂ Cl ₂	25	78 ^c	17

^a Conditions: *N*-propargyl amide (0.5 mmol); [Rh(COD)Cl]₂ (0.01 mmol)/dppf (0.02 mmol) (for entries 3 and 7) or Rh(PPh₃)₃Cl (0.01 mmol) (for other entries); CH₂Cl₂ (1.5 mL).

^b NMR yields using 1,2,3-trimethoxybenzene as an internal standard. ^c Isolated yield.

Finally, in order to investigate if NH group plays an important role in this dimerization reaction, methyl-substituted substrate TsN(CH₃)CH₂C≡CH was applied in this reaction (eq 5.2).

The result showed that dimerization product **18** was obtained in 81% yield, which indicated that NH group is not a pre-requisition for this efficient head-to-tail dimerization process.



5.3. Conclusion

In summary, we have developed a highly efficient head-to-tail dimerization of functionalized propargyl amines under mild conditions, and $\text{Rh}(\text{PPh}_3)_3\text{Cl}$ and $[\text{Rh}(\text{COD})\text{Cl}]_2/\text{dppf}$ showed higher catalytic activity among a series of rhodium catalysts. In contrast, propargyl sulfonamides are more efficient substrates than carbamates and structurally related *N*-propargyl amides. Interestingly, amide with $\text{R} = \textit{tert}$ -butyl can dimerize efficiently (78%), which attributes to a stronger donor capacity of the amide group in this substrate. Further experimental results have proven that NH group is not necessary to efficient catalysis of dimerization.

5.4. Experimental Section

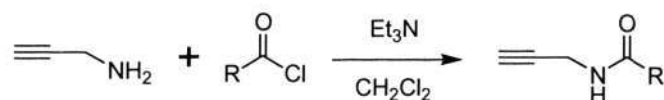
5.4.1. General Information

All commercial solvents were dried using 4Å molecule sieves, and all commercial reagents were used as received. Analytical thin layer chromatography (TLC) was performed using Merck 60 F254 precoated silica gel plates (0.2 mm thickness). TLC plates were visualized using UV radiation (254 nm) on Spectroline Model ENF-24061/F 254 nm. Further visualization was possible by staining with a basic solution of KMnO_4 . Flash chromatography was conducted by Merck silica gel 60 with freshly distilled solvents. Columns were typically packed as slurry and equilibrated with the appropriate solvent system prior to use.

IR spectra were recorded on a Horiba FT 300-S by ATR method and on a Shimadzu IR Prestige-21 FT-IR Spectrometer. High-resolution mass spectra were obtained with a Finnigan MAT 95 XP mass spectrometer (EI) and a Waters Micromass Q-Tof Premier Mass Spectrometer

(ESI). ^1H and ^{13}C NMR spectra were recorded on a Bruker Avance DPX 300, Bruker AMX 400, or Bruker DRX 500 spectrophotometer. Chemical shifts for ^1H NMR spectra were reported as δ in units of parts per million (ppm) downfield from SiMe_4 (δ 0.0) and relative to the signal of chloroform-*d* (δ 7.26, singlet). Multiplicities were given as: s (singlet); d (doublet); t (triplet); or m (multiplets). The number of protons (n) for a given resonance was indicated by nH. Coupling constants were reported as a *J* value in Hz.

5.4.2. Synthetic Procedures and Data



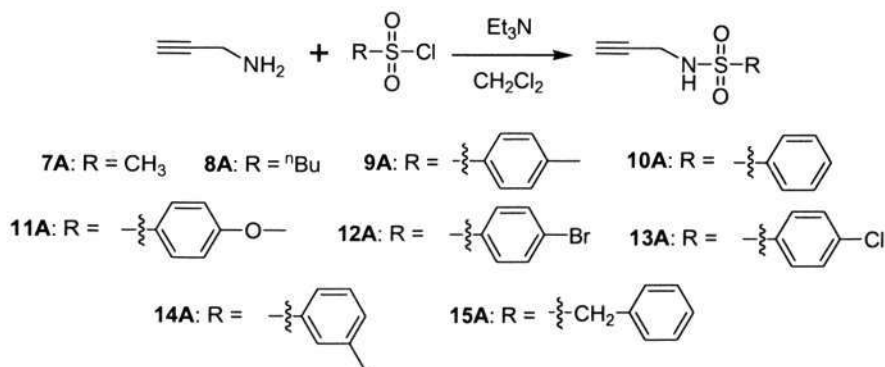
1A: R = *i*-Bu, **2A:** R = OCH_2Ph , **3A:** R = OEt, **4A:** R = Ph, **5A:** R = *t*-Bu, **6A:** R = $\text{N}(\text{CH}_3)_2$.

Literature reports were followed to prepare the following *N*-propargylamide monomers: **1A**,²² **3A**,²³ **4A**,²³ **5A**,²³ **8A**,²⁴ **9A**,^{24,25} **10A**,²⁴ and **15A**.²⁵ Other *N*-propargylamide monomers were synthesized using the following procedure: to a stirred solution of propargyl amine (5 mmol) in CH_2Cl_2 (8 mL) was added a corresponding acyl chloride (for **2A** and **6A**) or a sulfonyl chloride (1.1 equiv) at 0 °C. Et_3N (1.5 equiv) was then injected by syringe. The reaction mixture was allowed to slowly warm up to rt and was stirred for 10 h. The mixture was then washed with a 1 M HCl solution and subsequently a brine solution, and the combined organic layer was dried by anhydrous Na_2SO_4 . Analytically pure products were obtained after the solvent was removed, except for **2A**, which was purified by silica gel chromatography using 5/1 hexane/ethyl acetate.

2A: colorless oil (it turns to a white solid when kept in a fridge); 832 mg; 4.4 mmol; 88%. ^1H NMR (400 MHz, CDCl_3): δ 7.35-7.29 (m, 5H), 5.12 (s, 2H), 5.04 (br, 1H, NH), 3.98 (d, *J* = 3.0 Hz, 2H, CH_2NH), 2.25 (t, *J* = 2.4 Hz, 1H); ^{13}C NMR (100 MHz, CDCl_3): δ 155.9 (CO), 136.2, 128.6, 128.24, 128.20, 79.6 (C_{alkyne}), 71.6 ($\text{CH}_{\text{alkyne}}$), 67.1, 30.8 (CH_2NH). **HRMS (ESI)** for $\text{C}_{11}\text{H}_{12}\text{NO}_2$ calcd: 190.0868, found: 190.0859.

6A: white solid; mp: 76-77 °C; 315 mg; 2.5 mmol; 50%. ^1H NMR (400 MHz, CDCl_3): δ 4.56 (br, 1H, NH), 4.02 (m, 2H, CH_2), 2.91 (s, 6H), 2.21 (t, *J* = 2.4 Hz, 1H); ^{13}C NMR (100 MHz,

CDCl_3): δ 157.7 (CO), 81.1 (C_{alkyne}), 71.0 ($\text{CH}_{\text{alkyne}}$), 36.2 (CH_3), 30.7 (CH_2). **HRMS (ESI)** for $\text{C}_6\text{H}_{11}\text{N}_2\text{O}$ calcd: 127.0871, found: 127.0869.



7A: white solid; 339 mg; 2.55 mmol; 51%. ^1H NMR (500 MHz, CDCl_3): δ 4.80 (br, 1H, NH), 3.97 (m, 2H, CH_2), 3.09 (s, 3H), 2.38 (t, $J = 2.4$ Hz, 1H); ^{13}C NMR (125 MHz, CDCl_3): δ 78.9 (C_{alkyne}), 73.4 ($\text{CH}_{\text{alkyne}}$), 41.5 (CH_3), 32.7 (CH_2). **HRMS (ESI)** for $\text{C}_4\text{H}_8\text{NO}_2\text{S}$ calcd: 134.0276, found: 134.0277.

11A: white solid; mp: 79-80 $^\circ\text{C}$; 1.1 g; 4.9 mmol; 98%. ^1H NMR (500 MHz, CDCl_3): δ 7.82 (d, $J = 8.8$ Hz, 2H), 6.98 (d, $J = 8.8$ Hz, 2H), 4.61 (t, $J = 5.3$ Hz, 1H, NH), 3.87 (s, 3H, OCH_3), 3.82 (m, 2H), 2.11 (t, $J = 2.4$ Hz, 1H); ^{13}C NMR (100 MHz, CDCl_3): δ 163.2 (COCH_3), 131.1, 129.6, 114.3, 78.1 (C_{alkyne}), 73.0 ($\text{CH}_{\text{alkyne}}$), 55.7 (CH_3), 32.9 (CH_2). Anal. Calcd for $\text{C}_{10}\text{H}_{11}\text{NO}_3\text{S}$ (225.26): C, 53.32; H, 4.92; N, 6.22; S, 14.23%. Found: C, 53.71; H, 5.05; N, 6.52; S, 14.51%.

12A: white solid; mp: 102-103 $^\circ\text{C}$; 1.36 g; 4.9 mmol; 99%. ^1H NMR (500 MHz, CDCl_3): δ 7.76 (d, $J = 8.4$ Hz, 2H), 7.66 (d, $J = 8.4$ Hz, 2H), 4.87 (br, 1H, NH), 3.87 (m, 2H), 2.10 (t, $J = 2.2$ Hz, 1H); ^{13}C NMR (100 MHz, CDCl_3): δ 138.8 (CSO_2), 132.4, 129.0, 128.0, 77.7 (C_{alkyne}), 73.3 ($\text{CH}_{\text{alkyne}}$), 32.9 (CH_2). Anal. Calcd for $\text{C}_9\text{H}_8\text{BrNO}_2\text{S}$ (274.13): C, 39.43; H, 2.94; N, 5.11; S, 11.70%. Found: C, 39.80; H, 2.64; N, 5.16; S, 11.51%.

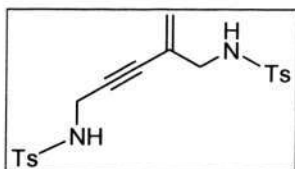
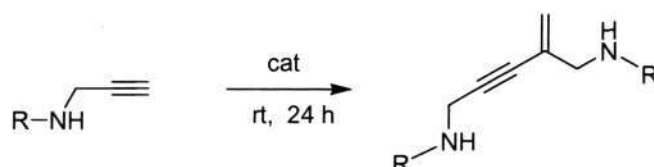
13A: white solid; mp: 102-103 $^\circ\text{C}$; 1.1 g; 4.8 mmol; 96%. ^1H NMR (400 MHz, CDCl_3): δ 7.82 (d, $J = 8.7$ Hz, 2H), 6.98 (d, $J = 8.7$ Hz, 2H), 5.05 (br, 1H, NH), 3.86 (m, 2H), 2.09 (t, $J = 2.4$ Hz, 1H); ^{13}C NMR (100 MHz, CDCl_3): δ 139.5 (CSO_2), 138.2, 129.4, 128.9, 77.7 (C_{alkyne}), 73.3 ($\text{CH}_{\text{alkyne}}$), 32.8 (CH_2). **HRMS (ESI)** for $\text{C}_9\text{H}_8\text{NO}_2\text{SClNa}$ calcd: 251.9862, found: 251.9857.

14A: colorless oil; 1.0 g; 4.8 mmol; 98%. ^1H NMR (500 MHz, CDCl_3): δ 7.71-7.68 (m, 2H), 7.40-7.39 (m, 2H), 4.80 (br, 1H, NH), 3.84 (m, 2H), 2.42 (s, 3H), 2.10 (t, $J = 2.4$ Hz, 1H);

^{13}C NMR (125 MHz, CDCl_3): δ 139.4 (CSO_2), 139.3, 133.8, 129.0, 127.7, 124.5, 77.9 (C_{alkyne}), 73.0 ($\text{CH}_{\text{alkyne}}$), 32.9 (CH_2), 21.3 (CH_3). **HRMS (ESI)** for $\text{C}_{10}\text{H}_{12}\text{NO}_2\text{S}$ calcd: 210.0589, found: 210.0581.

Dimerization of *N*-Protected Propargyl Amines:

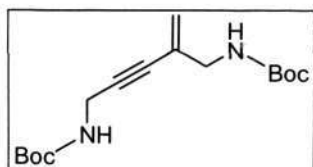
General procedure for the dimerization of alkynes (compounds **1-14**, **18**): A *N*-propargylamide monomer (0.5 mmol) and 2 mol% $[\text{Rh}(\text{COD})\text{Cl}]_2$ and 4 mol% dppf were weighted into a flask, which was kept in argon atmosphere. Subsequently, anhydrous CH_2Cl_2 (1.5 mL) was injected *via* a syringe, and the mixture was stirred at room temperature (for CH_2Cl_2) or 80 °C (for toluene) for 15- 24 h. The solvent was then removed under reduced pressure and the residue was purified by silica gel column chromatography.



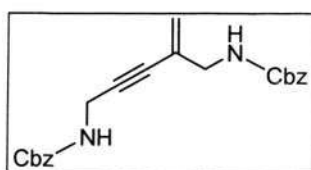
Compound 1: colourless viscous oil; yield: 83%; hexane/ethyl acetate:

5/3; ^1H NMR (400 MHz, CDCl_3): δ 7.77-7.72 (m, 4H, $\text{H}_{\text{aromatic}}$), 7.31-7.28 (m, 4H, $\text{H}_{\text{aromatic}}$), 5.30 (s, 1H, alkene), 5.14 (s, 1H, alkene), 4.86 (t, J = 6.1 Hz, 2H, 2NH), 3.86 (d, J = 6.0 Hz, 2H, CH_2), 3.48 (d, J = 6.4 Hz, 2H, CH_2), 2.43 (s, 3H, CH_3), 2.40 (s, 3H, CH_3); ^{13}C NMR (100 MHz, CDCl_3): δ 143.8, 143.6, 137.0, 136.6, 129.72 ($\text{CH}_{\text{aromatic}}$), 129.69 ($\text{CH}_{\text{aromatic}}$), 127.5 ($\text{CH}_{\text{aromatic}}$), 127.2 ($\text{CH}_{\text{aromatic}}$), 126.1 (C_{alkene}), 123.3 ($\text{CH}_2_{\text{alkene}}$), 85.6 (alkyne), 82.2 (alkyne), 47.6 (CH_2), 33.4 (CH_2), 21.55 (CH_3), 21.52 (CH_3). IR (KBr): 3318 (s), 3283 (s), 2924 (w), 2864 (w), 1618 (w), 1597 (w), 1441 (m), 1329 (s), 1306 (m), 1250 (w), 1159 (s), 1092 (s), 1028 (w), 932 (w), 816 (s), 687 (m), 664 (s), 546 (s), 515 (w) cm^{-1} .

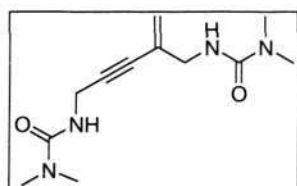
HRMS (ESI) for $\text{C}_{20}\text{H}_{23}\text{N}_2\text{O}_4\text{S}_2$ calcd: 419.1099, found: 419.1082.



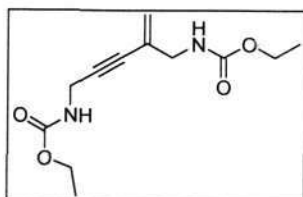
Compound 2: colourless viscous oil; yield: 62%; Hexane/ethyl acetate: 5/1 to 4/1; ^1H NMR (400 MHz, CDCl_3): δ 5.39 (s, 1H, alkene), 5.37 (s, 1H, alkene), 4.81 (br, 2H, NH), 4.03 (d, $J = 4.3$ Hz, 2H, CH_2), 3.75 (d, $J = 5.3$ Hz, 2H, CH_2), 1.44 (s, 18H); ^{13}C NMR (100 MHz, CDCl_3): δ 155.7 (CO), 155.3 (CO), 128.4 (C_{alkene}), 121.5 ($\text{CH}_2_{\text{alkene}}$), 86.7 (alkyne), 81.6 (alkyne), 80.0 ($\text{C}(\text{CH}_3)_3$), 79.6 ($\text{C}(\text{CH}_3)_3$), 45.3 (CH_2), 31.1 (CH_2), 28.4 ($2\text{C}(\text{CH}_3)_3$). IR (KBr): 3352 (m), 2980 (m), 2936 (w), 1701 (s), 1516 (s), 1456 (w), 1393 (m), 1368 (s), 1273 (m), 1252 (s), 1171 (s), 1049 (w), 860 (w), 779 (w) cm^{-1} . **HRMS (ESI)** for $\text{C}_{16}\text{H}_{27}\text{N}_2\text{O}_4$ calcd: 311.1971, found: 311.1967.



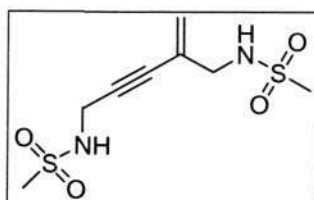
Compound 3: colourless viscous oil; yield: 68%; hexane/ethyl acetate: 10:3 to 2:1; ^1H NMR (400 MHz, CDCl_3): δ 7.36-7.32 (m, 10H, $\text{H}_{\text{aromatic}}$), 5.42 (s, 2H, alkene), 5.11 (s, 4H, $2\text{CH}_2\text{O}$), 5.00 (br, 1H, NH), 4.94 (br, 1H, NH), 4.08 (d, $J = 5.0$ Hz, 2H, CH_2), 3.84 (d, $J = 5.7$ Hz, 2H, CH_2); ^{13}C NMR (100 MHz, CDCl_3): δ 156.2 (CO), 155.9 (CO), 136.4 ($\text{C}_{\text{aromatic}}$), 136.3 ($\text{C}_{\text{aromatic}}$), 128.6 (2C overlap), 128.23, 128.19, 127.9 (C_{alkene}), 122.0 ($\text{CH}_2_{\text{alkene}}$), 86.5 (alkyne), 81.7 (alkyne), 67.1 (CH_2O), 66.9 (CH_2O), 45.7 (CH_2), 31.5 (CH_2). IR (KBr): 3327 (s), 3310 (s), 3067 (m), 3034 (m), 2963 (w), 2899 (w), 1952 (w), 1705 (s), 1682 (s), 1622 (m), 1528 (s), 1456 (m), 1360 (m), 1283 (s), 1215 (m), 1145 (m), 1063 (s), 980 (m), 909 (m), 781 (m), 698 (s), 584 (w), 496 (w) cm^{-1} . **HRMS (ESI)** for $\text{C}_{22}\text{H}_{23}\text{N}_2\text{O}_4$ calcd: 379.1658, found: 379.1658.



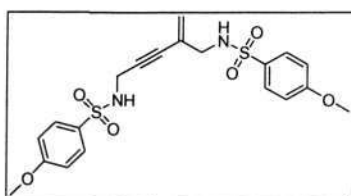
Compound 4: white solid; mp: 147-148 $^{\circ}\text{C}$; yield: 67%; ethyl acetate/methanol: 10/1; ^1H NMR (400 MHz, CDCl_3): δ 5.39 (s, 2H, $\text{CH}_2_{\text{alkene}}$), 4.67 (br, 2H, NH), 4.13 (d, $J = 5.1$ Hz, 2H, CH_2), 3.90 (d, $J = 5.9$ Hz, 2H, CH_2), 2.92 (s, 12H). ^{13}C NMR (100 MHz, CDCl_3): δ 158.2 (CO), 157.9 (CO), 129.2 (C_{alkene}), 121.0 (C_{alkene}), 87.9 (alkyne), 81.6 (alkyne), 45.6 (CH_2), 36.24 (CH_3), 36.20 (CH_3), 31.4 (CH_2). IR (KBr): 3329 (m), 2922 (w), 1638 (s), 1620 (w), 1537 (s), 1412 (m), 1379 (m), 1265 (m), 1229 (s), 1067 (w), 775 (w), 594 (w) cm^{-1} . **HRMS (ESI)** for $\text{C}_{12}\text{H}_{21}\text{N}_4\text{O}_2$ calcd: 253.1665, found: 253.1653.



Compound 5: pale yellow oil; yield: 66%; hexane/ethyl acetate: 5:1 to 5:2; ^1H NMR (500 MHz, CDCl_3): δ 5.40 (s, 2H, CH_2 alkene), 5.03 (br, 2H, 2NH), 4.13-4.09 (m, 4H, $2\text{CH}_2\text{CH}_3$), 4.08 (d, $J = 4.7$ Hz, 2H, CH_2), 3.80 (d, $J = 5.7$ Hz, 2H, CH_2), 1.23 (t, $J = 7.1$ Hz, 6H); ^{13}C NMR (125 MHz, CDCl_3): δ 156.5 (CO), 156.2 (CO), 128.1 (C_{alkene}), 121.7 (CH_2 alkene), 86.6 (alkyne), 81.6 (alkyne), 61.2 (CH_2CH_3), 61.0 (CH_2CH_3), 45.6 (CH_2), 31.4 (CH_2), 14.6 (2CH_3). IR (KBr): 3331 (m), 2984 (w), 2938 (w), 1705 (s), 1697 (s), 1533 (s), 1379 (w), 1258 (s), 1173 (m), 1040 (m), 872 (w), 779 (w) cm^{-1} . **HRMS (ESI)** for $\text{C}_{12}\text{H}_{19}\text{N}_2\text{O}_4$ calcd: 255.1345, found: 255.1336.

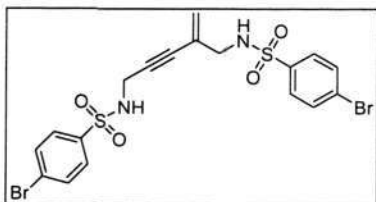


Compound 6: white solid; mp: 107-108 $^{\circ}\text{C}$; yield: 67%; hexane/acetone: 3:2 to 1:1; ^1H NMR (500 MHz, CDCl_3): δ 5.54 (s, 1H, alkene), 5.50 (s, 1H, alkene), 5.42 (br, 1H, NH), 5.39 (br, 1H, NH), 4.08 (d, $J = 5.9$ Hz, 2H, CH_2), 3.80 (d, $J = 6.4$ Hz, 2H, CH_2), 3.08 (s, 3H, CH_3), 3.00 (s, 3H, CH_3); ^{13}C NMR (125 MHz, CDCl_3): δ 127.0 (alkene), 124.1 (alkene), 86.9 (alkyne), 82.4 (alkyne), 48.0 (CH_2), 41.3 (CH_3), 41.1 (CH_3), 33.3 (CH_2). IR (KBr): 3304 (s), 3294 (s), 2982 (w), 2943 (w), 1867 (w), 1616 (w), 1439 (s), 1408 (m), 1319 (s), 1310 (s), 1250 (w), 1155 (s), 1148 (s), 1091 (s), 1045 (m), 959 (m), 930 (m), 758 (s), 513 (s) cm^{-1} . **HRMS (ESI)** for $\text{C}_{18}\text{H}_{15}\text{N}_2\text{O}_4\text{S}_2$ calcd: 267.0473, found: 267.0471.



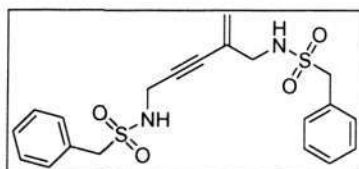
Compound 7: pale yellow oil; yield: 79%; hexane/ethyl acetate: 4/3; ^1H NMR (400 MHz, CDCl_3): δ 7.82-7.77 (m, 4H, $\text{H}_{\text{aromatic}}$), 6.97-6.95 (m, 4H, $\text{H}_{\text{aromatic}}$), 5.28 (s, 1H, alkene), 5.15 (s, 1H, alkene), 5.03 (t, $J = 5.4$ Hz, 2H, 2NH), 3.87-3.85 (m, 8H, $\text{CH}_2 + 2\text{CH}_3\text{O}$), 3.47 (d, $J = 6.4$ Hz, 2H, CH_2); ^{13}C NMR (125 MHz, CDCl_3): δ 163.2 (COCH_3), 163.0 (COCH_3), 131.6, 131.1, 129.6 ($\text{CH}_{\text{aromatic}}$), 129.4 ($\text{CH}_{\text{aromatic}}$), 126.3 (C_{alkene}), 123.4 (CH_2 alkene), 114.3 ($\text{CH}_{\text{aromatic}}$), 114.2 ($\text{CH}_{\text{aromatic}}$), 85.8 (alkyne), 82.2 (alkyne), 55.71 (OCH_3), 55.70 (OCH_3), 47.6 (CH_2), 33.4 (CH_2). IR (KBr): 3271 (s), 2963 (m), 2876 (s), 1597 (m), 1578 (w), 1499 (m), 1441 (w), 1325 (s), 1262 (s), 1155

(s), 1094 (m), 833 (m), 673 (w), 561 (m) cm^{-1} . **HRMS (ESI)** for $\text{C}_{20}\text{H}_{23}\text{N}_2\text{O}_6\text{S}_2$ calcd: 451.0998, found: 451.0974.



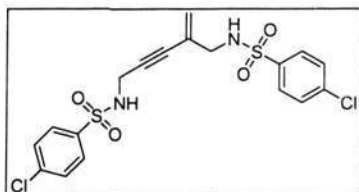
Compound 8: pale yellow oil; yield: 80%; hexane/ethyl acetate: 5:2 to 2:1; ^1H NMR (400 MHz, CDCl_3): δ 7.77-7.71 (m, 4H, $\text{H}_{\text{aromatic}}$), 7.66-7.63 (m, 4H, $\text{H}_{\text{aromatic}}$), 5.32 (s, 1H, alkene), 5.17 (s, 1H, alkene), 5.04 (t, $J = 6.0$ Hz, 2H, 2NH),

3.91 (d, $J = 6.0$ Hz, 2H, CH_2), 3.53 (d, $J = 6.4$ Hz, 2H, CH_2); ^{13}C NMR (100 MHz, CDCl_3): δ 139.2, 138.7, 132.4 (2C overlap, $\text{CH}_{\text{aromatic}}$), 129.1 ($\text{CH}_{\text{aromatic}}$), 128.7 ($\text{CH}_{\text{aromatic}}$), 128.1, 127.9, 125.9 (C_{alkene}), 124.0 ($\text{CH}_2_{\text{alkene}}$), 85.7 (alkyne), 82.4 (alkyne), 47.7 (CH_2), 33.5 (CH_2). IR (KBr): 3300 (s), 3288 (s), 3086 (w), 1616 (w), 1576 (m), 1433 (m), 1391 (m), 1331 (s), 1279 (w), 1163 (s), 1121 (m), 1092 (s), 1069 (s), 1011 (m), 822 (m), 739 (m), 627 (w), 548 (m) cm^{-1} . **HRMS (ESI)** for $\text{C}_{18}\text{H}_{17}\text{N}_2\text{O}_4\text{S}_2\text{Br}_2$ calcd: 546.8996, found: 546.8994.



Compound 9: pale yellow oil; yield: 64%; hexane/ethyl acetate: 5:2 to 5:3; ^1H NMR (400 MHz, CDCl_3): δ 7.44-7.37 (m, 10H, $\text{H}_{\text{aromatic}}$), 5.47 (s, 2H, alkene), 4.57 (br, 2H, 2NH), 4.32 (s, 2H,

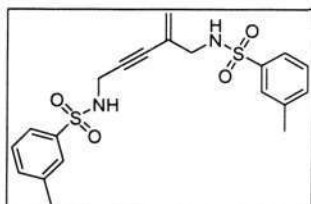
CH_2), 4.26 (s, 2H, CH_2), 3.90 (d, $J = 5.8$ Hz, 2H, CH_2), 3.60 (d, $J = 6.3$ Hz, 2H, CH_2); ^{13}C NMR (125 MHz, CDCl_3): δ 130.9, 130.8, 129.1 (one missing), 128.92, 128.88, 127.1 (C_{alkene}), 123.7 ($\text{CH}_2_{\text{alkene}}$), 86.9 (alkyne), 82.7 (alkyne), 59.8 (CH_2), 59.6 (CH_2), 48.2 (CH_2), 33.7 (CH_2). IR (KBr): 3277 (m), 3034 (w), 2930 (w), 1497 (w), 1456 (m), 1418 (w), 1319 (s), 1265 (w), 1153 (s), 1126 (s), 1074 (m), 889 (w), 839 (w), 781 (m), 698 (s), 605 (w), 542 (s) cm^{-1} . **HRMS (ESI)** for $\text{C}_{20}\text{H}_{22}\text{N}_2\text{O}_4\text{S}_2\text{Na}$ calcd: 441.0919, found: 441.0914.



Compound 10: pale yellow oil; yield: 81%; hexane/ethyl acetate: 5:2 to 2:1; ^1H NMR (400 MHz, CDCl_3): δ 7.84-7.79 (m, 4H, $\text{H}_{\text{aromatic}}$), 7.49-7.46 (m, 4H, $\text{H}_{\text{aromatic}}$), 5.31 (s, 1H, alkene),

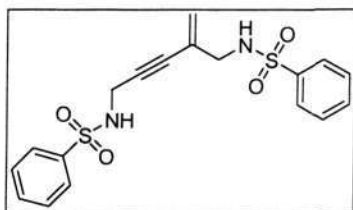
5.16 (s, 1H, alkene), 5.15 (br, 2H, 2NH), 3.90 (d, $J = 5.8$ Hz, 2H, CH_2), 3.52 (d, $J = 6.1$ Hz, 2H,

CH_2); ^{13}C NMR (125 MHz, CDCl_3): δ 139.6, 139.4, 138.6, 138.1, 129.4 (2C overlap, 2CH_{aromatic}), 129.0 (CH_{aromatic}), 128.7 (CH_{aromatic}), 125.9 (C_{alkene}), 123.9 (CH₂_{alkene}), 85.7 (alkyne), 82.4 (alkyne), 47.7 (CH₂), 33.5 (CH₂). IR (KBr): 3285 (s), 3094 (w), 1587 (w), 1478 (m), 1431 (m), 1397 (m), 1323 (s), 1277 (w), 1163 (s), 1096 (s), 1057 (m), 943 (w), 872 (m), 828 (m), 758 (s), 644 (m), 554 (m) cm^{-1} . HRMS (ESI) for $\text{C}_{18}\text{H}_{17}\text{N}_2\text{O}_4\text{S}_2\text{Cl}_2$ calcd: 459.0007, found: 458.9992.



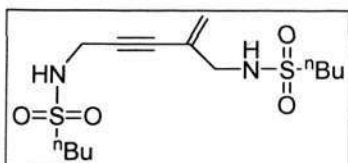
Compound 11: pale yellow oil; yield: 83%; hexane/ethyl acetate: 5:2 to 2:1; ^1H NMR (400 MHz, CDCl_3): δ 7.70-7.65 (m, 4H, H_{aromatic}), 7.39-7.37 (m, 4H, H_{aromatic}), 5.31 (s, 1H, alkene), 5.17 (s, 1H, alkene), 4.90 (t, J = 5.6 Hz, 2H, 2NH), 3.88 (d, J = 6.0 Hz, 2H, CH₂),

3.48 (d, J = 6.3 Hz, 2H, CH₂), 2.42 (s, 3H, CH₃), 2.41 (s, 3H, CH₃); ^{13}C NMR (100 MHz, CDCl_3): δ 139.9, 139.43, 139.42, 139.38, 133.8, 133.6, 129.01, 128.99, 127.8, 127.5, 126.2 (C_{alkene}), 124.6, 124.2, 123.4 (CH₂_{alkene}), 85.6 (alkyne), 82.3 (alkyne), 47.6 (CH₂), 33.5 (CH₂), 21.38 (CH₃), 21.36 (CH₃). IR (KBr): 3289 (s), 3275 (w), 2924 (m), 2857 (w), 1479 (m), 1418 (m), 1364 (m), 1331 (s), 1223 (w), 1173 (s), 1155 (s), 1090 (m), 870 (w), 787 (w), 700 (m), 590 (m), 552 (w) cm^{-1} . HRMS (ESI) for $\text{C}_{20}\text{H}_{23}\text{N}_2\text{O}_4\text{S}_2$ calcd: 419.1099, found: 419.1098.



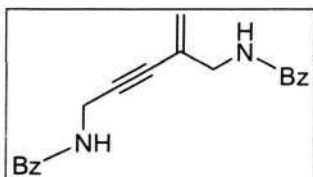
Compound 12: pale yellow oil; yield: 79%; hexane/ethyl acetate: 12/7; ^1H NMR (300 MHz, CDCl_3): δ 7.90 -7.84 (m, 4H, H_{aromatic}), 7.61-7.46 (m, 6H, H_{aromatic}), 5.27 (d, J = 0.9 Hz, 1H, alkene), 5.13-5.10 (m, 3H, 1H_{alkene} + 2NH), 3.88 (d, J = 6.0 Hz,

2H, CH₂), 3.47 (d, J = 6.4 Hz, 2H, CH₂); ^{13}C NMR (75 MHz, CDCl_3): δ 140.1, 139.7, 133.0, 132.9, 129.1 (2C overlap, 2CH_{aromatic}), 127.4 (CH_{aromatic}), 127.2 (CH_{aromatic}), 126.0 (C_{alkene}), 123.6 (CH₂_{alkene}), 85.6 (alkyne), 82.2 (alkyne), 47.6 (CH₂), 33.5 (CH₂). IR (KBr): 3271 (s), 3059 (w), 2857 (w), 1618 (w), 1481 (w), 1449 (s), 1358 (m), 1323 (s), 1292 (m), 1159 (s), 1094 (s), 1072 (m), 901 (m), 883 (m), 841 (m), 752 (m), 685 (s), 584 (s), 548 (m) cm^{-1} . HRMS (ESI) for $\text{C}_{18}\text{H}_{19}\text{N}_2\text{O}_4\text{S}_2$ calcd: 391.0786, found: 391.0771.



Compound 13: yellow oil; yield: 72%; hexane/ethyl acetate: 5/2;

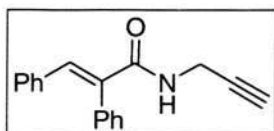
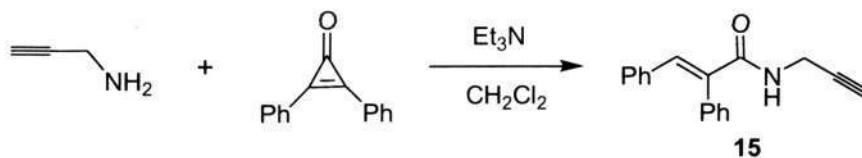
^1H NMR (400 MHz, CDCl_3): δ 5.53 (s, 1H, alkene), 5.48 (s, 1H, alkene), 5.03 (t, J = 6.0 Hz, 2H, 2NH), 4.06 (d, J = 5.9 Hz, 2H, alkene), 3.78 (d, J = 6.4 Hz, 2H, CH_2), 3.12 (t, J = 8.0 Hz, 2H, $\text{CH}_2\text{CH}_2\text{CH}_2\text{CH}_3$), 3.03 (t, J = 8.0 Hz, 2H, $\text{CH}_2\text{CH}_2\text{CH}_2\text{CH}_3$), 1.84-1.77 (m, 4H, $2\text{CH}_2\text{CH}_2\text{CH}_2\text{CH}_3$), 1.49-1.42 (m, 4H, $2\text{CH}_2\text{CH}_2\text{CH}_2\text{CH}_3$), 0.95 (t, J = 7.2 Hz, 6H, 2CH_3); ^{13}C NMR (100 MHz, CDCl_3): δ 127.4 (C alkene), 123.5 (CH_2 alkene), 87.0 (alkyne), 82.4 (alkyne), 53.6 ($\text{CH}_2\text{CH}_2\text{CH}_2\text{CH}_3$), 53.2 ($\text{CH}_2\text{CH}_2\text{CH}_2\text{CH}_3$), 47.9 (CH_2), 33.3 (CH_2), 25.60 ($\text{CH}_2\text{CH}_2\text{CH}_2\text{CH}_3$), 25.55 ($\text{CH}_2\text{CH}_2\text{CH}_2\text{CH}_3$), 21.58 ($\text{CH}_2\text{CH}_2\text{CH}_2\text{CH}_3$), 21.54 ($\text{CH}_2\text{CH}_2\text{CH}_2\text{CH}_3$), 13.6 (2CH_3). IR (KBr): 3279 (s), 2963 (s), 2938 (m), 2876 (m), 1620 (w), 1431 (m), 1321 (s), 1279 (m), 1144 (s), 1080 (m), 920 (w), 851 (m), 731 (w), 567 (m) cm^{-1} . HRMS (ESI) for $\text{C}_{14}\text{H}_{27}\text{N}_2\text{O}_4\text{S}_2$ calcd: 351.1412, found: 351.1403.



Compound 14: pale yellow oil; yield: 46%; hexane/ethyl acetate:

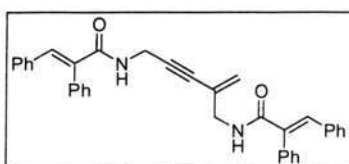
1/1; ^1H NMR (400 MHz, CDCl_3): δ 7.80-7.76 (m, 4H, $\text{H}_{\text{aromatic}}$), 7.49-7.31 (m, 6H, $\text{H}_{\text{aromatic}}$), 7.00 (br, 1H, NH), 6.88 (br, 1H, NH), 5.40 (s, 2H, CH_2 alkene), 4.30 (d, J = 5.0 Hz, 2H, CH_2NH), 4.09 (d, J = 5.9 Hz, 2H, CH_2NH); ^{13}C NMR (100 MHz, CDCl_3): δ 167.8 (CO), 167.3 (CO), 134.2, 133.7, 131.7, 131.6, 128.6 ($\text{CH}_{\text{aromatic}}$), 128.5 ($\text{CH}_{\text{aromatic}}$), 127.7 (C alkene), 127.2 ($\text{CH}_{\text{aromatic}}$), 127.0 ($\text{CH}_{\text{aromatic}}$), 122.1 (CH_2 alkene), 86.6 (alkyne), 82.0 (alkyne), 44.7 (CH_2), 30.5 (CH_2). IR (KBr): 3302 (s), 3063 (m), 2926 (w), 1724 (w), 1645 (s), 1578 (m), 1537 (s), 1489 (m), 1447 (w), 1354 (w), 1294 (m), 1076 (w), 802 (w), 710 (m), 692 (m) cm^{-1} . HRMS (ESI) for $\text{C}_{20}\text{H}_{19}\text{N}_2\text{O}_2$ calcd: 319.1447, found: 319.1428.

Synthesis of 15: Diphenylcyclopropanone (2 mmol) was weighted into a flask. 1,4-dioxane (3 mL) and propargyl amine (1.5 equiv) were then added *via* a syringe sequentially. The mixture was stirred at 80 $^{\circ}\text{C}$ for 6 h. Removal of solvent gave a residue which was purified by silica gel column chromatography to give a pale yellow solid.



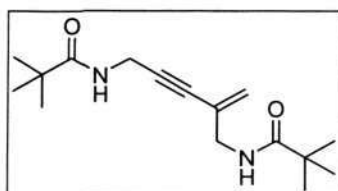
Compound 15: yellow solid; mp: 105-106 °C; yield: 85%; hexane/ethyl acetate: 5:1 to 5:2; ^1H NMR (400 MHz, CDCl_3): δ 7.89 (s, 1H, CH_{alkene}), 7.48-7.45 (m, 3H, H_{aromatic}), 7.28-7.26 (m, 2H, H_{aromatic}), 7.19-7.12 (m, 3H, H_{aromatic}), 7.00-6.98 (m, 2H, H_{aromatic}), 5.64 (br, 1H, NH), 4.12-4.10 (m, 2H, CH₂), 2.18 (s, 1H, CH_{alkyne}); ^{13}C NMR (100 MHz, CDCl_3): δ 166.7 (CO), 138.0, 135.8, 134.8, 133.6, 130.5 (CH_{aromatic}), 129.9 (CH_{aromatic}), 129.7 (CH_{aromatic}), 128.75, 128.73, 128.2 (CH_{aromatic}), 79.5 (alkyne), 71.5 (alkyne), 29.8 (CH₂). IR (KBr): 3292 (s), 3022 (m), 2911 (w), 1751 (w), 1655 (s), 1616 (s), 1516 (s), 1445 (m), 1335 (m), 1283 (s), 1070 (w), 930 (w), 773 (w), 714 (m), 669 (s) cm^{-1} . **HRMS (ESI)** for $\text{C}_{18}\text{H}_{16}\text{N}_2\text{O}$ calcd: 262.1232, found: 262.1223.

The following procedure was followed to prepare compounds **16** and **17**. A corresponding alkyne (0.5 mmol) and a catalyst $\text{Rh}(\text{PPh}_3)_3\text{Cl}$ (2%) were weighted into a flask, which was kept under argon atmosphere. Subsequently, anhydrous toluene (1.0 mL) was injected *via* a syringe, and the mixture was stirred at 80 °C for 24 h. After the reaction, removal of all volatiles gave a residue that was purified by silica gel column chromatography.



Compound 16: yellow oil; yield: 64%; hexane/ethyl acetate: 5:2 to 2:1; ^1H NMR (300 MHz, CDCl_3): δ 7.87 (s, 1H, CH_{alkene}), 7.86 (s, 1H, CH_{alkene}), 7.45-7.42 (m, 6H, H_{aromatic}), 7.27-7.24 (m, 4H, H_{aromatic}), 7.15-7.12 (m, 6H, H_{aromatic}), 6.99-6.96 (m, 4H, H_{aromatic}), 5.71 (t, J = 5.7 Hz, 1H, NH), 5.60 (t, J = 4.9 Hz, 1H, NH), 5.36 (s, 1H, CH₂_{alkene}), 5.31 (d, J = 1.1 Hz, 1H, CH₂_{alkene}), 4.16 (d, J = 5.4 Hz, 2H, CH₂NH), 3.93 (d, J = 5.9 Hz, 2H, CH₂NH); ^{13}C NMR (100 MHz, CDCl_3): δ 166.9 (CO), 166.7 (CO), 138.0 (CH_{alkene}), 137.6 (CH_{alkene}), 136.1, 135.7, 134.82, 134.76, 134.0, 133.7, 130.5 (CH_{aromatic}), 129.92 (CH_{aromatic}), 129.90 (CH_{aromatic}), 129.75 (CH_{aromatic}), 129.69 (CH_{aromatic}), 128.77 (CH_{aromatic}), 128.75 (CH_{aromatic}), 128.70 (CH_{aromatic}), 128.66 (CH_{aromatic}), 128.2

(CH_{aromatic}), 127.2, 122.1(CH_{2 alkene}), 86.3 (alkyne), 81.1 (alkyne), 44.3 (CH₂), 30.3 (CH₂). IR (KBr): 3422 (w), 3312 (m), 3055 (w), 2926 (w), 1722 (w), 1661 (s), 1614 (m), 1574 (w), 1510 (s), 1447 (m), 1352 (w), 1262 (m), 1072 (w), 770 (w), 710 (m), 692 (s) cm⁻¹. **HRMS (ESI)** for C₃₆H₃₁N₂O₂ calcd: 523.2386, found: 523.2382.

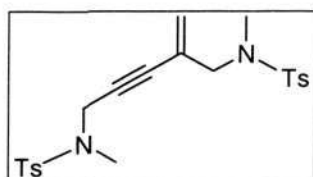


Compound 17: white solid; mp, 119-120 °C; yield: 59%;

hexane/ethyl acetate: 5:2 to 4:3; ¹H NMR (400 MHz, CDCl₃): δ

5.87 (br, 2H, 2NH), 5.42 (s, 1H, alkene), 5.38 (s, 1H, alkene), 4.13

(d, *J* = 4.9 Hz, 2H, CH₂), 3.92 (d, *J* = 5.9 Hz, 2H, CH₂), 1.22 (s, 9H, t-Butyl), 1.21 (s, 9H, t-Butyl); ¹³C NMR (100 MHz, CDCl₃): δ 178.4 (CO), 178.1 (CO), 128.0, 121.8 (CH_{2 alkene}), 86.5 (alkyne), 81.8 (alkyne), 44.0 (CH₂), 38.8 (C(CH₃)₃), 38.7 (C(CH₃)₃), 30.1 (CH₂), 27.6 (C(CH₃)₃), 27.5 (C(CH₃)₃). IR (KBr): 3339 (s), 3065 (w), 2967 (s), 2916 (m), 2872 (w), 1645 (s), 1533 (s), 1481 (m), 1418 (m), 1366 (m), 1298 (m), 1258 (m), 1213 (s), 1016 (w), 895 (w), 677 (m), 538 (w) cm⁻¹. **HRMS (ESI)** for C₁₆H₂₇N₂O₂ calcd: 279.2073, found: 279.2065.



Compound 18: yield: 81%; hexane/ethyl acetate: 5/3; ¹H NMR (500

MHz, CDCl₃): δ 7.70 (d, *J* = 8.3 Hz, 2H, H_{aromatic}), 7.63 (d, *J* = 8.3

Hz, 2H, H_{aromatic}), 7.33-7.28 (m, 4H, H_{aromatic}), 5.37 (d, *J* = 1.3 Hz,

1H, alkene), 5.25 (s, 1H, alkene), 4.10 (s, 2H, CH₂), 3.48 (s, 2H, CH₂), 2.82 (s, 3H, NCH₃), 2.58 (s, 3H, NCH₃), 2.42 (s, 3H, CH₃), 2.38 (s, 3H, CH₃); ¹³C NMR (125 MHz, CDCl₃): δ 143.6 (2C overlap), 134.6, 134.1, 129.8 (CH_{aromatic}), 129.5 (CH_{aromatic}), 128.0 (CH_{aromatic}), 127.3 (CH_{aromatic}), 125.7 (C_{alkene}), 123.9 (CH_{2 alkene}), 83.8 (alkyne), 83.4 (alkyne), 54.5 (CH₂), 40.5 (CH₂), 34.6 (NCH₃), 34.4 (NCH₃), 21.51 (CH₃), 21.48 (CH₃). IR (KBr): 2924 (w), 2864 (w), 1736 (w), 1597 (m), 1454 (m), 1341 (s), 1306 (m), 1163 (s), 1090 (m), 918 (m), 816 (m), 656 (m), 550 (s) cm⁻¹. **HRMS (ESI)** for C₂₂H₂₇N₂O₄S₂ calcd: 447.1412, found: 447.1410.

5.5. References

1. (a) Trost, B. M. *Science* **1991**, 254, 1471. (b) Trost, B. M. *Angew. Chem., Int. Ed.* **1995**, 34, 259. (c) Trost, B. M. *Acc. Chem. Res.* **2002**, 35, 695.
2. Bruneau, C.; Dixneuf, P. H. *Acc. Chem. Res.* **1999**, 32, 311.
3. (a) Pahadi, N. K.; Camacho, D. H.; Nakamura, I.; Yamamoto, Y. *J. Org. Chem.* **2006**, 71, 1152. (b) Liu, Y.; Nishiura, M.; Wang, Y.; Hou, Z. *J. Am. Chem. Soc.* **2006**, 128, 5592.
4. (a) Slugovc, C.; Mereiter, K.; Zobetz, E.; Schmid, R.; Kirchner, K. *Organometallics* **1996**, 15, 5275. (b) Yi, C. S.; Liu, N. *Organometallics* **1996**, 15, 3968.
5. Bianchini, C.; Peruzzini, M.; Zanobini, F.; Frediani, P.; Albinati, A. *J. Am. Chem. Soc.* **1991**, 113, 5453.
6. (a) Wakatsuki, Y. *J. Organomet. Chem.* **2004**, 689, 4092. (b) Puerta, M. C.; Valerga, P. *Coord. Chem. Rev.* **1999**, 193, 977. (c) Cowley, M. J.; Lynam, J. M.; Slattery, J. M. *Dalton Trans.* **2008**, 4552.
7. (a) Grotjahn, D. B.; Zeng, X.; Cooksy, A. L.; Kassel, W. S.; DiPasquale, A. G.; Zakharov, L. N.; Rheingold, A. L. *Organometallics* **2007**, 26, 3385. (b) Angelis, F. D.; Sgamellotti, A.; Re, N. *Dalton Trans.* **2004**, 3225.
8. (a) Korolev, A. V.; Guzei, I. A.; Jordan, R. F. *J. Am. Chem. Soc.* **1999**, 121, 11605. (b) Dash, A. K.; Eisen, M. S. *Org. Lett.* **2000**, 2, 737.
9. (a) Ge, S.; Norambuena, V. F. Q.; Hessen, B. *Organometallics* **2007**, 26, 6508. (b) Komeyama, K.; Kawabata, T.; Takehira, K.; Takaki, K. *J. Org. Chem.* **2005**, 70, 7260. (c) Tazelaar, C. G. J.; Bambirra, S.; van Leusen, D.; Meetsma, A.; Hessen, B.; Teuben, J. H. *Organometallics* **2004**, 23, 936. (d) Nishiura, M.; Hou, Z.; Wakatsuki, Y.; Yamaki, T.; Miyamoto, T. *J. Am. Chem. Soc.* **2003**, 125, 1184. (e) Heeres, H. J.; Teuben, J. H. *Organometallics* **1991**, 10, 1980. (f) Koneyama, K.; Takehira, K.; Takaki, K. *Synthesis* **2004**, 1062. (g) Nishiura, M.; Hou, Z. *J. Mol. Catal. A: Chem.* **2004**, 213, 101. (h) Janiak, C. *Coord. Chem. Rev.* **2006**, 250, 66.
10. (a) Haskel, A.; Straub, T.; Dash, A. K.; Eisen, M. S. *J. Am. Chem. Soc.* **1999**, 121, 3014. (b) Wang, J.; Kapon, M.; Berthet, J. C.; Ephritikhine, M.; Eisen, M. S. *Inorg. Chim. Acta* **2002**, 334, 183. (c) Wang, J. Q.; Dash, A. K.; Berthet, J. C.; Ephritikhine, M.; Eisen, M. S. *Organometallics* **1999**, 18, 2407. (d) Straub, T.; Haskel, A.; Eisen, M. S. *J. Am. Chem. Soc.* **1995**, 117, 6364. (e) Barnea, E.; Eisen, M. S. *Coord. Chem. Rev.* **2006**, 250, 855.

11. (a) Yoshida, M.; Jordan, R. F. *Organometallics* **1997**, *16*, 4508. (b) Horton, A. D. *J. Chem. Soc., Chem. Commun.* **1992**, 185. (c) Akita, M.; Yasuda, H.; Nakamura, A. *Bull. Chem. Soc. Jpn.* **1984**, *57*, 480. (d) Hagihara, N.; Tamura, M.; Yamazaki, H.; Fujiwara, M. *Bull. Chem. Soc. Jpn.* **1961**, *34*, 892.

12. Ruthenium catalyst: (a) Katayama, H.; Yari, H.; Tanaka, M.; Ozawa, F. *Chem. Commun.* **2005**, 4336. (b) Chen, X.; Xue, P.; Sung, H. H. Y.; Williams, I. D.; Peruzzini, M.; Bianchini, C.; Jia, G. *Organometallics* **2005**, *24*, 4330. (c) Bassetti, M.; Pasquini, C.; Raneri, A.; Rosato, D. *J. Org. Chem.* **2007**, *72*, 4558. (d) Hijazi, A.; Parkhomenko, K.; Djukic, J.-P.; Chemmi, A.; Pfeffer, M. *Adv. Synth. Catal.* **2008**, *350*, 1493. (e) Daniels, M.; Kirss, R. U. *J. Organomet. Chem.* **2007**, *692*, 1716. (f) Lee, J.-H.; Caulton, K. G. *J. Organomet. Chem.* **2008**, *693*, 1664. (g) Gao, Y.; Puddephatt, R. J. *Inorg. Chim. Acta*, **2003**, *350*, 101. (h) Lynam, J. M.; Nixon, T. D.; Whitwood, A. C. *J. Organomet. Chem.* **2008**, *693*, 3103.

13. (a) Singer, H.; Wilkinson, G. *J. Chem. Soc. (A)* **1968**, 849. (b) Carton, L.; Read, G. *J. Chem. Soc., Perkin Trans. I* **1978**, 1631. (c) Ohshita, J.; Furumori, K.; Matsuguchi, A.; Ishikawa, M. *J. Org. Chem.* **1990**, *55*, 3277.

14. Boese, W. T.; Goldman, A. S. *Organometallics* **1991**, *10*, 782.

15. Rhodium catalyst: (a) Weng, W.; Guo, C.; Çelenligil-Çetin, R.; Foxman, B. M.; Ozerov, O. V. *Chem. Commun.* **2006**, 197. (b) Katagiri, T.; Tsurugi, H.; Satoh, T.; Miura, M. *Chem. Commun.* **2008**, 3405. (c) Katagiri, T.; Tsurugi, H.; Funayama, A.; Satoh, T.; Miura, M. *Chem. Lett.* **2007**, *36*, 830. (d) Nishimura, T.; Guo, X.-X.; Ohnishi, K.; Hayashi, T. *Adv. Synth. Catal.* **2007**, *349*, 2669. (e) Lee, C.-C.; Lin, Y.-C.; Liu, Y.-H.; Wang, Y. *Organometallics* **2005**, *24*, 136.

16. Palladium catalyst: (a) Trost, B. M.; Chan, C.; Ruhter, G. *J. Am. Chem. Soc.* **1987**, *109*, 3486. (b) Trost, B. M.; Sorum, M. T.; Chan, C.; Harms, A. E.; Ruhter, G. *J. Am. Chem. Soc.* **1997**, *119*, 698. (c) Rubina, M.; Gevorgyan, V. *J. Am. Chem. Soc.* **2001**, *123*, 11107. (d) Yang, C.; Nolan, S. P. *J. Org. Chem.* **2002**, *67*, 591. (e) Tsukada, N.; Ninomiya, S.; Aoyama, Y.; Inoue, Y. *Org. Lett.* **2007**, *9*, 2919.

17. (a) Ogata, K.; Toyota, A. *J. Organomet. Chem.* **2007**, *692*, 4139. (b) Ogata, K.; Oka, O.; Toyota, A.; Suzuki, N.; Fukuzawa, S.-i. *Synlett* **2008**, *17*, 2663. (c) Ciclosi, M.; Estevan, F.; Lahuerta, P.; Passarelli, V.; Pérez-Prieto, J.; Sanaú, M. *Adv. Synth. Catal.* **2008**, *350*, 234. (d) Hirabayashi, T.; Sakaguchi, S.; Ishii, Y. *Adv. Synth. Catal.* **2005**, *347*, 872. (e) Ohmura, T.; Yorozuya, S.-i.; Yamamoto, Y.; Miyaura, N. *Organometallics* **2000**, *19*, 365.

18. (a) Ogoshi, S.; Ueta, M.; Oka, M.-i.; Kurosawa, H. *Chem. Commun.* **2004**, 2732. (b)

- Matsuyama, N.; Tsurugi, H.; Satoh, T.; Miura, M. *Adv. Synth. Catal.* **2008**, 350, 2274.
19. (a) Ritleng, V.; Sirlin, C.; Pfeffer, M. *Chem. Rev.* **2002**, 102, 1731, and references therein.
(b) Katayama, H.; Ozawa, F. *Coord. Chem. Rev.* **2004**, 248, 1703.
20. Larock, R. C.; Riefling, B. C. *J. Org. Chem.* **1978**, 43, 1468.
21. dppb = 1,3-bis(diphenylphosphine)butane; dppf = 1,1'-bis(diphenylphosphino)ferrocene;
dppp = 1,3-bis(diphenylphosphine)propane; dppm = bis(diphenylphosphine)methane;
xantphos = 4,5-Bis(diphenylphosphino)-9,9-dimethylxanthene; dppe = bis(diphenylphosphine)ethane.
22. (a) Williams, I.; Kariuki, B. M.; Reeves, K.; Cox, L. R. *Org. Lett.* **2006**, 8, 4389. (b) Wu, J.; Fang, F.; Lu, W.-Y.; Hou, J.-L.; Li, C.; Wu, Z.-Q.; Jiang, X.-K.; Li, Z.-T.; Yu, Y.-H. *J. Org. Chem.* **2007**, 72, 2897.
23. Wipf, P.; Aoyama, Y.; Benedum, T. E. *Org. Lett.* **2004**, 6, 3593.
24. Deng, J.; Tabei, J.; Shiotsuki, M.; Sanda, F.; Masuda, T. *Macromolecules* **2004**, 37, 5538.
25. Lo, M. M.-C.; Neumann, C. S.; Nagayama, S.; Perlstein, E. O.; Schreiber, S. L. *J. Am. Chem. Soc.* **2004**, 126, 16077.

CHAPTER 6

Gold-Catalyzed Intramolecular Hydroamination of Functionalized Enynes Affording Trisubstituted Pyrroles

6.1. Introduction

6.1.1. General Considerations

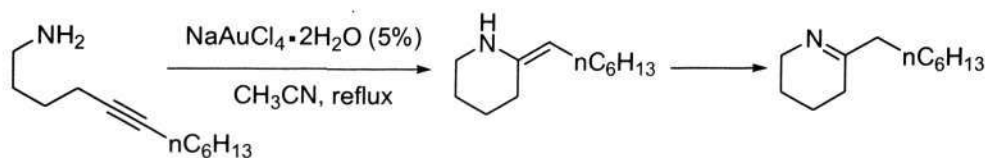
Gold is a well-known precious metal, which is widely used in various fields of our society. For example, it has been once used in monetary systems, and it has also been applied in medicinal industry.¹ However, the most important role of gold in synthetic chemistry is the catalytic applications in organic transformations. In recent years, tremendous progress has been achieved in gold-catalyzed organic reactions, and a number of review articles have been published which covered a broad scope of reactions on gold catalysis:² such as nucleophilic additions, C-H activations, reduction and oxidation. Importantly, some chiral catalysts showed notable activity and selectivity in enantio-selective catalysis.³

We are interested in gold-catalyzed nucleophilic additions, and the following paragraphs will briefly review this type of reaction. Particular attention will be given to recent developments of gold-catalyzed alkyne hydroamination. In view of the large volume of reported reviews, we will only cover representative literature.

6.1.2. Hydroamination of Alkynes

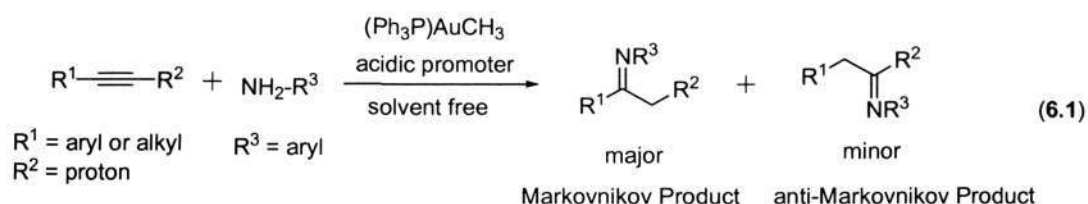
Hydroamination represents the addition reaction of N-H bond to non-activated alkenes, allenes or alkynes. A series of metal complexes have been developed as efficient catalysts for this transformation, including rare earth metals,^{4,5} Group 4 metals,^{5,6} and late transition metals such as Pd,^{5,7} Pt,⁸ Ir,⁹ and Au.^{2,10} Gold complexes used to be considered too inert to act as active catalysts, hence chemists had not paid much attention to gold-catalyzed hydroamination prior to 2001. In recent years, however, much attention has been focused on gold catalysis, largely due to their good functional-group tolerance and low air and moisture sensitivity.

Important pioneering work on gold-catalyzed hydroamination has been done by Utimoto and co-workers.¹¹ In 1987, they reported the first example of intramolecular hydroamination of 5-alkynylamines *via* 6-*exo*-cyclization using NaAuCl₄ hydrate as a catalyst, but the substrates are limited to alkyl-substituted internal alkynes (Scheme 6.1).^{11a}

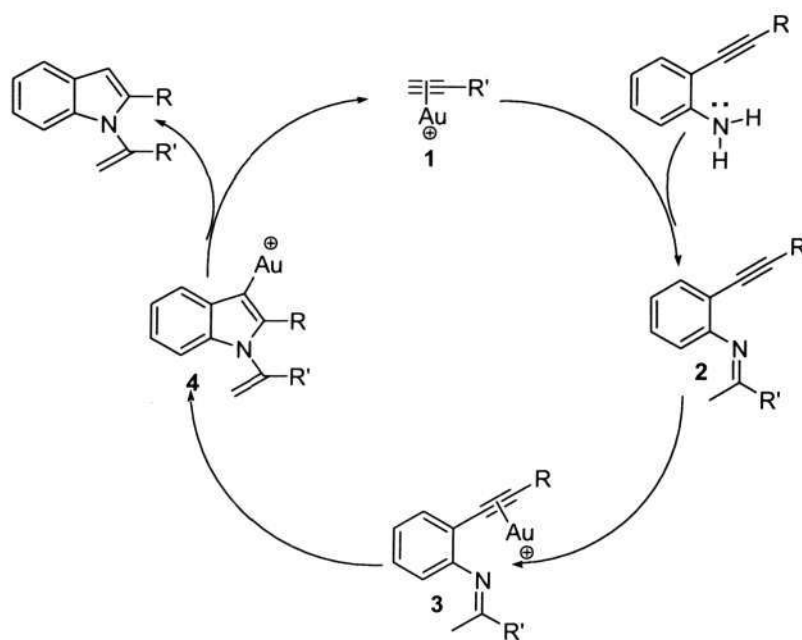
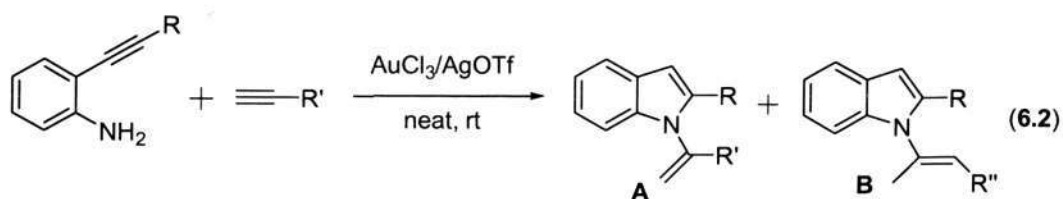


Scheme 6.1

In sharp contrast, intermolecular hydroamination was discovered rather late, and the first example was reported by Tanaka et al. in 2003.^{12a} They demonstrated the reaction between alkynes and anilines producing Markovnikov ketimines in the presence of (Ph₃P)AuCH₃ (0.01 mol %) and an acidic promoter (0.05 mol %, tungstophosphoric acid), but here aliphatic amines are not applicable (eq 6.1).

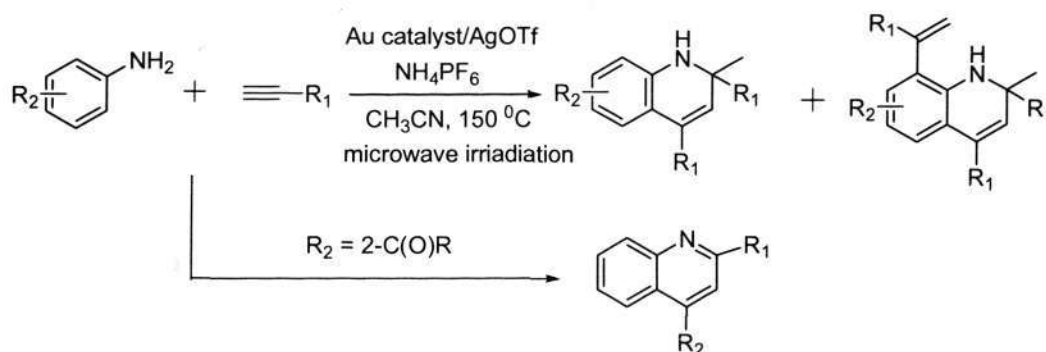


Later, Li et al. expanded the substrate scope of this type of reaction to aliphatic amines using AuCl₃ or AuCl₃/AgOTf.^{12b} Interestingly, they found that phenylacetylene could react with aniline to give poly-substituted 1,2-dihydroquinolines with AgBF₄/HBF₄, which cannot be realized by gold catalysts. In 2007, the same group synthesized a series of *N*-vinylindoles combining intermolecular and intramolecular hydroamination (eq 6.2).¹³ Both electron-rich and electron-poor arylacetylenes can efficiently give single product **A**, while aliphatic alkyl- and alkenylalkynes showed lower reactivity, and aliphatic alkylalkynes gave a mixture of **A** and **B**. Mechanistic studies indicated that intermolecular hydroamination proceeded first, followed by the subsequent intramolecular hydroamination (Scheme 6.2).



Scheme 6.2

Almost at the same time, Che et al. reported another example of tandem reaction combining intermolecular hydroamination and hydroarylation under microwave irradiation, which represented a feasible synthetic strategy for substituted 1,2-dihydroquinolines or quinolines (Scheme 6.3).¹⁴ The substituents attached to the aromatic ring of arylamines have great influences on the results. In some cases, the 1,2-dihydroquinoline species can undergo further hydroarylation with the third alkyne to give the mixture of products (for $\text{R}_2 = 4\text{-OMe}$, 4-OPh , 3-Me , $3,5\text{-2OMe}$). In addition, *o*-alkylcarbonyl or -arylcabonyl groups will produce 2,4-disubstituted quinolines in 63-94% yields through intermolecular hydroamination and condensation reactions.



Scheme 6.3

In comparison with the large number of examples of intermolecular addition of primary amines to alkynes, few examples are reported of the reaction between secondary amines and alkynes. More recently, Bertrand and co-workers designed cationic Au(I) carbene catalysts (Figure 6.1), which have been successfully applied to the hydroamination reaction between alkynes and ammonia or secondary amines.¹⁵ For instance, catalysts **1**, **2**, **3** in Figure 6.1 exhibited identical catalytic activity towards the addition of ammonia to a variety of unactivated alkynes and allenes affording linear or cyclic nitrogen-containing products (Scheme 6.4).^{15a} They also proved that substituted allenes could be synthesized from two alkynes using an amine (1,2,3,4-tetrahydroisoquinoline or dibenzylamine) as a hydrogen donor in the presence of catalyst **1** (Scheme 6.5).^{15b}

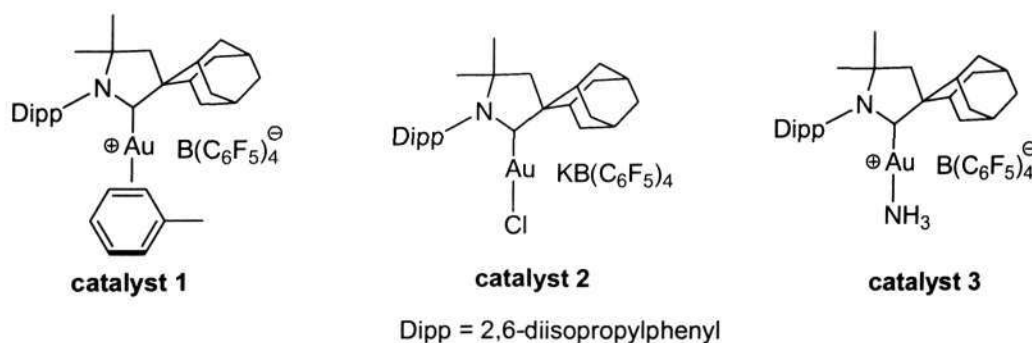
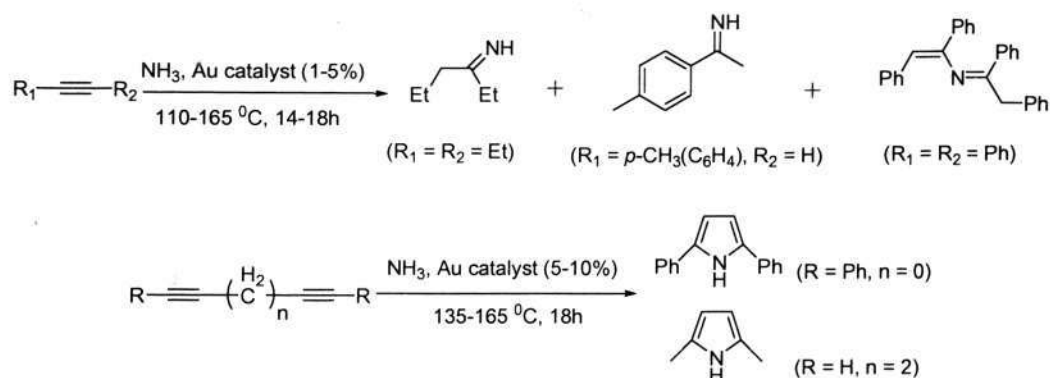
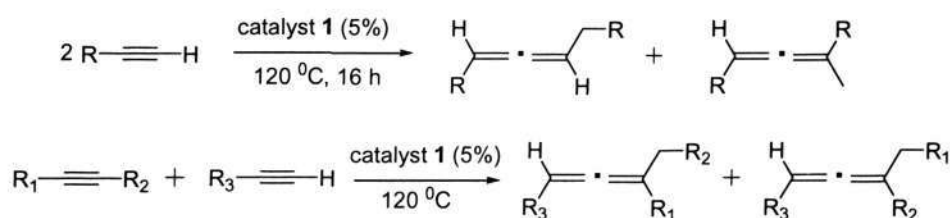


Figure 6.1



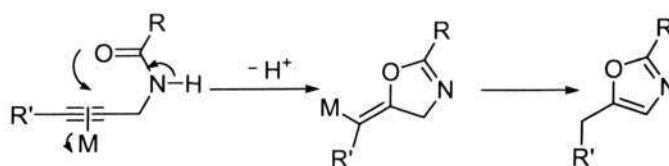
Scheme 6.4



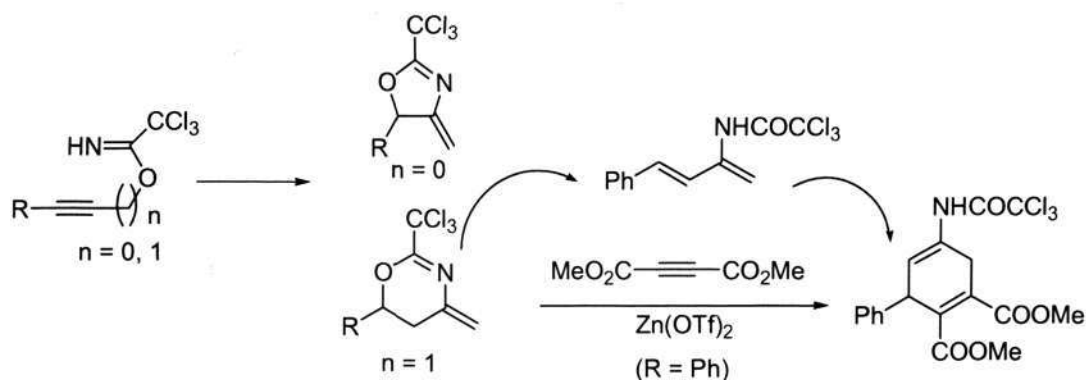
1,2,3,4-tetrahydroisoquinoline or dibenzylamine was added to both above reactions as hydrogen donors.

Scheme 6.5

In addition, in some cases it has been proven that the carbonyl group of the *N*-propargylcarboxamides could attack C≡C bond to afford the corresponding oxazoles *via* cycloisomerization, which indicated that oxygen attack took place (Scheme 6.6).¹⁶ For some imidate compounds, the nitrogen atom could also act as a nucleophile to attack triple bond affording oxazole products using Au(I) or Au(III) catalysts.¹⁷ For example, Shin et al. reported that trichloroacetimidates could undergo intramolecular hydroamination providing rare *exo*-methylene products, which did not isomerize to the thermodynamically more stable oxazole compounds.^{17a} Oxazoles are masked 2-acylamino-1,3-dienes which can undergo subsequent Diels-Alder cycloaddition reactions (Scheme 6.7).

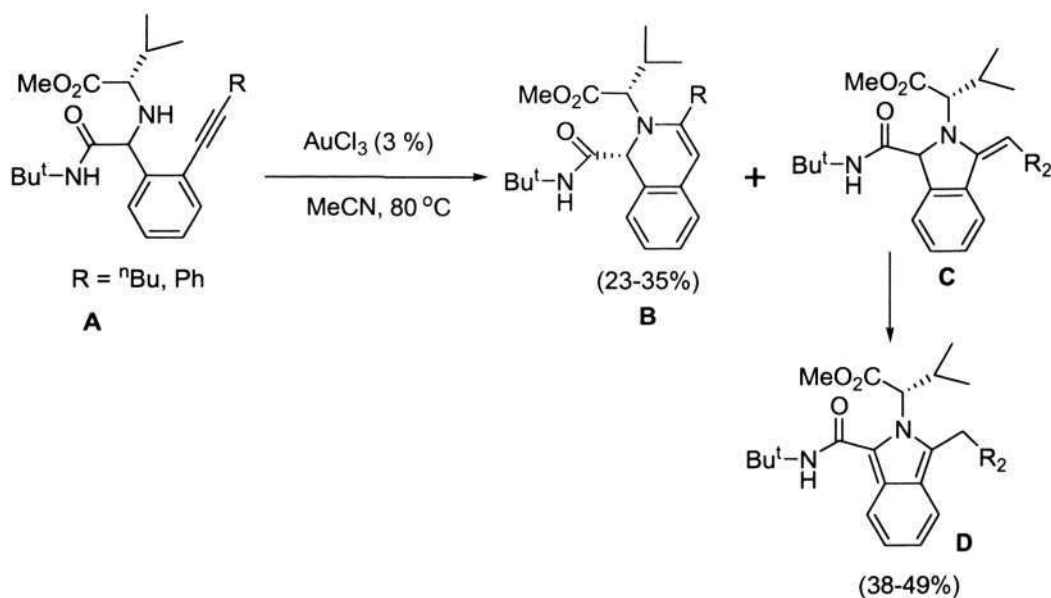


Scheme 6.6

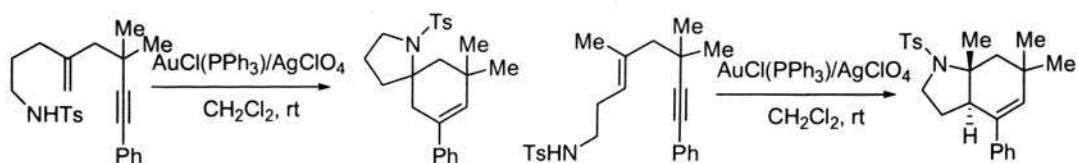


Scheme 6.7

Recently, this strategy has also been applied to the synthesis of some complex molecules. In 2006, Dyker et al. successfully synthesized dihydroisoquinolines **B** and isoindoles **D** from the same starting material using gold catalysts (Scheme 6.8).¹⁸ Obviously, compound **B** originates from a 6-*endo-dig* cyclization, whereas compound **C** isomerizes to the 5-*exo-dig* product **D**. Another example is gold-catalyzed synthesis of heterobicyclic alkenes *via* double cyclizations (Scheme 6.9), and diastereo-specificity of the product indicates that double cyclization is a highly concerted process.¹⁹

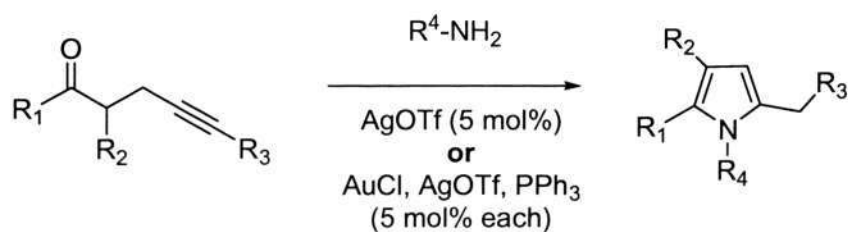


Scheme 6.8

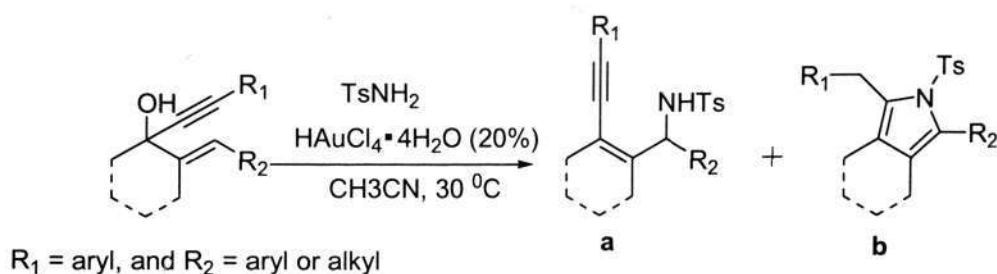


Scheme 6.9

As mentioned in the above substrates, NH_2 or NH acts as a nucleophile attacking the triple bond directly. In fact, combining a ketone or alcohol and a monoamine is also a good method for alkyne hydroamination. For example, the Dake group found that β -alkynyl ketones reacted with monoamines giving substituted pyrroles catalyzed by cationic Au(I) complexes or AgOTf (Scheme 6.10).²⁰ Experimental results showed that combination of $\text{AuCl}/\text{AgOTf}/\text{ligand}$ appeared to be more thermally stable compared to sole AgOTf , and the reaction can tolerate various functional groups, such as Boc , CO_2CH_3 , and SiMe_3 . Another example indicated that various substituents of propargyl alcohols and sulfonamides can undergo gold(III)-catalyzed tandem amination-intramolecular hydroamination in one pot affording highly substituted pyrroles.²¹ $\text{HAuCl}_4 \cdot 4\text{H}_2\text{O}$ was proved to be the most efficient catalyst, and CH_3CN was the most appropriate solvent. The reaction included two independent catalytic cycles: amination and hydroamination. The amination process afforded enynamines with high regio- and stereo-selectivity, which could undergo subsequent intramolecular hydroamination and isomerization giving pyrrole products **b** (Scheme 6.11). The distributions of these two products were affected by the catalysts and by the substituents on the substrates.



Scheme 6.10

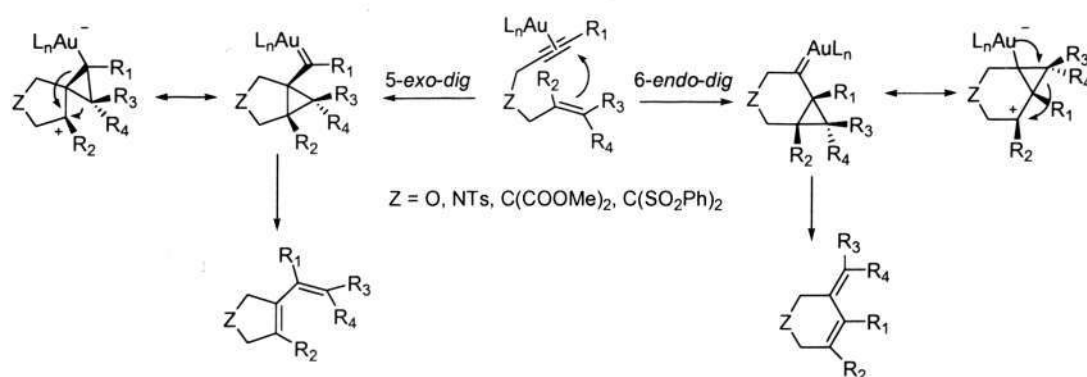


Scheme 6.11

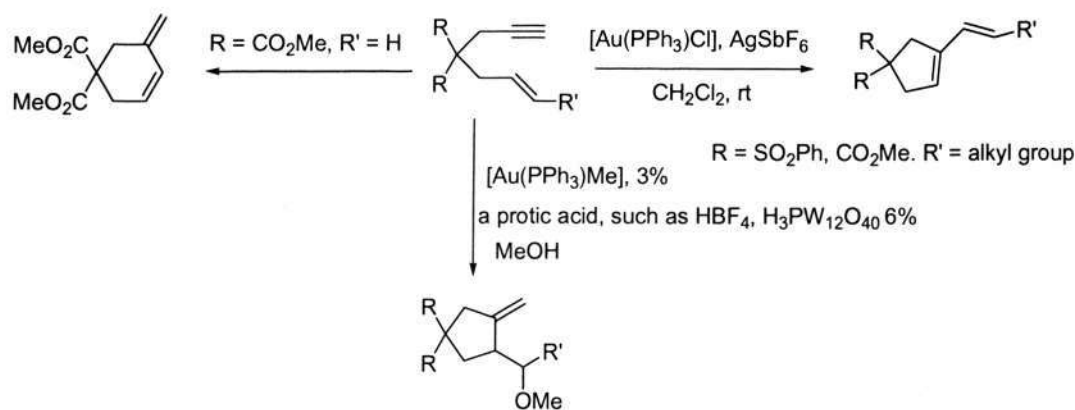
6.1.3. Other Nucleophilic Addition Reactions

Among various gold-catalyzed nucleophilic additions, in addition to nitrogen sources, many other substrates can also act as nucleophiles, such as olefins and alcohols. We take several typical examples to further illustrate nucleophilic additions using these substrates as nucleophiles.

Cyclization of enynes can build functionalized cyclic structures.²² Both gold(I) and gold(III) complexes can be used for this type reaction, although there are fewer examples for gold(III). Gold carbenes were considered as reactive intermediates in plausible mechanism studies. The first step is the coordination of the metal to the alkyne, which can react with alkene or allene affording 5-*exo-dig* or 6-*endo-dig* gold carbene intermediates. The final product was given by skeletal rearrangement (Scheme 6.12).²³ In 2004, Echavarren et al. reported the first example of a 6-*endo-dig* skeletal rearrangement using cationic gold(I) complex $[\text{Au}(\text{PPh}_3)]^+ \text{X}^-$ as a catalyst.^{23a} DFT calculations suggest that *exo*-cyclization should be favored for substrates such as (*E*)-6-octen-1-yne, because the activation energy is only 0.1 kcal mol⁻¹ for *exo*-cyclization and is 6.1 kcal mol⁻¹ for the 6-*endo-dig* process. As a matter of fact, most substrates will give 5-*exo-dig* products (Scheme 6.13). But, for R CO₂Me and R' H, a different pathway operates and produces an *endo*-cyclization product. Moreover, methoxycyclization of enynes was observed when the reactions were carried out in the presence of a gold catalyst and a protic acid using methanol as a solvent (scheme 6.13). Furthermore, recent examples showed that seven- or eight-membered rings can also be formed through cycloisomerization of 1,7- and 1,8-enynes.²⁴



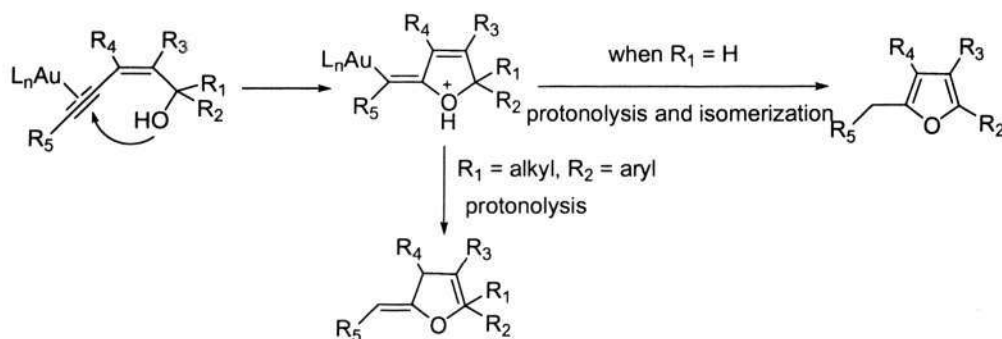
Scheme 6.12



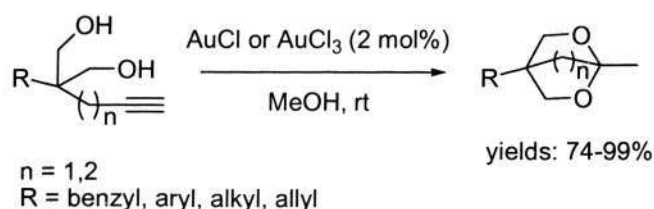
Scheme 6.13

The addition of alcohols to alkynes is an important method to construct oxygen heterocyclic compounds. Inspired by Hashmi's reported results,²⁵ Liu et al. developed a highly efficient gold-catalyzed cyclization of (Z)-2-en-4-yn-1-ols giving fully substituted dihydrofurans or furans (Scheme 6.14).^{26a} Both $AuCl_3$ and $Au(PPh_3)Cl$ can give efficient results, and this process is highly stereo-selectivity as a result of anti-oxyauration. Almost at the same time, Genêt, Michelet, and co-workers reported the first cycloisomerization of bis-homopropargylic diols in the presence of $AuCl$ or $AuCl_3$.^{26b} The reaction could occur smoothly under very mild reaction conditions (room temperature, 45 min), which gave dioxabicyclo[2.2.1] and [2.2.2] ketals products (Scheme 6.15). The proposed mechanism involves gold coordination and two intramolecular cyclization processes. Later, Barluenga et al. developed a highly efficient and diastereo-selective Pt or Au catalyzed protocol to prepare eight-membered carbocycles from allyl-substituted 5-hexyn-1-ol

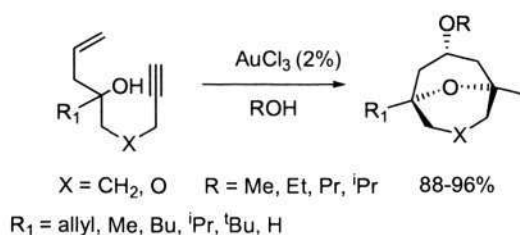
derivatives (Scheme 6.16).^{26c} 6-*exo* cycloisomerization and the following prins-type cyclization were involved in the proposed mechanism, and the configuration of the stereogenic centers was confirmed by labelling experiments.



Scheme 6.14



Scheme 6.15



Scheme 6.16

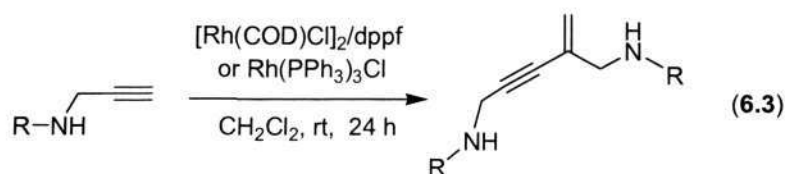
6.1.4. Summary

It has been widely noted that gold catalysis has attracted much attention in organic synthesis in recent years, owing to their soft and mild Lewis acidic nature. It has been demonstrated that many gold-catalyzed reactions show superior advantages, such as mild reaction conditions, low catalyst loading, and high atom-economy. Importantly, some methodologies have been applied to

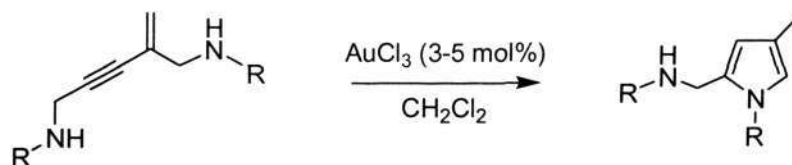
the synthesis of natural or non-natural molecules.²⁷ However, despite of the rapid and great progress in recent years, it is still necessary to further expand reaction scopes and to apply gold catalysts to asymmetric organic synthesis.

6.2. Results and Discussion

As shown in equation 6.3, in dimerization products, the proper orientation of a NH group and a triple bond allows further intramolecular elaboration. It is well-known that some transition-metal catalysts can activate alkenes or alkynes to allow catalytic hydroamination. Among them, gold-catalyzed alkyne hydroamination² and palladium-catalyzed alkene hydroamination^{7a-e} are especially efficient. In addition, examples have been reported for the cyclization of enynes to give furans,^{26a,28} thiophenes,²⁹ and pyrroles.³⁰



We thus initially attempted the hydroamination of a Ts-substituted enyne using AuCl_3 as a catalyst at room temperature.³¹ ^1H NMR analysis of the reaction mixture revealed that no starting material remained after 1 h, and the isolated product was confirmed to be a substituted pyrrole resulting from *5-endo-dig* cyclization. In fact, gold-catalyzed intramolecular alkyne hydroamination reactions have been reported to give substituted pyrroles.^{20,21,32} However, the reaction suffered from poor selectivity in that compound **1** was isolated in only 40% yield (entry 1, Table 6.1). We reason that the selectivity is likely improvable by lowering the reaction temperature to suppress the side reactions. Indeed, the isolated yield was augmented to 88% at -20°C after 0.7 h (entry 3, Table 6.1). The scope of the enyne substrates was extended to those with alkyl or arylsulfonamide functionalities. Under differently optimized conditions (entries 4-11, Table 6.1), the isolated yields range from 70% to 88%.

Table 6.1 Au-catalyzed hydroamination of propargyl sulfonamide enynes ^a

entry	R	temp (°C)	time (h)	yield (%)	product
1	Ts	25	1	40	1
2	Ts	0	4	63	1
3	Ts	-20	0.7	88	1
4	MeSO ₂	25	1	75	2
5	ⁿ BuSO ₂	25	1	76	3
6	<i>p</i> -Br(C ₆ H ₄)SO ₂	0	2	81	4
7	PhSO ₂	0	2	88	5
8	<i>p</i> -Cl(C ₆ H ₄)SO ₂	0	3	80	6
9	<i>p</i> -MeO(C ₆ H ₄)SO ₂	-20	3	83	7
10	<i>m</i> -Me(C ₆ H ₄)SO ₂	25	1	76	8
11	PhCH ₂ SO ₂	0	2	70	9

^aReaction conditions: enyne (0.2 mmol), AuCl₃ (3-5 mol%), CH₂Cl₂ (1 mL).

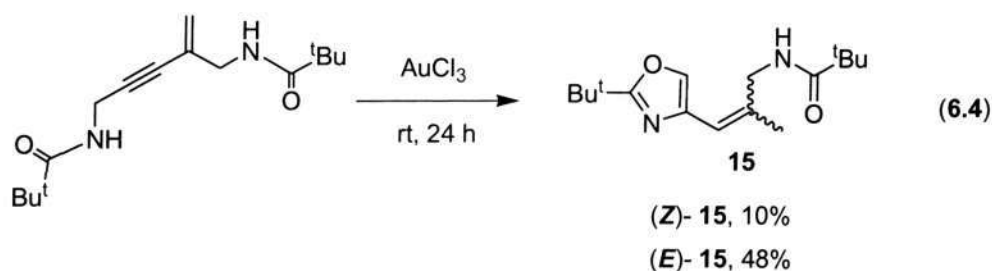
Carbamate- or amide-functionalized enynes are also applicable substrates in this type of reaction, and the results are given in Table 6.2. Pyrrole **10** was isolated in 80% yield starting from Cbz-substituted enyne (-40 °C, 1h, entry 2, Table 6.2). Here the R group has pronounced effects on the cyclization process. Pyrrole **11** was only obtained in 50 % yield (-40 °C, 2 h, entry 4, Table 6.2) for enyne with a Boc group. In line with the low yield of the dimerization step described in Chapter 5, only 36% yield was reached for the cyclization of benzoyl-functionalized enyne after initial optimization (entries 6 and 7, Table 6.2).

Table 6.2 Au-catalyzed hydroamination of functionalized enynes ^a

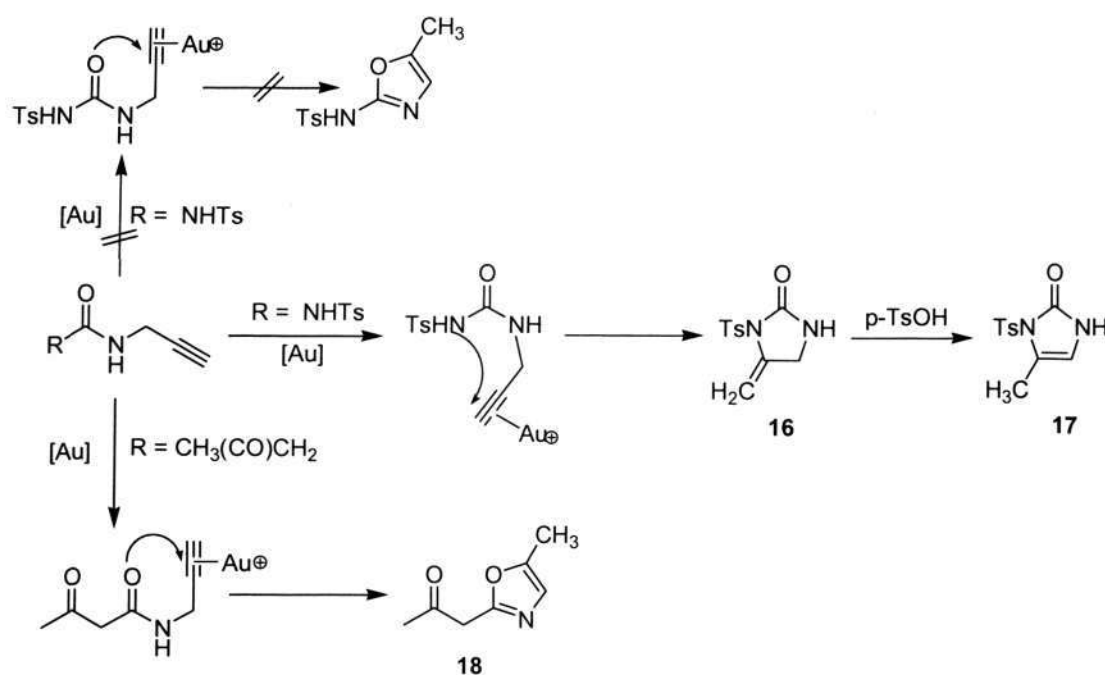
entry	R	temp (°C)	time (h)	yield (%)	product
1	Cbz	-20	0.7	58	10
2	Cbz	-40	1	80	10
3	Boc	-20	0.7	38	11
4	Boc	-40	2	50	11
5	-C(O)OEt	-40	2	52	12
6	-C(O)Ph	25	16	24	13
7	-C(O)Ph	80	24	36	13
8		25	16	38	14

^aReaction conditions: enyne (0.2 mmol), AuCl₃ (3-5 mol%), CH₂Cl₂ (1 mL).

In sharp contrast, the compound with ^tBu group cyclizes to give two isomeric oxazoles (eq 6.4), instead of a pyrrole, and the identity of these two products (*Z*- and *E*-**15**) was confirmed by NMR spectroscopy (HMBC). In comparison with other substrates, the introduction of a ^tBu group enhanced the nucleophilicity of the carbonyl group so that O-attack on the activated alkyne is favored. It seems that the reactivity of amide-substituted enynes is consistent with the acidity of the NH proton (entries 1-8, Table 6.2). In the cyclization of ^tBu-substituted enyne, only O-attack took place as a result of the low acidity of the NH group.



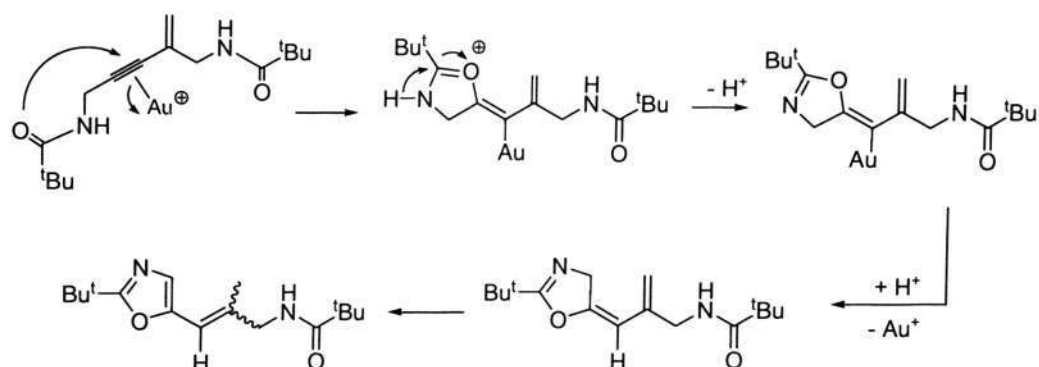
Several examples of metal-mediated carbonyl attack on terminal alkynes have been recently reported.¹⁶ For instance, Padwa and Verniest reported that the reaction routes varied with the R group of *N*-propargylcarboxamides $R(\text{CO})\text{NHCH}_2\text{C}\equiv\text{CH}$ (Scheme 6.17). When *N*-tosyl-*N'*-propargylurea was treated with AuCl_3 , NH group of TsNH attacked the $\text{C}\equiv\text{C}$ bond to give a cyclic urea derivative instead of O-attack. Here, *exo*-cyclic olefin product **16** can be isolated in 68% yield, which very slowly isomerized to the more stable product **17** only upon heating in toluene in the presence of *p*-TsOH. To 3-*oxo*-*N*-propargylbutanamide, the corresponding oxazole product **18** could be obtained.^{16d}



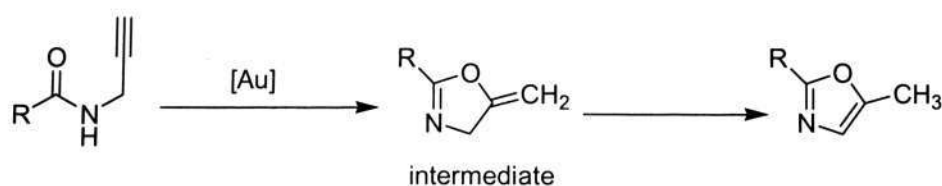
Scheme 6.17

A plausible mechanism of the overall transformation for equation 6.4 is proposed in scheme 6.18. The $\text{C}\equiv\text{C}$ bond in enyne is activated by AuCl_3 towards carbonyl attack (5-*exo-dig* cyclization) to give a Au vinyl intermediate, protonation of which afford an *exo*-cyclic olefin compound. The final product is obtained after isomerization of this olefin intermediate to the more stable aromatic oxazole products. *Exo*-methylene products are usually unstable, in most cases, they will convert to the thermodynamically more stable isomers (Scheme 6.19).¹⁶ Hashmi and co-workers once gave a detailed study to this isomerization process via ^1H NMR

spectroscopy, from which the intermediate (*exo*-double bond product) could be observed up to 95% yield.^{16b}



Scheme 6.18



Scheme 6.19

6.3. Conclusion

In summary, we proved that a series of head-to-tail dimerization products could further undergo Au-catalyzed hydroamination to afford functionalized pyrroles. Hydroamination works most efficiently for enynes with sulfonamide functionality, but it is relatively less efficient for carbamates. Both oxygen and nitrogen could attack the triple bond, depending on the substitutes attached to the carbonyl group. Although this is not a new methodology, it indeed provides a route for us to synthesize substituted pyrroles. Further study is necessary to extend this methodology to other substrates.

6.4. Experimental Section

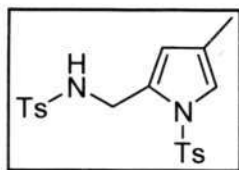
6.4.1. General Information

All commercial solvents were dried using 4Å molecule sieves, and all commercial reagents were used as received. Analytical thin layer chromatography (TLC) was performed using Merck 60 F254 precoated silica gel plates (0.2 mm thickness). TLC plates were visualized using UV radiation (254 nm) on Spectroline Model ENF-24061/F 254 nm. Further visualization was plausible by staining with a basic solution of KMnO_4 . Flash chromatography was conducted by Merck silica gel 60 with freshly distilled solvents. Columns were typically packed as slurry and equilibrated with the appropriate solvent system prior to use.

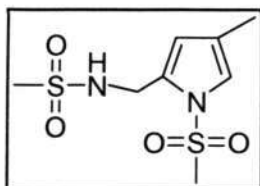
IR spectra were recorded on a Horiba FT 300-S by ATR method and on a Shimadzu IR Prestige-21 FT-IR Spectrometer. High-resolution mass spectra were obtained with a Finnigan MAT 95 XP mass spectrometer (EI) and a Waters Micromass Q-ToF Premier Mass Spectrometer (ESI). ^1H and ^{13}C NMR spectra were recorded on a Bruker Avance DPX 300, Bruker AMX 400, or Bruker DRX 500 spectrophotometer. Chemical shifts for ^1H NMR spectra were reported as δ in units of parts per million (ppm) downfield from SiMe_4 (δ 0.0) and relative to the signal of chloroform-*d* (δ 7.26, singlet). Multiplicities were given as: s (singlet); d (doublet); t (triplet); or m (multiplets). The number of protons (n) for a given resonance was indicated by nH. Coupling constants were reported as a *J* value in Hz.

6.4.2. Synthetic Procedures and Data

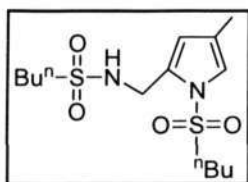
The following procedure was followed to prepare compounds **1-15**. The corresponding starting material (0.2 mmol) and AuCl_3 (3 mol%) were weighed into a flask in a glove box. CH_2Cl_2 (1 mL) was then added at temperatures indicated in Table 6.1. The mixture was then stirred for another 40 min to 20 h (see Table 6.1). Removal of the solvent gave a residue which was purified by silica gel column chromatography.



Compound 1: white solid; mp: 126-127 °C; yield: 88%; Hexane/ethyl acetate: 5/2; ^1H NMR (500 MHz, CDCl_3): δ 7.64 (d, J = 8.2 Hz, 2H, $\text{H}_{\text{aromatic}}$), 7.47 (d, J = 8.3 Hz, 2H, $\text{H}_{\text{aromatic}}$), 7.25-7.22 (m, 4H, $\text{H}_{\text{aromatic}}$), 6.82 (s, 1H, pyrrole), 5.82 (s, 1H, pyrrole), 5.34 (t, J = 6.5 Hz, H, NH), 4.10 (d, J = 6.6 Hz, 2H, CH_2), 2.41 (s, 3H, CH_3), 2.39 (s, 3H, CH_3), 1.87 (s, 3H, $\text{CH}_3_{\text{pyrrole}}$); ^{13}C NMR (100 MHz, CDCl_3): δ 145.2, 143.0, 137.3, 135.7, 130.1 ($\text{CH}_{\text{aromatic}}$), 129.4 ($\text{CH}_{\text{aromatic}}$), 129.0, 127.1 ($\text{CH}_{\text{aromatic}}$), 126.4 ($\text{CH}_{\text{aromatic}}$), 122.5, 120.4 ($\text{CH}_{\text{pyrrole}}$), 118.8 ($\text{CH}_{\text{pyrrole}}$), 39.9 (CH_2), 21.6 (CH_3), 21.5 (CH_3), 11.4 ($\text{CH}_3_{\text{pyrrole}}$). IR (KBr): 3308 (s), 2961 (w), 2922 (w), 1597 (m), 1457 (m), 1366 (s), 1327 (s), 1260 (m), 1163 (s), 968 (m), 812 (m), 679 (s), 594 (s), 540 (m) cm^{-1} . HRMS (ESI) for $\text{C}_{20}\text{H}_{23}\text{N}_2\text{O}_4\text{S}_2$ calcd: 419.1099, found: 419.1098.

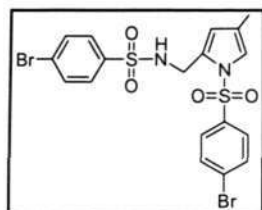


Compound 2: white solid; mp: 107-108 °C; yield: 75%; Hexane/ethyl acetate: 1/1; ^1H NMR (400 MHz, CDCl_3): δ 6.88 (s, 1H, pyrrole), 6.25 (s, 1H, pyrrole), 5.10 (br, 1H, NH), 4.37 (d, J = 6.5 Hz, 2H, CH_2), 3.14 (s, 3H, CH_3), 2.79 (s, 3H, CH_3), 2.04 (s, 3H, $\text{CH}_3_{\text{pyrrole}}$); ^{13}C NMR (100 MHz, CDCl_3): δ 130.1 (C-CH_2), 123.2 (C-CH_3), 120.5 ($\text{CH}_{\text{pyrrole}}$), 118.8 ($\text{CH}_{\text{pyrrole}}$), 42.8 (CH_3), 41.3 (CH_3), 39.7 (CH_2), 11.6 ($\text{CH}_3_{\text{pyrrole}}$). IR (KBr): 3331 (s), 3023 (m), 2928 (w), 1516 (w), 1427 (m), 1344 (s), 1321 (s), 1258 (s), 1152 (s), 1132 (s), 1078 (s), 978 (s), 841 (m), 791 (s), 529 (s) cm^{-1} . HRMS (EI) for $\text{C}_{18}\text{H}_{14}\text{N}_2\text{O}_4\text{S}_2$ calcd: 266.0389, found: 266.0386.



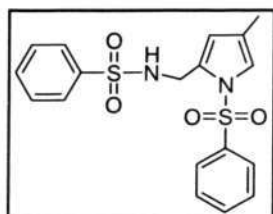
Compound 3: colourless oil; yield: 76%; Hexane/ethyl acetate: 1/1; ^1H NMR (400 MHz, CDCl_3): δ 6.85 (s, 1H, pyrrole), 6.22 (s, 1H, pyrrole), 5.07 (br, 1H, NH), 4.34 (s, 2H, CH_2), 3.20 (t, J = 7.8 Hz, 2H, $\text{CH}_2\text{CH}_2\text{CH}_2\text{CH}_3$), 2.77 (t, J = 8.0 Hz, 2H, $\text{CH}_2\text{CH}_2\text{CH}_2\text{CH}_3$), 2.03 (s, 3H, $\text{CH}_3_{\text{pyrrole}}$), 1.69-1.60 (m, 4H, $2\text{CH}_2\text{CH}_2\text{CH}_2\text{CH}_3$), 1.42-1.29 (m, 4H, $2\text{CH}_2\text{CH}_2\text{CH}_2\text{CH}_3$), 0.91 (t, J = 7.2 Hz, 3H, $\text{CH}_2\text{CH}_2\text{CH}_2\text{CH}_3$), 0.86 (t, J = 7.2 Hz, 3H, $\text{CH}_2\text{CH}_2\text{CH}_2\text{CH}_3$); ^{13}C NMR (100 MHz, CDCl_3): δ 130.7 (C-CH_2), 122.5 (C-CH_3), 120.8 ($\text{CH}_{\text{pyrrole}}$), 118.4 ($\text{CH}_{\text{pyrrole}}$), 55.6 ($\text{CH}_2\text{CH}_2\text{CH}_2\text{CH}_3$), 53.4 ($\text{CH}_2\text{CH}_2\text{CH}_2\text{CH}_3$), 39.7 (CH_2), 25.5 ($\text{CH}_2\text{CH}_2\text{CH}_2\text{CH}_3$), 25.0 ($\text{CH}_2\text{CH}_2\text{CH}_2\text{CH}_3$), 21.5

(CH₂CH₂CH₂CH₃), 21.2 (CH₂CH₂CH₂CH₃), 13.42 (CH₂CH₂CH₂CH₃), 13.41 (CH₂CH₂CH₂CH₃), 11.6 (CH₃ pyrrole). IR (KBr): 3279 (m), 2963 (s), 2876 (m), 1458 (m), 1364 (s), 1327 (s), 1279 (s), 1167 (s), 1140 (s), 1078 (m), 920 (w), 804 (w), 733 (w), 617 (w), 557 (m) cm⁻¹. HRMS (ESI) for C₁₄H₂₆N₂O₄S₂Na calcd: 373.1232, found: 373.1226.



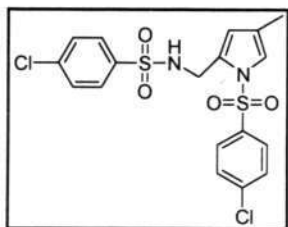
Compound 4: colourless oil; yield: 81%; Hexane/ethyl acetate: 5/2; ¹H NMR (400 MHz, CDCl₃): δ 7.62-7.57 (m, 6H, H_{aromatic}), 7.47-7.45 (m, 2H, H_{aromatic}), 6.79 (s, 1H, pyrrole), 5.84 (s, 1H, pyrrole), 5.42 (t, *J* = 6.4 Hz, H, NH), 4.13 (d, *J* = 6.6 Hz, 2H, CH₂), 1.88 (s, 3H, CH₃); ¹³C NMR

(100 MHz, CDCl₃): δ 139.6, 137.6, 133.0 (CH_{aromatic}), 132.0 (CH_{aromatic}), 129.5, 129.0, 128.6 (CH_{aromatic}), 127.8 (CH_{aromatic}), 127.2, 123.3, 120.6 (CH_{pyrrole}), 119.7 (CH_{pyrrole}), 39.9 (CH₂), 11.5 (CH₃ pyrrole). IR (KBr): 3306 (m), 3088 (w), 1576 (s), 1474 (m), 1393 (m), 1370 (s), 1260 (m), 1169 (s), 1096 (m), 1071 (s), 1011 (w), 824 (w), 739 (m), 627 (m), 586 (w) cm⁻¹. Anal. Calcd for C₁₈H₁₆Br₂N₂O₄S₂ (548.27): C, 39.43; H, 2.94; N, 5.11; S, 11.70%. Found: C, 39.70; H, 3.13; N, 5.30; S, 11.96%.

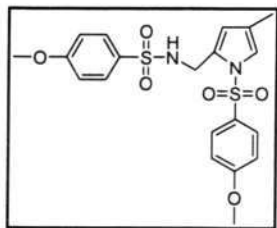


Compound 5: white solid; mp: 118-119 °C; yield: 88%; Hexane/ethyl acetate: 2/1; ¹H NMR (400 MHz, CDCl₃): δ 7.76 (d, *J* = 7.4 Hz, 2H, H_{aromatic}), 7.59-7.43 (m, 8H, H_{aromatic}), 6.82 (s, 1H, pyrrole), 5.86 (s, 1H, pyrrole), 5.40 (t, *J* = 6.2 Hz, H, NH), 4.12 (d, *J* = 6.6 Hz, 2H, CH₂), 1.87

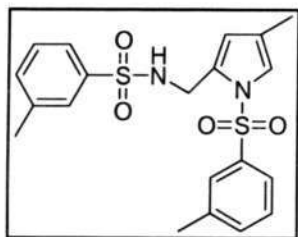
(s, 3H, CH₃); ¹³C NMR (100 MHz, CDCl₃): δ 140.4, 138.8, 134.1, 132.3, 129.6 (CH_{aromatic}), 129.1 (C_{pyrrole}), 128.8 (CH_{aromatic}), 127.0 (CH_{aromatic}), 126.3 (CH_{aromatic}), 122.7 (C_{pyrrole}), 120.6 (CH_{pyrrole}), 119.1 (CH_{pyrrole}), 39.9 (CH₂), 11.5 (CH₃ pyrrole). IR (KBr): 3310 (m), 3052 (w), 1584 (w), 1449 (m), 1362 (s), 1325 (s), 1258 (m), 1171 (s), 1098 (s), 1069 (m), 966 (w), 866 (w), 752 (m), 685 (m), 583 (m) cm⁻¹. HRMS (ESI) for C₁₈H₁₈N₂O₄S₂Na calcd: 413.0606, found: 313.0586.



Compound 6: white solid; mp: 120-121 °C; yield: 80%; Hexane/ethyl acetate: 3/1; ^1H NMR (500 MHz, CDCl_3): δ 7.65 (d, $J = 8.4$ Hz, 2H, $\text{H}_{\text{aromatic}}$), 7.55 (d, $J = 8.4$ Hz, 2H, $\text{H}_{\text{aromatic}}$), 7.44-7.39 (m, 4H, $\text{H}_{\text{aromatic}}$), 6.80 (s, 1H, pyrrole), 5.85 (s, 1H, pyrrole), 5.45 (t, $J = 6.6$ Hz, H, NH), 4.14 (d, $J = 6.6$ Hz, 2H, CH_2), 1.88 (s, 3H, CH_3); ^{13}C NMR (125 MHz, CDCl_3): δ 140.9, 139.0, 138.8, 137.0, 130.0 ($\text{CH}_{\text{aromatic}}$), 129.0 ($\text{CH}_{\text{aromatic}}$), 128.5 ($\text{CH}_{\text{aromatic}}$), 127.8 ($\text{CH}_{\text{aromatic}}$), 123.3 (one missing), 120.6 ($\text{CH}_{\text{pyrrole}}$), 119.6 ($\text{CH}_{\text{pyrrole}}$), 39.9 (CH_2), 11.4 ($\text{CH}_3_{\text{pyrrole}}$). IR (KBr): 3306 (m), 3098 (w), 1586 (w), 1479 (m), 1400 (m), 1370 (s), 1331 (s), 1262 (m), 1167 (s), 1092 (s), 1071 (m), 970 (w), 826 (w), 768 (s), 637 (s), 588 (s) cm^{-1} . HRMS (ESI) for $\text{C}_{18}\text{H}_{16}\text{N}_2\text{O}_4\text{S}_2\text{Cl}_2\text{Na}$ calcd: 480.9826, found: 480.9814.

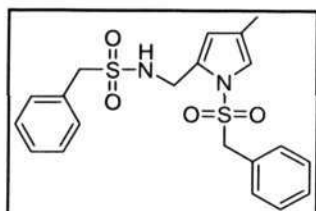


Compound 7: colourless oil; yield: 83%; Hexane/ethyl acetate: 5/2; ^1H NMR (400 MHz, CDCl_3): δ 7.70 (d, $J = 8.8$ Hz, 2H, $\text{H}_{\text{aromatic}}$), 7.54 (d, $J = 8.9$ Hz, 2H, $\text{H}_{\text{aromatic}}$), 6.92-6.88 (m, 4H, $\text{H}_{\text{aromatic}}$), 6.82 (s, 1H, pyrrole), 5.83 (s, 1H, pyrrole), 5.32 (t, $J = 6.5$ Hz, H, NH), 4.08 (d, $J = 5.8$ Hz, 2H, CH_2), 3.86 (s, 3H, OCH_3), 3.83 (s, 3H, OCH_3), 1.87 (s, 3H, CH_3); ^{13}C NMR (100 MHz, CDCl_3): δ 163.9, 162.7, 132.0, 130.1, 129.2 ($\text{CH}_{\text{aromatic}}$), 129.0, 128.8 ($\text{CH}_{\text{aromatic}}$), 122.4, 120.5 ($\text{CH}_{\text{pyrrole}}$), 118.7 ($\text{CH}_{\text{pyrrole}}$), 114.7 ($\text{CH}_{\text{aromatic}}$), 113.9 ($\text{CH}_{\text{aromatic}}$), 55.8 (OCH_3), 55.6 (OCH_3), 39.9 (CH_2), 11.5 ($\text{CH}_3_{\text{pyrrole}}$). IR (KBr): 3296 (s), 2963 (m), 2843 (w), 1597 (s), 1578 (w), 1499 (m), 1441 (w), 1327 (s), 1262 (s), 1155 (s), 1094 (m), 833 (w), 675 (w), 550 (w) cm^{-1} . HRMS (ESI) for $\text{C}_{20}\text{H}_{22}\text{N}_2\text{O}_6\text{S}_2\text{Na}$ calcd: 473.0817, found: 473.0815.



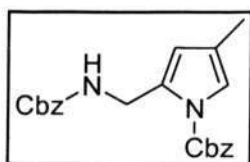
Compound 8: colourless oil; yield: 76%; Hexane/ethyl acetate: 5/2; ^1H NMR (400 MHz, CDCl_3): δ 7.56-7.54 (m, 2H, $\text{H}_{\text{aromatic}}$), 7.44 (s, 1H), 7.37-7.29 (m, 5H, $\text{H}_{\text{aromatic}}$), 6.81 (s, 1H, pyrrole), 5.84 (s, 1H, pyrrole), 5.40 (t, $J = 6.6$ Hz, H, NH), 4.12 (d, $J = 6.6$ Hz, 2H, CH_2), 2.37 (s, 3H, CH_3), 2.36 (s, 3H, CH_3), 1.86 (s, 3H, $\text{CH}_3_{\text{pyrrole}}$); ^{13}C NMR (100 MHz, CDCl_3): δ 140.2, 140.0, 139.0, 138.5, 134.9, 133.0, 129.4 ($\text{CH}_{\text{aromatic}}$), 129.1 ($\text{C}_{\text{pyrrole}}$), 128.6 ($\text{CH}_{\text{aromatic}}$),

127.3 (CH_{aromatic}), 126.6 (CH_{aromatic}), 124.1 (CH_{aromatic}), 123.4 (CH_{aromatic}), 122.5 (C_{pyrrole}), 120.4 (CH_{pyrrole}), 118.9 (CH_{pyrrole}), 39.9 (CH₂), 21.3 (CH₃), 21.2 (CH₃), 11.4 (CH₃_{pyrrole}). IR (KBr): 3327 (s), 2926 (w), 1479 (w), 1366 (s), 1333 (m), 1227 (w), 1173 (s), 1155 (s), 1092 (m), 868 (w), 783 (w), 700 (m), 617 (s), 565 (w) cm⁻¹. HRMS (ESI) for C₂₀H₂₃N₂O₄S₂ calcd: 419.1099, found: 419.1098.



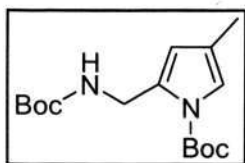
Compound 9: white solid; mp: ; 123-124 °C yield: 70%; Hexane/ethyl acetate: 5/2; ¹H NMR (400 MHz, CDCl₃): δ 7.39-7.29 (m, 6H, H_{aromatic}), 7.05 (d, *J* = 3.6 Hz, 2H), 6.95 (d, *J* = 7.5 Hz, 2H), 6.79 (s, 1H, pyrrole), 6.06 (s, 1H, pyrrole), 4.70 (t, *J* = 6.2 Hz, H,

NH), 4.42 (s, 2H, CH₂), 3.97 (s, 2H, CH₂), 3.50 (d, *J* = 6.5 Hz, 2H, CH₂NH), 2.04 (s, 3H, CH₃_{pyrrole}); ¹³C NMR (100 MHz, CDCl₃): δ 132.7(one missing), 130.8 (CH_{aromatic}), 130.5 (CH_{aromatic}), 129.8 (CH_{aromatic}), 129.0 (CH_{aromatic}), 128.8 (CH_{aromatic}), 128.6 (CH_{aromatic}), 126.5 (C_{pyrrole}), 122.8 (C_{pyrrole}), 120.2 (CH_{pyrrole}), 117.1 (CH_{pyrrole}), 61.9 (CH₂), 59.8 (CH₂), 39.1 (CH₂NH), 11.7 (CH₃_{pyrrole}). IR (KBr): 3325 (s), 3034 (w), 2982 (m), 1603 (w), 1495 (s), 1348 (s), 1325 (s), 1262 (s), 1175 (s), 1152 (s), 1082 (s), 966 (m), 889 (s), 795 (s), 696 (s), 615 (s), 540 (s) cm⁻¹. HRMS (ESI) for C₂₀H₂₃N₂O₄S₂ calcd: 419.1099, found: 419.1098.

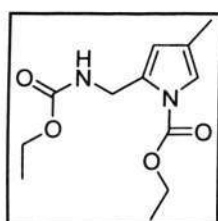


Compound 10: white solid; mp: 95-96 °C; yield: 80%; Hexane/ethyl acetate: 5/2; ¹H NMR (400 MHz, CDCl₃): δ 7.41-7.34 (m, 10H, H_{aromatic}), 6.97 (s, 1H, pyrrole), 6.11 (s, 1H, pyrrole), 5.67 (br, 1H, NH), 5.31 (s, 2H,

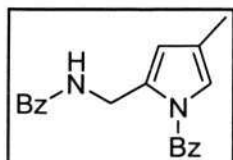
CH₂O), 5.07 (s, 2H, CH₂O), 4.45 (d, *J* = 6.4 Hz, 2H, CH₂), 1.99 (s, 3H, CH₃); ¹³C NMR (100 MHz, CDCl₃): δ 156.2 (CO), 150.7 (CO), 136.6, 134.8, 132.1, 128.8 (2C overlap, CH_{aromatic}), 128.5 (CH_{aromatic}), 128.4 (CH_{aromatic}), 128.2 (CH_{aromatic}), 128.1 (CH_{aromatic}), 121.7 (C_{pyrrole}), 118.4 (CH_{pyrrole}), 116.6 (CH_{pyrrole}), 68.8 (CH₂O), 66.7 (CH₂O), 38.2 (CH₂), 11.7 (CH₃_{pyrrole}). IR (KBr): 3300 (s), 3069 (w), 2965 (w), 1742 (s), 1694 (s), 1557 (s), 1414 (s), 1335 (s), 1250 (s), 1163 (m), 1057 (m), 990 (m), 739 (m), 696 (s), 588 (w) cm⁻¹. HRMS (ESI) for C₂₂H₂₃N₂O₄ calcd: 379.1658, found: 379.1643.



Compound 11: pale yellow oil; yield: 50%; Hexane/ethyl acetate: 8/1; ^1H NMR (400 MHz, CDCl_3): δ 6.89 (s, 1H, pyrrole), 6.03 (s, 1H, pyrrole), 5.37 (br, 1H, NH), 4.37 (d, $J = 6.0$ Hz, 2H, CH_2), 1.99 (s, 3H, CH_3 pyrrole), 1.58 (s, 9H, $\text{C}(\text{CH}_3)_3$), 1.43 (s, 9H, $\text{C}(\text{CH}_3)_3$); ^{13}C NMR (100 MHz, CDCl_3): δ 155.7 (CO), 149.5 (CO), 132.3, 120.8, 118.6 (CH pyrrole), 115.5 (CH pyrrole), 83.6 ($\text{C}(\text{CH}_3)_3$), 79.2 ($\text{C}(\text{CH}_3)_3$), 38.0 (CH_2), 28.5 ($\text{C}(\text{CH}_3)_3$), 28.1 ($\text{C}(\text{CH}_3)_3$), 11.7 (CH_3 pyrrole). IR (KBr): 3258 (m), 3071 (w), 2924 (w), 1728 (w), 1690 (s), 1551 (m), 1402 (m), 1343 (s), 1259 (w), 916 (w), 696 (m) cm^{-1} . **HRMS (ESI)** for $\text{C}_{16}\text{H}_{27}\text{N}_2\text{O}_4$ calcd: 311.1971, found: 311.1952.

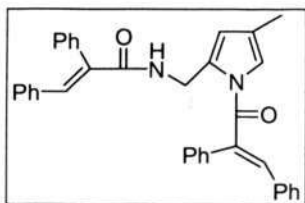


Compound 12: pale yellow oil; yield: 52%; Hexane/ethyl acetate: 5/2; ^1H NMR (500 MHz, CDCl_3): δ 6.95 (s, 1H, pyrrole), 6.08 (s, 1H, pyrrole), 5.58 (br, 1H, NH), 4.41 (d, $J = 6.3$ Hz, 2H, CH_2), 4.38-4.34 (m, 2H, CH_2CH_3), 4.10-4.06 (m, 2H, CH_2CH_3), 1.99 (s, 3H, CH_3), 1.40 (t, $J = 7.2$ Hz, 3H, CH_2CH_3), 1.21 (t, $J = 7.0$ Hz, 3H, CH_2CH_3); ^{13}C NMR (125 MHz, CDCl_3): δ 156.5 (CO), 150.9 (CO), 132.3, 121.4, 118.4 (CH pyrrole), 116.3 (CH pyrrole), 63.2 (CH_2CH_3), 60.7 (CH_2CH_3), 38.1 (CH_2), 14.7 (CH_2CH_3), 14.3 (CH_2CH_3), 11.7 (CH_3 pyrrole). IR (KBr): 3348 (m), 2986 (m), 2940 (w), 1774 (s), 1701 (s), 1528 (s), 1375 (m), 1250 (s), 1175 (w), 1032 (m), 862 (w), 777 (w) cm^{-1} . **HRMS (ESI)** for $\text{C}_{12}\text{H}_{19}\text{N}_2\text{O}_4$ calcd: 255.1345, found: 255.1336.



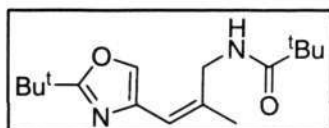
Compound 13: white solid; mp: 122-123 $^\circ\text{C}$; yield: 36%; Hexane/ethyl acetate: 5/2; ^1H NMR (400 MHz, CDCl_3): δ 7.83 (d, $J = 7.2$ Hz, 2H, H aromatic), 7.73 (d, $J = 7.3$ Hz, 2H, H aromatic), 7.62-7.59 (m, 2H, H aromatic), 7.53-7.40 (m, 5H, 4H aromatic + NH), 6.57 (s, 1H, pyrrole), 6.35 (s, 1H, pyrrole), 4.77 (d, $J = 6.2$ Hz, 2H, CH_2), 1.99 (s, 3H, CH_3); ^{13}C NMR (100 MHz, CDCl_3): δ 169.6 (CO), 166.7 (CO), 134.7, 134.0, 132.6 (C pyrrole), 132.4 (CH aromatic), 131.3 (CH aromatic), 129.6 (CH aromatic), 128.51 (CH aromatic), 128.47 (CH aromatic), 127.1 (CH aromatic), 122.0 (C pyrrole), 121.1 (CH pyrrole), 118.3 (CH pyrrole), 36.7 (CH_2), 11.7 (CH_3). IR (KBr): 3329 (w), 3061 (w), 2924 (w), 1734 (w), 1689 (s), 1645 (s), 1580 (w), 1532 (m), 1489 (m), 1392 (m), 1337 (s), 1262 (m), 910 (w), 720 (m), 696 (m) cm^{-1} . **HRMS**

(ESI) for $C_{20}H_{19}N_2O_2$ calcd: 319.1447, found: 319.1439.



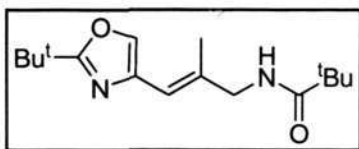
Compound 14: yield: 38%. 1H NMR (400MHz, $CDCl_3$): δ 7.85 (s, 1H), 7.36-7.29 (m, 6H, $H_{aromatic}$), 7.26-7.09 (m, 12H, $H_{aromatic}$), 7.00-6.98 (m, 2H, $H_{aromatic}$), 6.89 (s, 1H, CH_{alkene}), 6.86 (s, 1H, $CH_{pyrrole}$), 6.67 (t, $J = 6.0$ Hz, 1H, NH), 6.23 (s, 1H, $CH_{pyrrole}$), 4.62 (d, $J = 6.3$

Hz, 2H, CH_2NH), 1.98 (s, 2H, CH_3); ^{13}C NMR (100MHz, $CDCl_3$): δ 171.2 (CO), 169.4 (CO), 166.6, 136.8 (CH_{alkene}), 136.1, 135.8 (CH_{alkene}), 135.7, 135.2, 135.1, 134.8, 134.3, 132.5, 130.4 ($CH_{aromatic}$), 129.9 ($CH_{aromatic}$), 129.7 ($CH_{aromatic}$), 129.4 ($CH_{aromatic}$), 129.1 ($CH_{aromatic}$), 129.0 ($CH_{aromatic}$), 128.5 ($CH_{aromatic}$), 128.43 ($CH_{aromatic}$), 128.40 ($CH_{aromatic}$), 128.3 ($CH_{aromatic}$), 128.1 ($CH_{aromatic}$), 122.1, 120.4 ($CH_{pyrrole}$), 118.0 ($CH_{pyrrole}$), 37.3 (CH_2), 11.8 (CH_3). IR (KBr): 3418 (w), 3055 (w), 2924 (w), 1728 (w), 1684 (s), 1668 (s), 1616 (m), 1497(s), 1447 (m), 1331 (s), 1262 (m), 1142 (m), 758 (m), 710 (m), 692 (s) cm^{-1} . **HRMS (ESI)** for $C_{36}H_{31}N_2O_2$ calcd: 523.2386, found: 523.2378.



Compound (Z)-15: white solid; mp: 102-103 $^{\circ}C$; yield: 10%; Hexane/ethyl acetate: 2:1 to 3:2; 1H NMR (400 MHz, $CDCl_3$): δ

6.77 (s, 1H, oxazole), 6.12 (s, 1H, alkene), 5.75 (br, 1H, NH), 4.20 (d, $J = 5.7$ Hz, 2H, CH_2), 1.90 (s, 3H, CH_3), 1.38 (s, 9H, t-Butyl), 1.20 (s, 9H, t-Butyl); ^{13}C NMR (100 MHz, $CDCl_3$): δ 178.5 (CO), 170.3 (OCN), 148.4 ($CHCCH_2$), 136.9 (OCHC), 124.7 (OCHC), 113.5 ($CHCCH_2$), 41.2 (CH_2), 38.8 ($C(CH_3)_3$), 33.7 ($C(CH_3)_3$), 28.6 ($C(CH_3)_3$), 27.6 ($C(CH_3)_3$), 22.7 (CH_3). IR (KBr): 3362 (s), 2965 (s), 2916 (m), 2868 (w), 1730 (w), 1645 (s), 1541 (s), 1476 (m), 1366 (m), 1296 (m), 1265 (s), 1213 (m), 1161 (s), 986 (m), 837 (m), 669 (w) cm^{-1} . **HRMS (EI)** for $C_{16}H_{26}N_2O_2$ calcd: 278.1989, found: 278.1988.



Compound (E)-15: colourless oil; yield: 48%; Hexane/ethyl acetate: 2:1 to 3:2; ^1H NMR (400MHz, CDCl_3): δ 6.78 (s, 1H, oxazole), 6.09 (s, 1H, alkene), 5.86 (br, 1H, NH), 3.93 (d, J = 5.9 Hz, 2H, CH_2), 1.92 (s, 3H, CH_3), 1.35 (s, 9H, t-Butyl), 1.22 (s, 9H, t-Butyl); ^{13}C NMR (100MHz, CDCl_3): δ 178.4 (CO), 170.0 (OCN), 149.0 (CHCCH_2), 136.2 (OCHC), 124.6 (OCHC), 111.7 (CHCCH_2), 46.9 (CH_2), 38.8 ($\text{C}(\text{CH}_3)_3$), 33.6 ($\text{C}(\text{CH}_3)_3$), 28.5 ($\text{C}(\text{CH}_3)_3$), 27.6 ($\text{C}(\text{CH}_3)_3$), 16.8 (CH_3). IR (KBr): 3347 (s), 2972 (s), 2911 (m), 2872 (w), 1738 (w), 1645 (s), 1533 (s), 1481 (m), 1368 (m), 1294 (w), 1207 (m), 1148 (w), 980 (w), 662 (w) cm^{-1} . **HRMS (ESI)** for $\text{C}_{16}\text{H}_{27}\text{N}_2\text{O}_2$ calcd: 279.2073, found: 279.2065.

6.5. References

1. (a) Demann, E. T. K.; Stein, P. S.; Haubenrich, J. E. *J. Long-Term Effects Med. Implants* **2005**, *15*, 687. (b) Kostova, I. *Anti-Cancer Agents Med. Chem.* **2006**, *6*, 19.
2. Some reviews, see: (a) Li, Z.; Brouwer, C.; He, C. *Chem. Rev.* **2008**, *108*, 3239. (b) Gorin, D. J.; Sherry, B. D.; Toste, F. D. *Chem. Rev.* **2008**, *108*, 3351. (c) Arcadi, A. *Chem. Rev.* **2008**, *108*, 3266. (d) Müller, T. E.; Hultsch, K. C.; Yus, M.; Foubelo, F.; Tada, M. *Chem. Rev.* **2008**, *108*, 3795. (e) Skouta, R.; Li, C.-J. *Tetrahedron* **2008**, *64*, 4917. (f) Hashmi, A. S. K. *Chem. Rev.* **2007**, *107*, 3180. (g) Gorin, D. J.; Toste, F. D. *nature* **2007**, *446*, 395. (h) Widenhoefer, R. A.; Han, X. *Eur. J. Org. Chem.* **2006**, 4555. (i) Jiménez-Núñez, E.; Echavarren, A. M. *Chem. Commun.* **2007**, 333. (j) Fürstner, A.; Davies, P. W. *Angew. Chem., Int. Ed.* **2007**, *46*, 3410. (k) Hoffmann-Röder, A.; Krause, N. *Org. Biomol. Chem.* **2005**, *3*, 387.
3. (a) Widenhoefer, R. A. *Chem. Eur. J.* **2008**, *14*, 5382. (b) Hultsch, K. C. *Adv. Synth. Catal.* **2005**, *347*, 367. (c) LaLonde, R. L.; Sherry, B. D.; Kang, E. J.; Toste, F. D. *J. Am. Chem. Soc.* **2007**, *129*, 2452.
4. (a) Hong, S.; Marks, T. J. *Acc. Chem. Res.* **2004**, *37*, 673. (b) Arndt, S.; Okuda, J. *Adv. Synth. Catal.* **2005**, *347*, 339.
5. (a) Müller, T. E.; Beller, M. *Chem. Rev.* **1998**, *98*, 675. (b) Pohlki, F.; Doye, S. *Chem. Soc. Rev.* **2003**, *32*, 104. (c) Severin, R.; Doye, S. *Chem. Soc. Rev.* **2007**, *36*, 1407.
6. Bytschkov, I.; Doye, S. *Eur. J. Org. Chem.* **2003**, 935.
7. (a) Cochran, B. M.; Michael, F. E. *J. Am. Chem. Soc.* **2008**, *130*, 2786. (b) Patil, N. T.; Wu, H.; Yamamoto, Y. *J. Org. Chem.* **2007**, *72*, 6577. (c) Johns, A. M.; Liu, Z.; Hartwig, J. F. *Angew. Chem., Int. Ed.* **2007**, *46*, 7259. (d) Sakai, N.; Ridder, A.; Hartwig, J. F. *J. Am. Chem. Soc.* **2006**, *128*, 8134. (e) Bajracharya, G. B.; Huo, Z.; Yamamoto, Y. *J. Org. Chem.* **2005**, *70*, 4883. (f) Johns, A. M.; Utsunomiya, M.; Incarvito, C. D.; Hartwig, J. F. *J. Am. Chem. Soc.* **2006**, *128*, 1828. (g) Michael, F. E.; Cochran, B. M. *J. Am. Chem. Soc.* **2006**, *128*, 4246. (h) Cochran, B. M.; Michael, F. E. *Org. Lett.* **2008**, *10*, 329.
8. (a) Chianese, A. R.; Lee, S. J.; Gagné, M. R. *Angew. Chem., Int. Ed.* **2007**, *46*, 4042. (b) Brunet, J.-J.; Chu, N.-C.; Rodriguez-Zubiri, M. *Eur. J. Inorg. Chem.* **2007**, 4711.
9. (a) Lai, R.-Y.; Surekha, K.; Hayashi, A.; Ozawa, F.; Liu, Y.-H.; Peng, S.-M.; Liu, S.-T. *Organometallics* **2007**, *26*, 1062. (b) Bauer, E. B.; Andavan, G. T. S.; Hollis, T. K.; Rúbio, R.

- J.; Cho, J.; Kuchenbeiser, G. R.; Helgert, T. R.; Letko, C. S.; Tham, F. S. *Org. Lett.* **2008**, *10*, 1175. (c) Field, L. D.; Messerle, B. A.; Vuong, K. Q.; Turner, P.; Failes, T. *Organometallics* **2007**, *26*, 2058. (d) Burling, S.; Field, L. D.; Messerle, B. A.; Rumble, S. L. *Organometallics* **2007**, *26*, 4335. (e) Li, X.; Chianese, A. R.; Vogel, T.; Crabtree, R. H. *Org. Lett.* **2005**, *7*, 5437.
10. Some recent literatures about gold-catalyzed alkene hydroamination: (a) Kovács, G.; Ujaque, G.; Lledós, A. *J. Am. Chem. Soc.* **2008**, *130*, 853. (b) Giner, X.; Nájera, C. *Org. Lett.* **2008**, *10*, 2919. (c) Bender, C. F.; Widenhoefer, R. A. *Chem. Commun.* **2008**, 2741. (d) Bender, C. F.; Widenhoefer, R. A. *Chem. Commun.* **2006**, 4143. (e) Zhang, J.; Yang, C.-G.; He, C. *J. Am. Chem. Soc.* **2006**, *128*, 1798.
11. (a) Fukuda, Y.; Utimoto, K.; Nozaki, H. *Heterocycles* **1987**, *25*, 297; (b) Fukuda, Y.; Utimoto, K. *Synthesis* **1991**, 975.
12. (a) Mizushima, E.; Hayashi, T.; Tanaka, M. *Org. Lett.* **2003**, *5*, 3349. (b) Luo, Y.; Li, Z.; Li, C.-J. *Org. Lett.* **2005**, *7*, 2675.
13. Zhang, Y.; Donahue, J. P.; Li, C.-J. *Org. Lett.* **2007**, *9*, 627.
14. Liu, X.-Y.; Ding, P.; Huang, J.-S.; Che, C.-M. *Org. Lett.* **2007**, *9*, 2645.
15. (a) Lavallo, V.; Frey, G. D.; Donnadiou, B.; Soleilhavoup, M.; Bertrand, G. *Angew. Chem., Int. Ed.* **2008**, *47*, 5224. (b) Zeng, X.; Frey, G. F.; Kousar, S.; Bertrand, G. *Chem. Eur. J.* **2009**, *15*, 3056.
16. (a) Wipf, P.; Aoyama, Y.; Benedum, T. E. *Org. Lett.* **2004**, *6*, 3593. (b) Hashmi, A. S. K.; Weyrauch, J. P.; Frey, W.; Bats, J. W. *Org. Lett.* **2004**, *6*, 4391. (c) England, D. B.; Padwa, A. *Org. Lett.* **2008**, *10*, 3631. (d) Verniest, G.; Padwa, A. *Org. Lett.* **2008**, *10*, 4379.
17. (a) Kang, J.-E.; Kim, H.-B.; Lee, J.-W.; Shin, S. *Org. Lett.* **2006**, *8*, 3537. (b) Hashmi, A. S. K.; Rudolph, M.; Schymura, S.; Visus, J.; Frey, W. *Eur. J. Org. Chem.* **2006**, 4905.
18. Kadzimirsz, D.; Hildebrandt, D.; Merz, K.; Dyker, G. *Chem. Commun.* **2006**, 661.
19. Zhang, L.; Kozmin, S. A. *J. Am. Chem. Soc.* **2005**, *127*, 6962.
20. Harrison, T. J.; Kozak, J. A.; Corbella-Pané, M.; Dake, G. R. *J. Org. Chem.* **2006**, *71*, 4525.
21. Shu, X.-Z.; Liu, X.-Y.; Xiao, H.-Q.; Ji, K.-G.; Guo, L.-N.; Liang, Y.-M. *Adv. Synth. Catal.* **2008**, 350, 243.

22. (a) Jiménez-Núñez, E.; Echavarren, A. M. *Chem. Rev.* **2008**, 108, 3326. (b) Zhang, L.; Sun, J.; Kozmin, S. A. *Adv. Synth. Catal.* **2006**, 348, 227. (a) Nieto-Oberhuber, C.; Muñoz, M. P.; Buñuel, E.; Nevado, C.; Cárdenas, D. J.; Echavarren, A. M. *Angew. Chem., Int. Ed.* **2004**, 43, 2402. (b) Nieto-Oberhuber, C.; Muñoz, M. P.; López, S.; Jiménez-Núñez, E.; Nevado, C.; Herrero-Gómez, E.; Raducan, M.; Echavarren, A. M. *Chem. Eur. J.* **2006**, 12, 1677.
23. (a) Boyer, F.-D.; Goff, X. L.; Hanna, I. *J. Org. Chem.* **2008**, 73, 5163. (b) Ferrer, C.; Echavarren, A. M. *Angew. Chem., Int. Ed.* **2006**, 45, 1105. (c) Ferrer, C.; Amijs, C. H. M.; Echavarren, A. M. *Chem. Eur. J.* **2007**, 13, 1358.
24. Hashmi, A. S. K.; Schwarz, L.; Choi, J.-H.; Frost, T. M. *Angew. Chem. Int. Ed.* **2000**, 39, 2285.
25. (a) Liu, Y.; Song, F.; Song, Z.; Liu, M.; Yan, B. *Org. Lett.* **2005**, 7, 5409. (b) Antoniotti, S.; Genin, E.; Michelet, V.; Genêt, J.-P. *J. Am. Chem. Soc.* **2005**, 127, 9976. (c) Barluenga, J.; Diéguez, A.; Fernández, A.; Rodríguez, F.; Fañanás, F. *Angew. Chem., Int. Ed.* **2006**, 45, 2091.
26. (a) Sato, K.; Asao, N.; Yamamoto, Y. *J. Org. Chem.* **2005**, 70, 8977. (b) Xin, L.; Kennedy-Smith, J. J.; Toste, F. D. *Angew. Chem., Int. Ed.* **2007**, 46, 7671. (c) Jung, H. H.; Floreancig, P. E. *J. Org. Chem.* **2007**, 72, 7359. (d) Li, Y.; Zhou, F.; Forsyth, C. J. *Angew. Chem., Int. Ed.* **2007**, 46, 279.
27. (a) Zhang, J.; Zhao, X.; Lu, L. *Tetrahedron Lett.* **2007**, 48, 1911. (b) Zhang, D.; Yuan, C. *Eur. J. Org. Chem.* **2007**, 3916.
28. Gabriele, B.; Salerno, G.; Fazio, A. *Org. Lett.* **2000**, 2, 351.
29. (a) Istrate, F. M.; Gagosz, F. *Org. Lett.* **2007**, 9, 3181. (b) Gabriele, B.; Salerno, G.; Fazio, A. *J. Org. Chem.* **2003**, 68, 7853.
30. Pd(OAc)₂ and PtCl₂ can also be applied to this transformation, but the isolated yield is very low (5-20%).
31. Martin, R.; Rivero, M. R.; Buchwald, S. L. *Angew. Chem. Int., Ed.* **2006**, 45, 7079.